SENSITIVITY OF THE 2002 PAVEMENT DESIGN GUIDE TO TRAFFIC DATA INPUT

By

MICHAEL TODD BRACHER

A thesis submitted in partial fulfillment of
the requirements for the degree of

MASTER OF SCIENCE IN CIVIL ENGINEERING

WASHINGTON STATE UNIVERSITY
Department of Civil and Environmental Engineering

DECEMBER 2004

To the Faculty of Washington State University:

The members of the Committee appointed to examine the thesis of MICHAEL TODD BRACHER find it satisfactory and recommend that it be accepted.

_____
Chair

_____

_____

ACKNOWLEDGMENTS

I would like to thank my advisor, Dr. Tom Papagiannakis, who provided me with the guidance, mentoring and friendship necessary to see this thesis through to the end. I would also like to thank the FHWA for the funding that allowed me to perform the research presented here.

I also extend my thanks to Dr. Eyad Masad for making me believe in myself. Without him, these pages simply would not be. I would also like to thank Dr. Rollin Hotchkiss for challenging me in my undergraduate coursework. His advising and tutelage had a significant impact on my education.

Finally, I extend my thanks to the Washington State University Department of Civil and Environmental Engineering for providing me with an exceptional place to learn and work, and for hiring the people who taught me how to be an engineer.

SENSITIVITY OF THE 2002 PAVEMENT DESIGN GUIDE

TO TRAFFIC DATA INPUT

Abstract

by Michael Todd Bracher, M.S.
Washington State University
December 2004

Chair: Thomas Papagiannakis

The vehicle load input to the 2002 Pavement Design Guide (PDG) is in the form of axle load distributions by axle configuration and truck class. In practice they are obtained by combining data from a variety of traffic monitoring equipment operating over various lengths of time, such as weigh-in-motion (WIM), automated vehicle classification (AVC) and automated traffic recording (ATR) systems. Changes in the length of time that traffic data is available for causes variation in the estimated axle load, which results in variation of pavement life predictions.

The study at hand relates traffic data collection effort to variation in the predicted pavement life. At 50% reliability, scenarios 1-0, 1-1, and 1-2 all exhibit less than 10% overestimation of pavement life, suggesting that scenario 1-2 would be sufficient traffic data input at a 50% reliability level. Scenario 2-0 on average produced pavement life prediction overestimations less than 18% regardless of reliability level, and hence would represent a cost-effective data acquisition alternative to SS (site-specific) WIM. At 75%, 85%, 95%, and 99.9% reliability level, SS AVC data operating either one month (scenario 2-1) or one week (scenario 2-2) per season, combined with R (regional) WIM data, produces pavement life overestimation similar to that of the SS WIM system operating for one month per season (scenario 1-1).The average life

overestimation resulting from SS ATR counts taken 1 week per season is 47% at a 95% reliability level.

Pavement performance prediction using the 2002 PDG is highly dependent upon the traffic sampling scenario. Pavement life is also dependent upon the sources of the traffic data, and how much of it is site-specific. As expected, the more site-specific data, the more accurate the life prediction will be.

PDG Traffic Input Levels as they currently are written do not address variation in data collection time. Therefore, the time of data acquisition should be considered when choosing data acquisition equipment.

TABLE OF CONTENTS

Page

LIST OF TABLES

LIST OF FIGURES

Dedication

I dedicate this work to my father,

who showed me the meaning of integrity

and a hard day’s work.

CHAPTER ONE

INTRODUCTION

1.1 Background

1.1.1 Empirical Pavement Design

Flexible and rigid pavement (AC and PCC, respectively) performance depends on the complex interaction of environmental and traffic variables. Their performance is also significantly affected by their structural and material characteristics. The contribution of these factors to pavement performance has historically been described empirically. The American Association of State Highway Officials (AASHO) Road Test was performed in the late 1950s, and produced empirical equations for both flexible and rigid pavement design, as documented in [2]. These equations estimate the number of load repetitions to pavement failure based upon structure, present serviceability index, minimum acceptable serviceability and reliability. Traffic is input in the form of Equivalent Single Axle Loads (ESALs), which convert the damage from axles of all configurations and weights to the damage of a single, standard, eighteen-thousand pound, dual-tired axle. The equations for flexible and rigid pavement performance are given below (1.1 and 1.2, respectively).

$$\log_{10}(W_{18}) = Z_R \cdot S_0 + 9.36 \cdot \log_{10}(SN+1) - 0.20 + \frac{\log_{10}\left[\frac{\Delta PSI}{4.2-1.5}\right]}{0.40 + \frac{1094}{(SN+1)^{5.19}}} + 2.32 \cdot \log_{10}(MR) - 8.07 \qquad (1.1)$$

$$\log_{10}(W_{18}) = Z_R \cdot S_0 + 7.35 \cdot \log_{10}(D+1) - 0.06 + \frac{\log_{10}\left[\frac{\Delta PSI}{4.5-1.5}\right]}{1+\frac{1.624\cdot 10^7}{(D+1)^{8.46}}} + (4.22 - 0.32 \cdot p_t) \cdot \log_{10}\left[\frac{S'_c \cdot C_d\left(D^{0.75}-1.132\right)}{215.63 \cdot J\left[D^{0.75} - \frac{18.42}{(E_c/k)^{0.25}}\right]}\right] \quad (1.2)$$

The limitations of such empirical expressions are obvious. They do not address the damaging effect of the environment, and they aggregate damage from all axle configurations into a single value, ignoring the temporal variation in damage accumulation.

1.1.2 Mechanistic Pavement Design

Mechanistic pavement design principles have flourished since the advent of personal computers. Their philosophy involves mechanistic analysis of pavement response, translation of the response into damage, and accumulation of the damage into distinct pavement distresses. AC pavement response is computed using elastic layered theory, while PCC pavement response is computed using the finite element method.

1.1.3 The 2002 Pavement Design Guide

The 2002 Pavement Design Guide (PDG) [1] implements such a mechanistic approach into a software package that allows predicting pavement performance as a function of traffic, climatic and structural input. It uses actual axle load distributions for each axle configuration, and computes stresses and strains in the pavement structure for distinct time increments within the year. This means that material response is computed at intervals within the year, and the seasonal

material properties for each time increment are used in pavement response modeling. Traffic loads are input in the form of load distributions over each increment.

1.1.4 Traffic Input to the 2002 PDG

The 2002 PDG requires five traffic input in order to fully describe traffic behavior for a site. They are:

1. Annual Average Daily Truck Traffic (**AADTT**)
2. Vehicle Class Distribution (**VCD**) as a percent of total trucks
3. Monthly Adjustment Factors (MAFs) to distribute the VCD throughout a year
4. Number of Axles Per Truck (NOAPT) to calculate the number of axles
5. Normalized Axle Load Distribution Factors (NALDFs) to generate axles per truck

These five input can completely describe the axle load spectra applied at a pavement site. Load spectra are defined as the actual number of load passes by axle configuration and load interval over the defined time increment. In practice, this input is collected from a combination of traffic data acquisition systems. According to the PDG, the combination of data acquisition system types and their proximity to a pavement design site defines the traffic input level (TIL). For example, site-specific (SS) vehicle classification data represents a higher input level than vehicle classification data obtained for a similar site in the same state. The PDG does not differentiate TILs with respect to the length of time coverage of traffic data.

1.1.5 Resolution Of General Input Data

The PDG has three levels for most input, ranging from Level 1 data that has the highest relevance to the design site to Level 3 data that has the lowest. All input to the 2002 PDG follow this hierarchy. For example, there are three levels for characterizing asphalt binder:

- Level 1: Actual test values for G* and δ at five temperatures for the binder
- Level 2: Generic values for G* and δ at five temperatures for the binder
- Level 3: PG grade alone

Similarly, the traffic input hierarchy is:

- Level 1: Very good knowledge of past and future traffic characteristics
- Level 2: Modest knowledge of past and future traffic characteristics
- Level 3: Poor knowledge of past and future traffic characteristics

These descriptions are qualitative. Appendix A of the PDG elaborates on the traffic input levels with the following descriptions of data sources with respect to the design site:

- Level 1: Adequate site-specific axle load and truck classification spectra
- Level 2: Regional/state axle load spectra instead of site-specific axle load spectra
- Level 3: Regional truck distribution spectra instead of site-specific
- Level 4: Only site-specific Annual Average Daily Traffic (AADT) and percent truck information is required, (i.e., use of default classification and load data is implied)

According to these descriptions, the PDG distinguishes four traffic input levels in terms of the spatial relationship between the design site and the traffic data collection site. For example, the difference between traffic input Levels 1 and 2 is the source of the axle load distribution data and hence the location of the weigh-in-motion (WIM) system. When this data come from the same roadway in the proximity of the design site, then traffic data is assigned to Level 1.

Alternatively, when this data come from a regional WIM dataset, then traffic data is assigned to Level 2. These input levels involve no further differentiation with respect to the *time coverage* of traffic data.. Clearly, the accuracy in capturing the true load spectra experienced over the life of a pavement section varies with the combination of data acquisition technology, proximity of the systems to the site in question and the data time coverage of those systems. The accuracy in capturing this traffic input will obviously affect pavement performance prediction.

This work is part of a broader study conducted for the Federal Highway Administration (FHWA), *Optimization of Traffic Data Collection for Specific Pavement Design Applications* (contract DTFH61-02-D-00139).

1.2 Objective

The objective of this study is to evaluate the sensitivity of the 2002 PDG pavement performance predictions to the combination of traffic data acquisition technology, their proximity to the pavement design site being studied, and the data time coverage of those systems.

CHAPTER TWO

LITERATURE REVIEW

The literature review focuses on two main areas. First, study the relationship between traffic data collection effort and the resulting variability in traffic estimates. Second, evaluate the sensitivity of the pavement design process to the variability in traffic input.

2.1 Sensitivity of Traffic Estimates to Data Collection Effort

2.1.1 Annual Average Daily Traffic

Annual Average Daily Traffic (AADT) is the most common traffic statistic used to represent traffic volume, and is most commonly observed through the use of an automated traffic recorder (ATR). The American Association of State and Highway Transportation Officials (AASHTO) Joint Task Force on Traffic Monitoring Standards [3] proposes the following method for estimating AADT from short-term daily ATR counts:

- For each month, calculate the average day-of-week (DOW) traffic volume (Monday, Tuesday and Wednesday are each a DOW)
- For each DOW, compute an annual average value
- Average all seven of the annual DOW values to arrive at the AADT

This is expressed mathematically as:

$$AADT = \frac{1}{7}\sum_{i=1}^{7}\left[\frac{1}{12}\sum_{j=1}^{12}\left(\frac{1}{n}\sum_{k=1}^{n} VOL_{ijk}\right)\right] \tag{2.1}$$

where:

VOL_{ijk} = daily traffic volume for day k of DOW i and month j

i = annual average DOW ranging from 1 to 7 (i.e., Sunday to Saturday)

j = month of the year ranging from 1 to 12

k = day of the month

n = number of times day i occurs with traffic data within month j

This approach limits the bias that results from simply averaging traffic volumes for the days of the year available. In implementing this approach holidays, along with the days immediately preceding and following them, are excluded.

Early work by Ritchie and Hallenbeck [13] describes a relationship between the accuracy of an AADT estimate and the number of days with traffic data as a function of confidence interval and covariance of the observed. The accuracy of an *AADT* estimate is given by:

$$d = Z_{a/2} \frac{CV}{\sqrt{n}} \tag{2.2}$$

where:

d = probability that the sample mean is within 100d% of the true average for the level of confidence 100(1-α)%

α = total probability of failure

$Z_{\alpha/2}$ = standard normal statistic at a confidence level 100(1-α)%

CV = coefficient of variation in AADT (standard deviation in AADT divided by the mean)

n = number of days with volume measurements

For a given confidence interval, the precision in predicted AADT increases as the number of days of traffic volume counts n increases. As n increases, CV of the population decreases.

The 2001 Traffic Management Guide (TMG) [18] gives a slightly different expression than the one used by Ritchie and Hallenbeck. It is:

$$d = t_{\alpha/2,\,n-1}\,\frac{CV}{\sqrt{n}} \tag{2.3}$$

where,

d = probability that the sample mean is within 100d% of the true average for the level of confidence 100(1-α)%

α = total probability of failure

$t_{\alpha/2,\,n-1}$ = the Student's *t*-distribution statistic

CV = coefficient of variation in AADT (standard deviation in AADT divided by the mean)

n = number of days with volume measurements

The difference is the use of a *t*-distribution instead of a standard-normal one. This is because the variance of the daily traffic volume population is not actually known, and the number of days (n) is relatively small.

2.1.2 Monthly Adjustment Factors

Monthly adjustment factors (MAFs) are multipliers that define monthly variation in traffic volume throughout a year. From the 2002 PDG, the equation to compute a MAF is:

$$MAF_{ij} = \frac{ADTT_{ij}}{\frac{1}{12}\sum_{i=1}^{12} ADTT_{ij}} \tag{2.4}$$

where:

$MAFij$ = monthly adjustment factor for month i and vehicle class j

$ADTT_{ij}$ = average daily truck traffic for month i and vehicle class j

i = month of the year

j = vehicle class

This equation requires data collection for all months of the year. However, if volume counts are taken in only one month of the year, factors are necessary in order to reduce error in AADT predictions. Several methods for estimation of these factors are explained below.

Early work by Ritchie and Hallenbeck [13] describes different methods for obtaining these factors. Monthly seasonal factors for short-duration ATR counts (Tuesday to Thursday) were derived using a variation of linear regression. Monthly traffic volume data was grouped by highway geographic region *and* roadway functional class. Groups displaying similar seasonal patterns were combined. For each group, seasonal factors β were derived using a simple ratio-based method identical to the one later adopted by AASHTO [3], shown as:

$$\frac{AADT}{VOL} = \beta + e \tag{2.5}$$

where:

AADT = known annual average daily traffic

VOL = measured daily vehicle volume count obtained by averaging the counts for three weekdays (i.e., Tuesday to Thursday)

β = group seasonal factor

e = error

It was found that this method avoided the problem of heteroscedasticity present in other regression methods (condition where the variance of the regression error depends on the magnitude of the independent variable *VOL*).

Almost all short duration counts require adjustments, or factors to reduce the effects of temporal bias. These factored counts better reflect the variation in traffic volumes that occur from month to month. The 2001 version of the TMG [18] recommends that monthly or seasonal

factors be developed by analyzing data from *continuously* operating ATR stations. Data from these stations is combined into groups of similar characteristics, typically in terms of geographic and roadway functional class. Establishment of these roadway groups is best done using statistical clustering techniques [18]. The relationship used for computing AADT using these monthly factors is:

$$AADT_{hi} = VOL_{hi}\ M_h\ D_h\ A_i\ G_h \tag{2.6}$$

where,

h = roadway group

i = roadway location

M_h = monthly adjustment factor

D_h = daily adjustment factor

A_i = axle adjustment factor, (applicable only if conventional axle counters are used)

G_h = growth factor (applicable only if counts are from a different year)

This method is referred to as the combined month and DOW (CMDW) method. Site-specific axle factors for the Interstate and the National Highway System are developed using representative axle factors from other roads (e.g., state-wide or regional).

Axle factors are obtained from Automated Traffic Recorders (ATRs) and Automated Vehicle Classifiers (AVC) that are continuously operating together. These factors should be the non-weighted averages of the ratio of the number of axles to the number of vehicles from various sites in a region [5], and should be used for factoring axle counts obtained at nearby sites on the same road, but not at entry and exit ramps. They should also be recorded to two or three decimal places. For Interstate and National Highway System roads, road-specific factors are recommended.

For use on other roads, Cambridge Systematics recommends the development of axle-correction factors that vary by functional *system* and region. For each functional system within a region, a *system* factor is created as the un-weighted average of axle-to-vehicle ratios obtained for several sites within a system. These ratios can be from either annual counts of axles and vehicles from Data Pave, or estimates of AADT by vehicle class developed from short-term classification counts.

2.1.3 Missing Daily Data

The ratio of number of days *with* data per year to the total number of days in that same year is almost always less than one. This can be due to power outages, equipment malfunction, or down-time for equipment verification. Collected traffic data can also be thrown out by data quality control processes that disqualify days of data after collection has taken place.

The AASHTO procedure for averaging daily volumes (equation 2.1) imputes missing daily data implicitly. For example, if there are only three Mondays in June, the average of these three values is assigned to the missing Mondays in that same month. This is just one of many ways to impute daily traffic data.

A FHWA funded study conducted by Cambridge Systematics [5] utilized continuous ATR sites to evaluate the error in AADT estimates associated with certain methods of daily traffic volume data imputation. The results of that study suggest that the fore-mentioned AASHTO method (Table 2.1, No. 4 labeled CMDW, below) offers an acceptable compromise between accuracy and complexity. This is the same method recommended by the 2001 TMG for imputing the data of missing days.

Table 2.1: Accuracy of AADT Predictions as a Function of Factoring Procedure [5]

No	Factoring Procedure	Involves	Mean Absolute Error	Average % Error	P (e>0.2)
0	Unfactored	-	12.4%	-0.6%	18.2%
1	Separate month and DOW (MDW)	Set of 12 monthly factors and another set of 7 DOW factors (total of 19)	7.5%	-0.5%	6.2%
2	Combined month and average weekday (CMAWD)	Set of average weekday and average weekend factor for each month (total of 24)	7.6%	+0.4%	5.9%
3	Separate week and DOW (SWDW)	Set of 52 weekly factors and another set of 7 DOW factors (total of 59)	7.5%	-0.9%	6.0%
4	Combined month and DOW (CMDW)	Set of DOW factors for each month (total of 84)	7.4%	-0.2%	5.8%
5	Combined week and average weekday (CWAWD)	Set of average weekday and weekend factors for each week of year (total of 104)	7.3%	+0.5%	5.1%
6	Specific day, (SD)	Set of day factors for each day, (midnight-to-midnight) of the year (total of 365)	7.1%	+0.2%	5.1%
7	Specific day with noon-to-noon factors (SDNN)	Similar to the one above, except counts are noon-to-noon.	7.0%	+0.3%	4.8%

The relationship for the CMDW factor is:

$$CMDWF_{ijl} = \frac{AADT_l}{MADW_{ijl}} \tag{2.7}$$

where,

$CMDWF_{ijl}$ = combined month and day-of-week factor

$AADT_l$ = actual, known annual average daily traffic

$MADW_{ijl}$ = actual, known monthly average day-of-week traffic

i = month

j = DOW

l = road station

The use of this equation does not require continuous ATR data. For each month, one twenty-four hour sampling period is required for each DOW. Therefore, this procedure can be applied without completely continuous data. For more detailed information, see the paper by *Cambridge Systematics* [5].

2.1.4 Traffic Data Time Sampling

The 2001 TMG [18] recommends collecting traffic volume data through a combination of a limited number of continuously operating ATRs and a larger number of shorter-duration coverage locations. Traffic patterns established from continuously operating ATR sites can then be used to compute AADT from short-term volume counts at other comparable sites [5]. The TMG further recommends that short-term coverage ATRs record data over at least 24 hour, but preferably 48 hour, periods using systems that summarize data hourly. However, work by Cambridge Systematics suggests that the improvement in predicting AADT using a 48 weekday-

hour sample is marginal (a reduction in absolute error of 1%) [5] although 48 hour counts are useful for sampling reasons (if data sampling is interrupted in a 24 hr period, the data from the next 24 hours can be used to "patch" the data set). Counts of less than 24 hours are not recommended.

The 2001 TMG [18] recommends obtaining AVC counts following principals similar to those used for ATR counts. The main difference is that seasonal traffic volume adjustment factors (both monthly and daily) are to be developed for 3 or 4 broad vehicle classes (passenger cars, single unit trucks, single trailer trucks and multi-trailer trucks) rather than for all fourteen FHWA vehicle classes. This is one of the major differences between the 2001 version of the TMG and its earlier versions. This change was introduced to account for the seasonal variation in the traffic volume patterns of various vehicle classes.

2.1.5 Vehicle Classification

Seasonal factor groups are developed by analyzing data from continuously operating AVC stations. This data can then be used to represent the traffic conditions for the roadway group that the site belongs to. Seasonal factor groups can be established subjectively (e.g., based on roadway functional class) or through clustering techniques. The TMG contains no particular method for doing so.

Short-term AVC counts are to cover at least 48 consecutive hours, with a recommended monitoring cycle of 6 years. It is suggested that, unlike volume counts, an improvement of between 3% and 5% in the accuracy of predicting annual average traffic volumes can be achieved by increasing the duration of classification counts from 24 to 48 hours [9]. Low volume roads exhibited an even higher increase in accuracy due to the higher variation in daily traffic

counts [5]. The only exception to the 48-hour data collection recommendation is made for urban areas, where traffic congestion imposes variable vehicle speeds. In such situations, it is allowed to collect vehicle classification data over shorter periods of time (e.g., 15 minutes) during which time traffic is detected to move at a constant speed.

The annual average daily truck traffic for vehicle class *c* ($AADTT_c$) according to the FHWA classification scheme (Figure 2.1) is computed in the 2001 TMG using an expression similar to the one used for the *AADT*:

$$AADTT_c = \frac{1}{7}\sum_{i=1}^{7}\left[\frac{1}{12}\sum_{j=1}^{12}\left(\frac{1}{n}\sum_{k=1}^{n} AADTT_{ijkc}\right)\right] \tag{2.8}$$

where:

$AADTT_{ijkc}$ = daily truck traffic volume for day *k* of DOW *i* and month *j* for vehicle class *c*

i = DOW ranging from 1 to 7 (i.e., Sunday to Saturday)

j = month of the year ranging from 1 to 12

k = day of the month

n = number of times day *i* occurs with traffic data within month *j*

Consequently, adjustment factors are needed to convert short-duration counts for a particular vehicle class *c* to *AADTT* for that vehicle class. This principle is an extension of Equation 2.7 which, by dropping the subscript *l* for the shake of simplicity, is given by:

$$CMDWTF_{ijc} = \frac{AADTT_c}{MADWT_{ijc}} \tag{2.9}$$

where:

$CMDWTF_{ijc}$ = the combined month and DOW factor for truck class *c*

$MADWT_{ijc}$ = the daily average traffic count for month *i* and DOW *j* for truck class *c*

Finally, the 2001 TMG recommends calibration of AVC devices using roadside observers or roadside video cameras combined with manual post-processing.

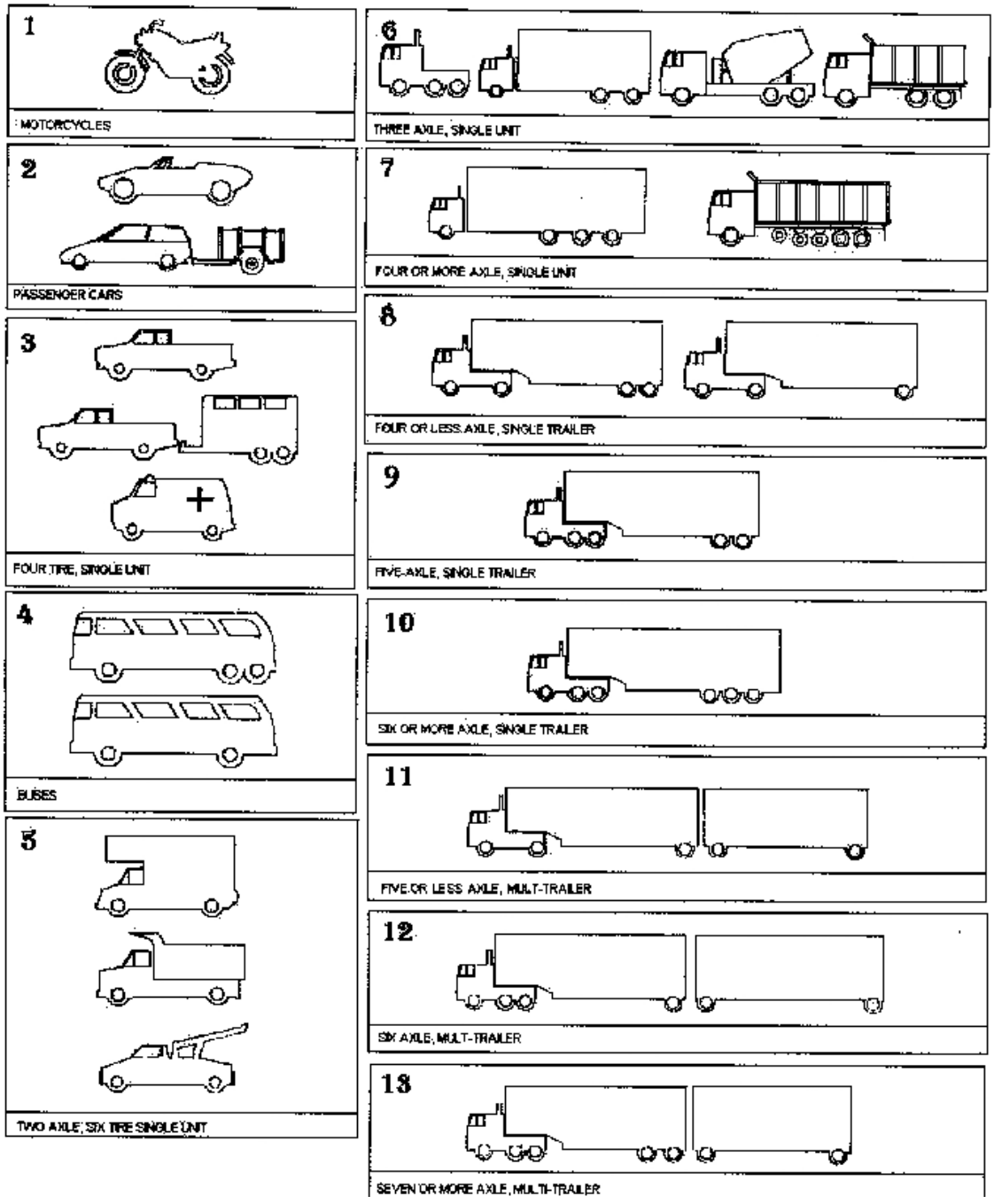

Figure 2.1: FHWA Vehicle Class Designations (from ODOT website)

2.1.6 Axle Load

The 2001 TMG defines truck axle load data collection as the means of obtaining the distribution of axle loads by axle configuration (single, tandem, triple, and quad) and vehicle class (FHWA 4 to 13, as per Figure 2.1) for selected roadway groups [18]. This information can be obtained only with Weigh In Motion (WIM) systems. In the absence of site-specific WIM systems, establishment of roadway groups with comparable axle load distribution patterns is essential in order to maximize the benefit of the limited number of WIM sites typically available in a jurisdiction. Roadway groups formed using axle load data from WIM sites need not be identical to the roadway groups formed using vehicle classification data obtained from AVC sites [18].

Roadway groups can be established subjectively (e.g., based on roadway functional class, predominant commodity being carried, etc.) or through clustering techniques, although no particular method for doing so is prescribed in the TMG. The number of WIM sites required per roadway group *n* can be found in the 2001 TMG as follows:

$$n = \left(t_{a/2,\nu} \frac{CV}{d} \right)^2 \tag{2.10}$$

where:

t = the value of the Student's t distribution for α and ν

α = total probability of failure

$\nu = n - 1$ degrees of freedom

CV = coefficient of variation of the total data, or standard deviation divided by the mean

d = the desired accuracy range in this traffic quantity

Numerous sources in the literature emphasize that it is more important to have accurate than continuous WIM data, although it is preferable to have at least one of six WIM sites in each roadway group operating continuously. This allows establishment of daily, weekly, and seasonal patterns in the traffic load data for a particular roadway group. Where continuous operation is not possible, WIM systems should operate for at least a period of seven continuous days to capture day-to-day variations [18].

2.2 Sensitivity of the Pavement Design to Traffic Input Variability

2.2.1 2002 Pavement Design Guide

NCHRP 1-37A [1] is the main study for the development of the 2002 PDG. In it, axle load information is synthesized by combining data from WIM, AVC and Automated Traffic Recording (ATR) systems from a specific pavement location (site-specific), or from other regional traffic data collection sites. The combination of data acquisition technology and spatial relationship constitute the traffic level input to the PDG (Table 2). These traffic input levels suggest similar levels for the other groups of input to the PDG, (i.e., layer properties and environmental data), but no actual connection between groups of input is made in the PDG. For example, a designer may have level 1 traffic data, but only level 3 structural. Furthermore, the PDG sets no criteria on the length of time that traffic data be collected in order to qualify for any of the traffic input levels defined below.

Table 2.2: Detailed Description of the PDG Traffic Input Levels

PDG Traffic Input Levels	Description
1	Site-specific vehicle classification and axle load data required. The traffic data measured at the site includes counts, classification, and weights by lane and direction over a sufficiently long period of time to reliably establish patterns in these traffic input. This is possible only with an on-site WIM installation, and is recommended for use in the design of high-volume highways.
2	Site-specific vehicle classification data required, with representative axle weight data by vehicle class and axle configuration taken from the regional data set. The regional axle load data are obtained from WIM installations on roadways that exhibit similar traffic load patterns as the design site. This is possible with an on-site AVC installation and sufficient WIM data from installations that have similar traffic load patterns. This input level is recommended for roadways of lesser importance.
3	Site-specific traffic volume counts with percent truck data are required, with representative vehicle classification and axle weight data taken from the regional dataset. This regional data is to be obtained from AVC and/or WIM installations from sites that exhibit similar traffic distributions and load patterns as the site in question. This is possible with an on-site ATR installation and on-site truck percentage counts. The latter can be either automated (e.g., vehicle length based algorithm) or manual. This input level is recommended for roadways of even lesser importance.
4	Similar to Level 3 input, this level uses default (i.e., national average) vehicle classification and axle load distributions in place of a regional classification and load data. This approach represents the minimum possible traffic input level, and should be used only for roadways of very low importance.

The traffic load information in the PDG is synthesized from input arranged into four modules of traffic information which are described below:

Module 1: Traffic Volume

- Annual average bi-directional, multi-lane daily truck traffic (FHWA classes 4 to 13)
- Number of lanes in the design direction
- Percent of trucks in the design direction

- Percent trucks in the design lane
- Operational speed

The first of these input components is updated annually through a user-specified growth rate (input module 2) while the remaining four components are treated as constant.

Module 2: Traffic Volume Adjustment Factors

- MAFs (Equation 2.4) for each month per truck class
- Truck class distribution, defined as the percentage of the traffic volume by vehicle class
- Hourly volume distribution
- Traffic growth factors, either the same for all classes or per individual vehicle class

Module 3: Load Distribution

- Normalized axle load distribution (percent of total axles by load level by axle configuration, by month and by truck class)

Module 4: General Traffic Input

- Number of axles by axle configuration and truck class
- Axle/tire configuration, spacing and tire inflation pressure
- Wheel base data

A summary of the traffic input components, the size of their associated input arrays, and the flow of calculations in the PDG software is given in Table 2.3. The number of axles by load level, axle configuration and month is further disaggregated by the distribution of truck traffic volume through the typical day. However, no differentiation is made in traffic volumes by the DOW within each month.

Table 2.3: PDG Flow Of Calculations in Assembling Axle Load Spectra

Traffic Input Component	Main Data Element	Input Array Size	Calculation and Result
1	Average annual daily trucks traffic in the design lane	1 (scalar)	-
2	Distribution of trucks by class (i.e., FHWA 4-13).	1x10	1x2 = annual average daily number of trucks by class
3	Monthly adjustment factors (MAF) by truck class	12x10	1x2x3 = adjusted average daily number of trucks by class, by month
4	Number of axles by axle configuration, (single, tandem, triple, quad) by truck class	4x10	1x2x3x4 = average number of axles by axle configuration, by month
5	Load frequency distribution (%) by axle configuration, by month, by truck class	4x12x10x41	1x2x3x4x5 = number of axles by load range, by axle configuration, by month

2.2.2 Pavement Performance Models in the PDG

For flexible pavements the PDG considers the following distresses:

- Fatigue cracking (both bottom-up alligator and top-down longitudinal)
- Plastic deformation in all pavement and subgrade layers
- Transverse (Thermal) cracking
- Roughness (IRI)

For rigid pavements, the PDG can analyze jointed-plain (JPCCP), jointed-reinforced (JRCP), and continuously-reinforced (CRCP) concrete pavements. The following distress mechanisms are modeled by the PDG for rigid pavement structures:

- Fatigue transverse cracking, both bottom-up and top-down (JPCCP, JRCP)
- Joint faulting (JPCCP, JRCP)

- Punchouts (CRCP)
- Roughness (JPCCP, JRCP and CRCP)

Fatigue damage for both flexible and rigid pavements is accumulated using a Miners rule approach, which consists of summing the damage ratios, which are calculated by dividing the actual number of strain cycles by the number of cycles that would cause fatigue failure at this strain level. The damage accumulation is given by:

$$Damage = \left(\sum_i \sum_j \sum_k \frac{n_{ijk}}{N_{ijk}} \right) 100\% \tag{2.11}$$

where,

Damage = percent of total life associated with particular distress mechanism

n_{ijk} = number of pavement response cycles from axle configuration *i*, load level *j* over time interval *k*

N_{ijk} = number of pavement response cycles that cause failure from axle configuration *i*, load level *j* over time interval *k*

The plastic deformation of flexible pavements and faulting damage of rigid pavements are simply cumulative. N_{ijk} comes from the calibration of the Long Term Pavement Performance (LTPP) data to traffic loading. More information on the damage functions used for each distress mechanism is given in the final report for the PDG [1], and is summarized in Appendix A. The findings of this study are specific to these damage functions, and the calibration performed by the time of release of the PDG (June 2004). Changes in any of the performance models used or their calibration could potentially alter the conclusions of this study.

2.2.3 PDG Data Input

NCHRP Study 1-39 [7] describes a method for processing the output of a combination of AVC and WIM systems from within a jurisdiction in order to synthesize the axle load spectra for a particular pavement design site necessary to run the 2002 PDG. This method consists of factoring the available, site-specific traffic data using the temporal axle load and vehicle classification distribution patterns from similar sites in the jurisdiction as prescribed by the 2001 TMG [18]. The type of technology and length of time coverage involved at these traffic data collection sites defines the value, or level of traffic input.

This method is implemented by a software package called *TrafLoad* [7] developed as part of NCHRP Study 1-39. The input to *TrafLoad* consist of the standard machine outputs of both AVC and WIM systems [18], namely the hourly summary *C Records* (*4 Cards)* and the individual vehicle *W Records* (*7 Cards)*, respectively. This data is assumed to have passed independent quality control (QC) tests prior to inputting into *TrafLoad*. The user must input the:

- Vehicle classification scheme (FHWA or other)
- Aggregation of these vehicle classes
- Grouping of traffic data sites with respect to vehicle classification distributions (TTC)
- Grouping of traffic data sites with respect to axle load distributions
- Seasonal load spectra by either month or by month and DOW

The latter is used in factoring incomplete sets of load spectra, as explained later. Some of this input, especially the site grouping and the seasonal load spectra computations, may require considerable pre-processing of the available WIM and AVC data.

TrafLoad distinguishes several levels of traffic input depending on the load and classification data available at a particular pavement design site. For complete, year-long, Level 1 WIM data *TrafLoad* produces all of the necessary input to the PDG. For incomplete WIM data, *TrafLoad* uses DOW and monthly factor ratios based upon complete Level 1 WIM sites belonging to the same truck weight road group (TWRG). This is done in terms of the pavement damage impacted by each vehicle class, month, and DOW as indexed by the average ESAL per vehicle (*AEPV*).

The approach used by *TrafLoad* to factor load spectra is fairly complex and has several limitations. First, it is applicable to continuous, site-specific WIM sites only, since lack of any site-specific WIM data precludes assigning this site to any load-based TWRG. Second, it indexes damage using ESALs, which the PDG does not use. The study at hand groups sites together based upon axle load distributions and vehicle class distributions using clustering techniques (described in Chapter 3).

CHAPTER THREE

METHODOLOGY

This study estimates pavement performance for a number of traffic data collection scenarios involving certain combinations of traffic data acquisition systems and lengths of data coverage. These scenarios are simulated from extended coverage WIM data extracted from the LTPP database. Throughout this analysis all other parameters are held constant, (i.e., structural and climatic). This is done for eleven pavement sites, selected from the LTPP database to represent a range of a AADTT levels and structural characteristics for both flexible and rigid pavements.

3.1 TRUTH in Traffic Data

The traffic experienced by a pavement structure is completely described by SS, continuous axle weight and vehicle classification data. This data is collected from a WIM system located on the site operating every day of the year. Therefore, pavement life computed from continuous SS WIM traffic data represents the TRUTH in traffic input to the 2002 PDG. Traffic data collection scenarios with less information than continuous SS WIM do not capture the full extent of pavement loading. Such scenarios may involve:

- Data Acquisition systems other than WIM (i.e., AVC or ATR)
- Sampling periods shorter than a year
- Locations other than SS

Use of such scenarios will generate traffic data estimates to the PDG that differ from the TRUTH, resulting in pavement life prediction variations. It is understood that these are merely estimates of pavement performance, and that they may differ from actual pavement performance.

Furthermore, it should be pointed out that if the PDG performance damage models change in the future, the results of this study should be revisited.

3.2 Sampling Scenarios

3.2.1 Selection

The traffic sampling scenarios selected expand upon the four TILs included in the PDG (listed in Section 1.1.5) by considering the length of sampling interval over which data is analyzed from the various data acquisition systems. The seventeen traffic sampling scenarios selected are shown in Table 3.1. As explained later, short-term data samples are extracted from extended coverage (i.e., greater that 299 days per year) WIM data. This allows comparison of traffic data input to the PDG to the TRUTH in traffic data.

Column two of this table lists the spatial relationship between the design site and the traffic data acquisition equipment location. Information in column two indicates the combination of data acquisition (e.g., both 3-0 and 3-1 use R WIM and AVC with SS ATR). The SS traffic data in column two is labeled as such, and is also shown in boldface for clarity.

Column 3 specifies the amount of time coverage that the SS data contains for each scenario. For example, scenario 3-0 has continuous SS ATR data coverage, while 3-1 has one month per season of SS ATR data coverage. The fourth column provides an identification code for each scenario consisting of two numbers separated by a dash. The first indicates the PDG TIL, and the second identifies the length of data coverage. For example, scenario 2-1 represents SS AVC data with a coverage of 1 month in each of the four seasons in a year, plus regional WIM data for the entire year. In selecting these scenarios two main considerations were adhered to:

- WIM and AVC systems are typically fixed, and therefore likely to operate over longer periods of time than ATRs
- Jurisdictions with neither AVC nor WIM data are less likely to have extended time coverage of SS ATR counts

Table 3.1: Selected Traffic Data Collection Scenarios

PDG Traffic Input Level (TIL)	**Traffic Data Sources for TIL**	**Time Coverage for the SS Traffic Data Source**	**Scenario ID**
1	**WIM Data = SS** AVC Data = R	Continuous	1-0
		1 month / 4 seasons	1-1
		1 week / 4 seasons	1-2
2	WIM Data = R **AVC Data = SS**	Continuous	2-0
		1 month / 4 seasons	2-1
		1 week / 4 seasons	2-2
		1 week	2-3
3	WIM Data = R AVC Data = R **ATR Data = SS**	Continuous	3-0
		1 month/4 seasons	3-1
4	WIM Data = N AVC Data = R **ATR Data = SS**	Continuous	4-0
		1 week / 4 seasons	4-1
		1 week	4-2
		1 weekday +1 weekend day	4-3
	WIM Data = N AVC Data = N **ATR Data = SS**	Continuous	4-4
		1 week / 4 seasons	4-5
		1 week	4-6
		1 weekday +1 weekend day	4-7

SS = Site Specific, R = Regional, N = National

N traffic data are simply the default input values already in the PDG. R traffic data are obtained by averaging data from sites with similar traffic characteristics within the same jurisdiction using a procedure known as clustering, which will be described in detail later.

3.2.2 Source Data

Obtaining traffic data input files for the 2002 PDG from short-term traffic samples involves considerable calculations in factoring the SS data using representative R and N vehicle classification and axle load data. The scenario traffic input is calculated as follows:

3.2.2.1 Scenario 1-0: SS Continuous WIM Data

This scenario represents the most complete traffic data set for generating traffic input to the PDG and is thus defined as the "truth" in traffic data. For the 11 sites analyzed, WIM data coverage ranged from more than 299 days per year to more than 359 days per year. The 5 traffic data input components to the PDG were computed as follows:

Axle Load Distributions

- Obtain the number of days per DOW (from Sunday to Saturday) for each month that has traffic records from the daily summary data table
- Sum the axle passes per truck class for each axle type and load bin for each month and DOW
- Divide each sum by the number of days of data to obtain the average number of daily axle passes per bin, per axle type, per truck class for each DOW and month
- Average the number of daily axle passes per bin for the 7 DOWs to obtain the monthly average number of axle passes by axle type, load bin and truck class for each month
- Translate the number of passes per bin into load distributions (percent) by axle type, truck class and month

Number of axles per vehicle

- Compute the average daily number of axles per axle type and truck class over the 12-month period
- Compute the average daily number of trucks by class
- Divide the two values to obtain the average number of axles by truck class and axle type

AADTT, VCD, and MAFs

- For each month and DOW, sum the number of trucks by class
- Divide each sum by the number of days of data to obtain the average number of daily vehicle passes by truck class per DOW and month
- Average the number of trucks by class for the 7 DOWs to obtain the monthly average number of trucks by class per month
- Average the number of trucks for the 12 months to obtain AADTT by trucks class.
- Translate these average values into frequencies (percent)
- Add the number of trucks for all classes to obtain AADTT
- Compute MAFs by truck class using the data above and Equation 2.4

The procedure described above accommodates WIM traffic datasets with some missing data days. For the WIM sites that have the largest number of missing days, (i.e., 299 days of WIM data per year or more), additional assumptions had to be made.

- Where entire months of data are missing, data is assumed to have values equal to the average of the data for the months available
- Where entire DOW are missing for a particular month, data is assumed to have values equal to the average of the data for the available DOWs for the same month

3.2.2.2 Scenario 1-1: SS WIM Data for 1 Month / 4 Seasons

This scenario involves WIM data that covers 1 month in each of 4 seasons. It is simulated from the continuous WIM dataset of the 11 sites selected, and is carried out by computing all of the necessary traffic input to the 2002 PDG from random combinations of sets of 4 months, each from a different season (81 possible combinations). Only months with more than 25 days of data were considered for this analysis. The challenge in simulating this scenario is that the traffic volume by truck class is not known for all months of the year. All that is known for the site is the volume for four months of the year. The following describes the computations used in obtaining each of the five traffic data input components to the PDG.

MAFs

There are a number of alternative algorithms for computing traffic volumes and MAFs by vehicle classification for the months without data. The one used here utilizes R MAF values for the average of all truck classes to estimate SS MAF values by class for the missing months. This algorithm is explained in the following example, and is demonstrated in Table 3.2.

Consider daily traffic volumes (VOL) for a given truck class are available only for January, April, July and October, summing to a total volume of 4150 trucks of a particular class for these months. The average R MAFs for all truck classes are taken from the AVC cluster that the design site is associated with (see Clustering, Section 3.4).The sum of the four R MAF values associated with the SS VOL measurements is 3.94 (shown in bold). Since the sum of all MAFs in a year is always 12, the sum of the R MAF values for the 8 months without VOL data is 8.06 (= 12 - 3.94). Using a proportion, the total volume for the missing months is 8489 (= 4150 * 8.06 /

3.94). The same proportion allows estimation of the traffic volume for each of the missing months (e.g., VOL for February is computed as 8489 * 0.9 / 8.06 = 948). As a check, the estimated SS MAFs by class sum to 12.

Table 3.2: Example of Computing MAFs from R Data

Month	**Measured VOL by Class**	**R MAF for All Truck Classes**		**Estimated VOL by Class**	**Estimated SS MAF by Class**
January	900	**0.8**		-	**0.85**
February	-		0.9	948	0.90
March	-		1.09	1148	1.09
April	1100	**1.05**		-	**1.04**
May	-		1.12	1180	1.12
June	-		1.15	1211	1.15
July	1200	**1.1**		-	**1.14**
August	-		1	1053	1.00
September	-		1	1053	1.00
October	950	**0.99**		-	**0.90**
November	-		0.95	1001	0.95
December	-		0.85	895	0.85
	Σ = 4150	**Σ = 3.94**	Σ = 8.06	Σ = 8489	Σ = 12.00
				AADTT = 1053	

Use of R MAF values for the average of all truck classes from the AVC cluster is a compromise between using MAF values from each vehicle class within the cluster and using the statewide average MAF data for all truck classes.

AADTT, Truck Class and Axle Load Distribution

The algorithm used for obtaining AADTT, Truck Class Distribution and Axle Load Distribution is identical to that of Scenario 1-0.

Number of axles per truck

The number of axles by axle configuration and truck class are assumed to be constant, and equal to the statewide average for the site analyzed. This assumption is justified considering that the number of axles for the most common truck classes (i.e., class 5 and 9) is relatively constant. Figures 3.1 and 3.2 below show the number of single and tandem axles per vehicle, respectively, for the Washington State sites analyzed. It can be seen that the number of single and tandem axles for vehicle classes 5 and 9 varies insignificantly between sites. This is not the case for vehicle classes 7 and 11, but they account for less than 4% of the total truck volumes. Additionally, the number of axles per vehicle type is expressed by a 4 x 10 matrix, and would have had to be input manually for each run of the PDG. This would have increased the time necessary to run the PDG, as well increase the chance for user error by inputting erroneous values.

3.2.2.3 Scenario 1-2: SS WIM Data for 1 Week/Season

This Scenario is simulated in a fashion similar to that described under scenario 1-1. The difference is that only one week per season of WIM data is available. For each season, one week is selected at random, *excluding* those with a national holiday or those having incomplete data. This yielded a higher number of combinations to be simulated, (depending on data coverage, up to 20,736 combinations). The one week chosen is assumed to be representative of the entire month. The handling of the remaining elements of the PDG input was identical to that described under scenario 1-1.

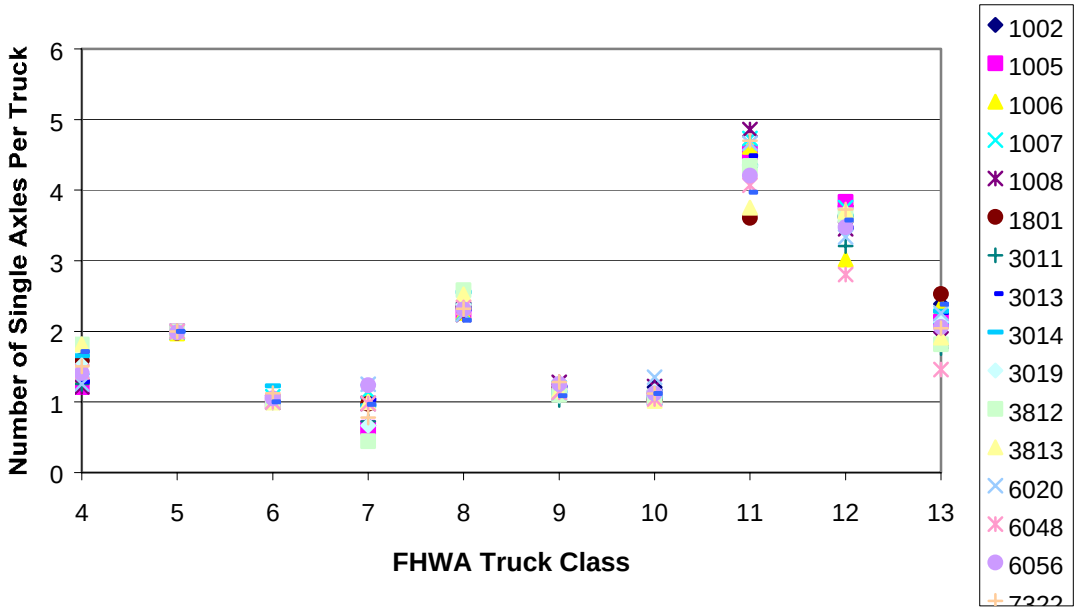

Figure 3.1: Single Axles Per Truck for All WA LTPP WIM Sites

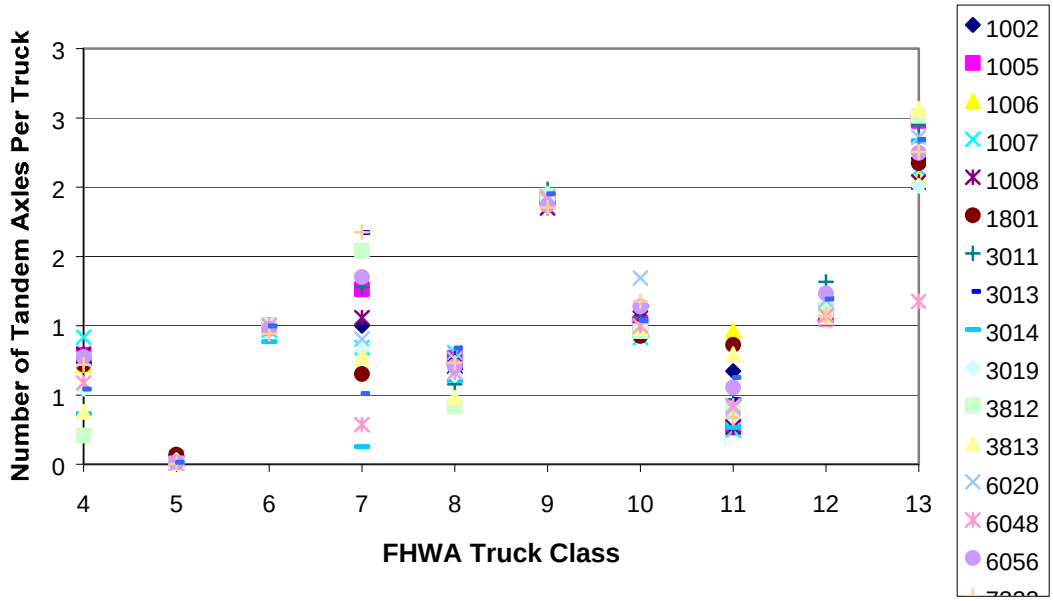

Figure 3.2: Single Axles Per Truck for All WA LTPP WIM Sites

3.2.2.4 Scenario 2-0: Continuous SS AVC Data and R WIM Data

The SS information from this scenario is the vehicle classification information. Therefore, all volume-related traffic input (AADTT, VCD, and MAFs) are obtained in an identical fashion to those of scenario 1-0. The number of axles per configuration and vehicle class is the statewide average for reasons explained earlier.

The load frequency distribution by axle configuration must be estimated from R WIM data. In doing so, it is assumed that although there is no SS WIM data, there is sufficient qualitative information regarding truck weights at the site to allow placement of the site into one of the axle load clusters within a particular state. As a result, normalized axle load distributions are obtained from the WIM data of the appropriate cluster, rather than from the statewide average.

3.2.2.5 Scenario 2-1: SS AVC Data for 1 Month/Season and R WIM Data

This scenario is simulated in a fashion similar to that of 1-1. The only difference is in computation of the normalized axle load distribution, which follows the method described in 2-0.

3.2.2.6 Scenario 2-2: SS AVC Data for 1 Week/Season and R WIM Data

This scenario is simulated in a fashion similar to that of 1-1. The only difference is in computation of the normalized axle load distribution, which follows the method described in 2-0.

3.2.2.7 Scenario 2-3: SS AVC Data for 1 Week/Year and R WIM Data

This scenario is simulated by assuming that the week of data available is representative of the month it belongs to. Weeks are selected at random, excluding those involving national holidays and those with incomplete data. MAFs are estimated in a fashion similar that described under

scenario 1-1 which uses R MAFs to fill data gaps. AADTT, VCD and NOAPT are calculated as per scenario 1-1. Axle load distributions are obtained from R WIM data as described under scenario 2-0.

3.2.2.8 Scenario 3-0: Continuous SS ATR Data, R AVC and R WIM Data

This scenario consists of continuous SS vehicle counts for an entire year, combined with R AVC and R WIM data. No site-specific vehicle classification or axle load information is available. It is assumed that there is enough qualitative information about the site to correctly assign it to both a state AVC cluster and a state WIM cluster. Also, the percent trucks at the site (total daily vehicles in FHWA classes 4 to 13 divided by AADT) is assumed equal to that of the AVC cluster for the site. This allows calculation of AADTT according to the method described under scenario 1-0.

MAFs are taken from the AVC cluster that the site belongs to. The number of axles by type and vehicle class is assumed equal to that of the state-wide average for reasons described under scenario 1-1. Axle load distributions by axle configuration and vehicle class are taken from the WIM cluster that the site belongs to.

3.2.2.9 Scenario 3-1: SS ATR Data for 1 Week/Season, R AVC and R WIM Data

This scenario is simulated in a fashion similar to that of scenario 3-0. The only difference is that vehicle volume data is known for only one month for each of four seasons. AADTT is computed as described under scenario 1-1. All other traffic data input are obtained in a similar fashion to scenario 3-0.

3.2.2.10 Scenario 4-0: Continuous SS ATR, R AVC and N WIM Data

The only difference between this scenario and 3-0 is that here the axle load information from the WIM cluster is replaced by the default, N average WIM data. All other traffic input are the same as scenario 3-0.

3.2.2.11 Scenario 4-1: SS ATR Data for 1 Week/Season, R AVC and N WIM Data

This scenario is simulated in a fashion similar to scenario 3-1. The only difference is that the axle load information from the WIM cluster is replaced by N WIM data.

3.2.2.12 Scenario 4-2: SS ATR Data for 1 Week/Year, R AVC and N WIM Data

This scenario is a variation of scenario 4-1, whereby only a single week of data is available for the entire year. Weeks are selected at random excluding those that contain national holidays or incomplete traffic data. This week is assumed to be representative of the entire month. As in scenario 3-0, R AVC cluster data is used to compute percent trucks, and average MAF values are used to obtain the traffic volumes by month and truck class. National, default WIM data are used for the normalized axle load distribution.

3.2.2.13 Scenario 4-3: SS ATR Data for 1Weekday+1Weekend/Year, R AVC and N WIM Data

This scenario involves ATR counts from one weekday and one weekend day in the same week. The weekday volume is assumed to represent all weekdays, and the weekend volume represents both weekend days. In other words, traffic volumes for weekdays and weekend days are multiplied by 5 and 2, respectively, to compute weekly traffic. All weeks that do not involve holidays or missing data were considered at random under this scenario. All traffic data input elements were computed as described under scenario 4-2.

3.2.2.14 Scenario 4-4 to 4-7: Various Coverage SS ATR Data, N AVC and N WIM Data

Scenarios 4-4, 4-5, 4-6, and 4-7 are almost identical to scenarios 4-0, 4-1, 4-2 and 4-3, respectively. The difference is in the data source alone. Besides traffic volume, all other traffic data input are N. The default vehicle classification distribution for a Truck Traffic Classification (TTC) type 1 was arbitrarily selected. TTC 1 is described as a major, single-trailer truck route (predominantly class 9 trucks). The default MAF values are 1.00 for all months and vehicle classes. All traffic volume computations were described previously.

3.2.2.15 Scenario Source Data Summary

The discussion above documents in detail the methods and assumptions used to obtain each of the five traffic data input elements of the PDG for each of the 17 traffic data collection scenarios. Table 3.3 summarizes the data sources used to compute each traffic data input element. Table 3.4 shows the number of possible combinations for each scenario.

Table 3.3: Summary of Traffic Data Input Source to the PDG

	PDG Input					
Scenario	**AADT**	**% Trucks**	**VCD**	**MAFs**	**NOAPT**	**NALDFs**
1-0	SS	SS	SS	SS	SS	SS
1-1	SS	SS	SS	AVC cluster	State	SS
1-2	SS	SS	SS	AVC cluster	State	SS
2-0	SS	SS	SS	SS	State	WIM cluster
2-1	SS	SS	SS	AVC cluster	State	WIM cluster
2-2	SS	SS	SS	AVC cluster	State	WIM cluster
2-3	SS	SS	SS	AVC cluster	State	WIM cluster
3-0	SS	AVC cluster	AVC cluster	AVC cluster	State	WIM cluster
3-1	SS	AVC cluster	AVC cluster	AVC cluster	State	WIM cluster
4-0	SS	AVC cluster	AVC cluster	AVC cluster	State	National
4-1	SS	AVC cluster	AVC cluster	AVC cluster	State	National
4-2	SS	AVC cluster	AVC cluster	AVC cluster	State	National
4-3	SS	AVC cluster	AVC cluster	AVC cluster	State	National
4-4	SS	National	National	National	National	National
4-5	SS	National	National	National	National	National
4-6	SS	National	National	National	National	National
4-7	SS	National	National	National	National	National

Table 3.4: Possible Combinations per Scenario

Scenario	Combinations per Scenario
1-0	1
1-1	81
1-2	20,736
2-0	1
2-1	81
2-2	20,736
2-3	48
3-0	1
3-1	81
4-0	1
4-1	20,736
4-2	48
4-3	480
4-4	1
4-5	20,736
4-6	48
4-7	480

3.3 Data Source and Pavement Site Selection

Continuous traffic data with daily resolution is required in order to simulate short-term traffic sampling scenarios. This data was obtained from the LTPP database [11]. Since the finest resolution necessary to simulate the scenarios described earlier is one day, daily traffic summaries was taken from Central Traffic Database (CTDB).

The first search of the LTPP database for sites with continuous data (WIM > 359 days per year) revealed 58 potential candidates. Some of these have multiple data years that met this continuous criterion. Figure 3.3 shows the total number of sites that meet this criterion versus the number of years of data coverage. Multiple data years are advantageous because they allow the calculation of SS traffic growth rates. This was not done as part of this thesis, but was a

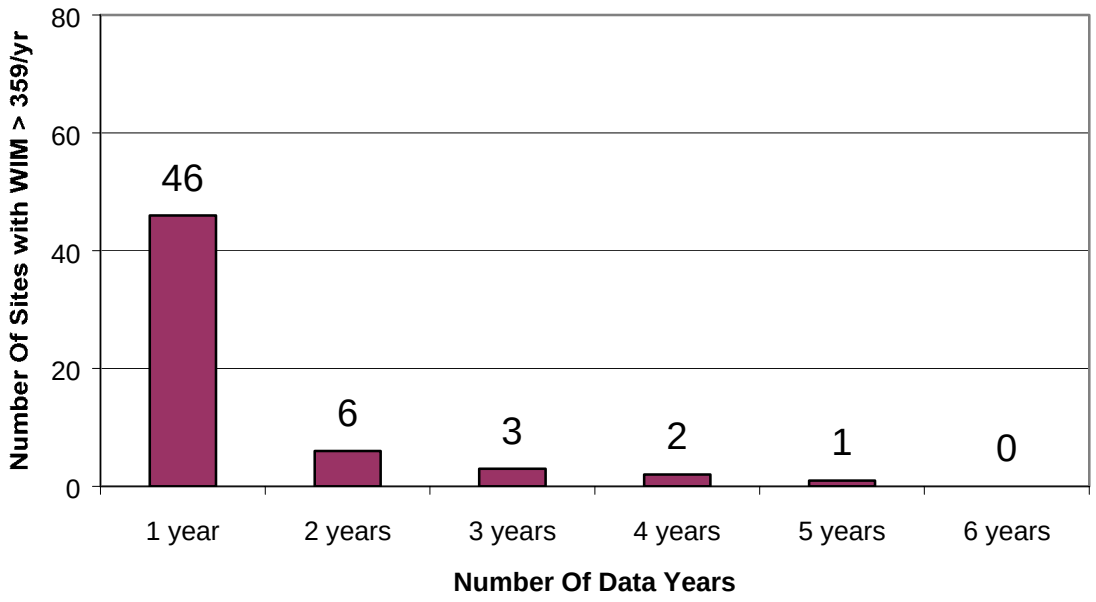

Figure 3.3: LTPP Sites With WIM Data For Periods Exceeding 359 Days Per Year

requirement for the parent study being performed (FHWA contract DTFH61-02-D-00139). Therefore the multiple-year criterion is used. Figure 3.3 shows that only 12 sites meet these criteria. Further analysis of the Technical Support Services Contractor (TSSC) reports revealed problems with the traffic data of 4 of these sites.

In order to increase the number of sites available for analysis, another search of the LTPP database was performed by relaxing the continuous criterion of data availability to WIM data > 299 days per year. The results of this search are shown in Figure 3.4. This change of the continuous criterion increased the number of sites available for study to 96 (i.e., sum of all multiple-year values in Figure 3.4). This is sufficient to perform the analysis, and will provide ample regional traffic data. Therefore, the LTPP sites chosen for study are based upon multiple

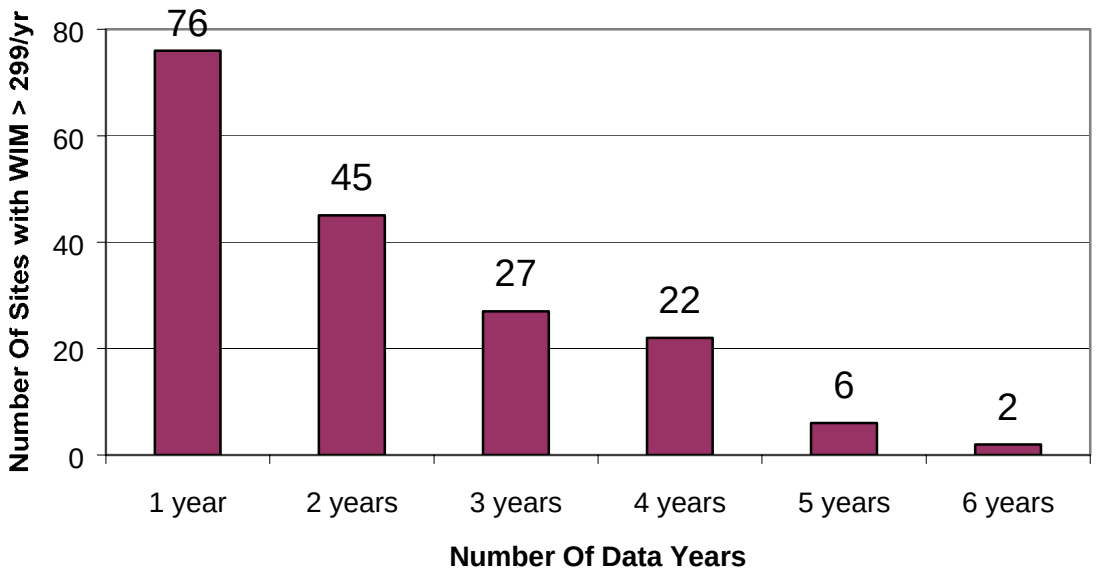

Figure 3.4: LTPP Sites With WIM Data For Periods Exceeding 299 Days Per Year

data years with WIM coverage in excess of 299 days per year. A number of these 96 sites were chosen for detailed pavement performance estimation using the 2002 PDG. They were selected to represent a range in both AADTT and structural configuration. The remainder of these sites was used to generate R traffic data essential in simulating the traffic data collection scenarios. The sites chosen included 5 flexible and 6 rigid pavements, as listed in Tables 3.5 and 3.6, respectively. These sites showed no problems as per the TSSC reports. The CTDB was further mined for detailed structural data for all 96 sites. Layer thicknesses for the 11 sites are shown in Table 3.7. The layout of the flexible sites is given in Figure 3.5. Subgrade moduli for these sites were assumed as a function of the SS Unified Soil Classification System (USCS) designation, (Table 3.8). The moduli of the pavement layers were defined by specifying binder, aggregate and Portland cement characteristics, assumed constant between sites. This information is detailed in Appendix D. It should be noted that although the material characteristics are the same between

sites, the environmental conditions specified in the pavement performance analyses, were those specific to each site, (i.e., as defined by the longitude and latitude and the corresponding climatic database information built into the PDG). This approach minimized non-traffic-related input variation in the PDG, while maintaining realistic design circumstances at each site.

Table 3.5: Flexible LTPP Sites Selected

Site ID	28_2807	26_1010	53_1007	18_1028	53_6048
State	MS	MI	WA	IN	WA
Data Cover (days)	> 359	> 359	> 359	> 299	> 359
Data Years	1995, **96**	1994, 95, **98**	1993, 94, **95**	1997, **98**	**1994**
Route No.	6	57	221	27	522
Functional Class*	2	6	2	6	2
Veh. Class	**Normalized Vehicle Class Distributions (percent)**				
4	3	2	0	2	1
5	19	76	10	13	45
6	6	4	4	9	12
7	0	1	1	3	1
8	11	5	3	11	7
9	59	6	47	53	20
10	1	2	8	4	7
11	0	0	4	2	0
12	0	0	6	2	1
13	0	4	18	0	7

* defined in Table 3.9, boldface indicates year chosen for analysis

Table 3.6: Rigid LTPP Sites Selected

Site ID	28_4024	50_1682	27_5076	9_4008	27_4055	18_5518
State	MS	VT	MN	CT	MN	IN
Data Cover (days)	>359	>359	>299	> 359	>299	>359
Data Years	**1995**	1992, 94, 95, **97**	**1997**	**1994**	**1994**, 97	**1997**
Route No.	1	7	694	84	94	65
Functional Class*	11	1	1	11	14	2
Configuration	Doweled JPCC	JPCC	CRC	Doweled JPCC	Doweled JPCC	CRC
Veh. Class	**Normalized Vehicle Class Distributions (percent)**					
4	29	3	1	1	2	1
5	28	30	18	20	18	22
6	8	7	8	4	3	2
7	0	1	7	2	0	2
8	8	10	4	10	4	4
9	24	47	55	55	68	59
10	1	2	3	1	2	1
11	2	0	2	7	3	4
12	0	1	1	0	0	1
13	0	0	0	0	0	2

* defined in Table 3.9, boldface indicates year chosen for analysis

Table 3.7: Layer Types and Thicknesses for All Sites

Site	**Layer 1 (Surface)**	**h_1 (in)**	**Layer 2 (USCS)**	**h_2 (in)**	**Layer 3 (USCS)**	**h_3 (in)**	**Layer 4 (USCS)**	**h_4 (in)**
18_1028	**ACP**	15.8	CL	12.0	CL	∞		
26_1010	**ACP**	2.3	GW	11.0	SW	20.0	ML	∞
28_2807	**ACP**	10.5	GW	30.0	ML	∞		
53_1007	**ACP**	1.8	GW	13.2	MH	∞		
53_6048	**ACP**	6.0	GW	3.4	GW	10.0	GW	∞
18_5518	**CRCP**	9.0	GW	6.0	ML	∞		
27_5076	**CRCP**	9.0	GW	6.0	SM	∞		
9_4008	**JCP**	9.0	GW	18.0	SW	∞		
27_4055	**JCP**	8.9	GW	2.3	SW	∞		
28_4024	**JCP**	8.0	ACP	4.0	GW	6.0	CL	∞
50_1682	**JCP**	8.0	GW	10.0	SW	20.0	GW	∞

Table 3.8: Assumed Layer Moduli

Layer Type (USCS)	Layer Description	Modulus (ksi)
GW	Gravel	100
SW	Sand	40
SM	Silty Sand	20
CL	Silty Clay	20
ML	Clayey Silt	20
MH	Silt	20

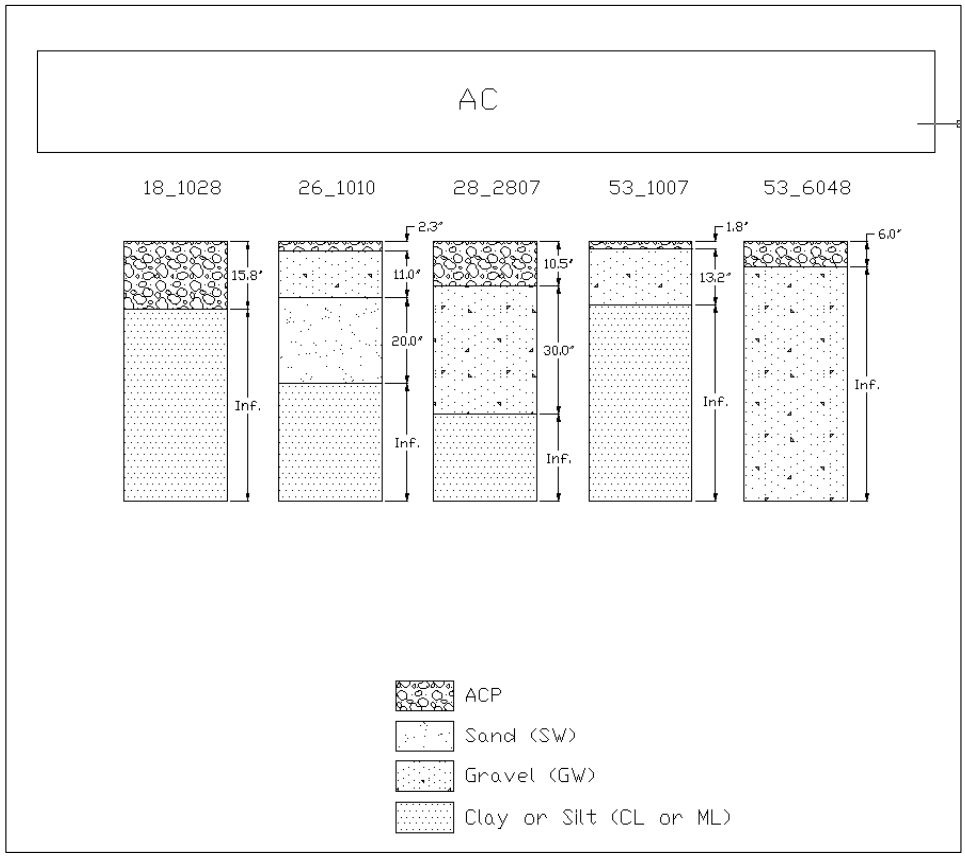

Figure 3.5: Flexible Pavement Sections Studied

3.4 Clustering

Where N traffic data is required, the default traffic values of the 2002 PDG are used. For R traffic data, the grouping of traffic data collection sites for the purpose of establishing representative traffic data can be done according to three criteria. These are roadway functional classification (Table 3.9, from LTPP [10]), truck classification distribution (the percentage of each of the FHWA classes 4 to 13), and pavement loading.

The grouping of sites according to roadway functional class is largely subjective. R data generated using functional class showed large internal variation for both vehicle classification distribution and tandem axle loading. Consequently sites are grouped according to truck classification distribution and pavement loading.

The annual average axle load spectra for a site consists of load spectra (40 load bins) for all axle configurations (4 axles). Grouping sites based upon 160 values (40 * 4) would be complex and time consuming.

Study of the traffic data files reveals that class 9 trucks are the most common heavy truck on most roads. This implies that tandem axles are the most populous heavy truck axle configuration. Therefore, tandem axle load distribution is the axle configuration most indicative of pavement loading, and is used in this study to cluster WIM data.

Presented in the 2001 TMG as the preferred method for identifying similarities in traffic volume seasonality ([18] appendix 2-b), clustering is used here as a means of quantifying the similarity of LTPP sites based upon both annual vehicle classification distributions (AVC) and annual normalized tandem axle load distributions (WIM data). An example of how this was done is given below with Washington State's LTPP tandem axle load data.

Table 3.9: Identification Codes for Roadway Functional Classes

ID	Roadway Functional Class
1	Rural Principal Arterial – Interstate
2	Rural Principal Arterial – Other
6	Rural Minor Arterial
7	Rural Major Collector
8	Rural Minor Collector
9	Rural Local Collector
11	Urban Principal Arterial – Interstate
12	Urban Principal Arterial - Other Freeways or Expressways
14	Urban Other Principal Arterial
16	Urban Minor Arterial
17	Urban Collector
19	Urban Local

Clustering is a mathematical method for identifying groups of objects based upon similarities between their attributes [14]. For this example (regional data formation), objects are the LTPP WIM sites in Washington State that meet the criteria (WIM coverage and data quality), and attributes are the tandem axle load values in the load bins of the normalized distribution. Since there are 40 load bin values, each object has 40 attributes to be compared. Attribute values do not need to be standardized because all values share the same limits (0 and 1). The total number of LTPP continuous WIM sites nationwide can be seen in Figure 3.6.

The Euclidean Distance *e* is defined as the distance between two points *i* and *j*, and is expressed by the following in two-dimensional space:

$$e_{ij} = \sqrt{\left(x_i - x_j\right)^2 + \left(y_i - y_j\right)^2} \tag{3.1}$$

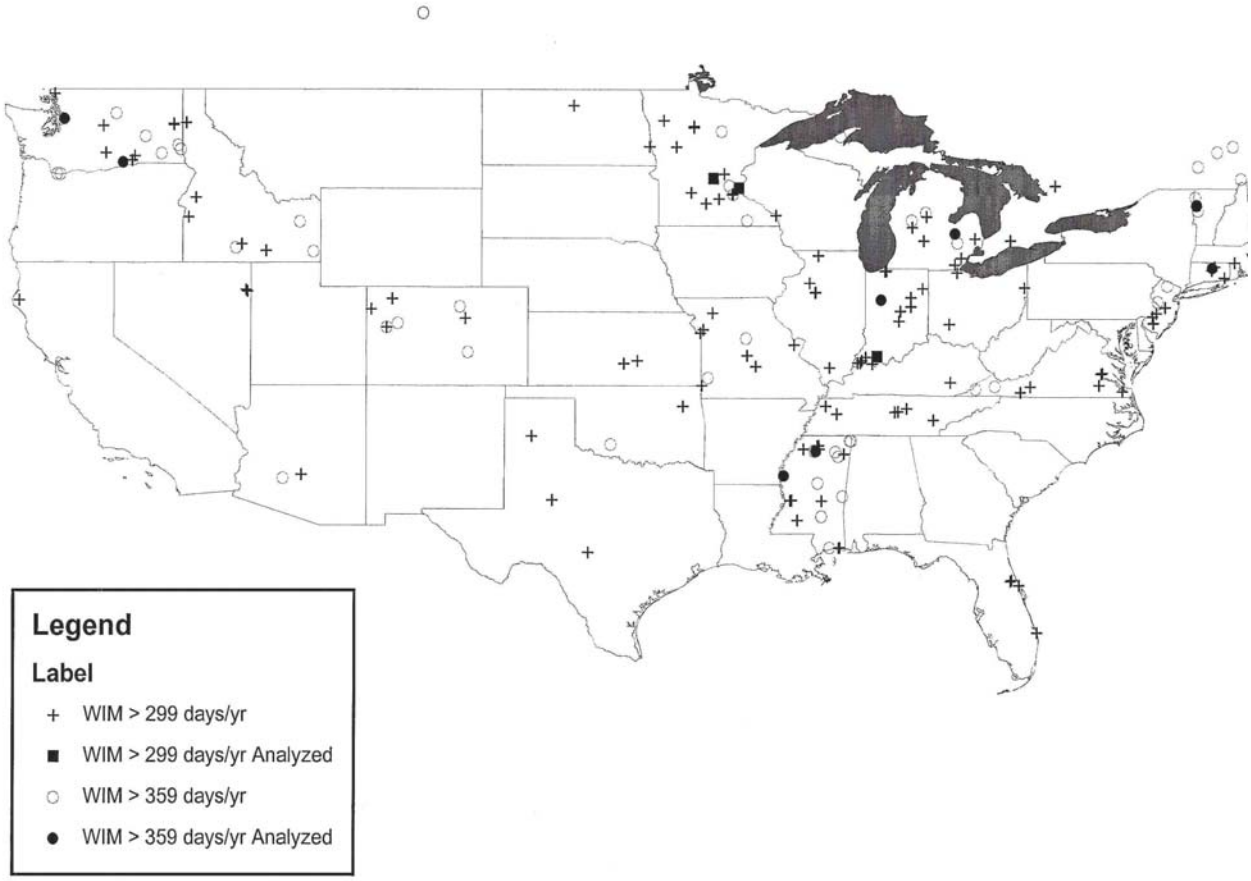

Figure 3.6: USA WIM Systems, WIM > 299 Days Per Year

If each dimension represents a property, or attribute of the points plotted, then this distance represents the similarity between the two points, or objects *i* and *j* with respect to their attributes *x* and *y*. The greater the distance e_{ij}, the greater the total dissimilarity between the two objects based on all attributes. It is for this reason that e_{ij} is referred to as the dissimilarity coefficient in clustering.

Ward's Minimum Variance is the chosen clustering algorithm. For a detailed explanation of this method see the text by Romesburg 1984 [14]. This method uses the square of the Euclidean Distance. At each iteration, the squares of the distances between each point within the potential

cluster and the cluster mean are computed, totaled for each cluster, and added for all clusters. The cluster scheme with the lowest total variance is chosen. This provides fast computation and reliable results [14].

The total variance for all clusters is measured as *E*. A *clustering tree* is then constructed based upon *E*, and pairs of objects are sequentially grouped together and compared with the remaining objects in order of increasing *E*. The clustering tree for the example presented is shown graphically in Figure 3.7. Clustering calculations were performed using an add-on function to *Excel*® found in the *StatistiXL*® library [16].

The only qualitative aspect to clustering is the acceptable amount of dissimilarity between objects within a cluster. In this study no limits were predefined. Instead, clusters were simply compared to one another. If sites share a trend, they belong to the same cluster. If not, they were assigned to another cluster.

For example, in Figure 3.7, site 7409 is at the top of the tree's vertical axis. The normalized annual average tandem axle load for this site is plotted along with that of site 3812. The dissimilarity (measured by the x-axis in Figure 3.7) is very low since these spectra are almost identical. The trend observed is that neither heavy nor light axles dominate (Figure 3.8). Therefore, they remain clustered.

The spectra from sites in the next sub-cluster (sites 6048, 3813 and 3011) are then added to the plot. The new data has approximately the same trend even though dissimilarity for the entire cluster has increased. The spectra for sites 1006, 1002 and 3014 are also added. Their contribution increases total cluster dissimilarity as well, but the original trend is maintained.

Finally, the tandem axle load spectra from the next sub-cluster (consisting of sites 3019 and 1005) are added to the plot. It is obvious that these two spectra have peaks to the right,

representing a dominance of heavy tandem axles (Figure 3.9). These spectra therefore belong in a different cluster, making the limit of acceptable dissimilarity equal to 0.059. Again, this is the square of the distances between objects within the cluster and the cluster mean.

Figure 3.7 identifies three WIM clusters for the state of Washington (thickly-lined boxes), each with similar annual tandem axle load distributions using a dissimilarity limit of 0.06. Figures 3.8 and 3.9 show the frequency distributions of tandem axle loads for two of the three clusters in WA, and illustrate the distinct differences between their respective loading patterns. The first cluster contains the design site 6048, and reflects the dominance of lighter tandem axles; the second, contains design site 1007, and represents heavier tandem axles.

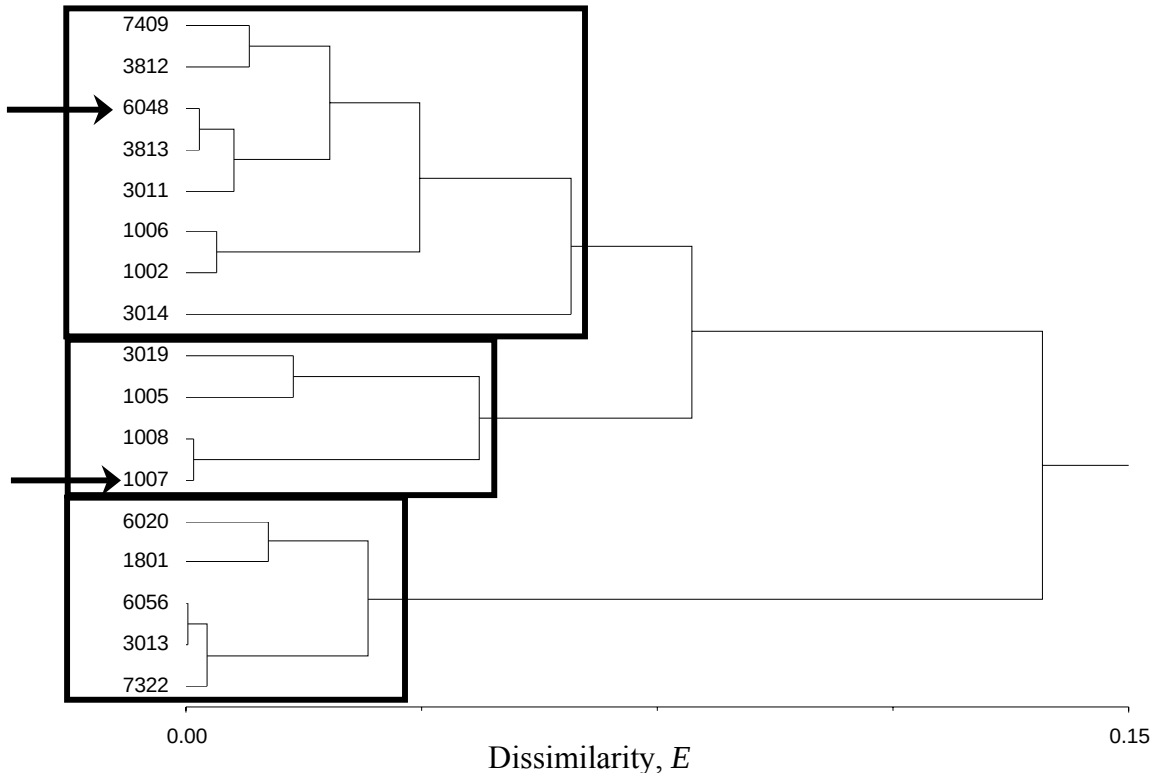

Figure 3.7: Clustering Tree; Annual Distributions of Tandem Axle Loads, WA

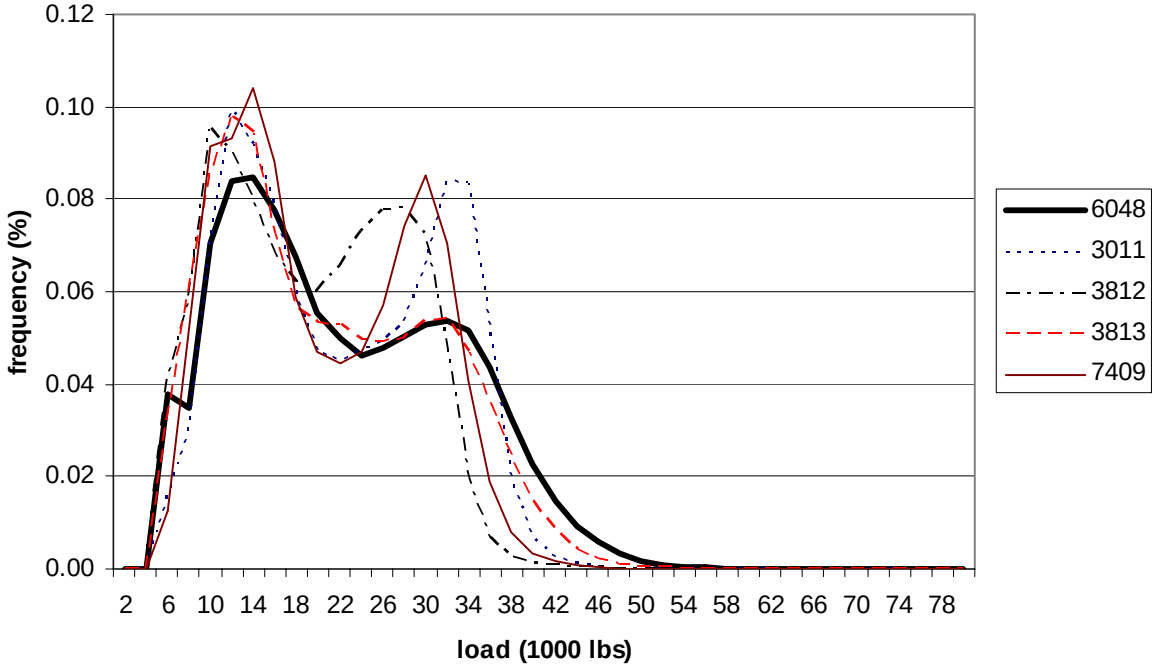

Figure 3.8: Tandem Axle Load Distributions for WA site 6048 Cluster

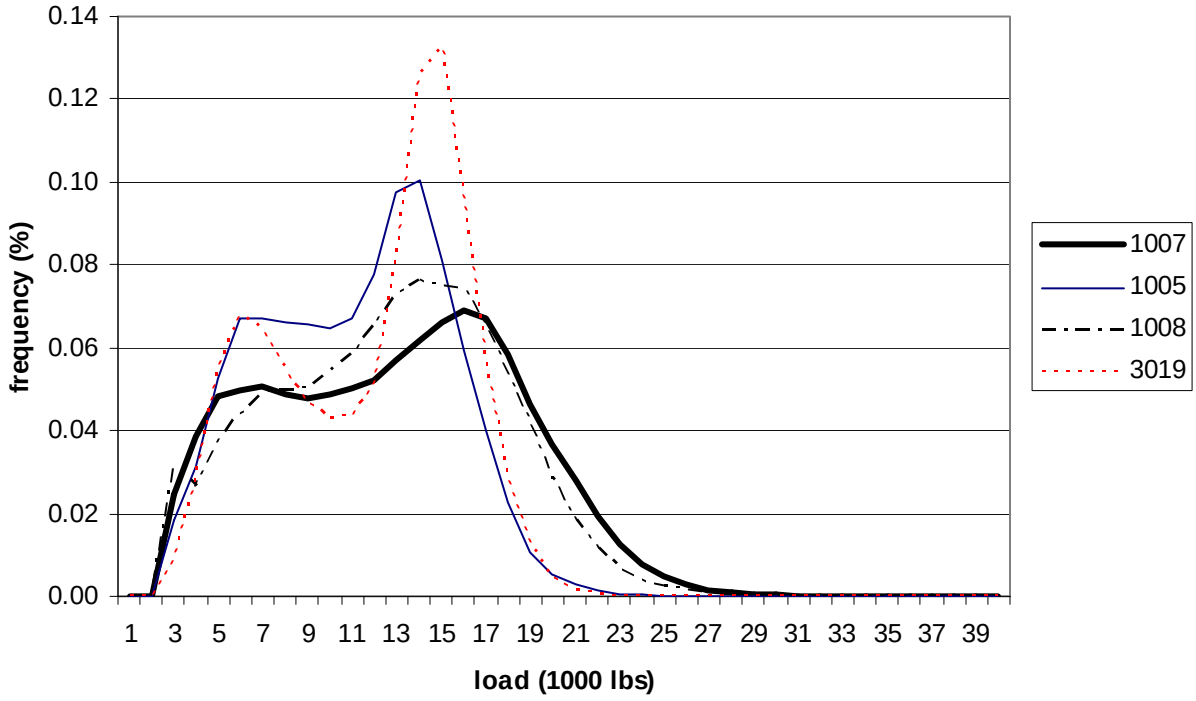

Figure 3.9: Tandem Axle Load Distributions for WA site 1007 Cluster

The analysis presented above is based on annual average data. The temporal stability of a site is examined here to test the validity of the use of average annual axle load distributions. Figure 3.10 shows the average monthly tandem axle load distributions for site 3019 over the course of a year's time. The heavy-axle trend is constant throughout the year. This consistency of trend is common for other sites analyzed. The cluster averages result in even less monthly variation over the course of a year, but that is the cosmetic effect of averaging several sites per month. Based upon the relatively small monthly variation in axle loading and vehicle distribution, R data generated from the clustering of annual traffic data alone is sufficiently representative of monthly traffic patterns as well. Annual average axle load spectra for the 11 sites analyzed are listed in Appendix C.

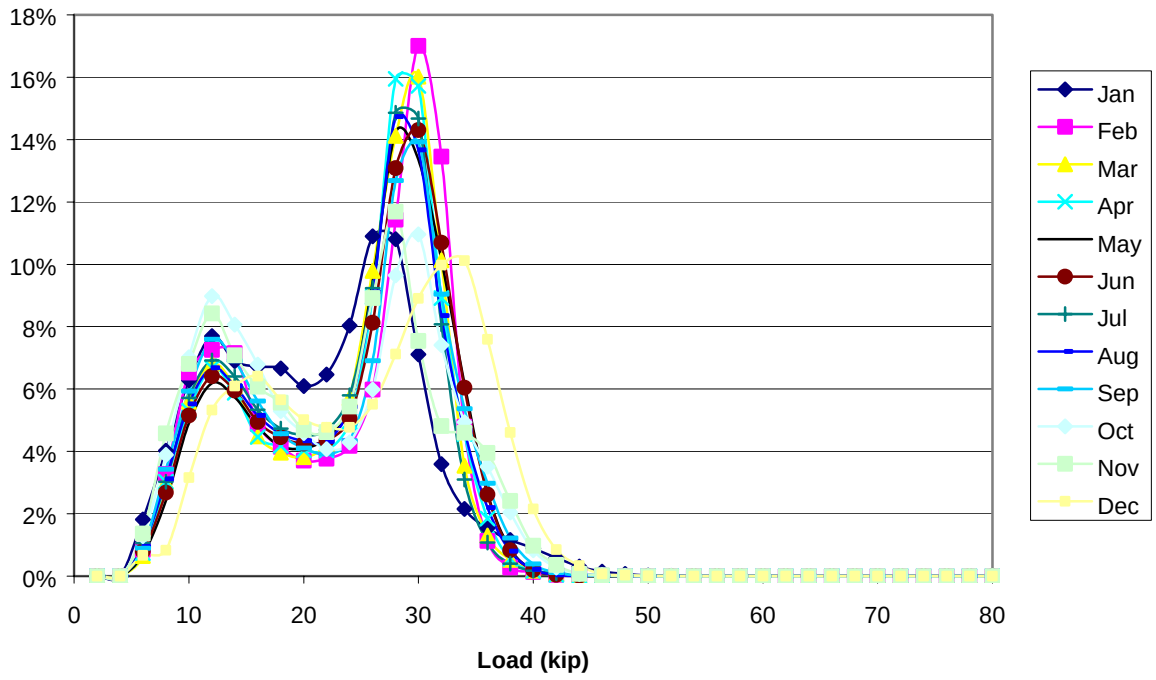

Figure 3.10: Site 3019 Monthly Average Tandem Axle Loads

For each site studied, all LTPP WIM sites (except the one being designed) within the same state are clustered. Two or three clusters for each state are then generated for both tandem axle load spectra and annual average vehicle classification data. Finally, the daily traffic values for each site within a cluster are averaged together with all of the other sites from the same cluster. This produces the R data required for the study at hand.

The partitioning of nationwide data into states simulates the common practice of DOTs from each state working primarily within their own databases. However, clustering can be performed with data from any dataset so long as the vehicles traveling within the jurisdiction abide by the same rules governing gross vehicle weight and axle configuration. The resulting cluster assignments by state are shown in tables 3.10 and 3.11 below. All clusters used in this study are presented in Appendix B.

Table 3.10: WIM Cluster Analysis Results

State	**Cluster**	**LTPP Sites within each WIM Cluster** (based upon annual average tandem axle load)													
9	1	4008	1803	4020	5001										
18	1	1028	2009	3030	3031	4042	5022	5043	5518	9020					
	2	6012	1037	2008											
	3	5538	5528												
26	1	1010	1001	1004	1004	1012	1013	3069	4015	5363	7072	9029	9030		
27	1	4055	1023	1028	4054	5076									
	2	6251	4050	4040	4037	4033	1019	1016	9075	1085	7090	1087	3003		
	3	3013													
28	1	2807	1001	1016	1802	3018	3019	3083	3085	3087	3089	3090	3091	4024	5025
	2	9030	3099	3094	3093	5805	5006	3081	7012						
50	1	1682	1002	1004	1681	1683									
53	1	1007	1005	1008	3019										
	2	6020	1801	6056	3013	7322									
	3	6048	1002	1006	3011	3014	3812	3813	7409						

Table 3.11: AVC Cluster Analysis Results

State	Cluster	LTPP Sites within each WIM Cluster (based upon annual average tandem axle load)													
9	1	4008	5001												
	2	4020													
	3	1803													
18	1	1028	5518	6012	9020										
	2	4042	3031	2008	1037										
	3	5538	5528	2009	5022	5043	3030								
26	1	1010	1001	1004											
	2	9030	9029	5363											
	3	7072	4015	3069	1012	1013									
27	1	4055	1023	1028	1085	3003	4033	4040	4054	5076	6251	7090	9075		
	2	3013	1087												
	3	4037	1019	1016	4050										
28	1	2807	1001	1016	3087	3089	4024	5025							
	2	5006	3081	9030	7012	3094	3093	3019	3018	3099	5805	3091	1802		
	3	3085	3083	3090											
50	1	1682	1002	1681	1683										
	2	1004													
53	1	1007	10005	1801	3014	3019	7409								
	2	7322	6056	3013	3813	3011	1002								
	3	6048	1006	1008	3812	6020									

3.5 Establishing Range in PDG Input

For each site and scenario, all possible combinations are used to compute the PDG traffic input. Mean and standard deviation are then computed for each of the traffic input, and confidence intervals for those input are generated.

For large populations it is reasonable to assume a normal distribution. The populations in this experiment are statistically large ($n > 48$). Therefore, properties of a normal distribution are assumed, such that a confidence interval for reliability level 100(1-α)%, or CI_α, can be expressed as:

$$CI_\alpha = \mu \pm Z_{\alpha/2} \cdot SD \tag{3.2}$$

where:

CI_α = confidence interval for reliability 100(1-α)%

μ = population mean

$Z_{\alpha/2}$ = standard normal deviate for reliability 100(1-α)% (where $0 < \alpha < 1$)

SD = population standard deviation

In practical terms, the value of a traffic statistic will fall within the confidence interval CI_α 100(1-α)% of the time. Table 3.12 lists the standard normal deviates for the reliability levels being studied.

If traffic is underestimated, pavement life will be overestimated, and the design will be made weaker by decreasing the layer thicknesses. Inversely, if traffic is overestimated, pavement life will be underestimated, and the design will be strengthened by increasing layer thicknesses. Clearly, the former is less conservative, and therefore controls the design situation. This underestimation of traffic is represented by the lower boundary of the confidence interval for all traffic input, identified here as CI_{lower}. Hence, performing a PDG analysis using all input at their CI_{lower} gives the highest life estimate, referred to as T_f in years. T_f estimates for the various scenarios are compared to the pavement life resulting from scenario 1-0 (i.e., TRUTH).

Table 3.12: Standard Normal Deviate for Two-Sided Test

Probability of Survival/Failure	**Standard Normal Deviate $Z_{a/2}$**
50/50	0.00
75/25	1.15
85/15	1.44
95/5	1.96
99.9/0.1	3.18

3.6 Traffic Input Data Creation

The extraction of axle load data from the CTDB was straightforward. Extracting vehicle classification information from the CTDB was more complex. The CTDB contains two types of classification files, namely *class_weight* and *class*_class. Both files contain vehicle counts by vehicle class using the FHWA classification scheme. However, analysis of these files reveals a significant difference between them. The data file *class_weight* omits most counts for vehicle classes 1, 2, and 3 (motorcycles, passenger cars, and four-tire, single-unit vehicles, respectively). On the other hand, the data file *class_class* contains data for the three light vehicle classes. Therefore, the percent trucks is calculated using the vehicle classification file *class_class*. All other traffic input use *class_weight*.

Daily traffic summaries are extremely large database files. Determination of traffic data mean and standard deviation is required for all traffic input. To simplify this task, a macro was written in *Visual Basic* ™ by Jingjuan Li that computes the traffic mean and standard deviation for all traffic input (see Table 2.3) for all possible combinations of a scenario within a year (see Table 3.4). For example, if a database file contains traffic data for a full year, the macro computes the mean and standard deviation for each of the five PDG traffic input components for every possible sampling combination. These statistics are then entered into Equation 3.2 using a spreadsheet to arrive at the PDG input files for all reliabilities. All other non-traffic input (i.e., climatic, structural and general) are listed in Appendices D and E.

3.7 Predict Pavement Life Using the 2002 PDG

With input files generated, pavements are analyzed using the PDG. Pavement performance is computed using the damage models incorporated into the June 2004 release (Appendix A). However, some pavements did not fail within the chosen 20 year analysis. In some cases, performance perditions to failure had to be extrapolated beyond the 20-year analysis period. A linear extrapolation method was used. This was justified since no tertiary damage is accounted for in the damage model used, causing linear trends in distress progression towards the end of the 20-year analysis period. An example of this is shown in Figure 3.11. Assumed failure criteria are listed in Table 3.13.

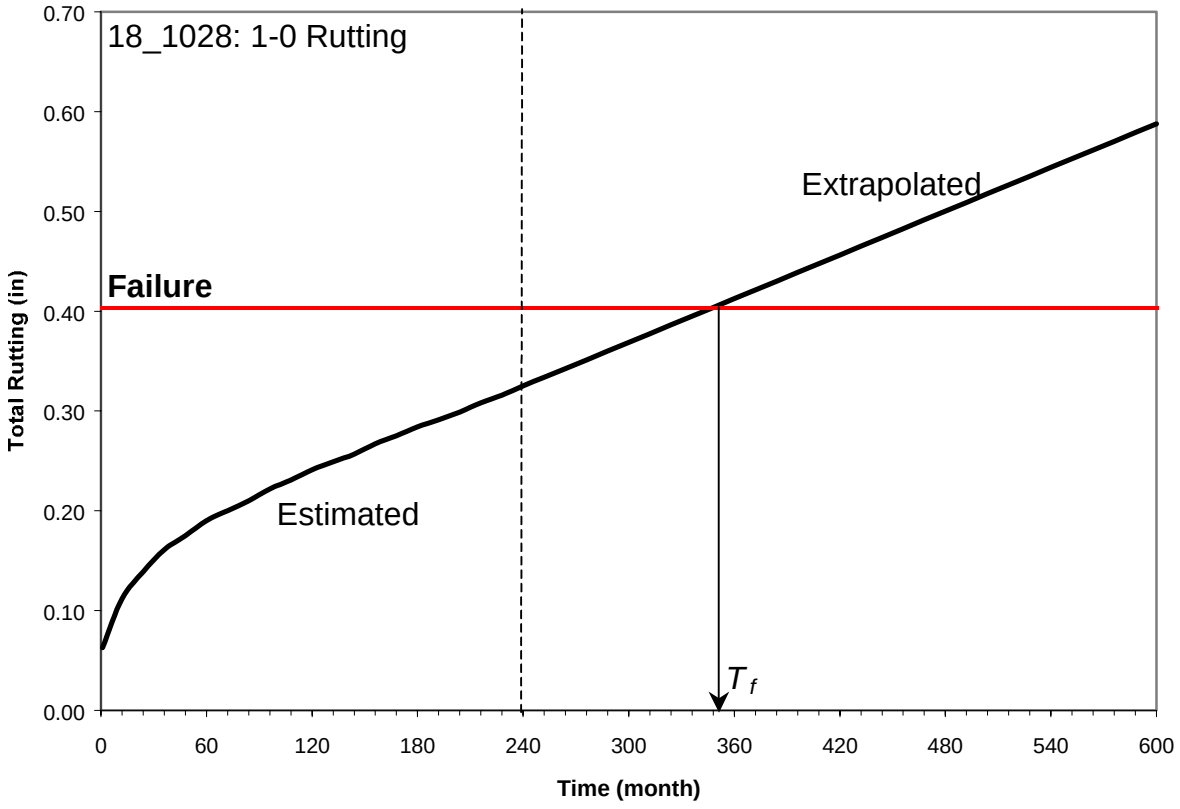

Figure 3.11: Performance Extrapolation Beyond 20 Years

Table 3.13: Failure Criteria for Each Pavement Type

Pavement Type	Failure Mode	Limit
AC	Rutting	0.40 inches (or 10 mm)
AC	Longitudinal Cracking	20% (or 1028 feet per mile)
JPCC	Slabs Cracked	50% of total slabs
CRC	Punchouts	30 per mile

CHAPTER FOUR

RESULTS

The PDG considers several distress prediction models for each pavement type. In this analysis the distress that first reaches its failure criterion defines failure for the pavement section, and hence the time to failure, or T_f. The failure mode for each flexible pavement site is listed in Table 4.1. It can be seen that site 53_1007 (Washington site with 2 inches of AC) failed prematurely, exhibiting total rut depths in excess of 0.4 inches (10.2 mm) within the first two years. Therefore, the performance results of this site are not used for further analysis.

Table 4.1: Failure Mode for Flexible Sites

Type	Site	Failure Mode
AC	18_1028	Rut > 0.4 inch
AC	28_2807	Crack >20% area
AC	26_1010	Rut > 0.4 inch
AC	**53_1007**	**Premature failure**
AC	53_6048	Rut > 0.4 inch

Failure modes for the rigid pavements analyzed are listed in Table 4.2. Two of these sites, 27_4055 and 28_4024, experienced no distress for the 20-year period, and are therefore not considered further. This lack of damage is most likely due to the small amount of traffic experienced at these two rigid pavement sites.

A total of 520 PDG analyses were performed in order to predict pavement performance for the eight remaining sites and all 17 sampling scenarios. As seen in Figure 3.11, the result of interest produced by a PDG analysis is the time to failure of a pavement site (T_f) for each sampling scenario and reliability level. These results are displayed in two formats. The first is in

Table 4.2: Failure Mode for Rigid Sites

Type	Site	Failure Mode
CRC	18_5518	Punchouts > 30/mile
CRC	27_5076	Punchouts > 30/mile
JPCC	9_4008	Slab Cracking > 50% slabs
JPCC	**27_4055**	**No distresses**
JPCC	**28_4024**	**No distresses**
JPCC	50_1682	Slab Cracking > 50% slabs

absolute terms (i.e., years). The second is in relative terms, expressed as the percent difference in life for a particular scenario and the life from the TRUTH.

The first type of graph gives, for each scenario, the mean and the range in life predictions for a given reliability level. Examples of this type of graph are shown for site 26_1010 in Figures 4.2 to 4.6. These graphs contain the TRUTH (dotted, horizontal line representing the life prediction using continuous WIM data for the site), the sampling scenario mean (circle), and the variation in life (vertical thick black line) for reliability 100(1-α)%. The large numbers in boldface at the top are the PDG TILs. These plots are given for each site and reliability level in Appendix F.

To explain interpretation of these year plots, Figure 4.1 represents a magnified set of results for a scenario. A is the difference between the life prediction using the TRUTH (scenario 1-0) and life prediction using the mean traffic inputs for a particular scenario. B is the difference between the life prediction using the critical traffic inputs, $CI_{\alpha\, lower}$, and the scenario mean for a particular scenario. A could be above or below TRUTH depending on the relationship between the traffic properties at a particular site and those of the R or N traffic data. To be conservative, the absolute value of A is added to the value of B. The difference between this statistic and life prediction from TRUTH gives the maximum possible overestimation of pavement life for a particular scenario.

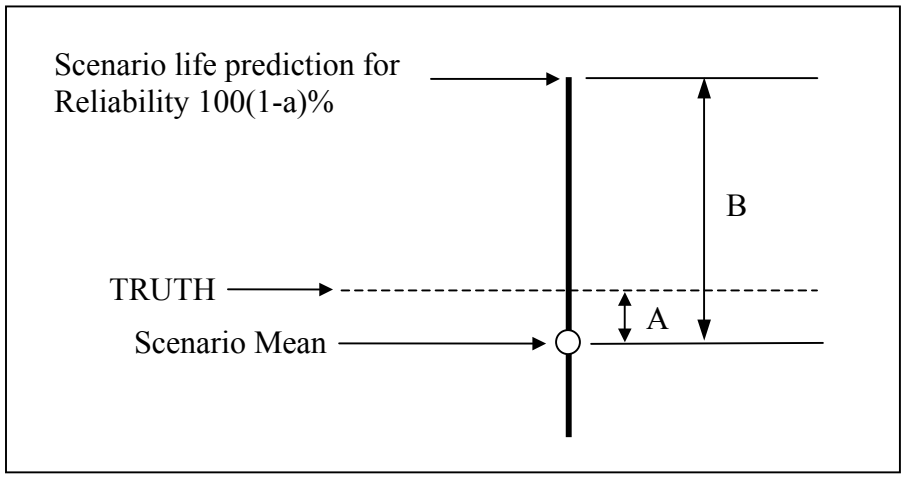

Figure 4.1: Example of a Life Plot and Maximum Life Variation

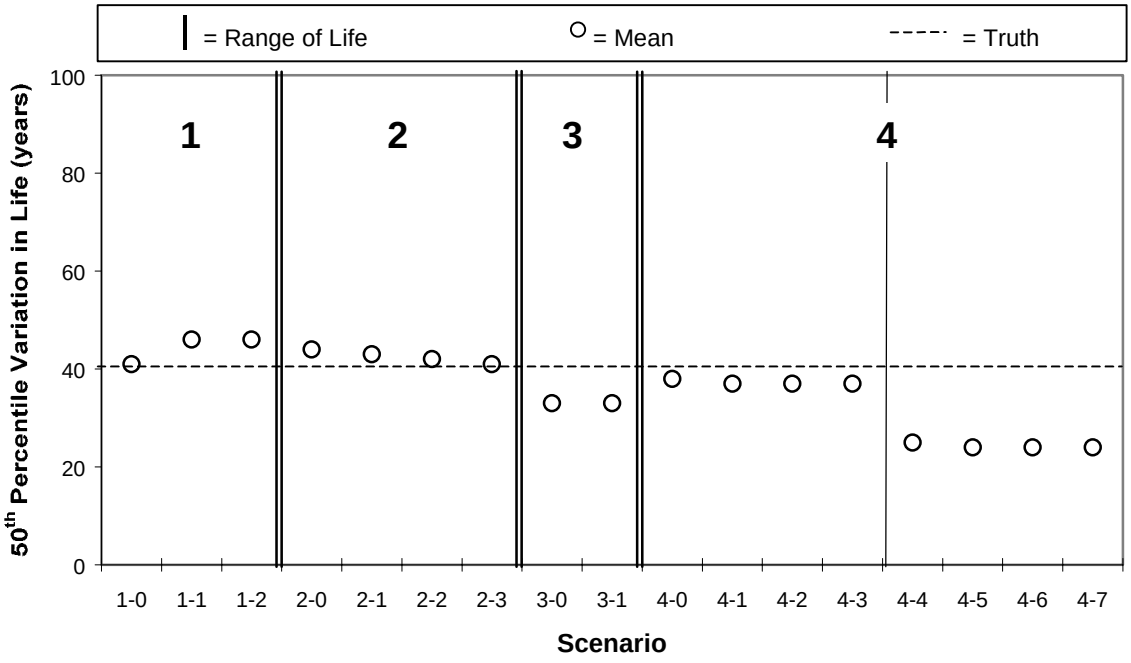

Figure 4.2: Flexible Site 26_1010, 50th Percentile, Range in Life

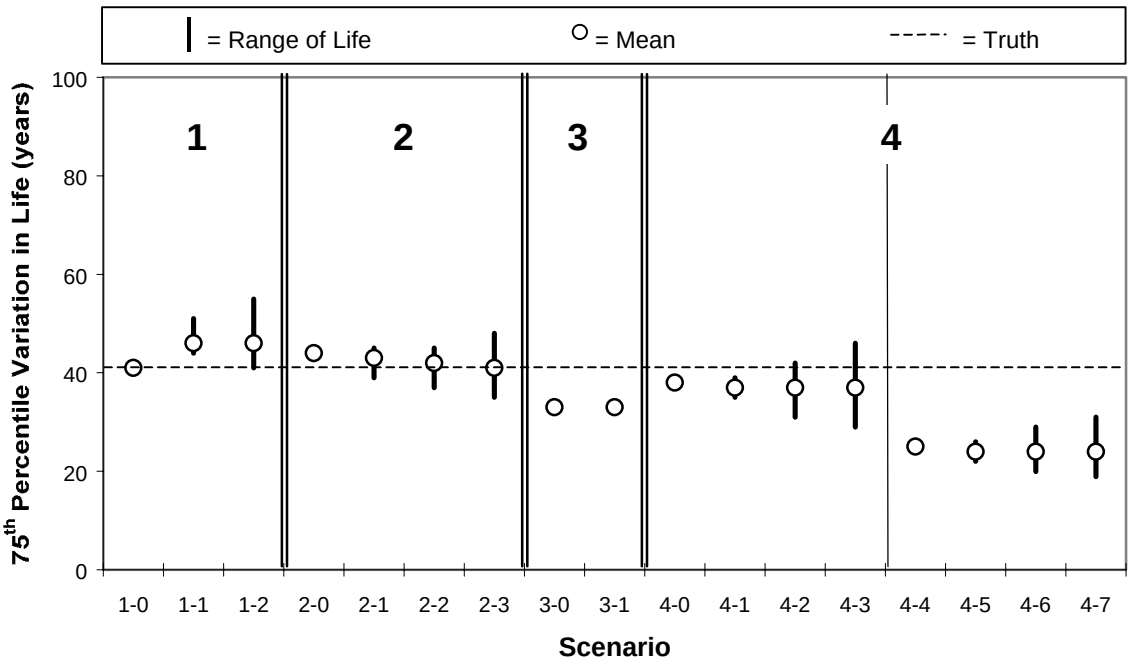

Figure 4.3: Flexible Site 26_1010, 75th Percentile, Range in Life

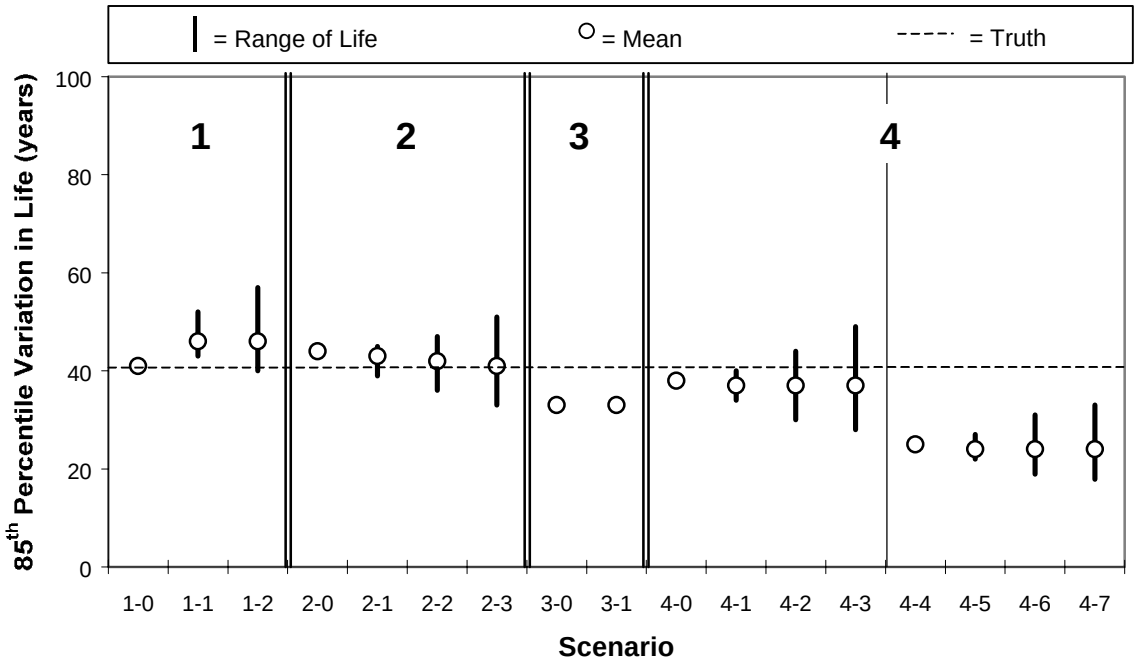

Figure 4.4: Flexible Site 26_1010, 85th Percentile, Range in Life

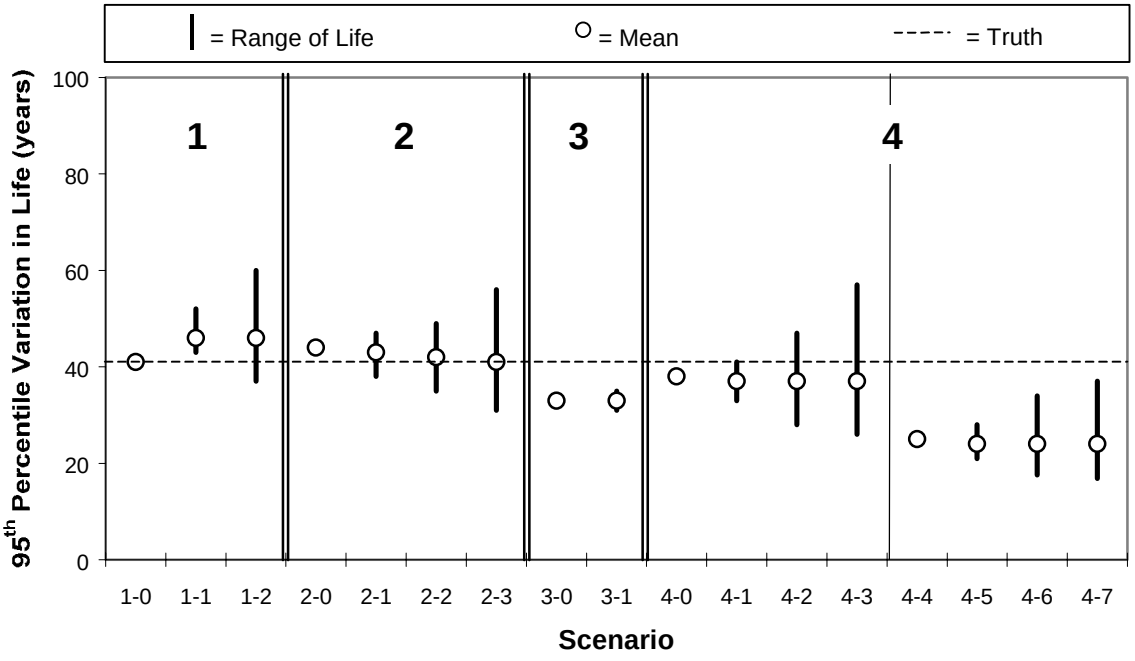

Figure 4.5: Flexible Site 26_1010, 95th Percentile, Range in Life

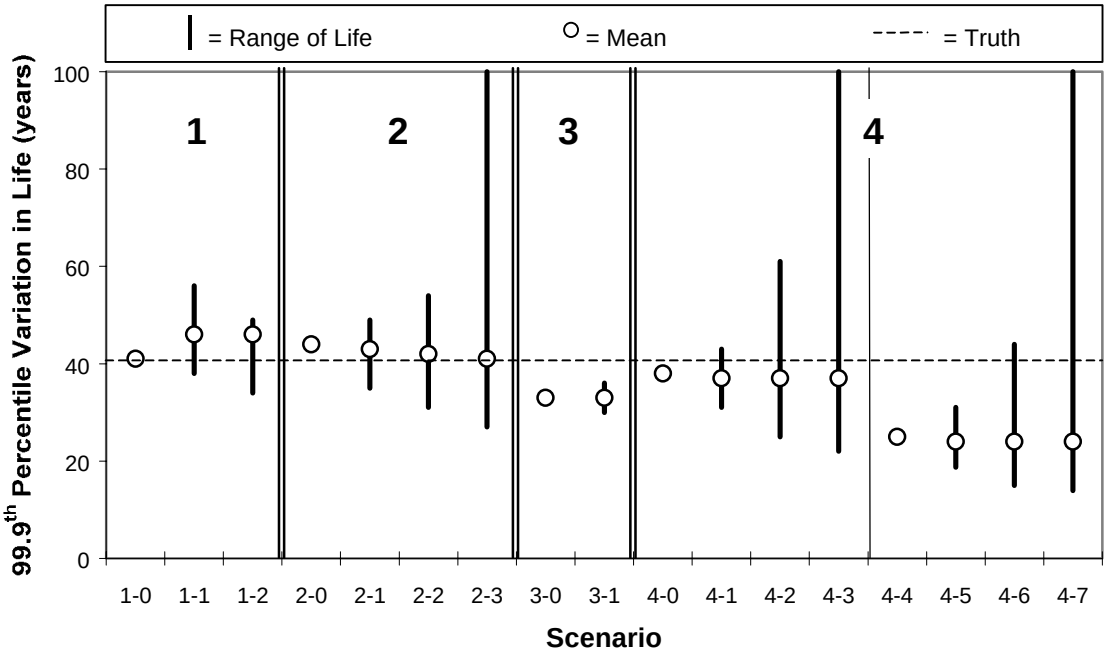

Figure 4.6: Flexible Site 26_1010, 99.9th Percentile, Range in Life

The 50th percentile plot (Figure 4.2) contains no vertical lines because there is no variation in traffic input (i.e., $Z_{\alpha/2} = 0$). Consequently, for all scenarios, the mean will remain in the same location at each reliability level. At 75% reliability (Figure 4.3) there is variation in life predictions. This variation increases from left to right within each TIL.

The second type of graph is produced by plotting the ratio of maximum possible overestimation of pavement life to the TRUTH for that site (i.e., {TRUTH + |A| + B} / TRUTH, where A and B are depicted in Figure 4.1). This takes the plots of pavement life from an absolute space (years) and transforms them to a relative space (percentage of TRUTH). This also facilitates the comparison of scenario results from sites with significantly different life predictions. Examples of these percent plots for site 26_1010 are given in Figures 4.7 to 4.11. In them, the bar shading represents similarity in the traffic data sources between scenarios. For example, scenarios 1-2 and 2-2 both use SS AVC data, and are thus shaded similarly. A complete list of percent life plots for all eight sites can be found in Appendix G.

An interpretation of the results for site 26_1010, scenario 3-1, as presented in Figure 4.8, is as follows: Using an on-site axle counter combined with regional AVC and regional WIM data, there is a 75% chance that the pavement life will be overestimated by the PDG by 25%. In other words, using scenario 3-1, if the design life is 10 years, then the life estimate from the PDG can be as high as 12.5 years at 75% confidence.

The horizontal dashed line fixed at 10% life overestimation represents a reasonable criterion for maximum allowable life overestimation. In practice, this limit is set by the designer. Here it serves as a point of reference from which variation in maximum pavement life overestimation can be measured.

In these plots, as reliability increases so does variation. For some sites, variation exceeds 500% of TRUTH. This was the case for sites with very light traffic. Conceptually, as reliability level increases, so does the size of the *CI*, making the lower boundary of the *CI* (i.e., critical traffic input) smaller. Therefore, as reliability level increases, traffic input values decrease, resulting in a pavement life overestimate increase. Furthermore, as traffic input values approach zero, pavement life overestimation approaches infinity, i.e. no distresses observed over the period analyzed. In these cases a pavement life value of 100 years was assumed.

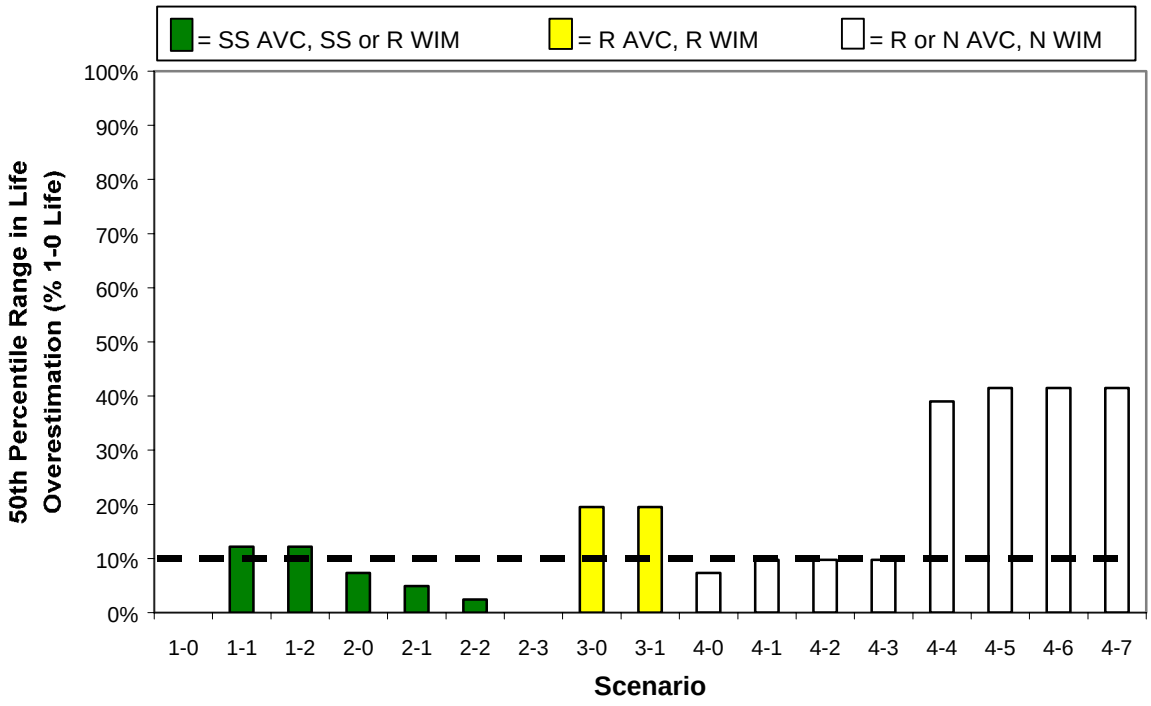

Figure 4.7: Flexible Site 26_1010, 50th Percentile, % Life Overestimation

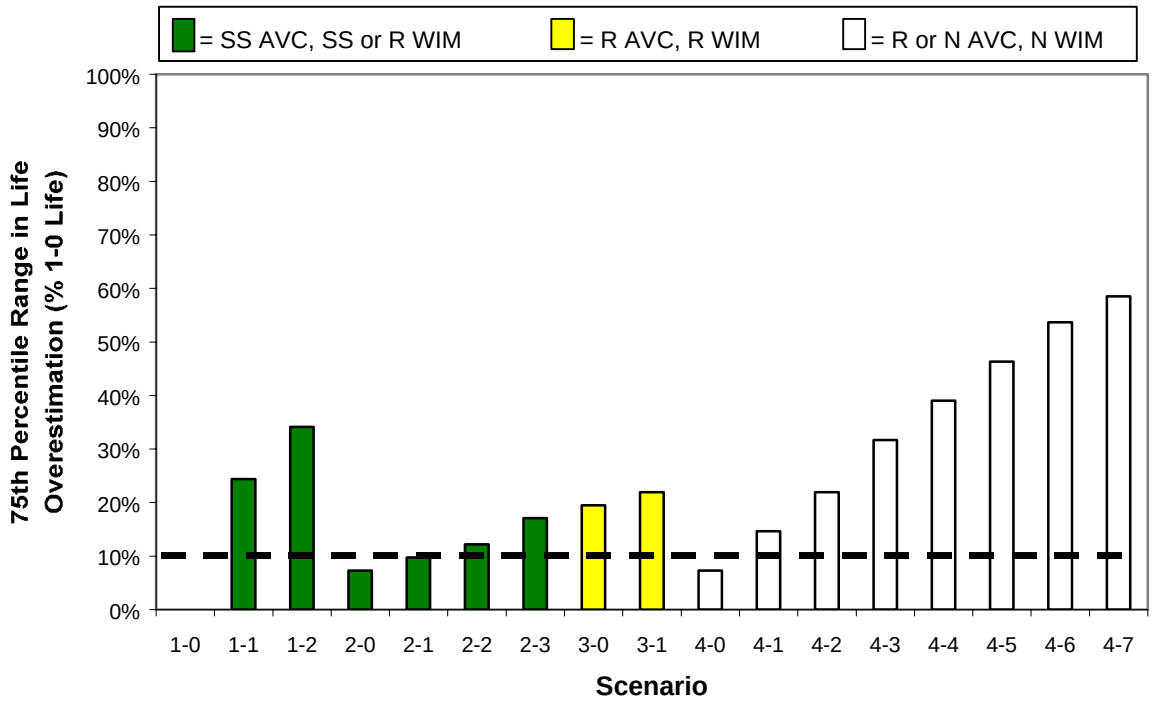

Figure 4.8: Flexible Site 26_1010, 75th Percentile, % Life Overestimation

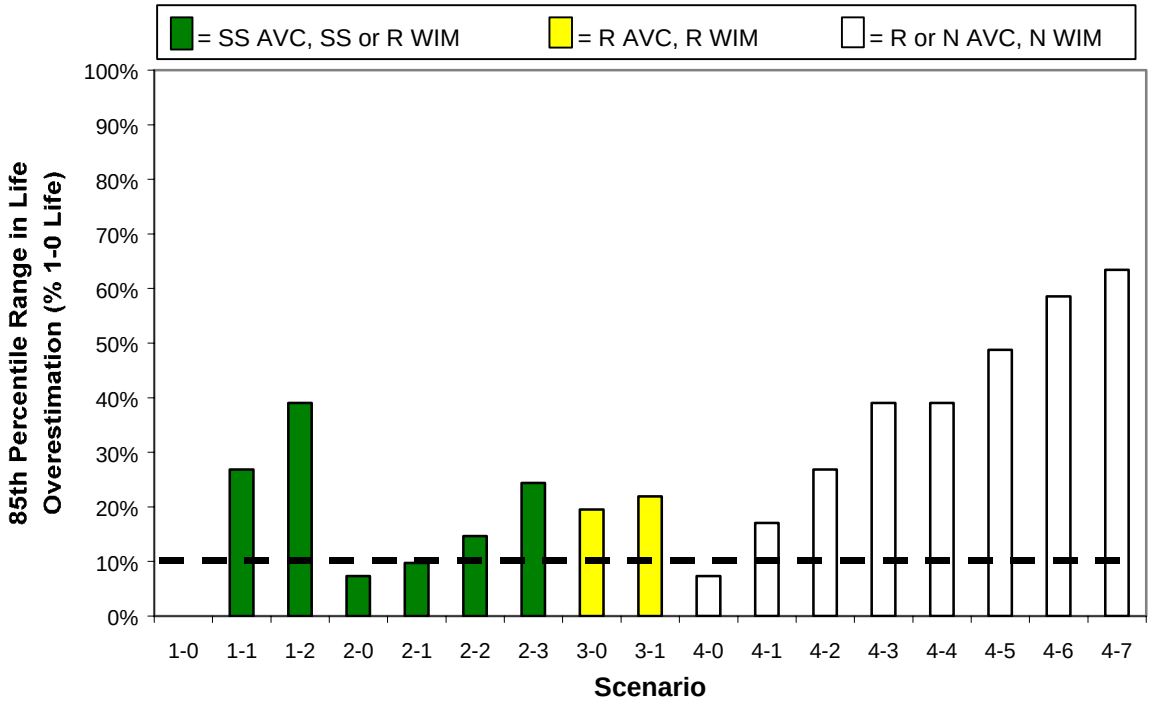

Figure 4.9: Flexible Site 26_1010, 85th Percentile, % Life Overestimation

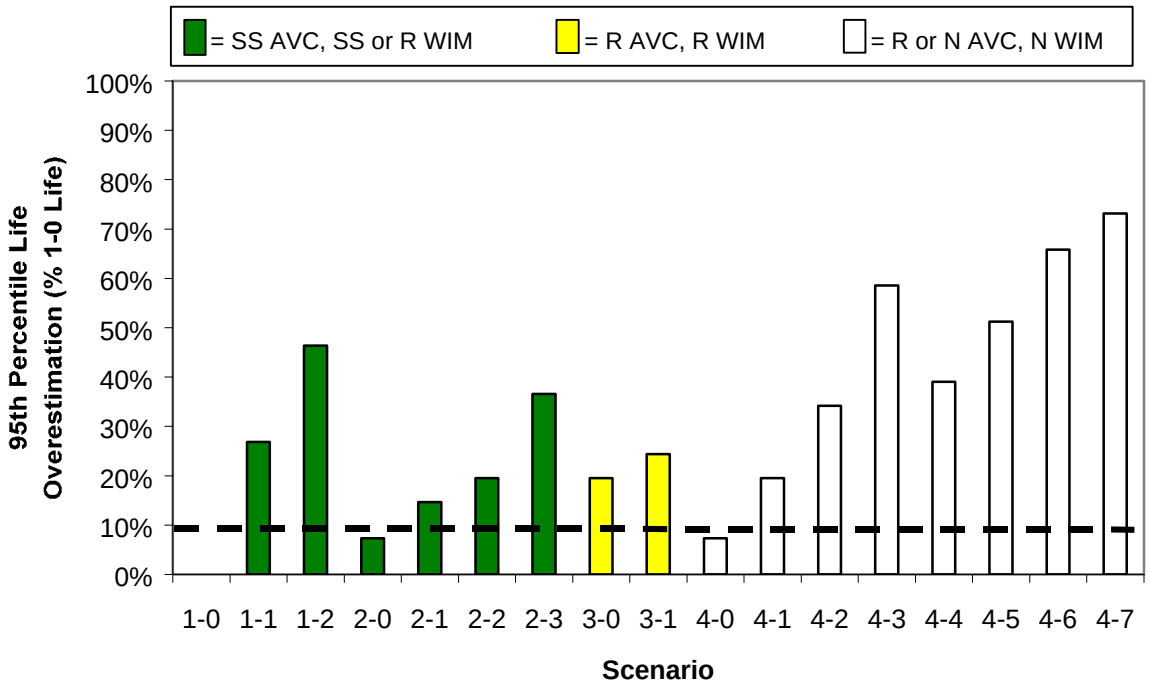

Figure 4.10: Flexible Site 26_1010, 95th Percentile, % Life Overestimation

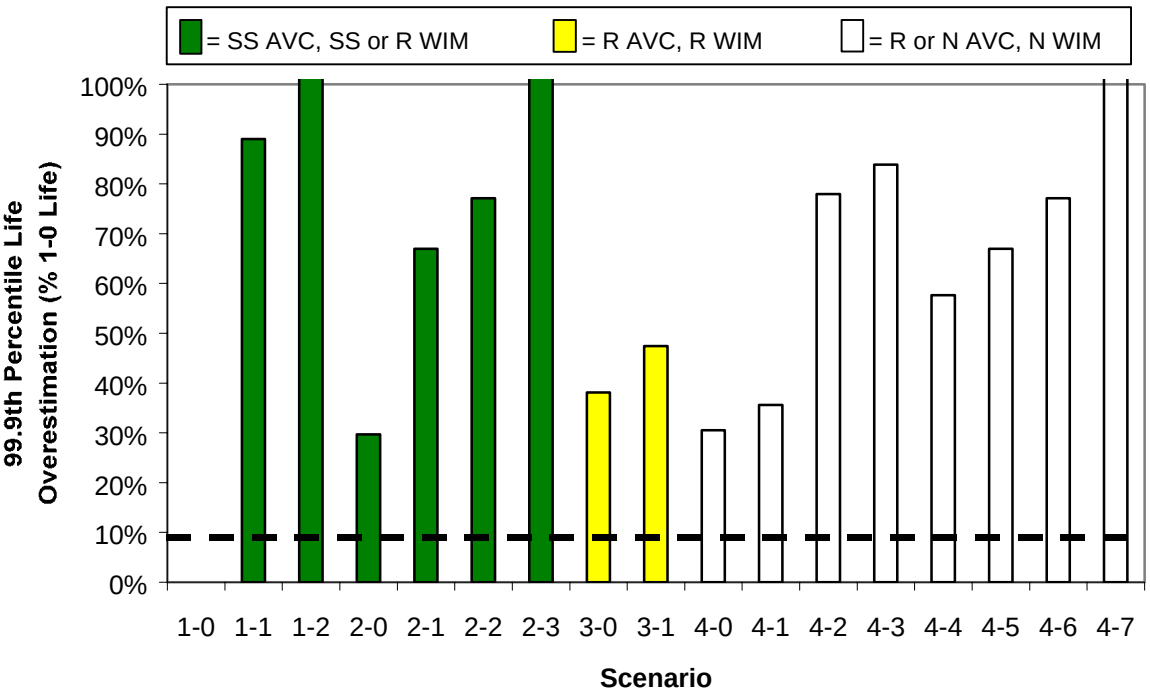

Figure 4.11: Flexible Site 26_1010, 99.9th Percentile, % Life Overestimation

Figures 4.7 to 4.11 are an alternative view of the same data presented in Figures 4.1 to 4.6. Therefore the same trends from the life plots apply here as well. The maximum range was set to 100%. However, the actual maximum overestimation of pavement life prediction by far exceeded 100% of TRUTH.

With maximum pavement life overestimation plotted in a common range (0 to 100%), an average is computed for all sites for each scenario and reliability level. This results in five plots, one for each reliability level. The average maximum pavement life overestimation by traffic sampling scenario and reliability level is presented in both graphical (Figures 4.12 to 4.16) and tabular (Table 4.3) form. The standard deviations are also computed (Table 4.4).

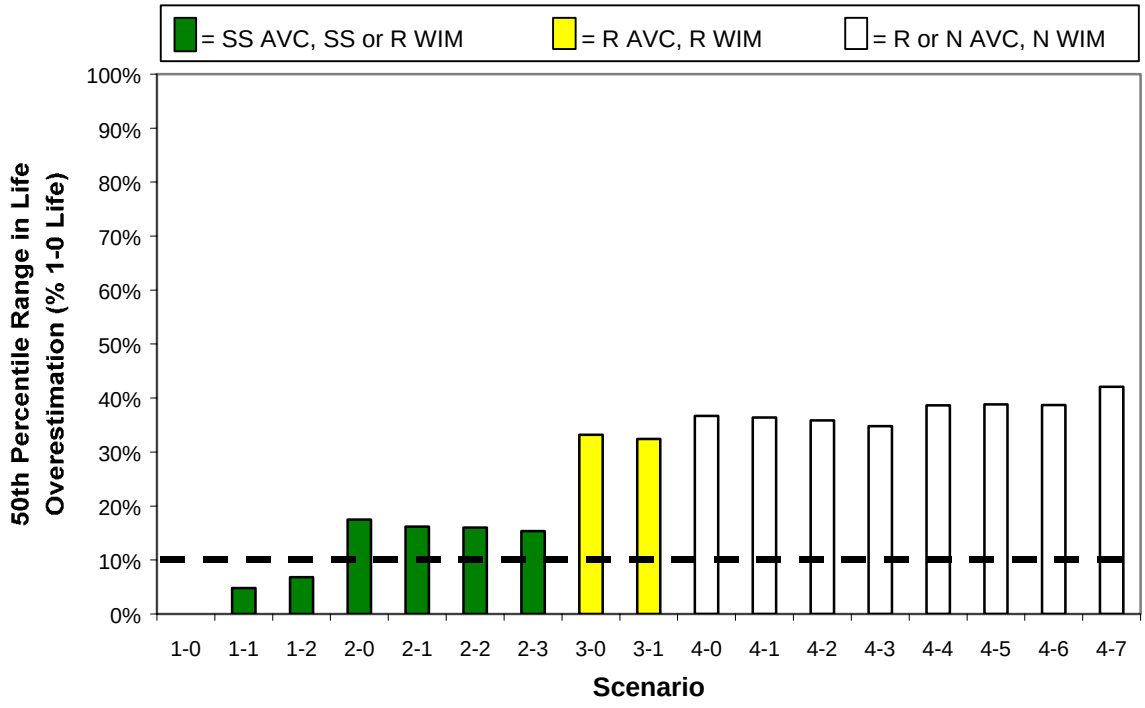

Figure 4.12: Average All Sites, 50th Percentile, % Life Overestimation

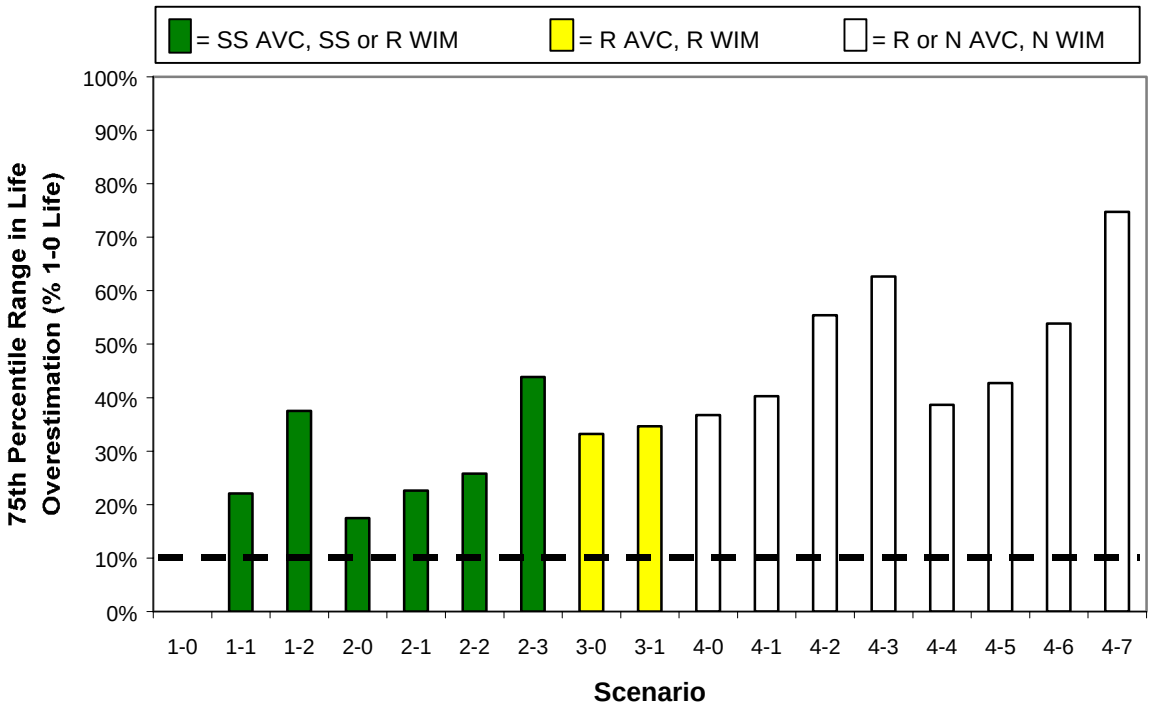

Figure 4.13: Average All Sites, 75th Percentile, % Life Overestimation

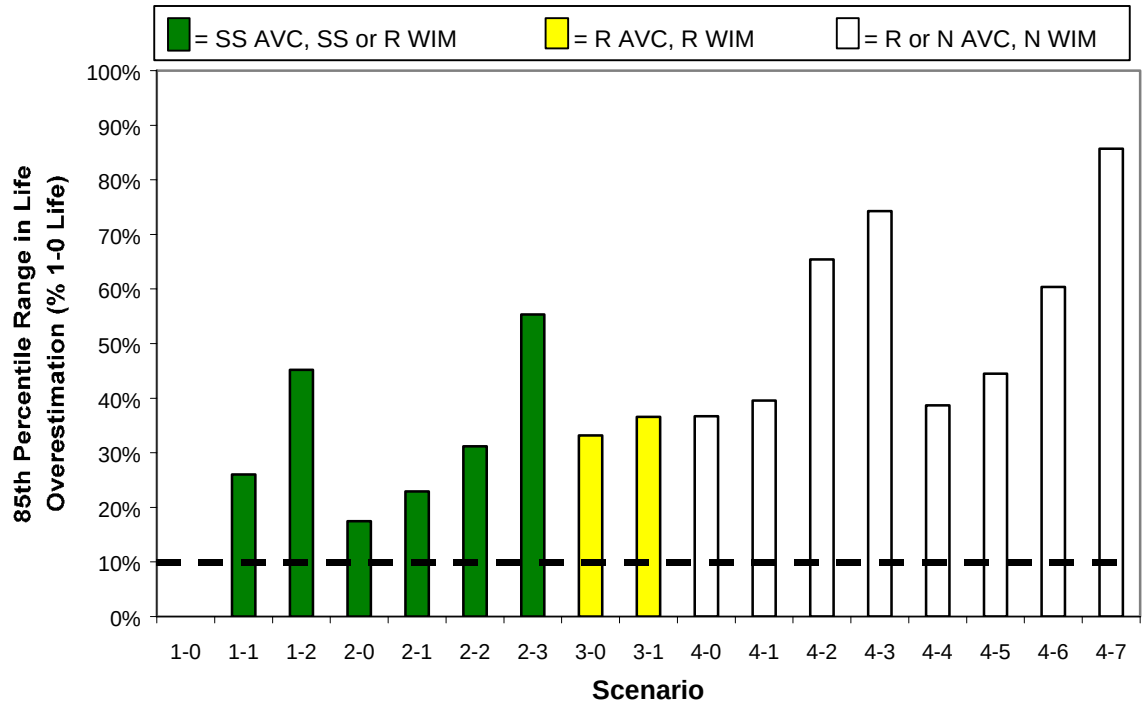

Figure 4.14: Average All Sites, 85th Percentile, % Life Overestimation

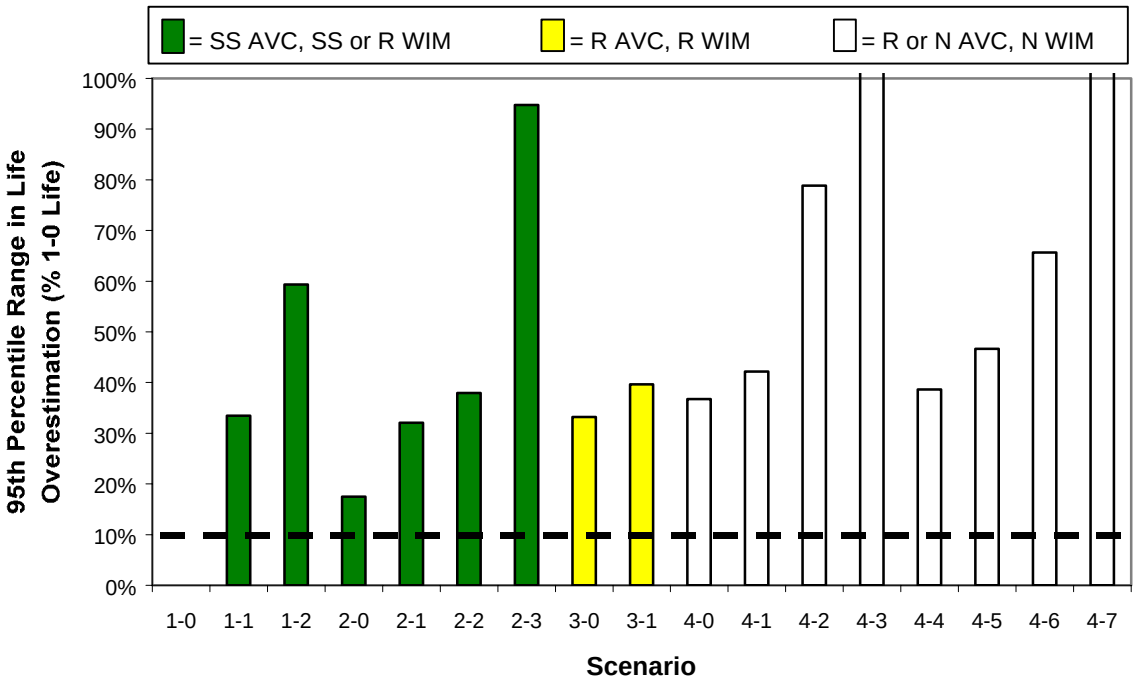

Figure 4.15: Average All Sites, 95th Percentile, % Life Overestimation

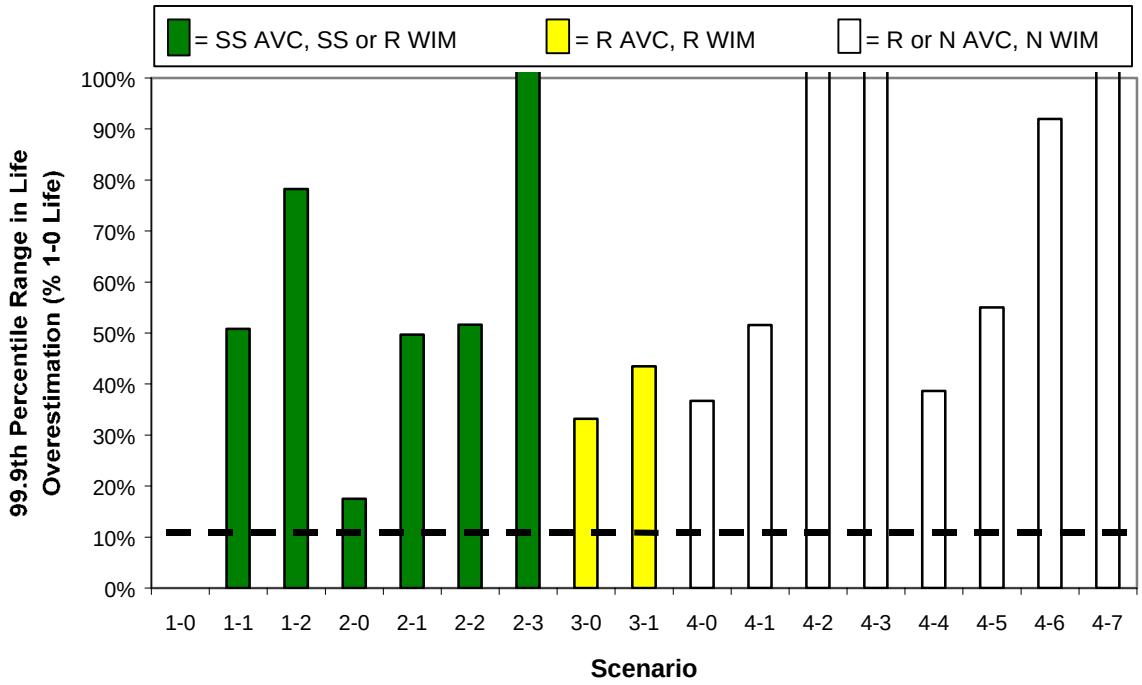

Figure 4.16: Average All Sites, 99.9th Percentile, % Life Overestimation

Table 4.3: Average Pavement Life Overestimation by Traffic Sampling Scenario and Reliability Level

			Average Pavement Life Overestimation as a Percentage of TRUTH for Reliability Levels 50%, 75%, 85%, 95%, and 99.9%				
Traffic Data Sources	**Time Coverage for the SS Traffic Data Source***	**Scenario ID**	**50%**	**75%**	**85%**	**95%**	**99.9%**
WIM Data = SS AVC Data = R	Continuous (**TRUTH**)	1-0	0%	0%	0%	0%	0%
	1 month / 4 seasons	1-1	5%	22%	26%	33%	51%
	1 week / 4 seasons †	1-2	7%	38%	45%	59%	78%
WIM Data = R **AVC Data = SS**	Continuous	2-0	17%	17%	17%	17%	17%
	1 month / 4 seasons †	2-1	16%	23%	23%	32%	50%
	1 week / 4 seasons †	2-2	16%	26%	31%	38%	52%
	1 week	2-3	15%	44%	55%	95%	165%
WIM Data = R AVC Data = R **ATR Data = SS**	Continuous	3-0	33%	33%	33%	33%	33%
	1 month/4 seasons	3-1	32%	35%	37%	40%	44%
WIM Data = N AVC Data = R **ATR Data = SS**	Continuous	4-0	37%	37%	37%	37%	37%
	1 week / 4 seasons	4-1	36%	40%	40%	42%	52%
	1 week	4-2	36%	55%	65%	79%	591%
	1 weekday +1 weekend day	4-3	35%	63%	74%	108%	343%
WIM Data = N AVC Data = N **ATR Data = SS**	Continuous	4-4	39%	39%	39%	39%	39%
	1 week / 4 seasons	4-5	39%	43%	44%	47%	55%
	1 week	4-6	39%	54%	60%	66%	92%
	1 weekday +1 weekend day	4-7	42%	75%	86%	113%	462%

*Time coverage pertains only to the site-specific data source in column one.
† Shaded scenarios exhibit similar pavement life overestimations

Table 4.4: Standard Deviation of Average Pavement Life Overestimation by Traffic Sampling Scenario and Reliability Level

	Reliability Level				
Scenario	**50%**	**75%**	**85%**	**95%**	**99.9%**
1-0	0%	0%	0%	0%	0%
1-1	5%	12%	15%	20%	32%
1-2	6%	22%	27%	35%	57%
2-0	10%	10%	10%	10%	10%
2-1	10%	15%	15%	21%	38%
2-2	11%	14%	16%	20%	30%
2-3	11%	31%	46%	99%	168%
3-0	31%	31%	31%	31%	31%
3-1	30%	31%	35%	34%	39%
4-0	35%	35%	35%	35%	35%
4-1	33%	33%	37%	36%	40%
4-2	34%	42%	48%	64%	550%
4-3	34%	48%	60%	105%	535%
4-4	26%	26%	26%	26%	26%
4-5	25%	22%	23%	23%	27%
4-6	25%	26%	31%	31%	51%
4-7	27%	40%	45%	70%	561%

* Shaded values represent similar variations per reliability

CHAPTER FIVE

CONCLUSIONS AND RECOMMENDATIONS

5.1 Conclusions

Average life overestimation ranged from 5% to over 400%. Standard deviations in life overestimation vary widely (Table 4.4). Within each TIL, the continuous scenario (2-0, 3-0, 4-0, and 4-4) produced the least variation. Also, for each TIL, as the time coverage decreased, variation in life overestimation increased within each TIL.

At 50% reliability, scenarios 1-0, 1-1, and 1-2 all exhibit less than 10% overestimation of pavement life, suggesting that scenario 1-2 would be sufficient traffic data input at a 50% reliability level. At higher reliability levels, no scenario other than 1-0 met this criterion. Scenario 2-0 on average produced pavement life prediction overestimations less than 18% regardless of reliability level, and hence would represent a cost-effective data acquisition alternative to SS WIM. The reason that continuous SS AVC outperforms short-term WIM data coverage is that it yields accurate, SS MAFs, and hence allows accurate modeling of seasonal pavement damage.

At 75%, 85%, 95%, and 99.9% reliability level, SS AVC data operating either one month (scenario 2-1) or one week (scenario 2-2) per season combined with R WIM data produces pavement life overestimation similar to that of the SS WIM system operating for one month per season (scenario 1-1). These values are highlighted in Table 4.3, and plotted together in Figure 5.1. Hence it appears that these traffic data collection scenarios are equivalent for pavement design.

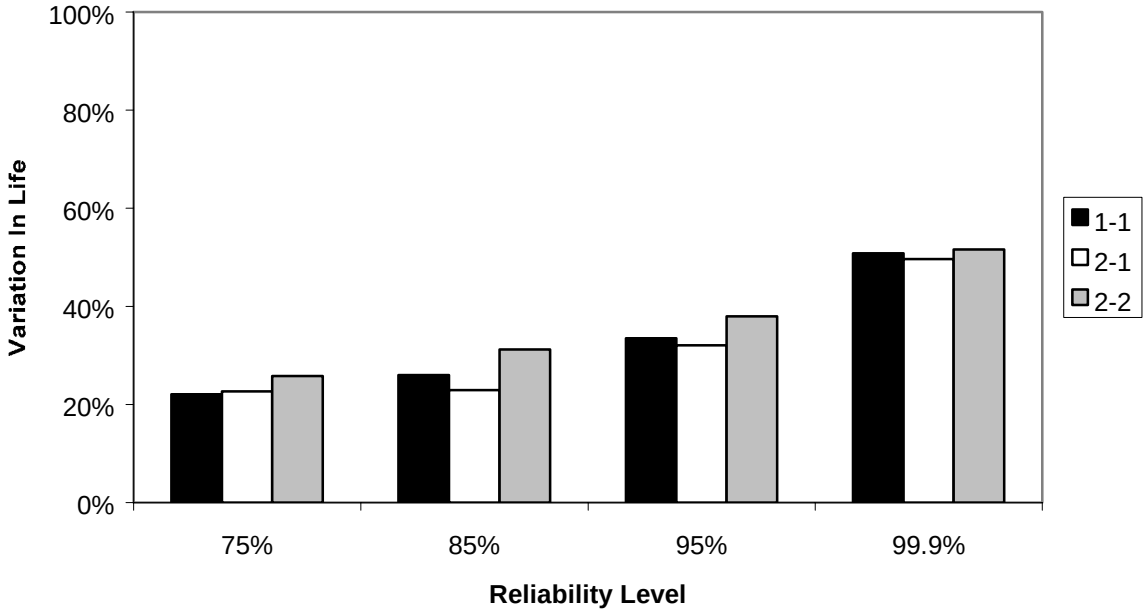

Figure 5.1: Average Maximum Variation in Life for Three Scenarios

ATR counts are the most common type (and least costly) means of gathering SS traffic data. These systems are typically used for short durations. The average maximum life overestimation resulting from SS ATR counts taken 1 week per season is 47% at a 95% reliability level. In other words, as a result of relying solely upon national default values for %Trucks, Vehicle Class Distributions, Normalized Axle Load Distribution Factors, and Monthly Adjustment Factors (the expensive data), pavements in this study on average failed half way through their intended service life.

In summary, pavement performance prediction using the 2002 PDG is highly dependent upon the traffic sampling scenario. Pavement life is also dependent upon the sources of the traffic data, and how much of it is site-specific. As expected, the more site-specific data, the more accurate the life prediction will be.

PDG Traffic Input Levels as they currently are written do not address variation in data collection time. For instance, site-specific ATR counts (TIL 2) performed better than SS WIM operating for one month or one week per season (both TIL 1). Therefore, the time of data acquisition should be considered when choosing data acquisition equipment.

5.2 Recommendations

The sites chosen for this study reflect only eight pavement designs. It is recommended that more sites be chosen in order to perform a factorial experiment where AADTT is the factor being studied. If five or six sites per factorial level were analyzed at three AADTT levels (high, medium, and low), then recommendations could be made per traffic level.

BIBLIOGRAPHY

1. AASHTO 2002 Pavement Design Guide, Design of New and Rehabilitated Pavement Structures, Draft Final Report, NCHRP Study 1-37A, July 2004

2. AASHTO Guide for the Design of Pavement Structures, American Association of State Highway and Transportation Officials, Washington DC, 1993.

3. AASHTO Guidelines for Traffic Data Programs, Joint Task Force on Traffic Monitoring Standards, ISBN 1-56051-054-4, 1992.

4. Accuracy of Traffic Load Monitoring and Projections Related to Traffic Data Collection Parameters, FHWA pool Fund Study SPR-2 (193), Presentation in A2B08 Committee Meeting during 82nd Annual TRB Meeting, January 2003.

5. Cambridge Systematics, "Use of Data from Continuous Monitoring Sites", Vol. I Recommendations and Vol. II Documentation , FHWA, August 1994.

6. Cambridge Systematics, "Accuracy of Traffic Load Monitoring and Projections Related to Traffic Data Collection Parameters", SPR-2 (193), Federal Highway Administration, August 1998.

7. Cambridge Systematics, "Traffic Data Collection, Analysis and Forecasting for Mechanistic Pavement Design", National Cooperative Highway Research Program, NCHRP Study 1-39, Draft Final Report, October 2003.

8. *DataPave* Release 16.0, Federal Highway Administration, July 2003.

9. Hallenbeck, M.E. and Soon-Gwam Kim, "Final Technical Report for Task A: Truck Loads and Flows", WSDOT Report WA-RD 320.3, Nov., 1993.

10. Long Term Pavement Performance Program, Guide to LTPP Traffic Data Collection and Processing, Federal Highway Administration, March 21, 2001.

11. LTPP IMS Data Release 16.0, VR 2003.05, July 2003 Upload, Volume 1: Primary Data set

12. Progress in the Development of the 2002 Guide for the Design of New and Rehabilitated Pavement Structures – 82nd Annual Transportation Research Board Meeting Washington DC, January 2003.

13. Ritchie, S.G. and Hallenbeck, M.E., State-Wide Highway Data Rationalization Study, Washington State DOT Research Report WA-RD-83.1, 1986.

14. Romesburg, H.C., Cluster Analysis for Researchers, Lifetime Learning Publications, Belmont CA, 1984.

15. Standard Specification for Highway Weigh-in-Motion (WIM) Systems with User Requirements and Test Method, American Society of Testing of Materials, ASTM E 1318-90, pp. 701-712, 1990.

16. *StatistiXL*®, Statistical Functions for *Excel*®, www.statistixl.com

17. Thickness Design for Concrete Highway and Street Pavements, Portland Cement Association, 1984/1995.

18. Traffic Monitoring Guide, US Dep. of Transportation, Federal Highway Administration, Versions 1992, 1995 and 2001.

APPENDIX A

SUMMARY OF FLEXIBLE AND RIGID PAVEMENT DAMAGE FUNCTIONS IN THE 2002 PAVEMENT DESIGN GUIDE

The 2002 Pavement Design Guide (PDG) uses pavement response models to calculate stress and strain throughout pavement layers. Flexible uses a Linear Equivalent Algorithm, and rigid uses Finite Element Method. With stress computed, models are then used to predict performance of the pavement assuming certain structural properties and environmental conditions.

The following provides an overview of the traffic-associated flexible and rigid pavement damage functions incorporated into the AASHTO PDG as well as the pavement response models. The software for the latter relies upon two mechanistic response engines; flexible uses JULEA, while rigid uses ISLAB2000.

FLEXIBLE PAVEMENT PREDICTIVE MODELS

For flexible pavements, three traffic-associated distress mechanisms are considered:

- Fatigue cracking – top-down longitudinal
- Fatigue cracking – bottom-up alligator
- Rutting – plastic deformation in all layers including native

<u>Fatigue Cracking</u> (F.C.) – Bottom-up alligator

$$F.C. = \left(\frac{1}{60}\right) \cdot \left(\frac{6000}{1 + EXP(C_1 \cdot C_1' + C_2 \cdot C_2' \cdot \log_{10}(D \cdot 100))}\right) \quad \text{(A.1)}$$

where:

C_1 = 1.0

C_2 = 1.0

C_1' = - 2·C_2'

C_2' = -2.40874 - 39.748·(1+h_{AC})$^{-2.856}$

h_{AC} = AC thickness (in)

$$D = \sum_{i=1}^{T} \frac{n_i}{N_f}$$

n_i = number of load repetitions experienced at time t of total time T

$$N_f = 0.00432 \cdot \beta_{f1}' \cdot k_1' \cdot C \left(\frac{1}{\varepsilon_t}\right)^{3.9492} \left(\frac{1}{E}\right)^{1.281} \quad \text{(A.2)}$$

ε_t = tensile strain at the bottom of the AC layer

E = layer stiffness (psi)

β_{fi}' = 1.0

$$k_1' = \frac{1}{0.000398 + \frac{1}{1 + EXP(11.02 - 3.49 \cdot h_{AC})}} \quad \text{(A.3)}$$

$C = 10^{M}$

$$M = 4.84\left(\frac{V_b}{V_a + V_b} - 0.69\right) \quad \text{(A.4)}$$

V_b = Volume of binder (% total mix volume)

V_a = Volume of air (% total mix volume)

Fatigue Cracking (F.C.) – Top-down Longitudinal

$$F.C. = 10.56 \cdot \left(\frac{1000}{1 + EXP(7 - 3.5 \cdot \log_{10}(D \cdot 100))} \right) \quad \text{(A.5)}$$

$$D = \sum_{i=1}^{T} \frac{n_i}{N_f}$$

n_i = number of load repetitions experienced at time t of total time T

$$N_f = 0.00432 \cdot \beta_{f1}' \cdot C \left(\frac{1}{\varepsilon_t} \right)^{3.9492} \left(\frac{1}{E} \right)^{1.281} \quad \text{(A.6)}$$

$\beta_{fi}' = 1.0\ k_1'$

$$k_1' = \frac{1}{0.0001 + \frac{29.844}{1 + EXP(30.544 - 5.7357 \cdot h_{AC})}} \quad \text{(A.7)}$$

$C = 10^{M}$

$$M = 4.84 \left(\frac{V_b}{V_a + V_b} - 0.69 \right) \quad \text{(A.8)}$$

V_b = Volume of binder (% total mix volume)

V_a = Volume of air (% total mix volume)

ε_t = tensile strain at the bottom of the AC layer

E = layer stiffness (psi)

Plastic Deformation – Total

The design guide models primary and secondary-stage rutting by calculating plastic deformation in sublayers and summing deformation in all sublayers, which is expressed mathematically as:

$$PD = \sum_{i=1}^{n} \varepsilon_p^i \, h^i \tag{A.9}$$

where,

PD = permanent pavement deformation

n = number of sublayers

$\varepsilon_p^{\,i}$ = total plastic deformation in sublayer i

h^i = thickness of sublayer i

Plastic Deformation – AC

To find the plastic deformation experienced by an AC layer, the design guide uses the following series of equations:

$$\frac{\varepsilon_p}{\varepsilon_r} = k_1 \cdot 10^{-3.4488} \, T^{1.5606} N^{0.479244} \tag{A.10}$$

where,

ε_p = plastic compressive strain in AC sublayer

The vertical elastic strain ε_r is computed from the normal stresses σ_x, σ_y, σ_z and Poisson's ratio μ in a Cartesian coordinate system using:

$$\varepsilon_r = \frac{1}{E}\left(\sigma_z - \mu\sigma_x - \mu\sigma_y\right) \tag{A.11}$$

where

E = layer stiffness (psi)

μ = Poisson's ratio

σ_x = stress in the x direction

σ_y = stress in the y direction

σ_z = stress in the z direction

$$k_1 = (C_1 + C_2 \cdot depth) \cdot 0.328196^{depth} \quad \text{(A.12)}$$

$$C_1 = -0.1039 \cdot H_{AC}^2 - 17.342 \quad \text{(A.13)}$$

$$C_2 = 0.0172 \cdot H_{AC}^2 - 1.7331 \cdot H_{AC}^2 + 27.428 \quad \text{(A.14)}$$

H_{AC} = total thickness of the AC layer (in)

$depth$ = depth at which the rut is calculated (in)

T = asphalt concrete layer temperature (ºF)

N = number of loading cycles experienced

The plastic deformation in each AC sublayer is summed to produce the total plastic deformation in a season. For the next season, the accumulation of plastic strains begins at a traffic level equivalent to that which would produce the same plastic deformation as the previous season. This allows continuous accumulation of strain increments derived from the plastic deformation expression above as the number of load applications increases.

Plastic Deformation – Granular Unbound Layers

The plastic deformation in the granular layers is similarly computed by summing the plastic deformation in all sublayers. Plastic deformation is computed using:

$$\frac{\varepsilon_0}{\varepsilon_r} = \frac{1}{2}\left(0.15\, e^{(\rho)^{\beta}} + 20\, e^{\left(\frac{\rho}{10^9}\right)^{\beta}} \right) \tag{A.15}$$

where:

$$\rho = 10^9 \left(\frac{-4.89285}{1-(10^9)^{\beta}} \right)^{\frac{1}{\beta}} \tag{A.16}$$

$$\beta = 10^{(-0.61119-0.017638 \cdot W_c)}$$

$$W_c = 51.712\, CBR^{-0.3586 \cdot GWT^{\,0.1192}}$$

CBR = CBR ratio of the unbound layer

GWT = the ground water table depth (ft)

RIGID PAVEMENT DAMAGE FUNCTIONS

The PDG considers 2 types of Portland Cement Concrete (PCC) pavement structures, namely Jointed (JCP) and Continuously Reinforced (CRCP) Concrete Pavement. JCP can be either un-doweled or doweled. The following damage mechanisms are considered in this study:

- Fatigue transverse cracking, both bottom-up and top-down (JPCP)
- Joint faulting (JPCP)
- Punchouts (CRCP)

The structural response of rigid slabs is a function of many parameters. In the PDG, they are designated as either fixed or variable. Examples of fixed parameters are slab thickness and PCC modulus of elasticity, while the variable parameters are age, month of opening to traffic, load configurations, load levels, temperature, and load position. If critical stress calculations were performed for all possible combinations of the variable parameters listed above millions of

computations would be required. Instead, the PDG software performs structural response calculations for a limited number of variable combinations and uses the output as input to a neural network routine which predicts the critical response parameters. The variable combinations used are:

- Temperature and wheel loads
- Loss of support due to slab curling
- Subgrade stiffness and
- Slab-to-slab interaction

Based on these response parameters pavement damage is accumulated in monthly increments. Within each increment the following are held constant:

1. PCC strength and modulus
2. Base modulus
3. Subgrade modulus
4. Joint load transfer efficiency (transverse and longitudinal)
5. Base erosion and loss of support (for CRCP)

Within each increment, an average temperature distribution through the slab is considered with a resolution of 2°F. Because the entire damage functions are exhaustive, a brief description of the damage functions by distress mechanism follows.

Fatigue (Transverse) Cracking - JPCP

The total amount of slab cracking *TCRACK* is determined by adding the top-down and bottom-up components, but excluding their combination. This is expressed as:

$$TCRACK = \left(CRK_p + CRK_q - CRK_p \cdot CRK_q\right)100\% \quad \text{(A.17)}$$

where:

$CRK_{p,q}$ = predicted percentage of cracking

p = bottom-up crack type

q = top-down crack type

Each specific cracking type is modeled as a function of its respective fatigue damage using:

$$CRK_{p,q} = \frac{1}{1 + FD_{p,q}^{-1.68}} \quad \text{(A.18)}$$

where,

$$FD_{p,q} = \sum \frac{n_{i,j,k,l,m,n}}{N_{i,j,k,l,m,n}} \quad \text{(A.19)}$$

and,

$FD_{p,q}$ = total fatigue damage for bottom-up or top-down cracking

$n_{i,j,k,...}$ = applied number of load applications at condition *i, j, k, l, m, n*

$N_{i,j,k,...}$ = number of load applications to failure, (i.e., 50% slab cracking) under conditions *i, j, k, l, m, n*

i = age (accounts for change in PCC modulus of rupture, layer bond condition, deterioration of shoulder LTE)

j = month (accounts for change in base and effective modulus of subgrade reaction

k = axle type (single, tandem, tridem for bottom-up cracking; short, medium, and long wheelbases for top-down cracking)

l = load level for each axle type

m = temperature difference between top and bottom of slab

n = traffic path, assuming a normally distributed lateral wheel wander.

The number of load application to failure $N_{i,j,k,l,m,n}$ under conditions *i, j, k, l, m, n* is given by:

$$\log\left(N_{i,j,k,l,m,n}\right) = 2.0 \cdot \left(\frac{MR_i}{\sigma_{i,j,k,l,m,n}}\right)^{1.22} + 0.4371 \qquad \text{(A.20)}$$

where,

MR_i = PC slab modulus of rupture at age *i* (psi)

$\sigma_{i,j,k,,l,m,n}$ = critical stresses under load conditions *i, j, k, l, m, n* (psi)

In performing these fatigue calculations, the locations of calculated stresses are crucial. These differ as a function of axle type, lateral placement, temperature difference between top and bottom of slab, subgrade support, and so on. As mentioned earlier, a neural network approach is used to establish critical stress locations and their magnitudes. This approach drastically reduces software running time in performing PC pavement design.

Faulting

Faulting is computed using a monthly incremental approach, whereby the faulting accumulated each month is added up to produce total faulting. The major steps are listed and explained below.

Process temperature profile data

The Enhanced Integrated Climatic Model (EICM) produces temperatures at eleven evenly spaced points throughout the thickness of a PCC slab for every hour of the day. For faulting, the equivalent linear temperature difference for night time is determined for each calendar month as

the mean difference between top and bottom PCC surfaces from 8 p.m. to 8 a.m. For each month of the year, the equivalent temperature gradient for the month is then determined as follows:

$$\Delta T_m = \Delta T_{t,m} - \Delta T_{b,m} + \Delta T_{sh,m} + \Delta T_{PCW} \quad \text{(A.21)}$$

where,

ΔT_m = effective temperature differential for month *m*

$\Delta T_{t,m}$ = mean PCC top surface night time temperature (8 p.m. to 8 a.m.) for month *m*

$\Delta T_{b,m}$ = mean PCC bottom surface night time temperature (8 p.m. to 8 a.m.) for month *m*

$\Delta T_{sh,m}$ = equivalent temperature differential due to reversible shrinkage for month *m* for old concrete (i.e. shrinkage is fully developed)

ΔT_{PCWt} = equivalent temperature differential due to permanent curl/warp

This process accounts for slab curling during the evenings. PCC temperature data are also used to find other base and LTE parameters that vary with temperature.

Determine initial maximum faulting

$$FAULTMAX_0 = C_{12} \cdot \delta_{curling} \cdot \left[Log\left(1 + C_5 \cdot 5.0^{EROD}\right) \cdot Log\left(\frac{P_{200} \cdot WetDays}{P_s}\right)\right]^{C_6} \quad \text{(A.22)}$$

where,

$FAULTMAX_0$ = initial maximum mean transverse joint faulting (in)

$\delta_{curling}$ = maximum mean monthly slab corner upward deflection due to temperature curling and moisture warping (units are unclear)

$EROD$ = erodibility class ($1 \le \text{EROD} \le 5$)

P_s = overburden on subgrade (lb)

P_{200} = percent subgrade material passing #200 sieve

WetDays = average annual number of wet days (greater than 0.1 in rainfall)

C_1 = 1.29

C_2 = 1.1

C_5 = 250

C_6 = 0.4

FR = base freezing index, defined as the percentage of time the top base temperature is below freezing.

$$C_{12} = C_1 + C_2 \ FR^{0.25} \quad \text{(A.23)}$$

Evaluate initial joint Load Transfer Efficiency (LTE)

In the PDG, total LTE is contributed from 3 sources, namely vertical resistance from aggregate interlock, dowels (if present), and base/subgrade resistance. Each of these LTE components is computed separately.

LTE from aggregate interlock

To find aggregate interlock LTE, joint width (*jw*) size must first be calculated. To calculate the joint width for each time increment, use the following equation:

$$jw = Max\left(12{,}000 \cdot L \cdot \beta\left(\alpha_{PCC}\left\{T_{constr} - T_{mean}\right\} + \varepsilon_{sh,m}\right), 0\right) \quad \text{(A.24)}$$

where,

jw = joint opening, mils (0.001 in)

L = joint spacing, ft

β = friction coefficient between the base and PCC (assumed as 0.65 for stabilized base, 0.85 for granular base)

α_{PCC} = PCC coefficient of thermal expansion (in/in/°F)

T_{mean} = mean monthly nighttime mid depth temperature, (°F)

T_{const} = PCC temperature at set (°F)

$\varepsilon_{sh,m}$ = PCC slab mean shrinkage strain

The last variable ($\varepsilon_{sh,m}$) is mean shrinkage strain, and is defined as:

$$\varepsilon_{sh,m} = \varepsilon_{sh,b} + \varepsilon_{sh,t} - \varepsilon_{sh,b} \cdot \frac{h_d}{h_{PCC}} \tag{A.25}$$

where,

$\varepsilon_{sh,b}$ = shrinkage strain at the bottom of the slab

$\varepsilon_{sh,t}$ = shrinkage strain at the top of the slab

h_d = depth of a drier portion of the PCC slab (set equal to 2 in)

h_{PCC} = PCC slab thickness (in)

Shrinkage at the top of the slab ($\varepsilon_{sh,t}$) is found by:

$$\varepsilon_{sh,t} = \varepsilon_{su} S_t \left(S_{h\max} - \phi \cdot S_{h\,i} \right) \tag{A.26}$$

where,

ε_{su} = ultimate shrinkage (10^{-6}) (see below)

S_t = time factor for moisture related slab warping

$S_{h\,max}$ = maximum average relative humidity factor

ϕ = (not defined in the PDG)

$S_{h\,i}$ = relative humidity factor for month *i*

The ultimate shrinkage strain (ε_{su}) of PCC is the shrinkage strain that will develop under prolonged exposure to drying conditions, (i.e., 40% relative humidity). The estimation of ε_{su} depends on the input level of the given data for the design analysis.

Shrinkage at the bottom of the slab ($\varepsilon_{sh,b}$) is found by:

$$\varepsilon_{sh,b} = \varepsilon_{su} S_t S_{h\,bot} \tag{A.28}$$

where,

ε_{su} = ultimate shrinkage (10^{-6})

S_t = time factor for moisture related slab warping

$S_{h\,bot}$ = relative humidity factor at the bottom of the PCC slab (assumed 90%)

The LTE due to aggregate interlock, LTE_{AGG}, is given by:

$$LTE_{AGG} = \frac{100}{1 + 0.012\, J_{AGG}^{-0.849}} \tag{A.29}$$

where,

J_{AGG} = transverse joint stiffness

The joint transverse stiffness on the transverse joint for the increment *i*:

$$Log\left(J_{AGG}\right) = -28.4 \cdot \exp\left\{-0.35^{\left(\frac{e-s}{0.38}\right)}\right\} \tag{A.30}$$

where:

J_{AGG} = transverse joint stiffness

S = joint shear capacity, equal to s_0 (initial joint shear capacity)

The initial joint shear capacity s_0 is given by:

$$s_0 = 0.05 \cdot h_{PCC} \cdot \exp(-0.032 \cdot jw) \quad \text{(A.31)}$$

where h_{PCC} and jw are explained above.

LTE from dowels

Dowel LTE, if present, is found using a non-dimensional stiffness factor expressed as:

$$J_d = J_d^* + (J_0 - J_d^*)\exp(-DAM_{dowels}) \quad \text{(A.32)}$$

where,

Jd = *non-dimensional dowel stiffness*

J_0* = *initial dowel stiffness*

$$= \frac{120 \cdot d^2}{h_{PCC}} \quad \text{(A.33)}$$

d = dowel diameter (in) (d > 0.75 in)

J_d^* = critical dowel stiffness

$$= Min\left(118,\ Max\left[165 \cdot \frac{d^2}{h_{PCC}} - 19.8120,\ 0.4\right]\right) \quad \text{(A.34)}$$

DAM_{dowels} = cumulative damage of a dowel joint depending on dowel bearing stress and number of load repetitions. Initially, set equal to 0

Finally, the LTE due to dowels (LTE_{dowel}) is computed using:

$$LTE_{dowel} = \frac{100}{1 + 0.012 \cdot J_d^{-0.849}} \quad \text{(A.35)}$$

LTE from subgrade

The base/subgrade LTE (LTE_{base}) can be found from the following table:

Table A1: Base Type LTE

Base Type	$\boldsymbol{LTE_{base}}$
Aggregate	20%
ATB or CTB base	30%
LCB base	40%

After all components of LTE (LTE_{dowel}, LTE_{AGG}, and LTE_{base}) have been found, LTE_{joint}, which represents the total joint load transfer efficiency, can be found using the following:

$$LTE_{joint} = 100\left(1-\left\{1-\frac{LTE_{dowel}}{100}\right\}\left\{1-\frac{LTE_{AGG}}{100}\right\}\left\{1-\frac{LTE_{base}}{100}\right\}\right) \quad \text{(A.36)}$$

Determine Current Max Faulting

The current maximum faulting is computed by adjusting the maximum faulting equation ($FAULTMAX_0$) to include past traffic damage using the past differential energy accumulated from axle load applications for all months prior to the current month. The first month has a differential energy of zero. The equations used to quantify this are as follows:

$$FAULTMAX_i = FAULTMAX_0 + C_7 \cdot \sum_{j=1}^{m} DE_j \cdot Log\left(1 + C_5 \cdot 5.0^{EROD}\right)^{C_6} \quad \text{(A.37)}$$

$$FAULTMAX_0 = C_{12} \cdot \delta_{curling} \cdot \left[Log\left(1 + C_5 \cdot 5.0^{EROD}\right) \cdot Log\left(\frac{P_{200} \cdot WetDays}{P_s}\right)\right]^{C_6} \quad \text{(A.38)}$$

where,

$FAULTMAX_i$ = maximum mean transverse joint faulting for month i (in)

$FAULTMAX_0$ = initial maximum mean transverse joint faulting (in)

DE_i = differential deformation energy accumulated during month *i* (for calculation, see step 8, Critical Pavement Responses)

$EROD$ = erodibility class ($1 \leq \text{EROD} \leq 5$) (pp. 2.2.58)

$\delta_{curling}$ = maximum mean monthly slab corner upward deflection due to temperature curling and moisture warping (in)

P_s = overburden on subgrade (lb)

P_{200} = percent subgrade material passing #200 sieve

$WetDays$ = average annual number of wet days (greater than 0.1 in rainfall)

FR = base freezing index defined as the percentage of time the top base temperature is below freezing.

$C_5 = 250$

$C_6 = 0.4$

$C_7 = 1.2$

$$C_{12} = C_1 + C_2 \ FR^{0.25} \tag{A.39}$$

Determine critical pavement responses for the increment

For each load condition, deflections at the loaded and unloaded corner of the slab are calculated using neural networks. With these deflections, the differential deformation energy of subgrade deformation (*DE*), shear stress at the slab corner (τ), and maximum dowel bearing stress (σ_b) are calculated:

$$DE = k/2\left(\delta^2_{loaded} - \delta^2_{unloaded}\right) \tag{A.40}$$

$$\tau = \frac{AGG}{h}\left(\delta_{loaded} - \delta_{unloaded}\right) \tag{A.41}$$

$$\sigma_b = \frac{D_d}{d \cdot dsp}\left(\delta_{loaded} - \delta_{unloaded}\right) \tag{A.42}$$

where,

δ_{loaded} = loaded corner deflection (in)

$\delta_{unloaded}$ = loaded corner deflection (in)

AGG = Aggregate interlock stiffness factor (psi/in)

k = coefficient of subgrade reaction (psi/in)

D_d = dowel stiffness factor = $J_d \cdot k \cdot l \cdot dsp$

d = dowel diameter (in)

dsp = dowel spacing (in)

l = radius of relative stiffness, defined by:

$$l = \sqrt[4]{\frac{E_{PCC} h_e^3}{12 \cdot k\left(1 - \mu_{PCC}^2\right)}} \tag{A.43}$$

where,

E_{PCC} = elastic modulus of PCC (psi)

h_e = effective slab thickness (in)

μ_{PCC} = PCC Poisson's ratio

k = modulus of subgrade reaction (psi/in)

Evaluate loss of shear capacity and dowel damage

$$\Delta s = \begin{cases} 0 & \text{if } jw < 0.001\ h \quad \text{(A.44)} \\ \sum_j \dfrac{0.005}{1.0 + (jw/h)^{-5.7}} \left(\dfrac{n_j}{10^6}\right)\left(\dfrac{\tau_j}{\tau_{ref}}\right) & \text{if } jw < 3.8\ h \quad \text{(A.45)} \\ \sum_j \dfrac{0.068}{1.0 + 6.0 \cdot \left(\dfrac{jw}{h} - 3\right)^{-1.98}} \left(\dfrac{n_j}{10^6}\right)\left(\dfrac{\tau_j}{\tau_{ref}}\right) & \text{if } jw > 3.8\ h \quad \text{(A.46)} \end{cases}$$

where,

n_j = number of laod applications for the current increment by load group j

jw = joint opening, mils (0.001 in)

h_{PCC} = PCC slab thickness

τ_j = shear stress on the transverse crack from the response model for the load group j

τ_{ref} = reference shear stress derived from the PCA test results, found using:

$$\tau_{ref} = 111.1 \cdot \exp\left[-\exp\left(0.9988 \cdot \exp\left\{-0.1089 \cdot \log J_{AGG}\right\}\right)\right] \quad \text{(A.47)}$$

where,

J_{AGG} = joint stiffness on the transverse crack computed for the time increment

Dowel damage is calculated using the following:

$$DAM_{dow} = C_8 \sum_j \left(\frac{n_j}{10^6}\right)\left(\frac{\tau_j}{f_c'}\right) \quad \text{(A.48)}$$

where,

DAM_{dow} = damage at dowel-concrete interface

C_8 = coefficient equal to 400

n_j = number of laod applications for the current increment by load group j

τ_j = shear stress on the transverse joint from the response model for the load group j

f_c' = PCC compressive strength, psi

Calculate incremental faulting

Use the following equation to calculate the change in faulting for a particular time increment.

$$\Delta Fault_i = C_{34} \cdot \left(FAULTMAX_{i-1} - Fault_{i-1}\right)^2 \cdot DE_i \quad \text{(A.49)}$$

where,

$\Delta Fault_i$ = incremental change (monthly) in mean transverse joint faulting during month *i* (in)

$FAULTMAX_{i-1}$ = maximum mean transverse joint faulting for month *i-1* (in)

$Fault_{i-1}$ = mean faulting for the month *i-1* (in)

DE_i = differential energy (see Step 8)

FR = base freezing index defined as the percentage of time the top base temperature is below freezing.

$$C_{34} = C_3 + C_4 FR^{0.25} \quad \text{(A.50)}$$

where,

$$C_3 = 0.001725 \quad \text{(A.51)}$$

$$C_4 = 0.0008 \quad \text{(A.52)}$$

Calculate mean joint faulting at the end of the month

$$Fault_m = \sum_{i=1}^{m} \Delta Fault_i \quad \text{(A.53)}$$

where,

$Fault_m$ = mean joint faulting at the end of month m (in)

$\Delta Fault_i$ = incremental change (monthly) in mean transverse joint faulting during month i (in)

Punchouts

The major steps in computing punchout damage are described below.

Calculate crack spacing

If crack control is used in CRCP design, (i.e., crack spacing is not random), the mean crack spacing should be used for crack width and fatigue computations. If CRCP is allowed to crack randomly, external software like CRCP8, or the procedure described next should be used to compute mean crack spacing:

$$\overline{L} = \frac{f_1 - C\sigma_0\left(1 - \frac{2\zeta}{H}\right)}{\frac{f}{2} + \frac{U_m P_b}{c_1 d_b}} \tag{A.54}$$

where,

$\overline{L}$ = mean crack spacing (in)

f_t = concrete tensile strength (psi)

f = subbase friction coefficient

U_m = peak bond stress (psi)

P_b = percent steel, fraction equal to area of steel reinforcement (A_s) per area of concrete (Ac) (%)

$= A_s / Ac$

d_b = reinforcing steel bar diameter (in)

c_1 = first bond stress coefficient (unclear how this is defined)

σ_{env} = tensile stress in the PCC due to environmental curling (psi)

H = slab thickness (in)

ζ = depth to steel layer (in)

C = Bradbury's curling/warping stress coefficient

σ_0 = Westergard's nominal stress factor, found with :

$$\sigma_0 = \frac{E_{PCC} \cdot \Delta\varepsilon_{tot}}{2(1 - f\mu_{PCC})} \quad \text{(A.55)}$$

where,

μ_{PCC} = PCC Poisson's ratio

$\Delta\varepsilon_{tot}$ = unrestrained curling and warping strain, found by:

$$\Delta\varepsilon_{tot} = \alpha_{PCC}\Delta t_{eqv} + \varepsilon_\infty \Delta\left(1 - rh_{PCC}^3\right)_{eqv} \quad \text{(A.56)}$$

where,

α_{PCC} = PCC coefficient of thermal expansion (/°F)

Δt_{eqv} = equivalent temperature (not clearly defined)

ε_∞ = utlimate shrinkage of PCC

$\Delta(1\text{-}rh_{PCC}^3)_{eqv}$ = relative humidity differences between the pavement surface and bottom based on formulations given by Mohamed and Hansen (40)

Calculate crack width and crack LTE for one month

To predict the mean estimate of the opening of the transverse cracks at the level of the steel due to shrinkage, thermal contraction, and counteracted by the restraint of the reinforcing steel and subbase friction, the following formula is used:

$$cw = Max\left\{ L \cdot \left(\varepsilon_{shr} + \alpha_{PCC} \cdot \Delta T_{\xi} - \frac{c_2 \cdot f_{\sigma}}{E_{PCC}} \right) \cdot 1000 \cdot CC, 0.001 \right\} \quad \text{(A.57)}$$

where,

cw = average crack width at the depth of the steel (mils)

L = crack spacing based on design crack distribution (in)

ε_{shr} = unrestrained concrete drying shrinkage at the depth of the steel (10^{-6})

α_{PCC} = PCC coefficient of thermal expansion (/ °F)

ΔT_{ξ} = drop in PCC temperature from concrete set temperature at the depth of the steel for each season (°F)

c_2 = second bond stress coefficient (unclear how this is defined)

f_{σ} = maximum longitudinal tensile stress in PCC at the steel level (psi)

E_{PCC} = PCC elastic modulus

CC = local calibration constant, with a default value of 1.00

The unrestrained shrinkage at any time, $\varepsilon_{shr}(t)$, at the reinforcing steel level for an atmospheric relative humidity corresponding to month i is given by the following equation :

$$\varepsilon_{shr}(t) = \varepsilon_{su} \cdot \left(1 - \left(\frac{RH_c}{100} \right)^3 \right) \quad \text{(A.58)}$$

where,

$\varepsilon_{shr}(t)$ = unrestrained shrinkage strain for month *i* at any time *t* days from placement (10^{-6})

ε_{su} = ultimate shrinkage strain (10^{-6})

RH_c = relative humidity in the concrete, percent, given by:

$$RH_c = RH_{ai} + \left(100 - RH_{ai}\right) \cdot f(t) \tag{A.59}$$

where,

$RH_{a\,i}$ = atmospheric relative humidity for month *i* (%)

$f(t)$ = 1/(1+(t/b)) (A.60)

t = time since concrete placement (days)

$$b = \frac{35}{4} \cdot d^{1.35}\left(w/c - 0.19\right) \tag{A.61}$$

d = depth to steel (mm)

w/c = water-to-cement ratio

The maximum longitudinal stress in PCC at the steel level are calculated using the following:

$$f_\sigma = \frac{L \cdot f}{2} + \frac{L \cdot U_m \cdot P_b}{c_1 \cdot d_b} + C \cdot \sigma_0 \left(1 - \frac{2\zeta}{H}\right) \tag{A.62}$$

where,

f_σ = tensile stress in the PCC due to environmental curling (psi)

L = crack spacing (in)

f = subbase friction coefficient

U_m = peak bond stress (psi)

P_b = percent steel, fraction equal to area of steel reinforcement (A_s) per area of concrete (*Ac*) (%)

c_1 = first bond stress coefficient (unclear how this is defined)

d_b = reinforcing steel bar diameter (in)

C = Bradbury's curling/warping stress coefficient

σ_0 = Westergard's nominal stress factor (see equation above)

ζ = depth to steel layer (in)

H = PCC slab thickness (in)

Like joints in JPCP, cracks occurring in CRCP have load transfer properties. This ability to transfer load is essential to pavement performance. As shown earlier, crack width (*cw*) is a function of pavement temperature at the elevation of the reinforcing steel. Therefore, average monthly slab temperatures produced by the EICM are used to predict incremental (monthly) crack widths. This crack width is related to the ability of the crack to transfer vertical loads. Therefore, the load transfer capability varies seasonally over the life of the pavement. Initial shear capacity of a non-damaged joint could be expressed as:

$$s_{o\,i} = 0.05 \cdot h_{PCC} \cdot \exp\left(-0.032 \cdot cw_i\right) \tag{A.63}$$

where,

$s_{o\,i}$ = dimensionless initial shear capacity based on crack width for time increment (month) *i*

h_{PCC} = slab thickness (in)

cw_i = crack width for time increment *i* (mils)

The current shear capacity of the transverse cracks for any given instance in pavement life *i* can be characterized using the following formula :

$$s = s_{o\,i} - \Delta S_{i-1} \tag{A.64}$$

where,

s = current crack shear capacity computed for time increment i

$s_{o\,i}$ = initial crack shear capacity based on crack width for increment i

ΔS_{i-1} = loss in shear load capacity accumulated from all previous time increments (computed at the end of the previous time increment i-1, set equal to 0 for first month)

Transverse crack stiffness is then determined from crack shear capacity using the following equation :

$$Log(J_c) = -2.2 \cdot \exp\left\{-\exp\left(-\frac{J_s + 11.26}{7.56}\right)\right\} - 28.85 \cdot \exp\left\{-\exp\left(\frac{e - s}{0.38}\right)\right\} + 49.8 \cdot \exp\left\{-\exp\left(-\frac{J_s + 11.26}{7.56}\right)\right\} \cdot \exp\left\{-\exp\left(\frac{e - s}{0.38}\right)\right\} \tag{A.65}$$

where,

J_c = joint stiffness on the transverse crack for current time increment

s = dimensionless shear capacity (unclear how this is defined)

J_s = load transfer across lane-shoulder joint (see table below)

e = current joint shear capacity

Table A.2: Typical Joint Stiffness Values from Different Shoulder Types

Shoulder Type	J_s
Granular	0.04
Asphalt	0.04
Tied PCC	4

In order to quantify the total load transfer capabilities of a crack, the influence of base layer and reinforcing steel is added to the model through the following equation :

$$LTE_{TOT} = 100 \cdot \left[1 - \left\{ 1 + Log^{-1} \left(\frac{0.214 - 0.183 \frac{a}{l} - \log(J_c) - R}{1.18} \right) \right\}^{-1} \left\{ 1 - \frac{LTE_{Base}}{100} \right\} \right] \quad \text{(A.66)}$$

where,

LTE_{TOT} = total crack LTE due to aggregate interlock, steel reinforcement, and base support (%)

a = radius of loaded area (in)1

l = radius of relative stiffness computed for time increment i (in)

R = residual dowel-action factor to account for residual load transfer provided by the steel reinforcement, calculated as follows:

$$R = 2.5 \cdot P_b - 1.25 \quad \text{(A.67)}$$

where,

P_b = percent of longitudinal reinforcement

LTE_{Base} = base layer (from table below)

Table A.3: LTE_{base} as a Function of Base Type

Base Type	$\boldsymbol{LTE_{base}}$
Aggregate	20%
ATB or CTB base	30%
LCB base	40%

Calculate loss of support along longitudinal edge of slab for one month

This section, referenced as Chapter 2 Section 2 in the PDG, is entirely missing.

Process monthly relative humidity data

The effects of moisture warping are a function of relative humidity. For a time increment (monthly), effects of variation in moisture warping are expressed in terms of equivalent temperature differences, and are added to the equivalent linear temperature difference during stress calculations.

$$ETG_{Shi} = \frac{3 \cdot \phi \cdot \varepsilon_{su} \cdot h_s \left(S_{h\,i} - S_{h\,ave}\right)\left(\frac{h}{2} - \frac{h_s}{3}\right)}{\alpha \cdot h^2 \cdot 100} \quad \text{(A.68)}$$

where,

ETG_{Shi} = temperature difference equivalent of the deviation of moisture warping in month *i* from the annual average (°F)

ϕ = reversible shrinkage factor, fraction of total shrinkage (use 0.5 unless better data is available)

ε_{su} = ultimate shrinkage (10^{-6}) *may be estimated using PCC mix properties using equation in Chapter 2 Section 2)

S_{hi} = relative humidity factor for month *i* determined by the following:

$S_{hi} = 1.1 \cdot RH_a$ for $RH_a < 30\%$ (A.69)

$S_{hi} = 1.4 - 0.01 \cdot RH_a$ for $30\% < RH_a < 80\%$ (A.70)

$S_{hi} = 3.0 - 0.03 \cdot RH_a$ for $RH_a \geq 80\%$ (A.71)

RH_a = ambient average relative humidity (%)

$S_{h\,ave}$ = annual average relative humidity factor (annual average of S_{hi})

h_s = depth of shrinkage zone (typically 2 in)

h = PCC slab thickness

a = PCC coefficient of thermal expansion (/ ºF)

The equivalent temperature gradient for any time after placement is determined by the following :

$$ETG_{Sht} = S_t \cdot ETG_{Shi} \tag{A.72}$$

where,

ETG_{Sht} = ETG_{Shi} at any time t days from PCC placement (ºF)

ETG_{Shi} = temperature difference equivalent of the deviation of moisture warping in month i from the annual average (°F)

S_t = time factor for moisture-related slab warping, found using :

$$S_t = \frac{Age}{n + Age} \tag{A.73}$$

Age = PCC age since placement (days)

N = time to develop 50% ultimate shrinkage strain esu (unless more accurate data is available, use 35, the ACI recommended value)

Calculate critical stress

Use finite element or neural networks to find critical top of slab transverse stress for all cases to be analyzed. For CRCP punchouts, the following increments must be considered :

- Load configuration (axle type)

- Load level
- Temperature gradient
- Lateral load position

Deterioration of crack stiffness and crack LTE

As cracks are subjected to vertical loading, crack walls are subjected to repetitious shear loading. This leads to aggregate wear-out which decreases LTE due to exposed aggregate interlocking. Crack shear capacity shows deterioration potential if the crack width-to-PCC thickness ratio is greater than 0.0037 (*cw* and h_{PCC} expressed in the same units). The loss of shear at the end of any time increment t is expressed by the following equations :

$$\Delta s_i = \sum_j \left(\frac{0.005}{1 + \left(\frac{cw_i}{h_{PCC}} \right)^{-5.7}} \right) \left(\frac{n_{ji}}{10^6} \right) \left(\frac{\tau_{ij}}{\tau_{ref\ i}} \right) ESR \qquad if \quad \frac{cw_i}{h_{PCC}} < 3.7 \qquad \text{(A.74)}$$

$$\Delta s_i = \sum_j \left(\frac{0.068}{1 + 6\left(\frac{cw_i}{h_{PCC}} - 3 \right)^{-1.98}} \right) \left(\frac{n_{ji}}{10^6} \right) \left(\frac{\tau_{ij}}{\tau_{ref\ i}} \right) ESR \qquad if \quad \frac{cw_i}{h_{PCC}} > 3.7 \qquad \text{(A.75)}$$

where,

Δs_i = loss in shear capacity for crack spacing as a summation over shear capacity losses due to each load application in each weight/axle group *j*

cw_i = crack width for time increment i (mils)

h_{PCC} = slab thickness (in)

n_{ji} = number of axle load applications for load level *j*

τ_{ij} = shear stress on the transverse crack at the corner due to load j (psi)

$\tau_{ref\,i}$ = reference shear stress derived from the PCA test results (psi)

ESR = equivalent shear ratio to adjust traffic load applications for lateral traffic wander

$$ESR = a + \frac{b \cdot l}{L} + c\frac{LTE_{crack}}{100} \tag{A.76}$$

where:

$$\begin{aligned} a &= 0.0026\overline{D}^2 - 0.1779\overline{D} + 3.2206 \\ b &= 0.1309Ln\left(\overline{D}\right) - 0.4627 \\ c &= 0.5798Ln\left(\overline{D}\right) - 2.061 \end{aligned} \tag{A.77}$$

L = crack spacing (in)

l = radius of relative stiffness (in) (discussed earlier)

LTE_{crack} = load transfer efficiency of transverse crack (%)

Reference shear stresses (τ_{ref}) are computed as follows:

$$\tau_{ref} = (111.1)\exp\{-\exp(x')\} \tag{A.78}$$

where :

$$x' = 0.9988 \cdot \exp(-0.1089 \cdot Ln(J_c))^{1.0} \tag{A.79}$$

where,

J_c = computed joint stiffness of the transverse crack

The constants for the *x'* equation may vary by aggregate type. However, preliminary test results indicate that this variation is small, as long as the aggregates are coarse.

Finally, as load applications increase, losses in shear capacity calculated for each time increment are accumulated as follows :

$$\Delta S_i = \sum_{i=1}^{current} \Delta s_i = \Delta S_{i-1} + \Delta s_i \quad \text{(A.80)}$$

where,

ΔS_i = loss in shear capacity accumulated over all previous time increments, including current time increment *i*

Δs_i = loss in shear capacity during current time increment i due to all weight/axle type group *j*

ΔS_{i-1} = loss in shear capacity accumulated over all previous time increments excluding the current time increment *i*

Calculate fatigue damage

Accumulated fatigue damage due to slab bending in the transverse direction is found using incremental analysis. This is the main parameter in prediction of CRCP punchouts. While the effects of concrete strength gain, subgrade support, and climatic conditions are broken into monthly time increments, all effects due to temperature gradients within the slab are calculated in hourly increments, (i.e., temperature conditions in PCC slabs vary continuously throughout each day and have a dramatic effect on pavement response).

For each time increment, the number of applied traffic loads (n_{ij}) in the traffic lane are computed using input traffic data for the analysis period. The following are also considered in the analysis :

- Estimated traffic load spectra
- Axle load distributions by axle type

- Lateral offsets from slab edge

Maximum bending stress is calculated and used in the following equation to determine the maximum number of allowable axle load applications :

$$\log\left(N_{i,j}\right) = 2.0 \cdot \left(\frac{MR_i}{\sigma_{i,j}}\right)^{1.22} - 1 \qquad \text{(A.81)}$$

where,

$N_{i,j}$ = number of allowable axle load applications during time increment *i* due to load of magnitude *j*

MR_i = PCC modulus of rupture at age i (psi)

$\sigma_{i,j}$ = maximum bending stress at time increment *i* due to load of magnitude *j*

Fatigue damage from all design wheel loads and all traffic increments are summed using Miner's rule as follows :

$$FD = \sum \frac{n_{i,j}}{N_{i,j}} \qquad \text{(A.82)}$$

where,

FD = accumulated fatigue damage over the design period for the current crack spacing occurring at the critical fatigue location of the slab

$n_{i,j}$ = number of applied axle loads of the j^{th} magnitude evaluated during the i^{th} time increment

$N_{i,j}$ = number of allowable axle load applications of the j^{th} magnitude evaluated during the i^{th} time increment

i = number of time increment

j = number of load magnitude

Determine the amount of punchouts

CRCP punchouts (PO) are predicted using the following nationally calibrated model:

$$PO = \frac{106.3}{1 + 4.0\left(FD^{-0.40}\right)} \tag{A.83}$$

where,

F.D. = accumulated fatigue damage.

APPENDIX B

CLUSTER ANALYSIS RESULTS

This appendix contains the clustering trees produced for both AVC and WIM R data in each state where a design site exists.

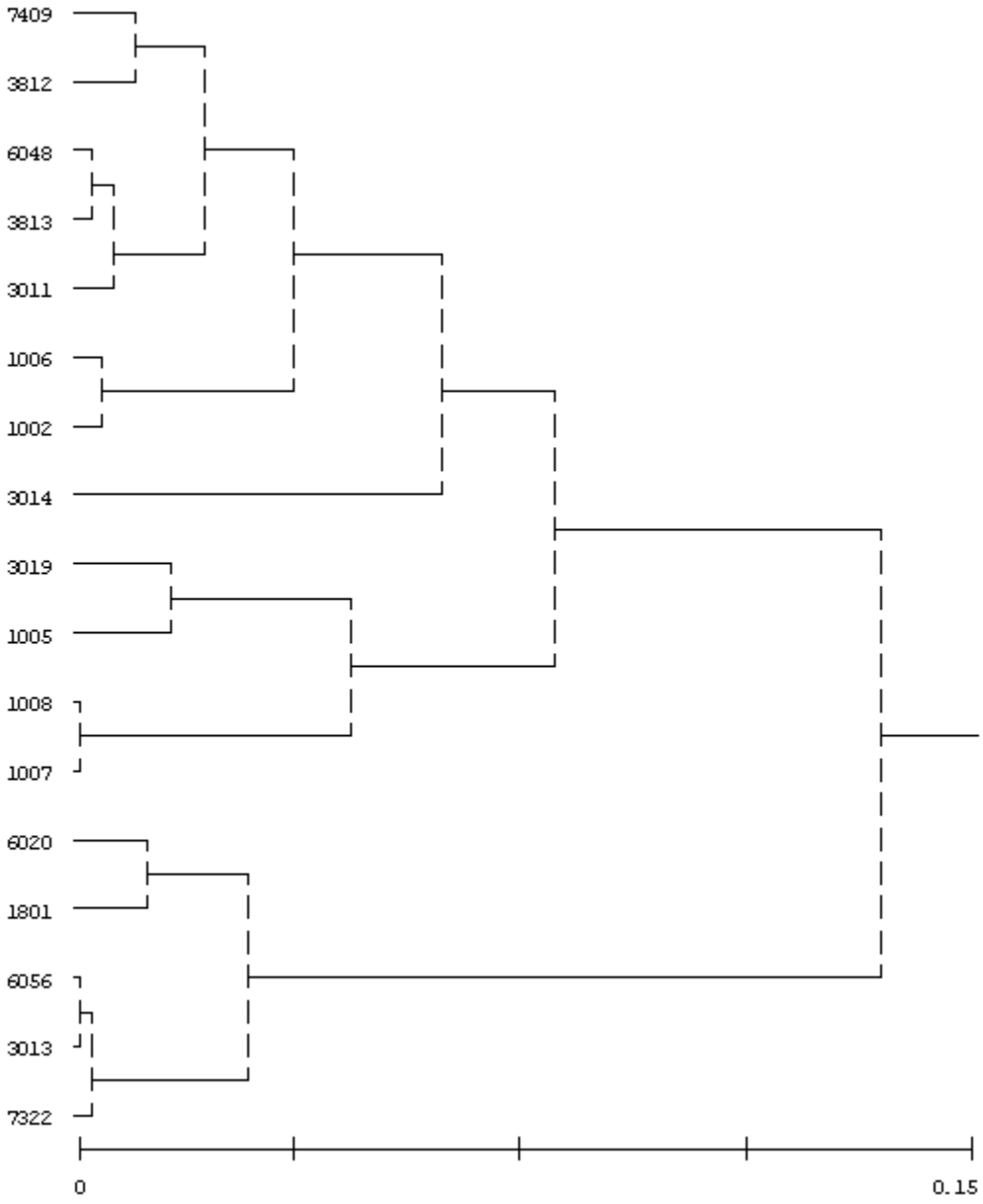

Figure B.1: Clusters of LTPP Sites by Annual Tandem Axle Load Distribution; WA

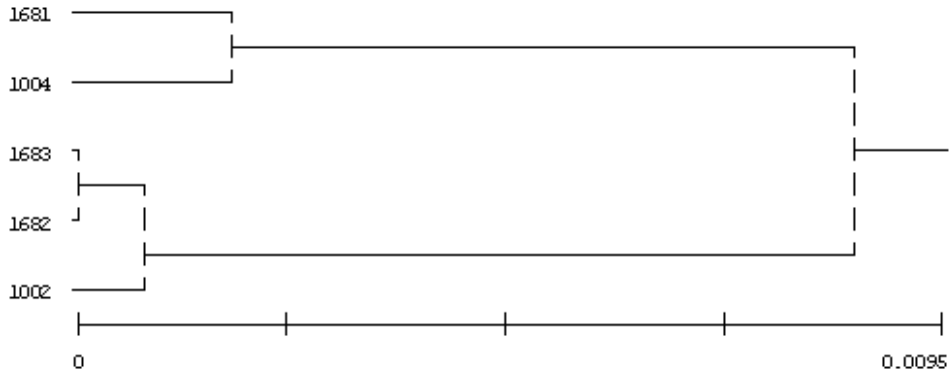

Figure B.2: Clusters of LTPP Sites by Annual Tandem Axle Load Distribution; VT

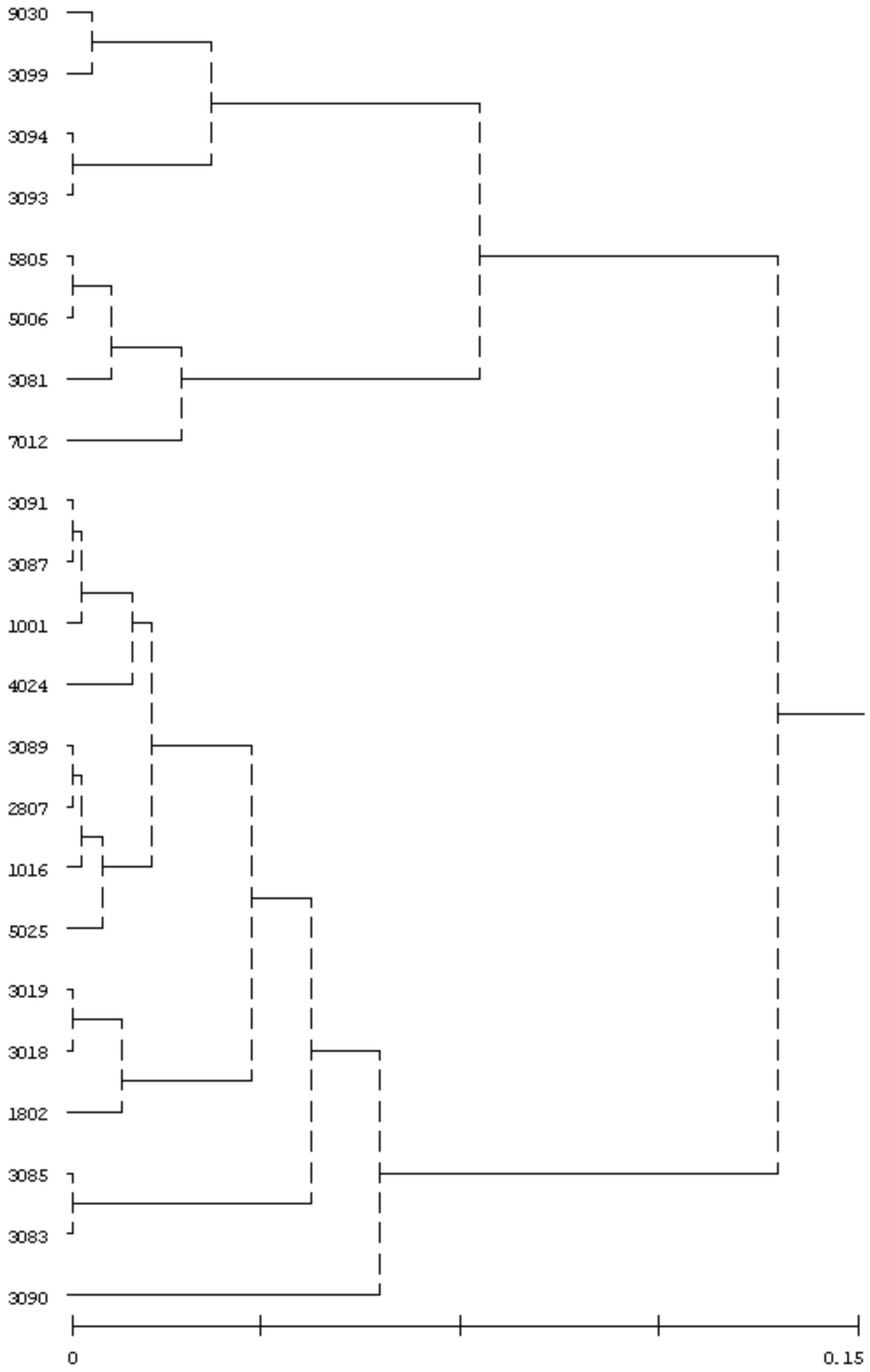

Figure B.3: Clusters of LTPP Sites by Annual Tandem Axle Load Distribution; MS

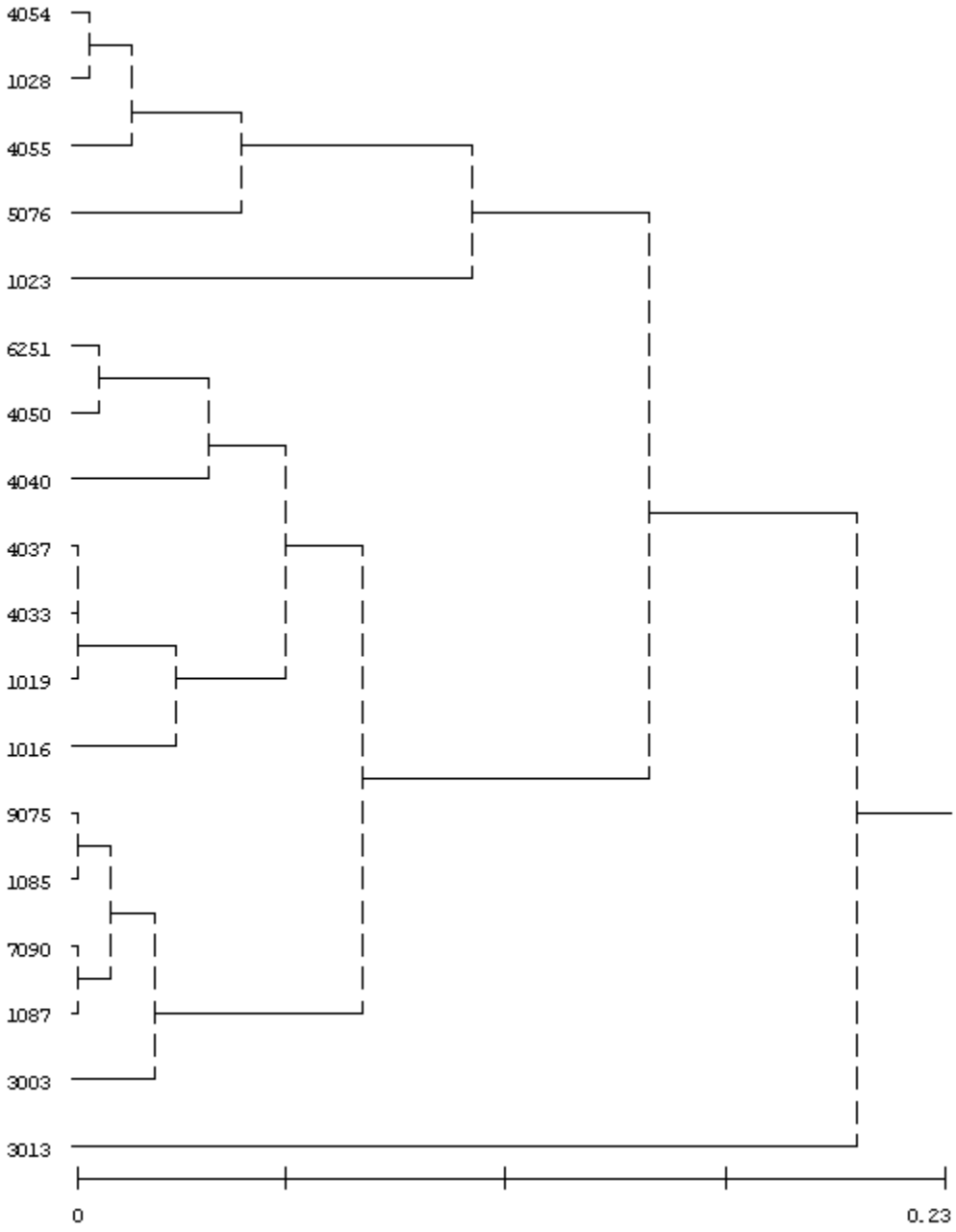

Figure B.4: Clusters of LTPP Sites by Annual Tandem Axle Load Distribution; MN

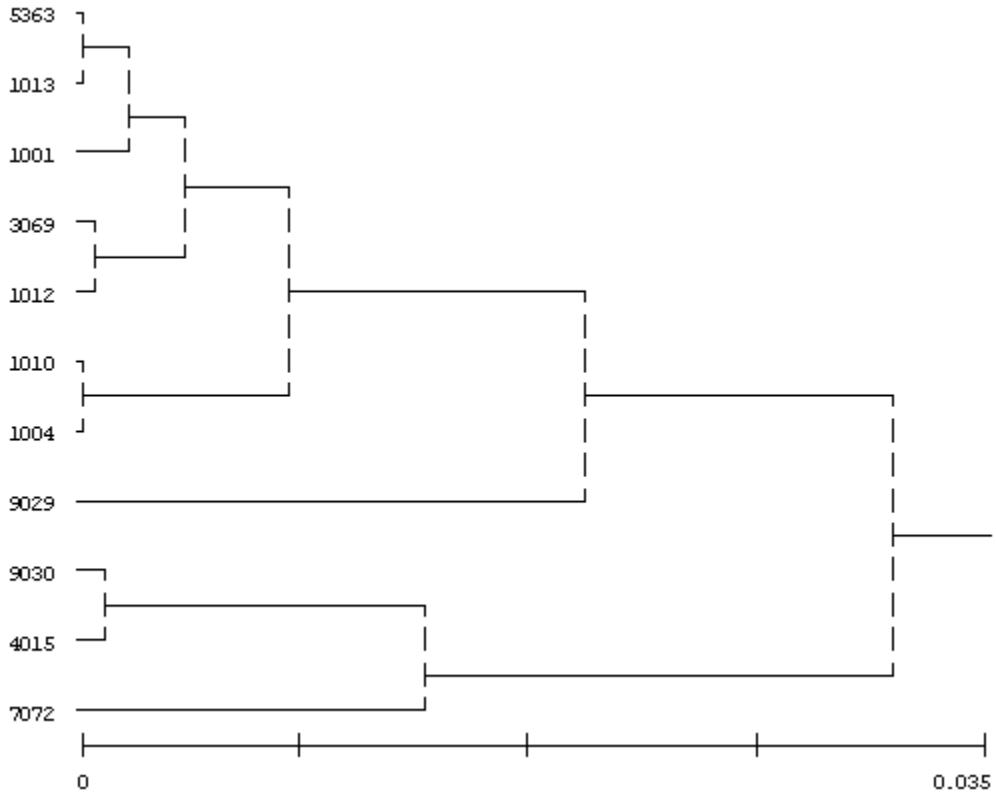

Figure B.5: Clusters of LTPP Sites by Annual Tandem Axle Load Distribution; MI

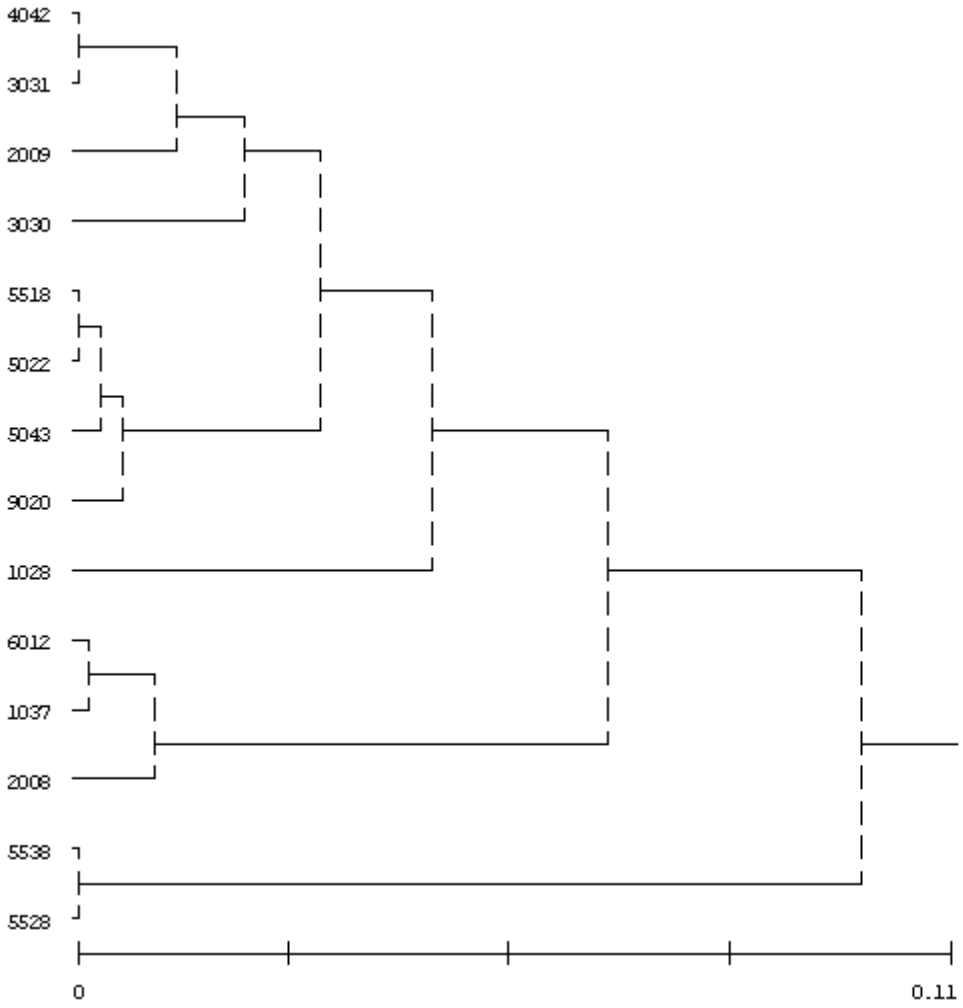

Figure B.6: Clusters of LTPP Sites by Annual Tandem Axle Load Distribution; IN

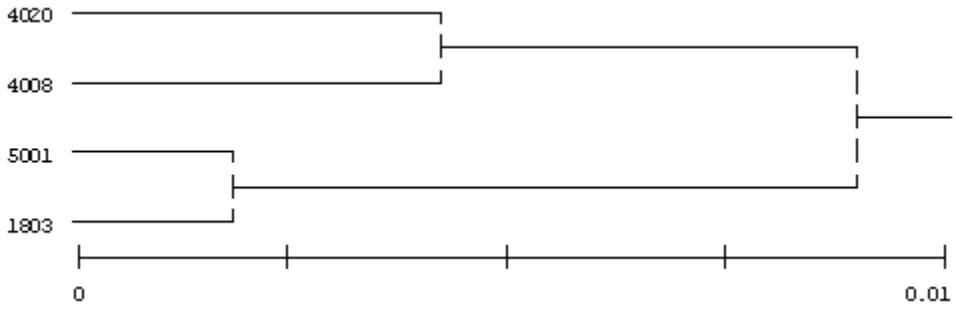

Figure B.7: Clusters of LTPP Sites by Annual Tandem Axle Load Distribution; CT

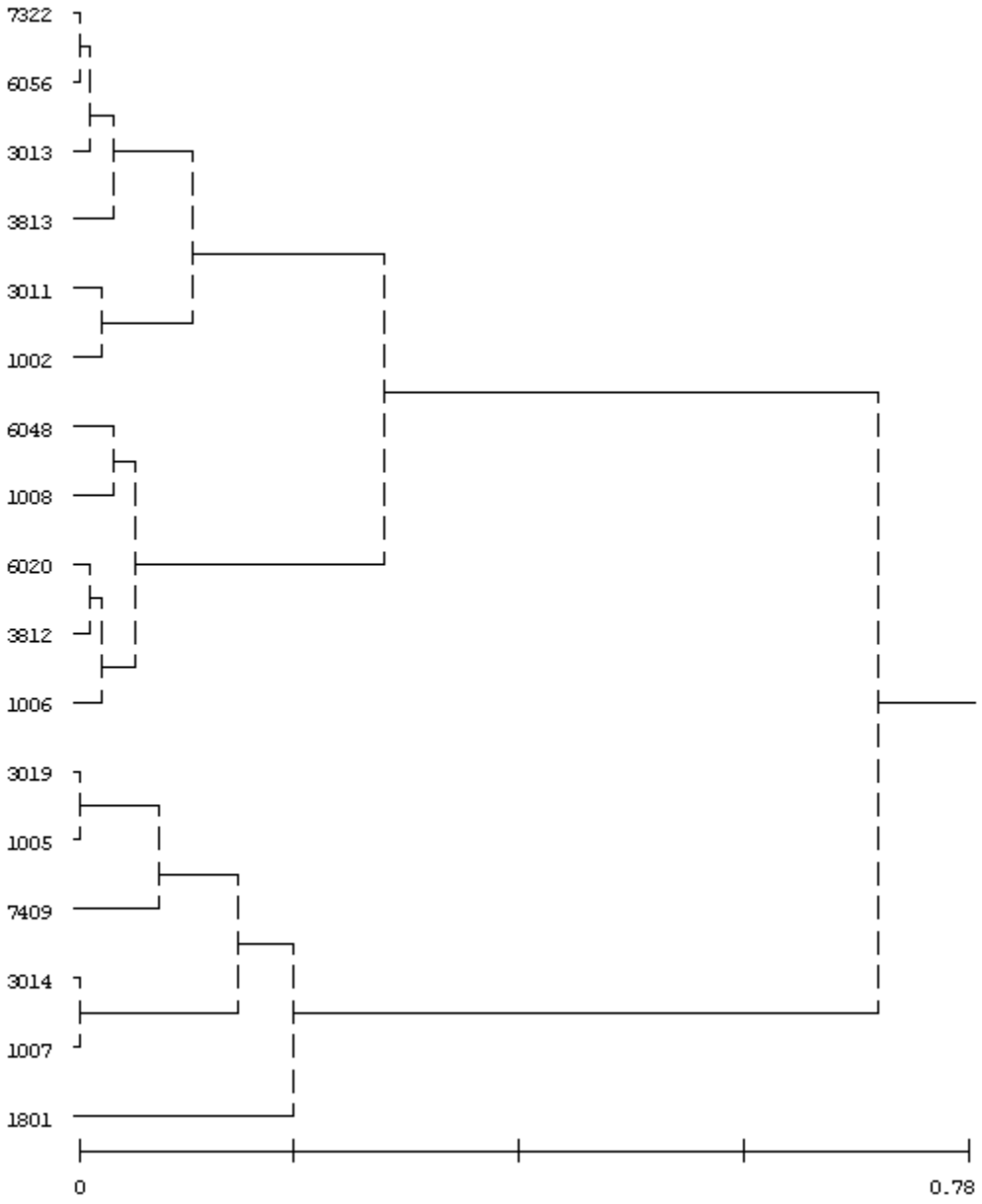

Figure B.8: Clusters of LTPP Sites by Annual Average Truck Class Distribution; WA

Figure B.9: Clusters of LTPP Sites by Annual Average Truck Class Distribution; VT

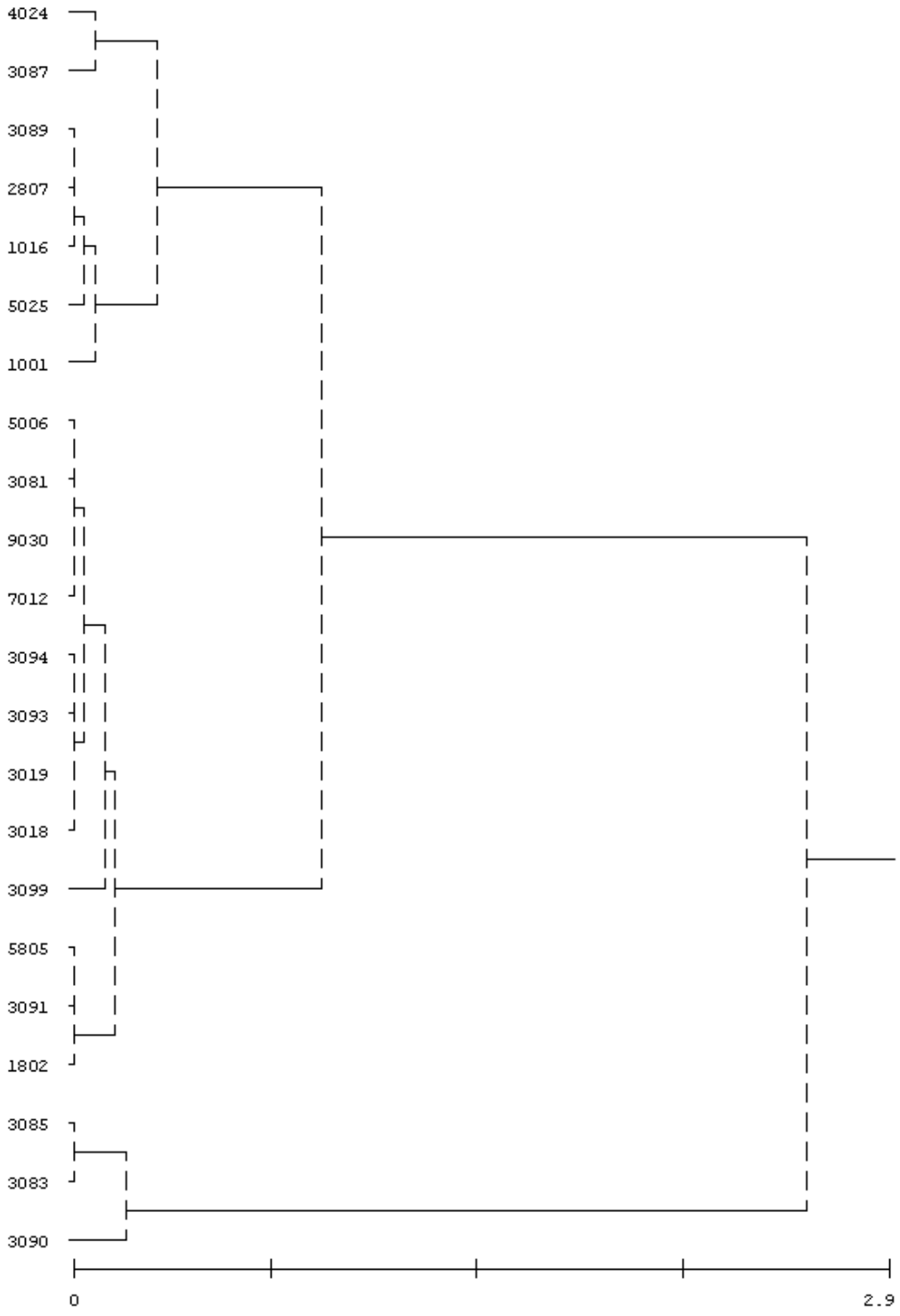

Figure B.10: Clusters of LTPP Sites by Annual Average Truck Class Distribution; MS

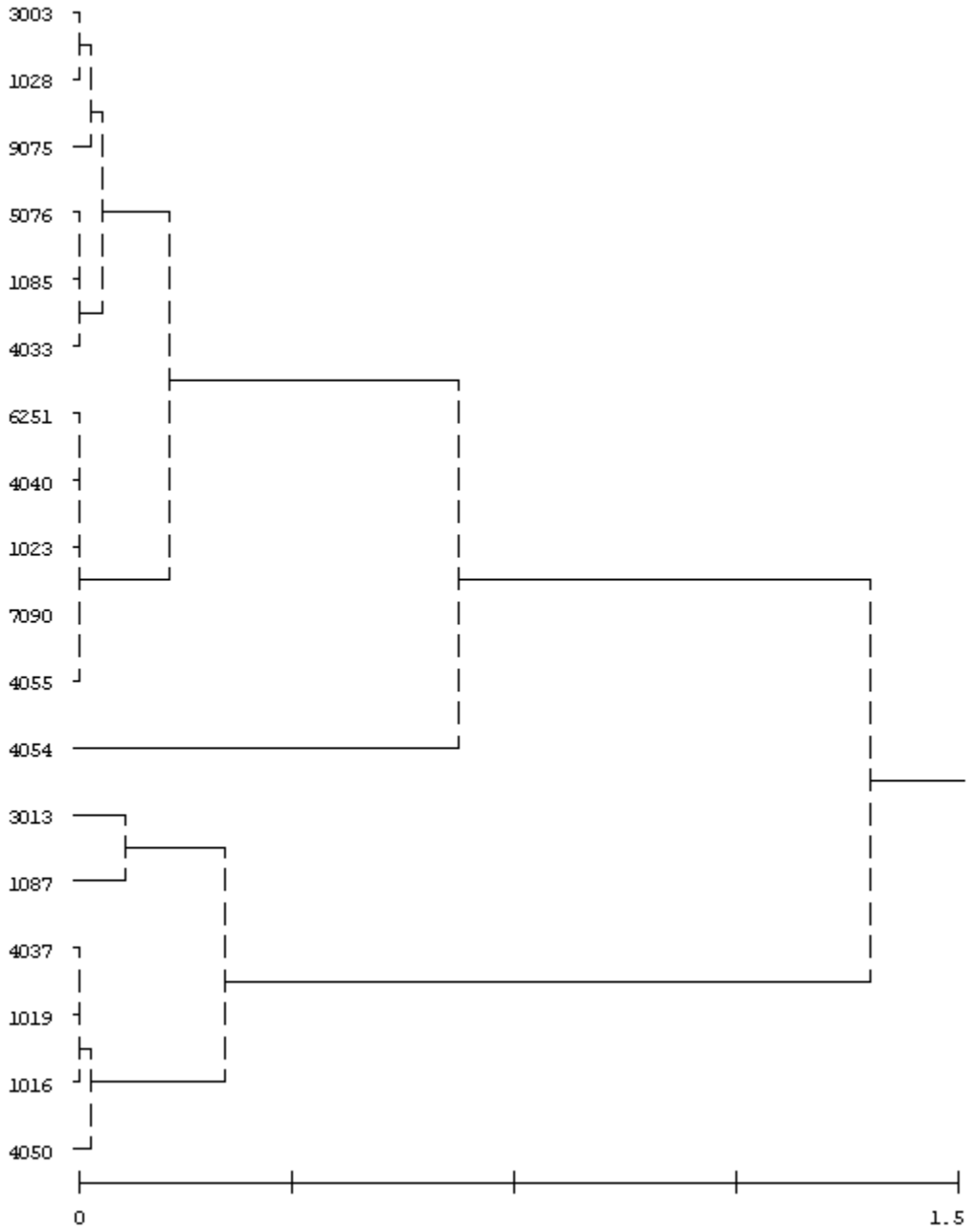

Figure B.11: Clusters of LTPP Sites by Annual Average Truck Class Distribution; MN

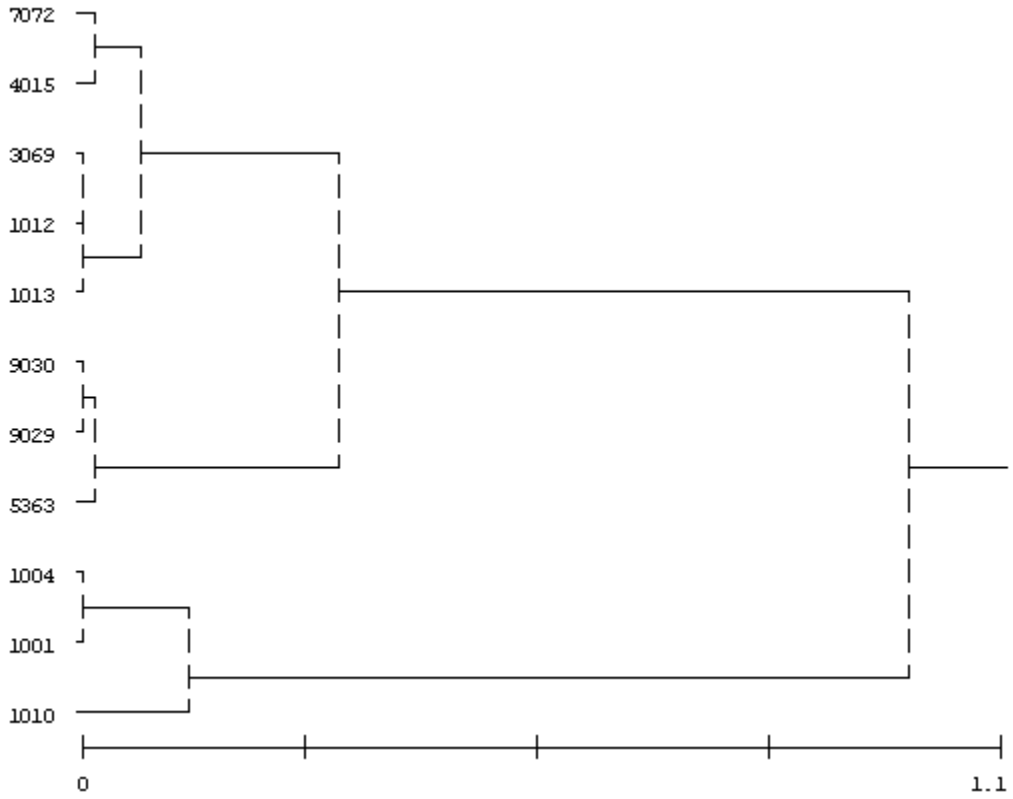

Figure B.12: Clusters of LTPP Sites by Annual Average Truck Class Distribution; MI

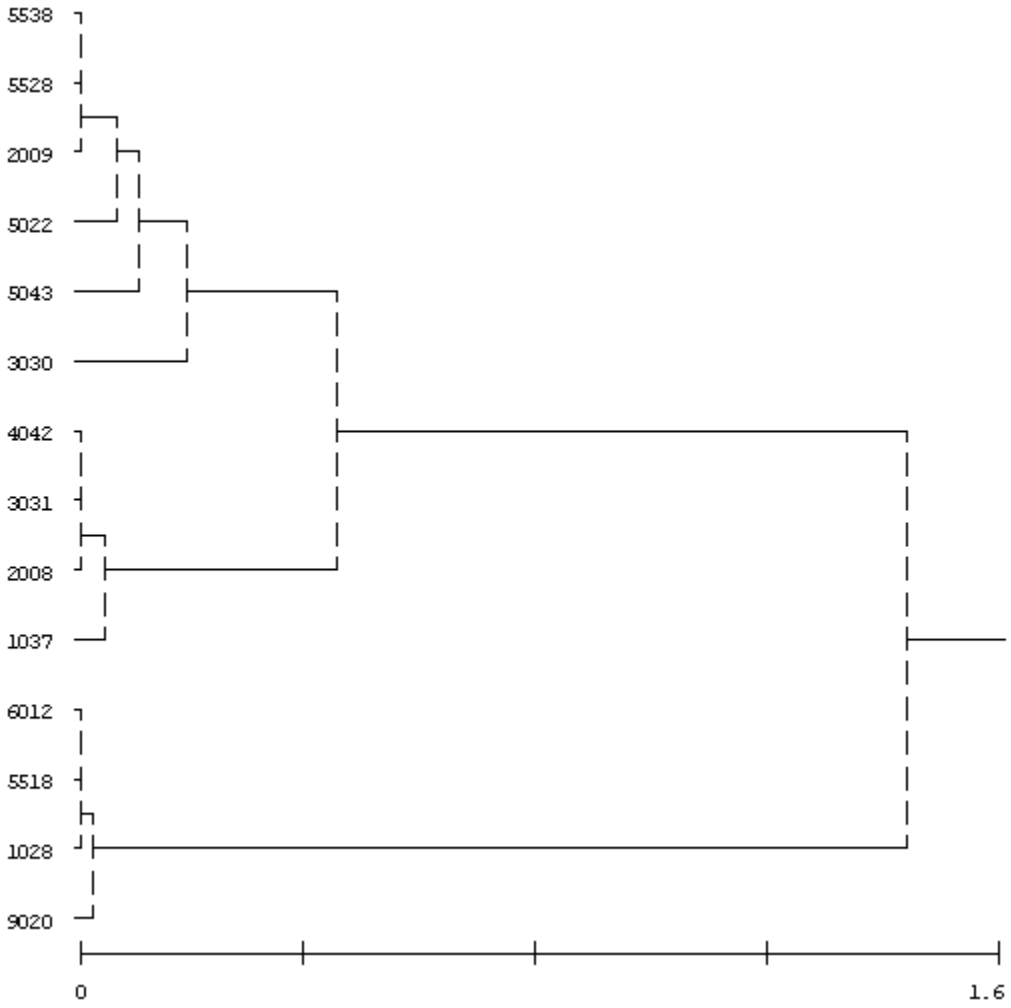

Figure B.13: Clusters of LTPP Sites by Annual Average Truck Class Distribution; IN

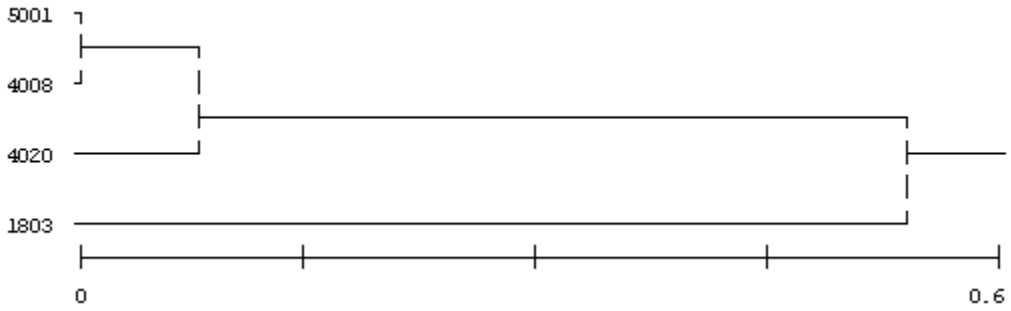

Figure B.14: Clusters of LTPP Sites by Annual Average Truck Class Distribution; CT

APPENDIX C

Axle Load Spectra

This appendix contains single, tandem, triple, and quadruple normalized annual average axle load spectra used for each design site.

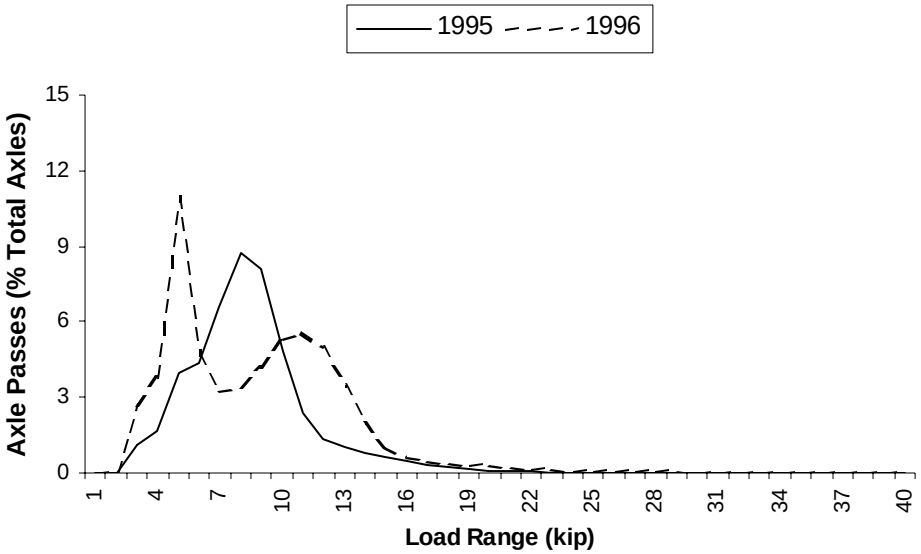

Figure C.1; Single Axles, 28-2807

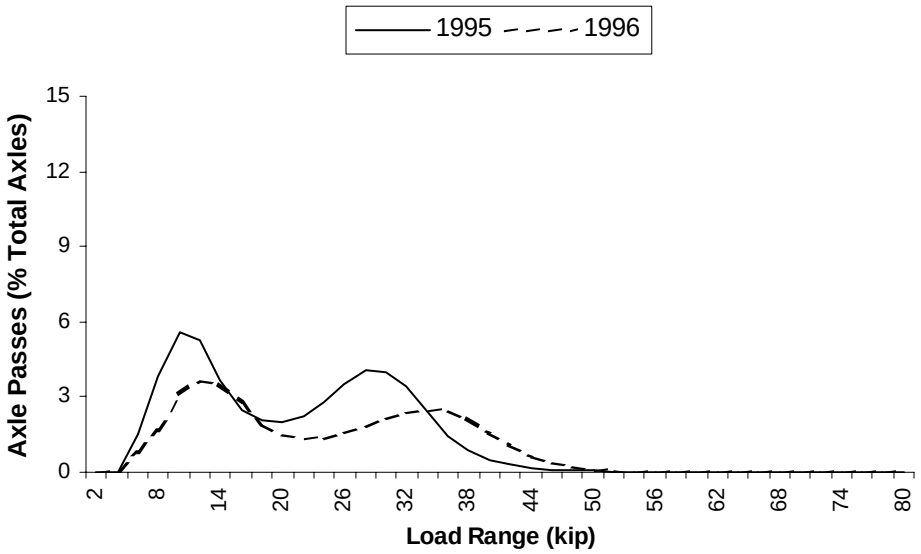

Figure C.2; Tandem Axles, 28-2807

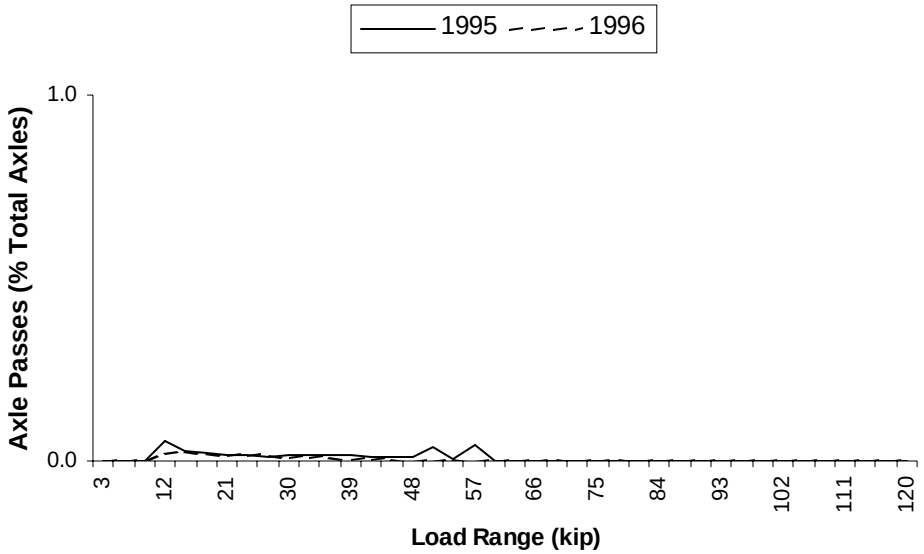

Figure C.3; Tridem Axles, 28-2807

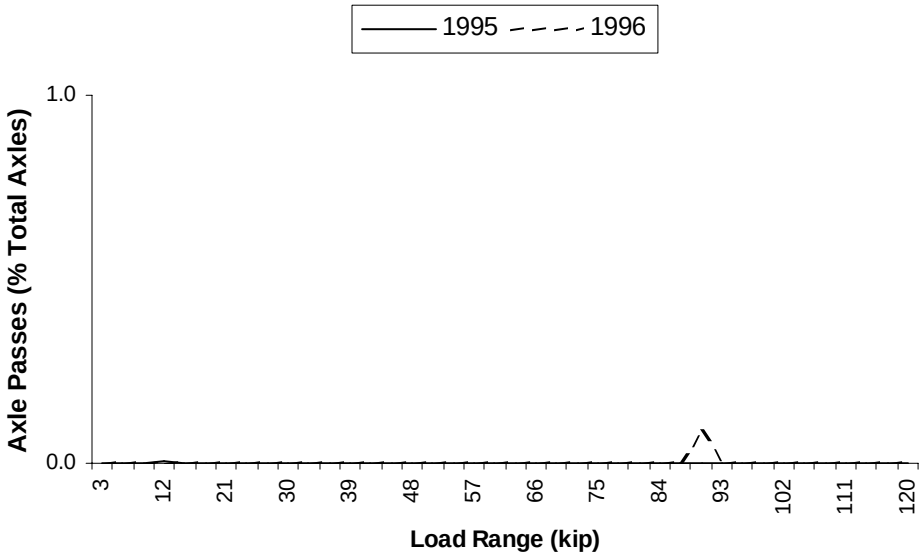

Figure C.4; Quad Axles, 28-2807

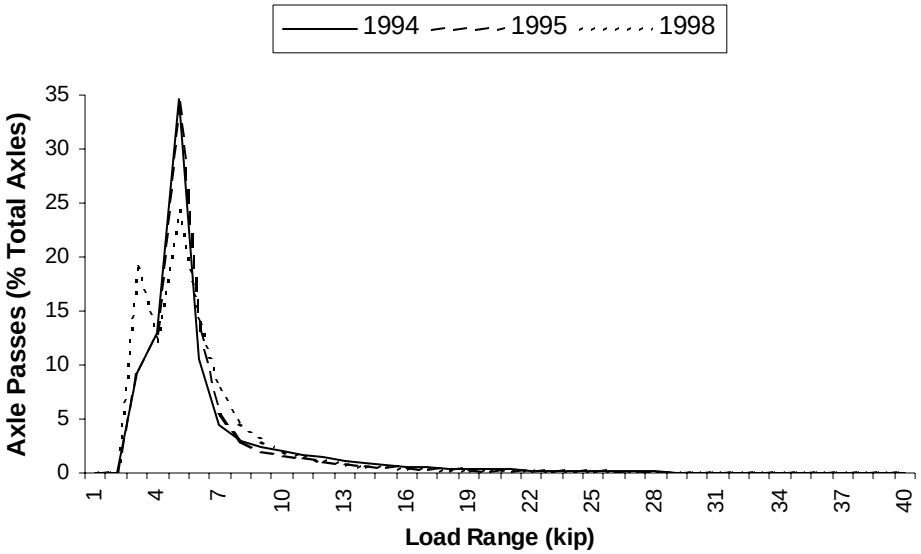

Figure C.5; Single Axles, 26-1010

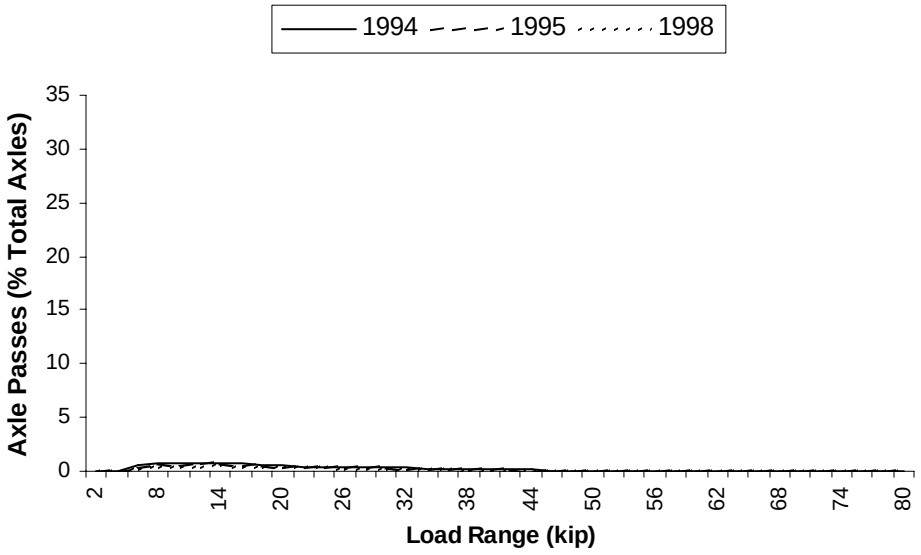

Figure C.6; Tandem Axles, 26-1010

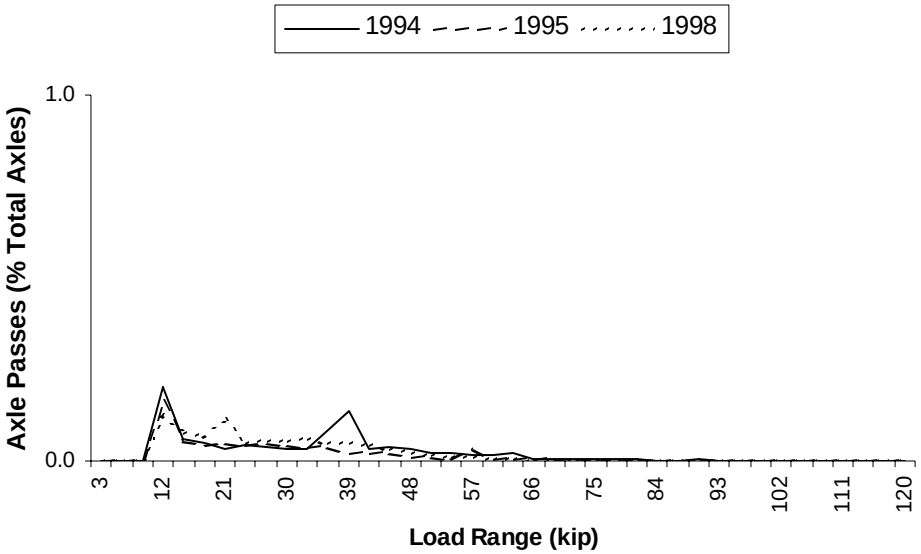

Figure C.7; Tridem Axles, 26-1010

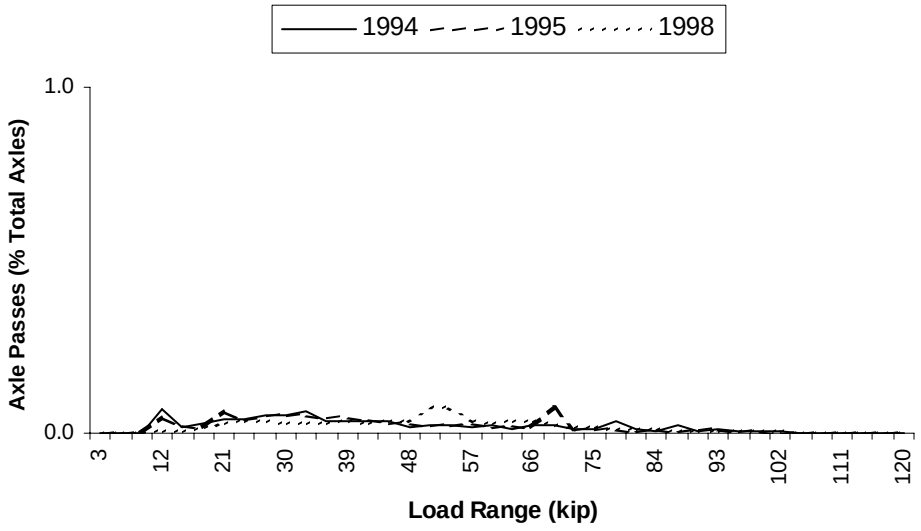

Figure C.8; Quad Axles, 26-1010

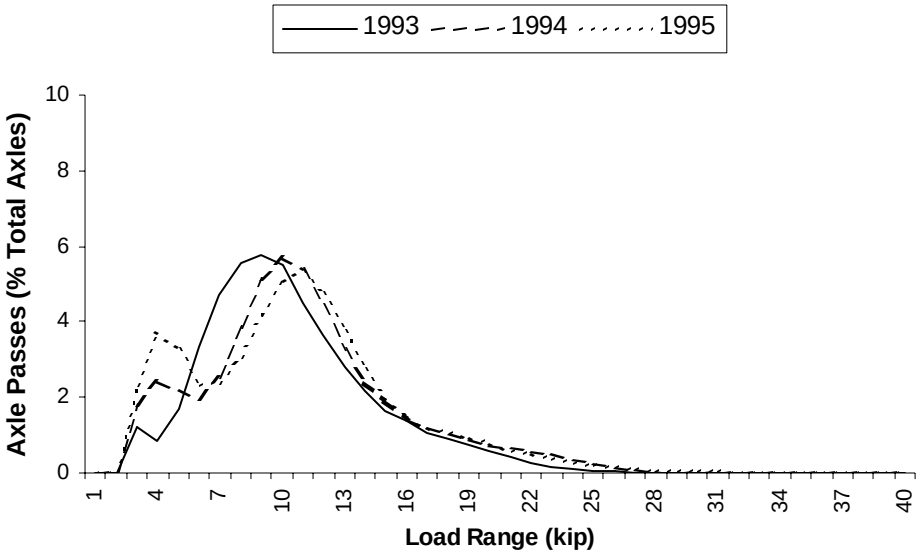

Figure C.9; Single Axles, 53-1007

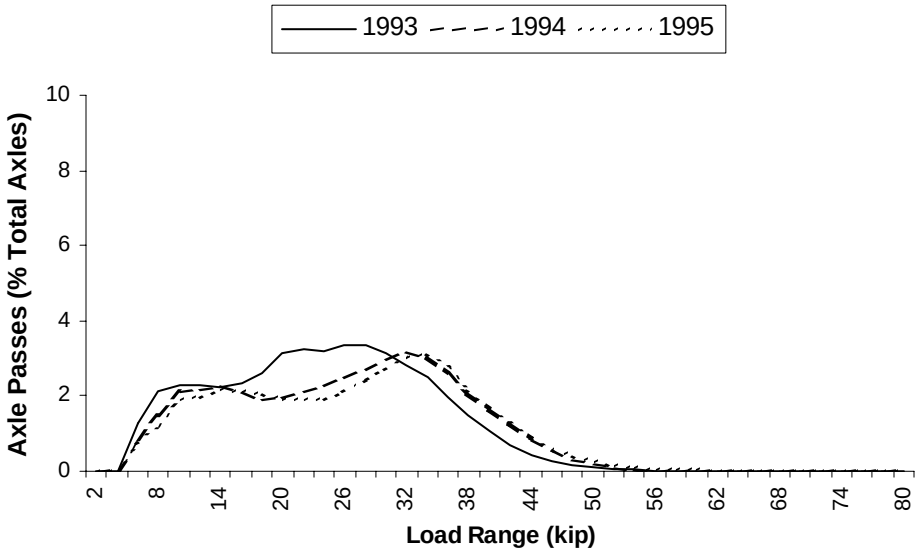

Figure C.10; Tandem Axles, 53-1007

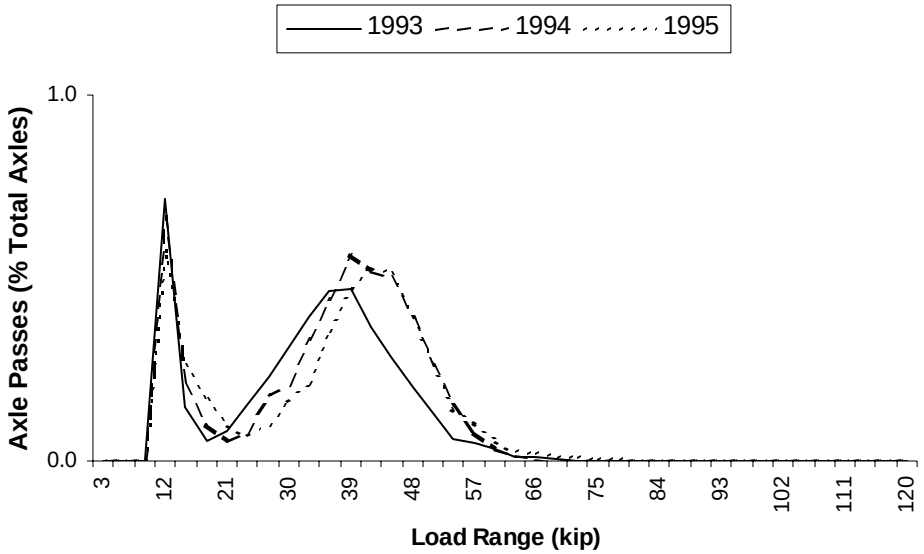

Figure C.11; Tridem Axles, 53-1007

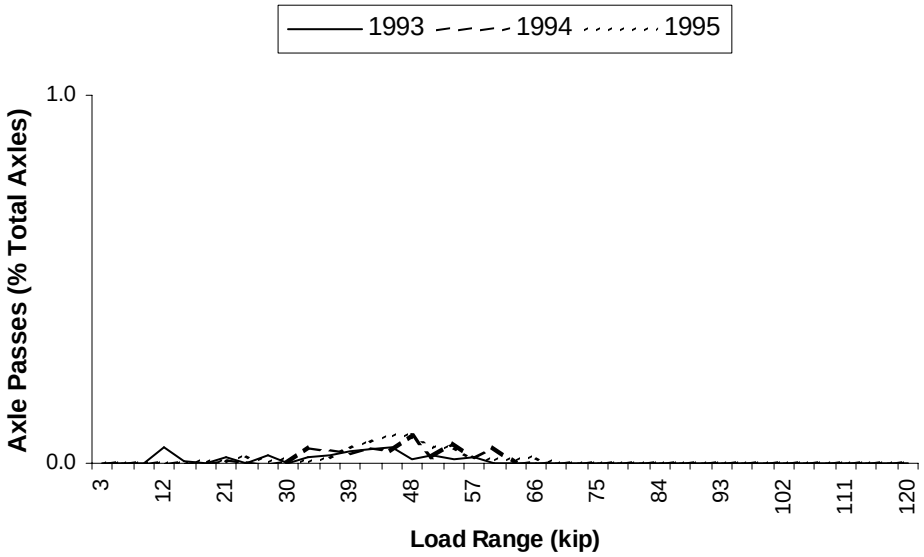

Figure C.12; Quad Axles, 53-1007

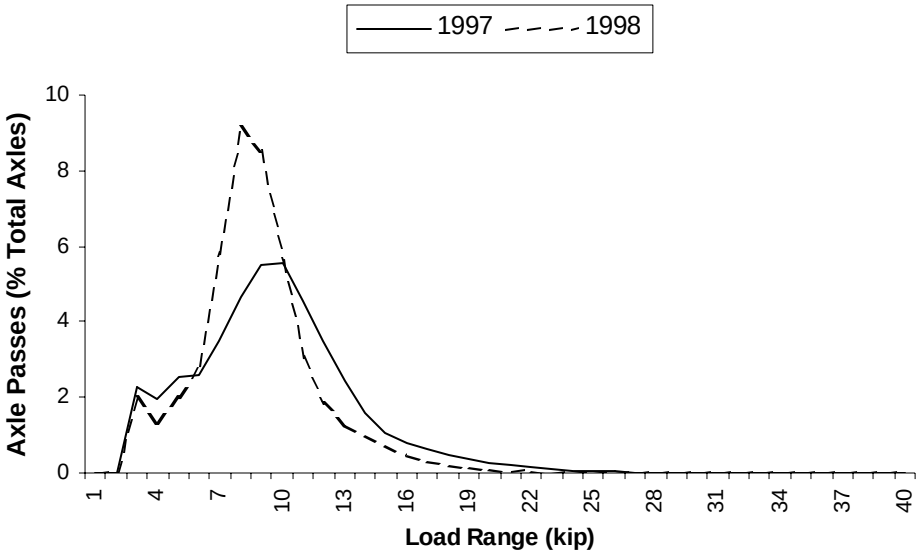

Figure C.13; Single Axles, 18-1028

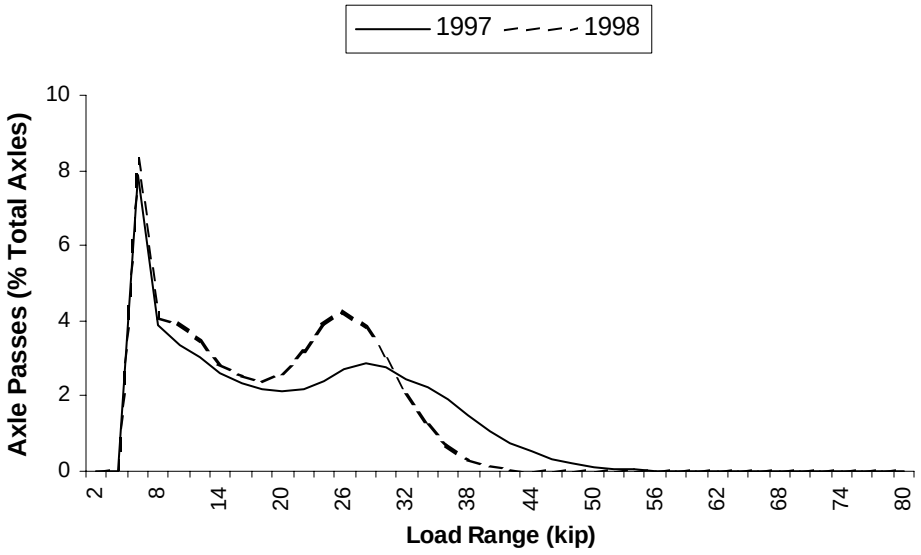

Figure C.14; Tandem Axles, 18-1028

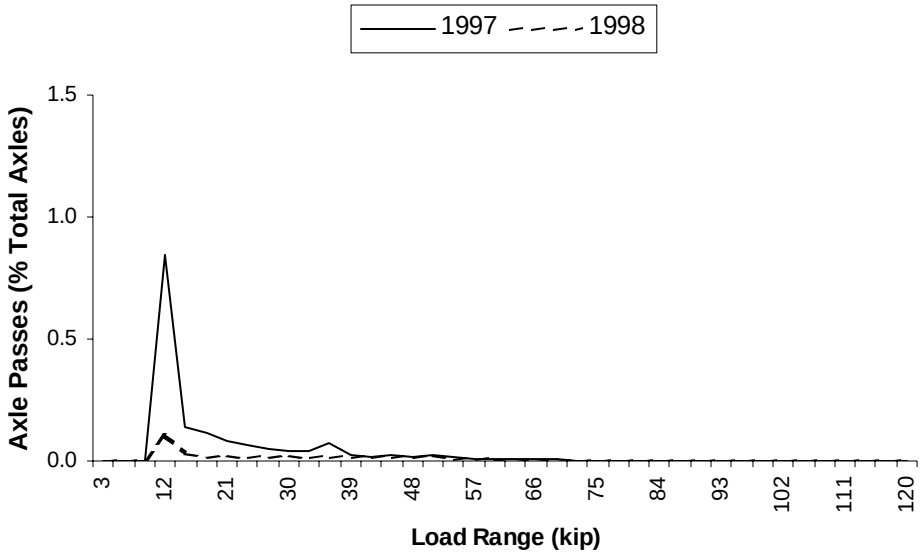

Figure C.15; Tridem Axles, 18-1028

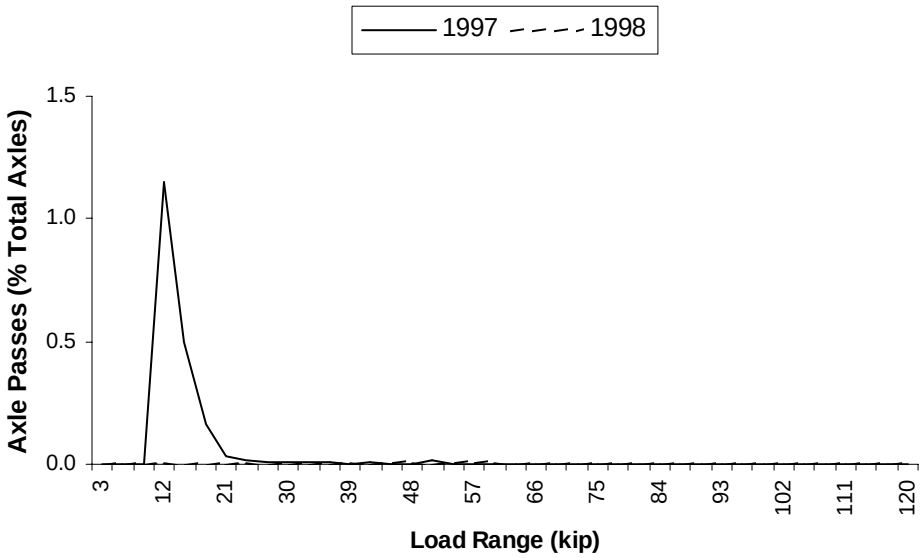

Figure C.16; Quad Axles, 18-1028

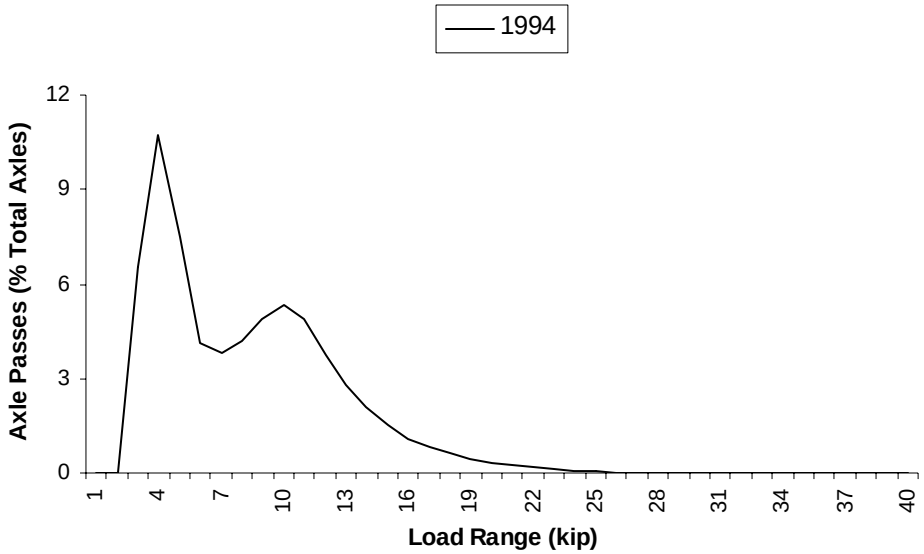

Figure C.17; Single Axles, 53-6048

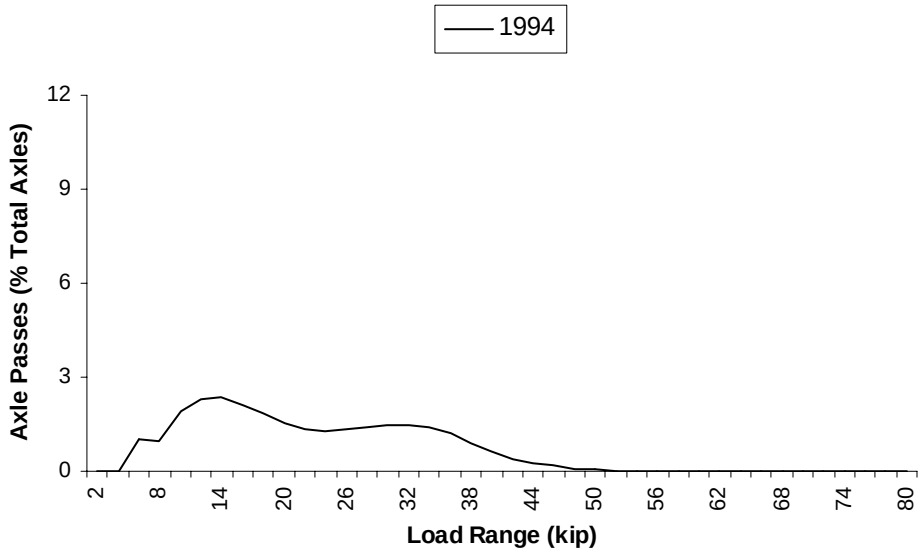

Figure C.18; Tandem Axles, 53-6048

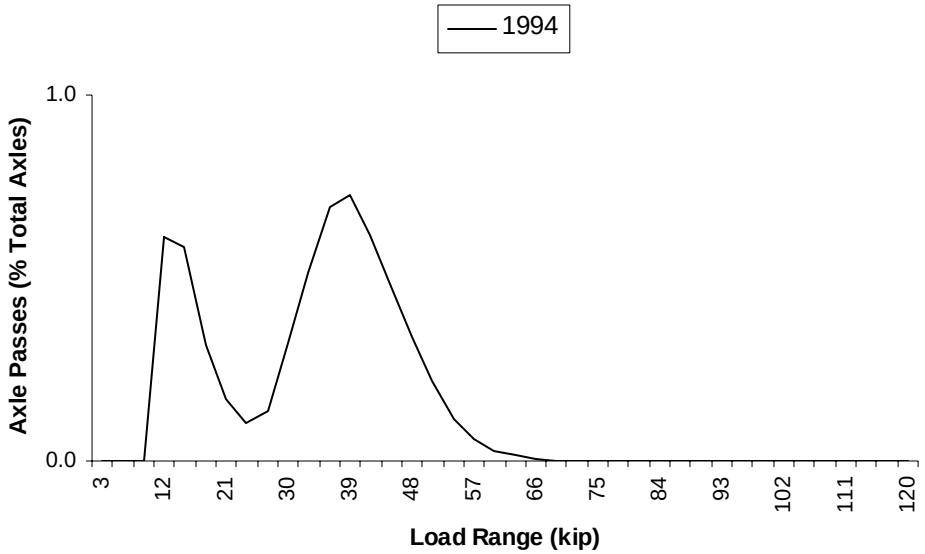

Figure C.19; Tridem Axles, 53-6048

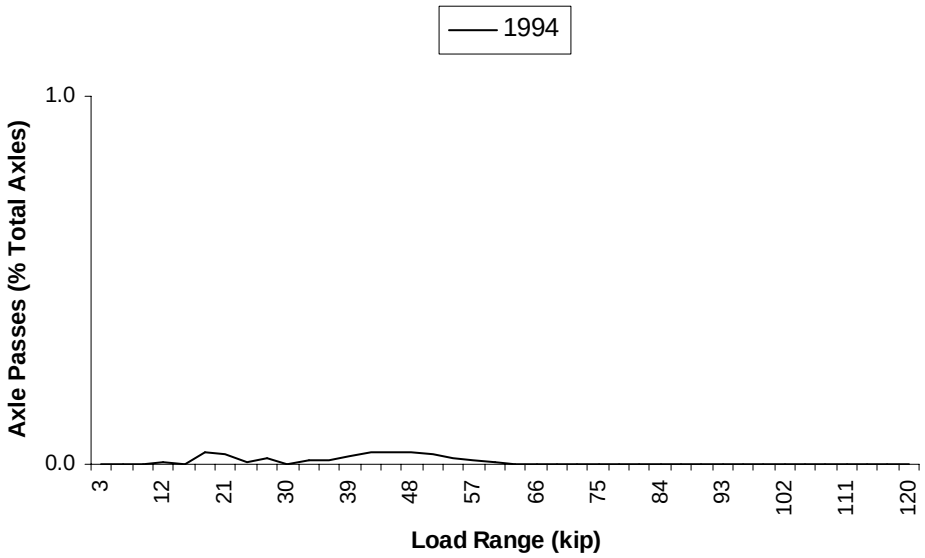

Figure C.20; Quad Axles, 53-6048

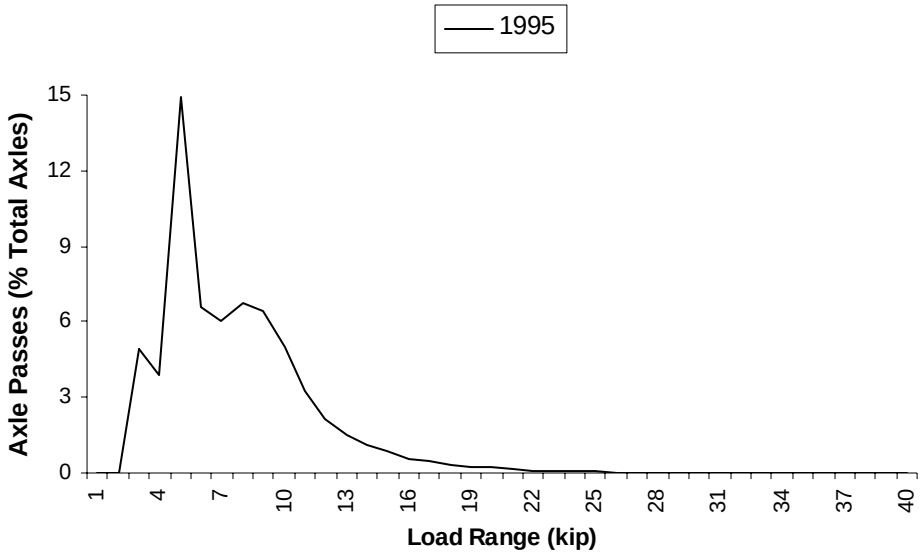

Figure C.21; Single Axles, 28-4024

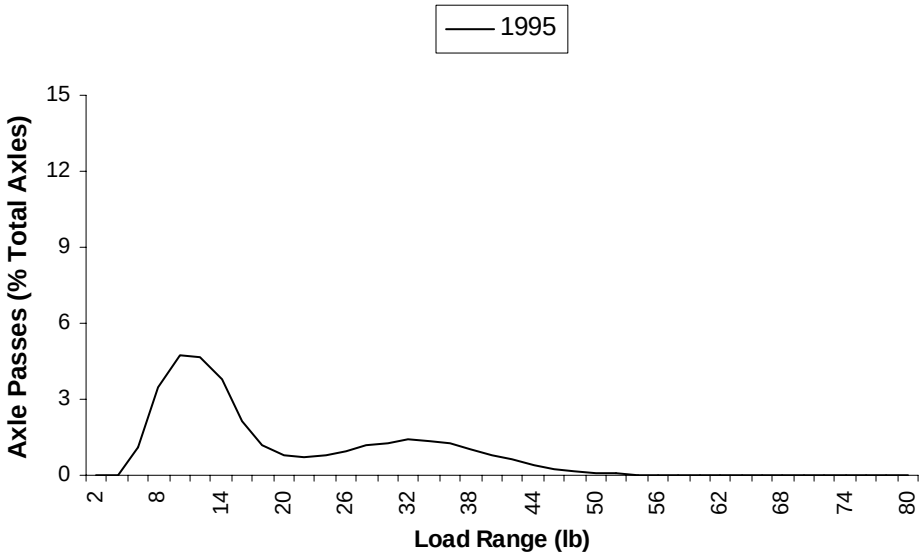

Figure C.22; Tandem Axles, 28-4024

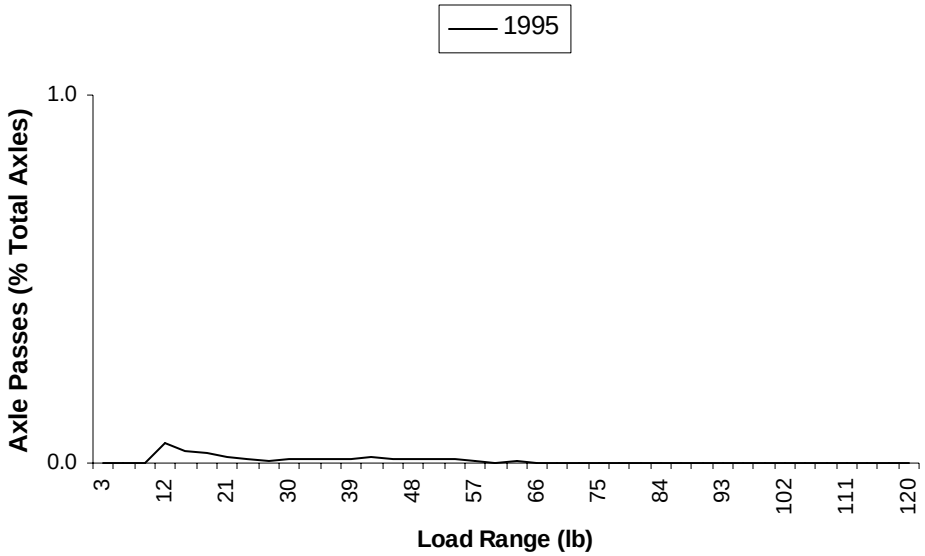

Figure C.23; Tridem Axles, 28-4024

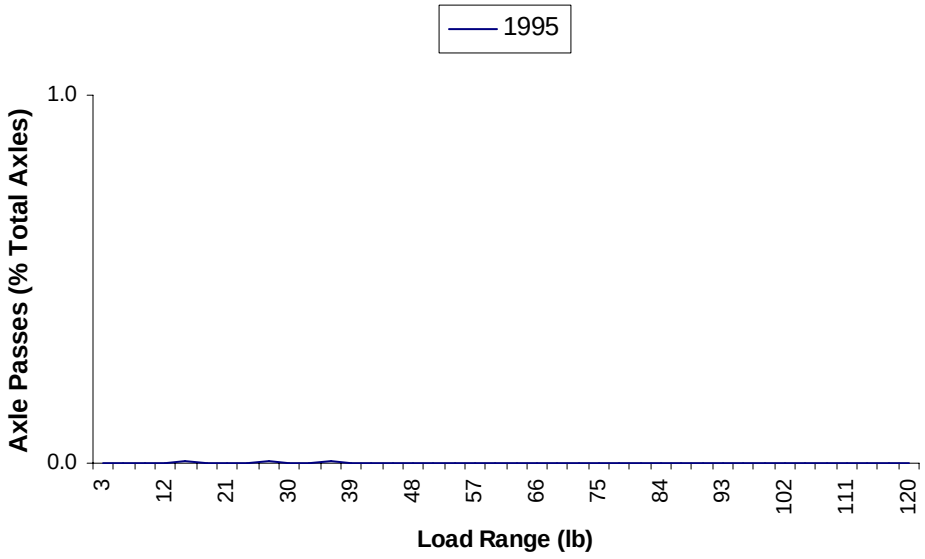

Figure C.24; Quad Axles, 28-4024

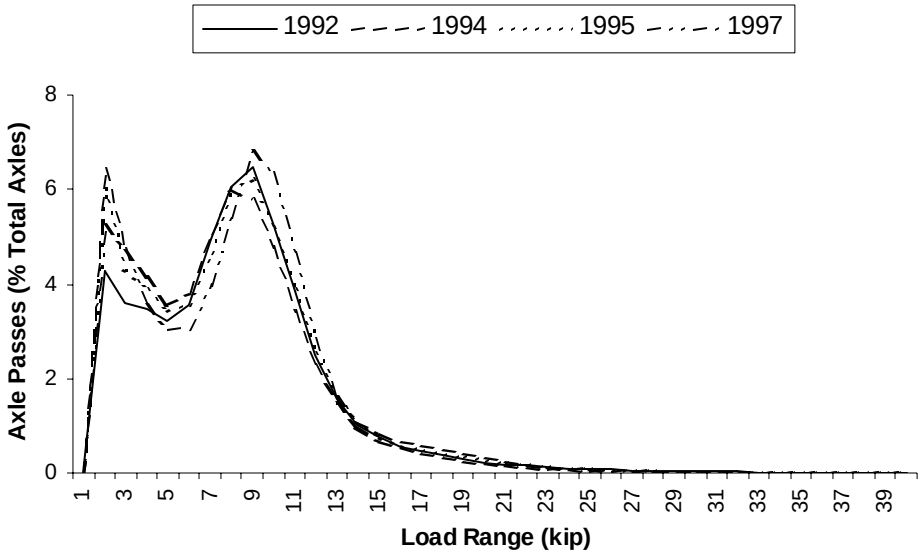

Figure C.25; Single Axles, 50-1682

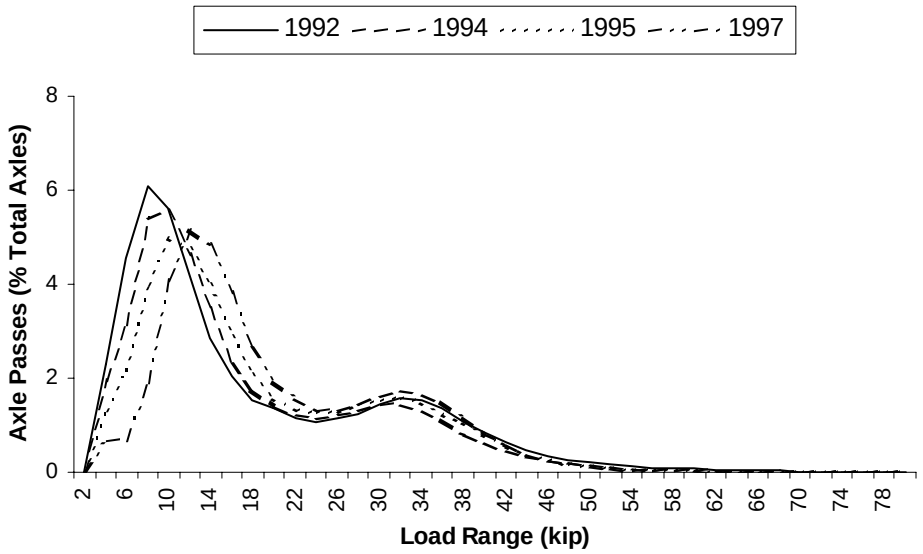

Figure C.26; Tandem Axles, 50-1682

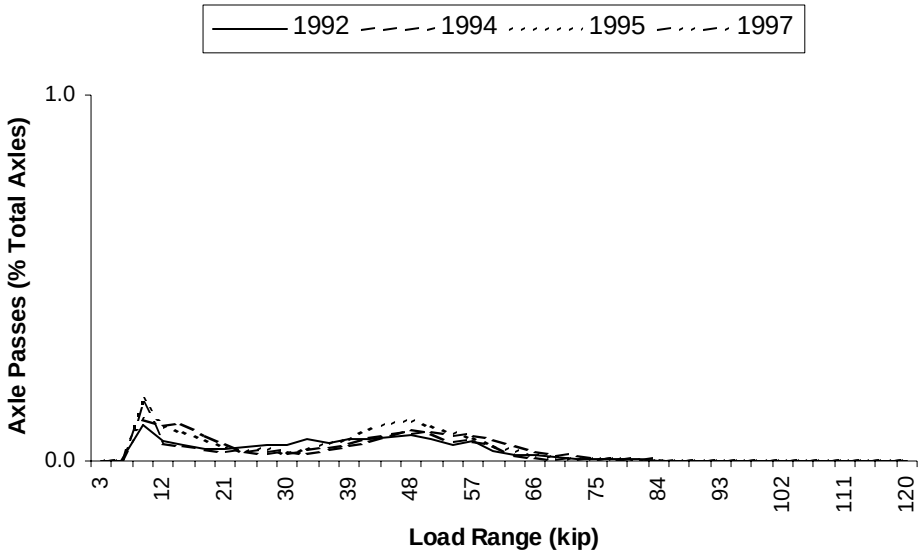

Figure C.27; Tridem Axles, 50-1682

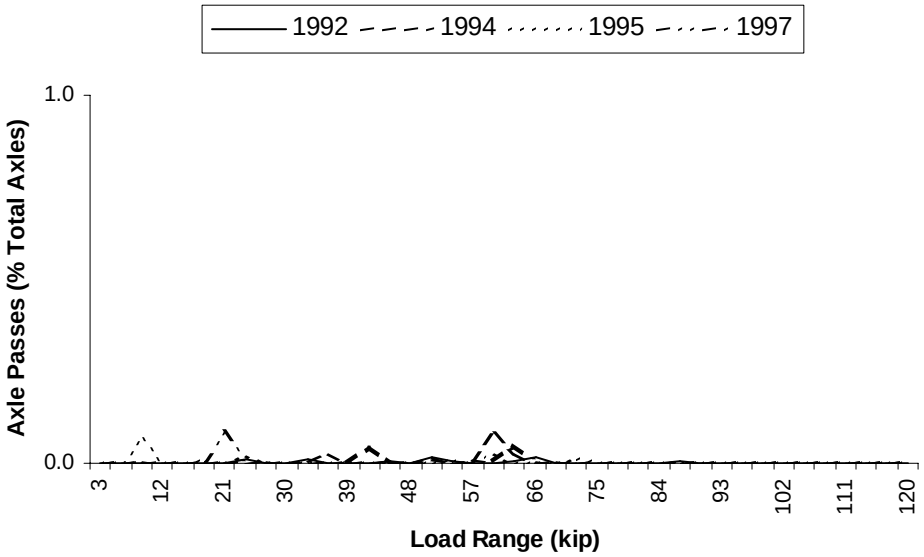

Figure C.28; Quad Axles, 50-1682

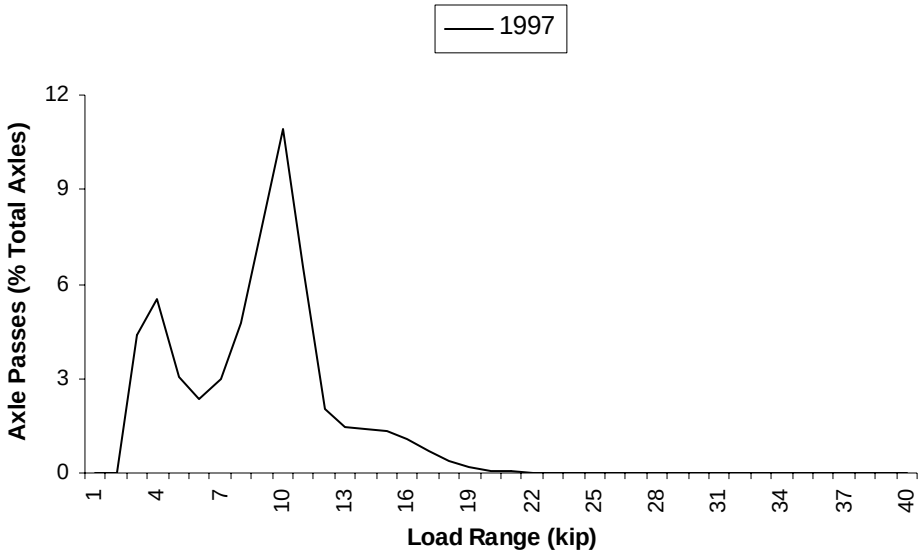

Figure C.29; Single Axles, 27-5076

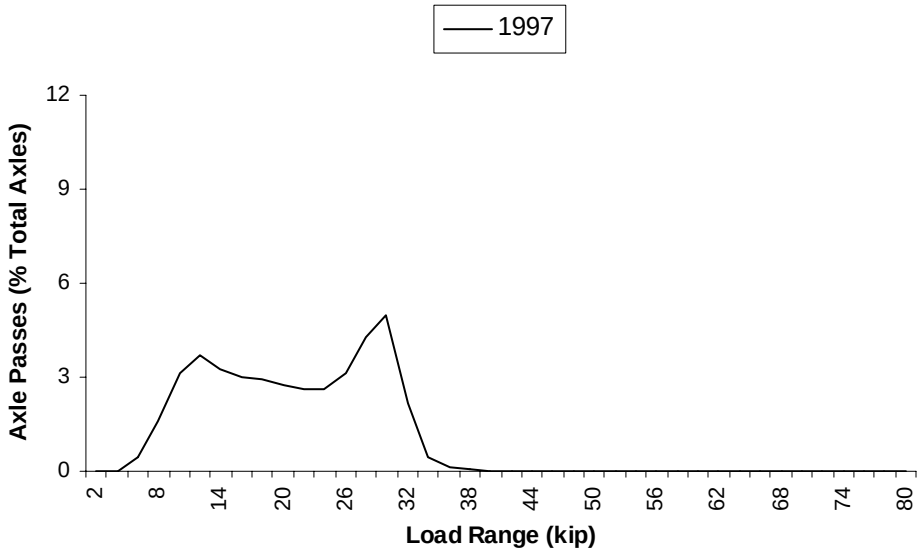

Figure C.30; Tandem Axles, 27-5076

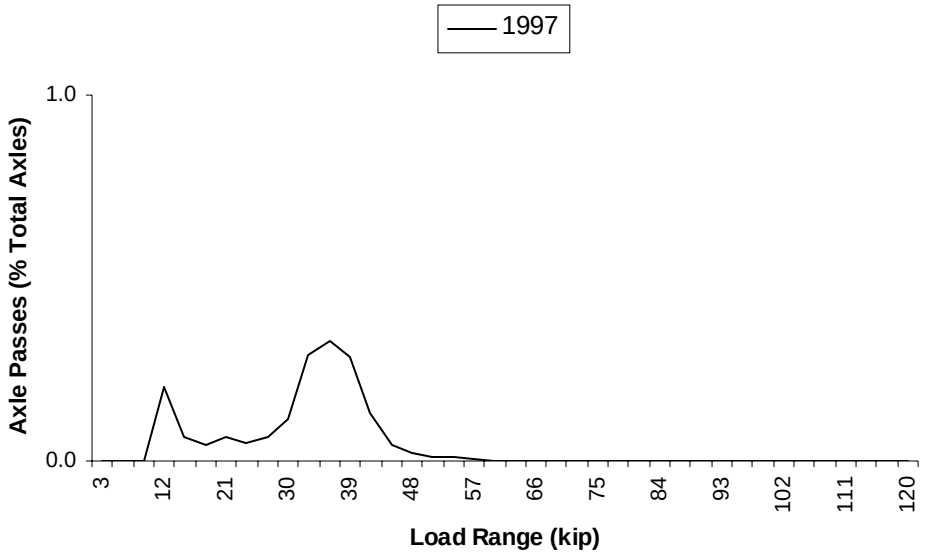

Figure C.31; Tridem Axles, 27-5076

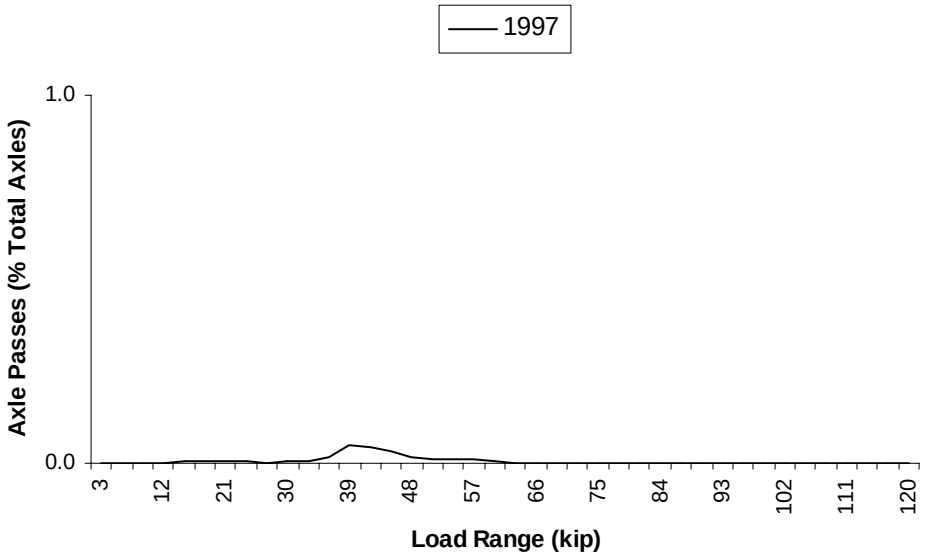

Figure C.32; Quad Axles, 27-5076

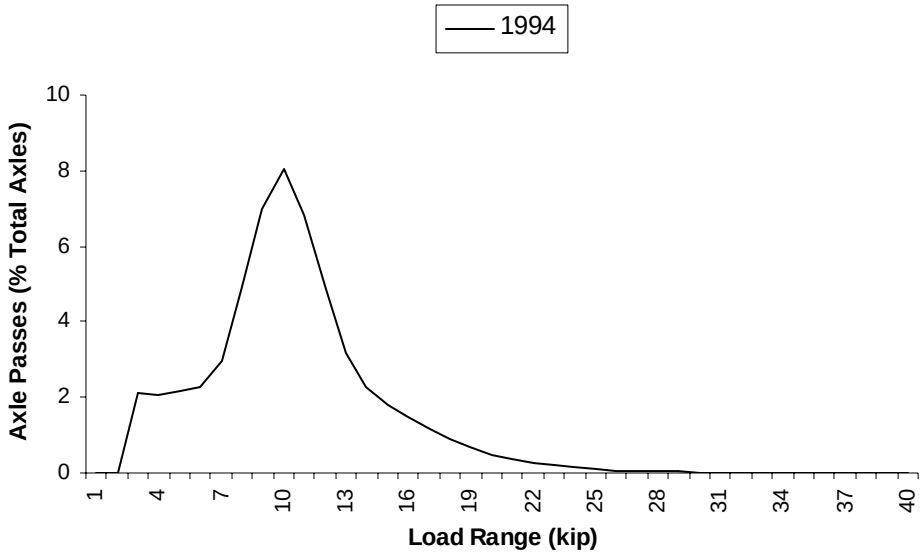

Figure C.33; Single Axles, 9-4008

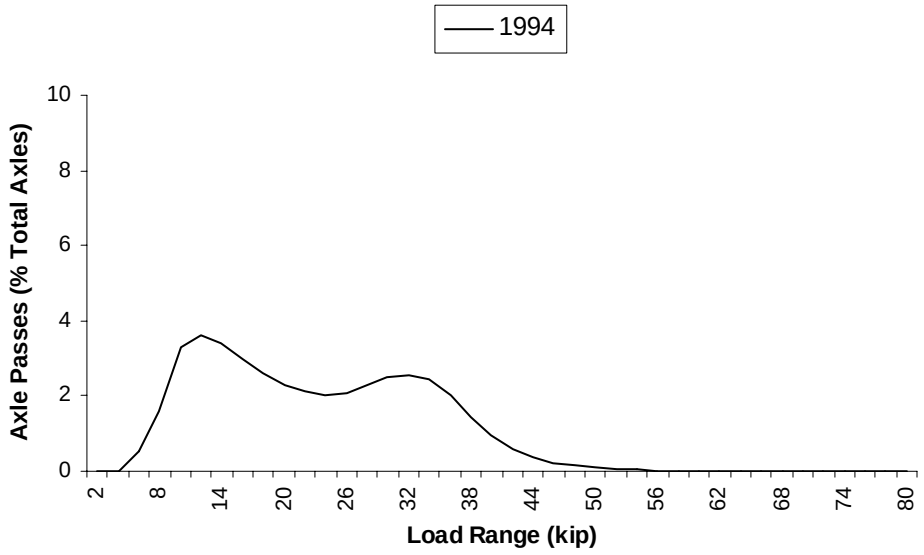

Figure C.34; Tandem Axles, 9-4008

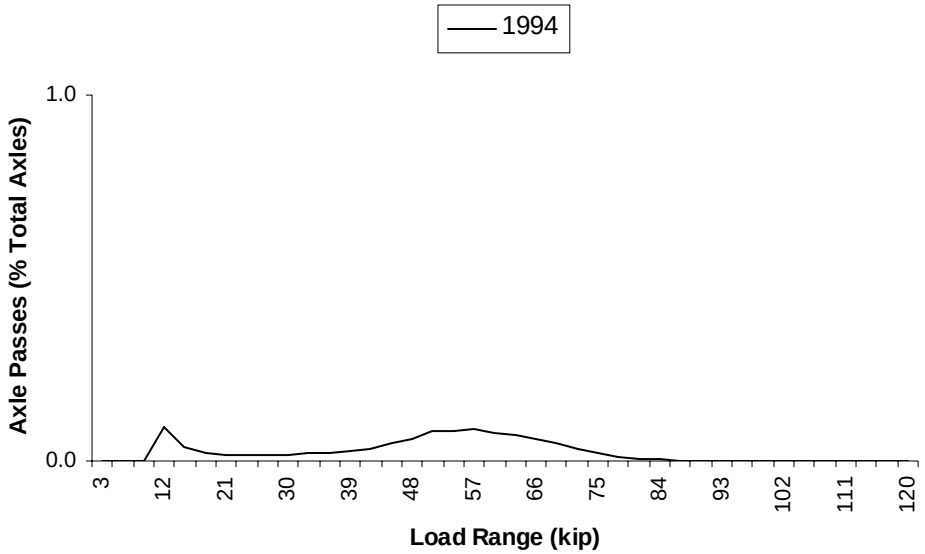

Figure C.35; Tridem Axles, 9-4008

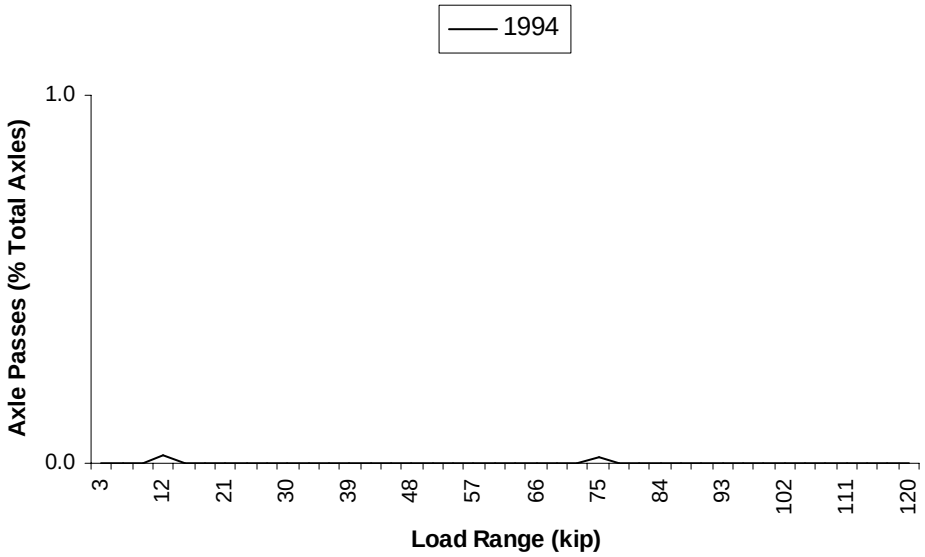

Figure C.36; Quad Axles, 9-4008

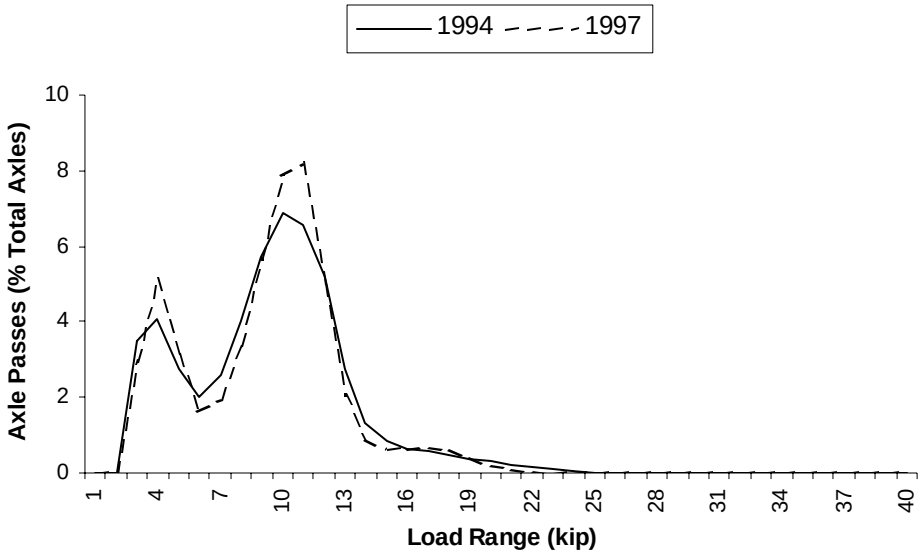

Figure C.37; Single Axles, 27-4055

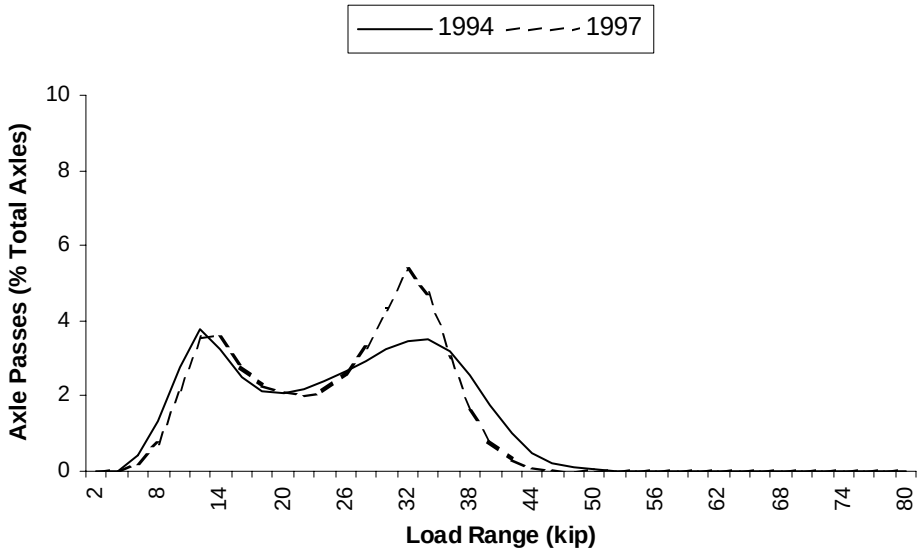

Figure C.38; Tandem Axles, 27-4055

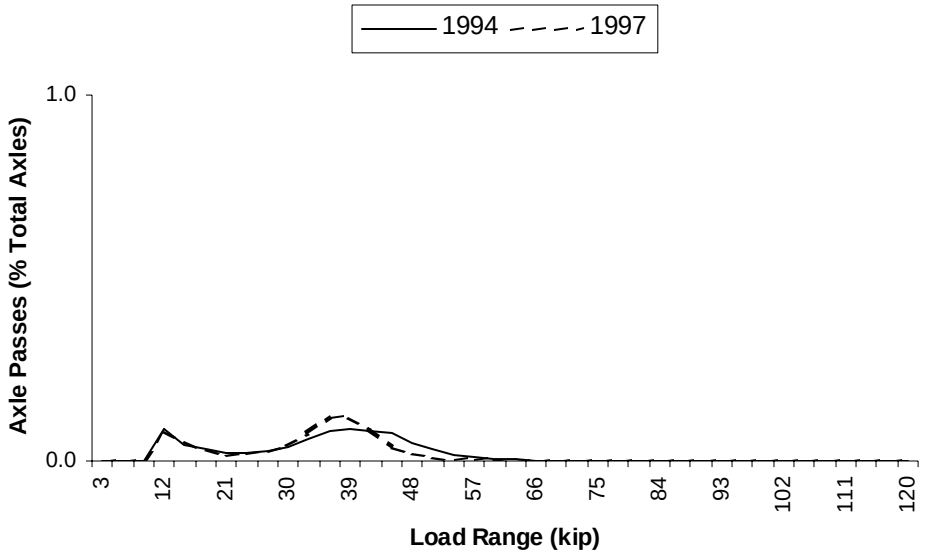

Figure C.39; Tridem Axles, 27-4055

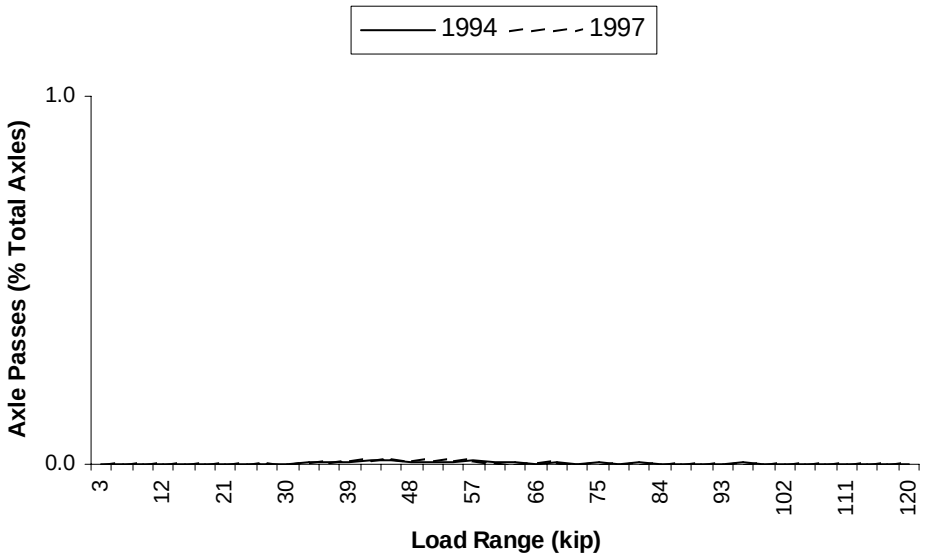

Figure C.40; Quad Axles, 27-4055

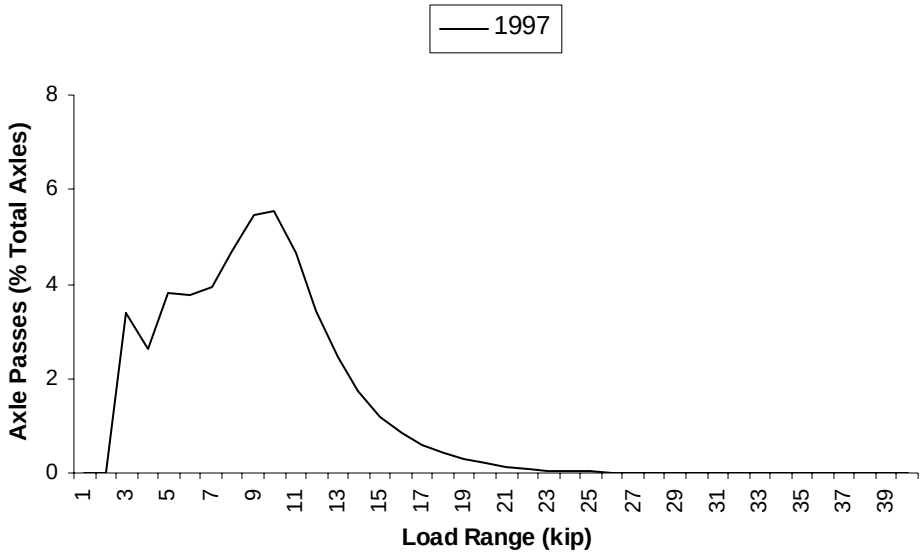

Figure C.41; Single Axles, 18-5518

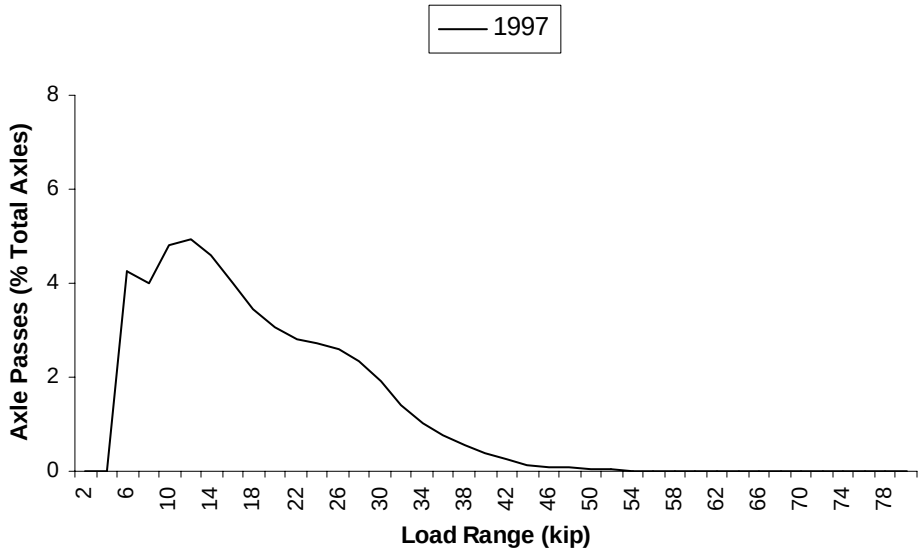

Figure C.42; Tandem Axles, 18-5518

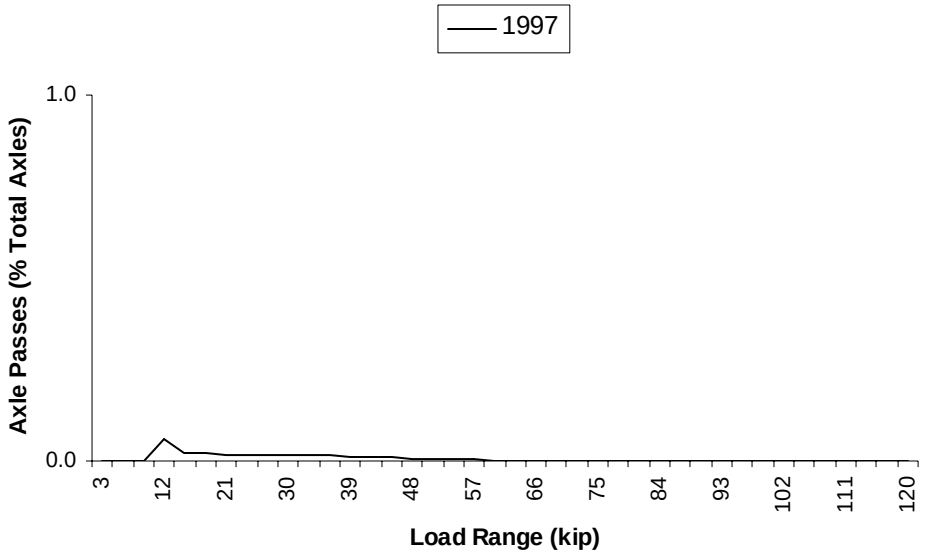

Figure C.43; Tridem Axles, 18-5518

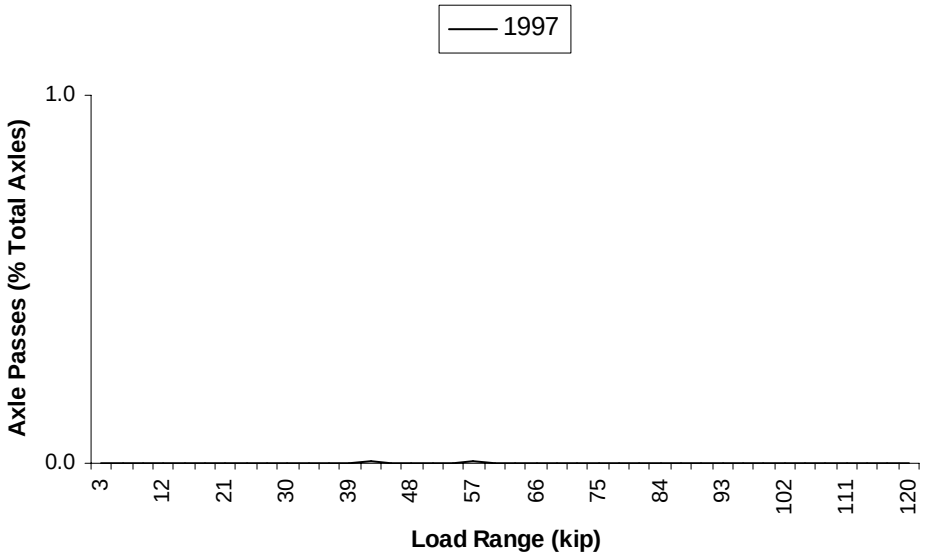

Figure C.44; Quad Axles, 18-5518

APPENDIX D

STRUCTURAL AND CLIMATIC INPUTS

TO THE 2002 PAVEMENT DESIGN GUIDE

This appendix lists the structural and climatic input values used for the 2002 PDG for all sites analyzed. For ease of entry, structural inputs are listed in the order in which the data is entered in to the PDG. For the climatic data, the actual coordinates of the sites are listed. Weather station data was used for the nearest three or four weather sites to interpolate a virtual, site-specific weather station. All ground water table values were set at 100 feet to remove ground water table effects between sites.

<u>Structure</u> – Jointed Portland Cement Concrete Pavement

1) Design Features
    a) Slab Thickness (in): Variable (Table 3.7)
    b) Permanent curl/warp effective temperature difference (ºF): -10
    c) Joint Spacing (ft): 12
    d) Sealant Type: Liquid
    e) Doweled Transverse Joints
    f) Dowel Diameter (in): 1.25
    g) Dowel Bar Spacing (in): 12
    h) Edge Support: None
    i) Base Type: Granular
    j) PCC-Base Interface: Bonded
    k) Erodibility Index: Erosion Resistant (3)
    l) Loss of bond age (months): 60
2) Drainage and Surface Properties
    a) Surface shortwave absorptivity: 0.85
    b) Infiltration: Minor (10%)
    c) Drainage path length (ft): 12
        i) Pavement Cross Slope (%): 2
3) Layers
    a) PCC
        i) Thermal
            (1) PCC material: JPCP

(2) Layer Thickness (in): Variable (Table 3.7)

(3) Unit Weight (pcf): 150

(4) Poisson's Ratio: 0.20

(5) Coefficient of thermal expansion (per F^o x 10-6): 5.5

(6) Thermal conductivity (BTU / hr-ft-F^o): 1.25

(7) Heat capacity (BTU / lb-F^o): 0.28

ii) Mix

(1) Cement Type: Type II

(2) Cementitious material content (lb/yd3): 600

(3) Water-cement ratio: 0.4

(4) Aggregate Type: Gabbro

(5) PCC zero-stress temperature (F^o): Computed by PDG

(6) Ultimate shrinkage at 40% R.H. (microstrain): Computed by PDG

(7) Reversible shrinkage (% of ultimate shrinkage): Computed by PDG

(8) Time to develop 50% of ultimate shrinkage (days): Computed by PDG

(9) Curing method: curing compound

iii) Strength: Level 2 (Table D.1)

Table D.1: PC Strength Properties for Level 2

Time	Compressive Strength (psi)
7 day	3560
14 day	3900
28 day	4200
90 day	4700
20 year / 28 day	1.44

Structure – Continuously Reinforced Concrete Pavement

1) Design Features
    a) Slab Thickness (in): Variable (Table 3.7)
    b) Shoulder Type: Asphalt
        i) Permanent curl/warp effective temperature difference (ºF): -10
    c) Steel Reinforcement
        i) Percent Steel (%): 0.7
        ii) Bar Diameter (in): 0.625
        iii) Steel Depth (in): 4
    d) Base Properties
        i) Base Type: Granular
        ii) Erodibility Index: Erosion Resistant (3)
        iii) Base/slab friction coefficient: 4
    e) Crack Spacing: Generate using model
2) Drainage and Surface Properties
    a) Surface shortwave absorptivity: 0.85

b) Infiltration: Minor (10%)

c) Drainage path length (ft): 12

i) Pavement Cross Slope (%): 2

3) Layers

a) PCC

i) Thermal

(1) PCC material: CRCP

(2) Layer Thickness (in): Variable (Table 3.7)

(3) Unit Weight (pcf): 150

(4) Poisson's Ratio: 0.20

(5) Coefficient of thermal expansion (per F^o x 10-6): 5.5

(6) Thermal conductivity (BTU / hr-ft-F^o): 1.25

(7) Heat capacity (BTU / lb-F^o): 0.28

ii) Mix

(1) Cement Type: Type II

(2) Cementitious material content (lb/yd3): 600

(3) Water-cement ratio: 0.4

(4) Aggregate Type: Gabbro

(5) PCC zero-stress temperature (F^o): Computed by PDG

(6) Ultimate shrinkage at 40% R.H. (microstrain): Computed by PDG

(7) Reversible shrinkage (% of ultimate shrinkage): Computed by PDG

(8) Curing method: curing compound

iii) Strength: Level 2 (Table D.1)

Structure – Asphalt Cement Concrete Pavement

1) Drainage and Surface Properties
    a) Surface shortwave absorptivity: 0.85
2) Layers
    a) AC
        i) Input Level: 3
        ii) Asphalt Material Type: Asphalt Concrete
        iii) Layer Thickness: Variable (Table 3.7)
        iv) Asphalt Mix
            (1) Cumulative percent retained on the 3/4 inch sieve: 0
            (2) Cumulative percent retained on the 3/8 inch sieve: 5
            (3) Cumulative percent retained on the #4 sieve: 30
            (4) Percent passing the #200 sieve: 5
        v) Asphalt Binder
            (1) Conventional Viscosity Grade: AC 20
        vi) Asphalt General
            (1) Reference Temperature (Fº): 70
            (2) Volumetric Properties as built
                (a) Effective Binder Content (%): 11.0
                (b) Air Voids (%): 8.5
                (c) Total Unit Weight (lb/ft3): 148

(3) Poisson's ratio: 0.35

(4) Thermal Properties

(a) Thermal conductivity asphalt (BTU / hr-ft-F^{o}): 0.67

(b) Heat capacity asphalt (BTU / lb-F^{o}): 0.23

<u>Structure</u> – Unbound Base

1) Unbound Material: Variable (Table 3.8)
2) Thickness (in): Variable (Table 3.7)
3) Strength Properties
    a) Input Level: 3
    b) Poisson's ratio: 0.35
    c) Coefficient of lateral earth pressure, K0: 0.5
    d) Material Property
        i) Modulus (psi): Variable (Table 3.8)
    e) Analysis Type:
        i) ICM calculated modulus: ICM inputs
4) ICM
    a) Gradation and Plasticity Index: Computed by PDG
    b) Calculated/Derived Parameters: Computed by PDG
    c) Soil Characteristic Curve Fit Parameters: Computed by PDG
    d) Compacted, Unbound Materials

Climate

Table D.2: Site Locations Used for Interpolation of Weather Station Data

Site	Longitude (decimal of deg.)	Latitude (decimal of deg.)	Elevation (ft)	Depth to Water Table (ft)
9_4008	-72.558	41.798	155	100
18_1028	-87.016	38.196	441	100
18_5518	-86.853	40.477	65	100
26_1010	-83.656	43.179	792	100
27_4055	-94.074	45.424	980	100
27_5076	-92.975	45.034	985	100
28_2807	-89.655	34.356	295	100
28_4024	-91.041	33.359	125	100
50_1682	-73.241	44.326	400	100
53_1007	-119.602	46.048	903	100
53_6048	-122.138	47.788	120	100

APPENDIX E

Summary of General and Traffic Inputs to the 2002 AASHTO PDG

General Information

- Design Life (years): 20
- Base/Subgrade Construction Month: August, 1998 (if applicable)
- Pavement Construction Month: August, 1988
- Traffic Open Month: September, 1988
- Type of design: **JPCP**

Traffic

- Initial two-way AADTT: **Variable**
- Number of lanes in design direction (%): 1
- Percent of trucks in design direction (%): 50.0
- Percent of trucks in design lane (%): 100.0
- Operational speed (mph): 60
- Traffic Volume Adjustment Factors
  - Monthly Adjustment Factors: **Variable**
  - Vehicle Class Distribution: **Variable**
  - Hourly Truck Distribution: See figure 1 (below)
  - Traffic Growth Factor: Compound, 4%

Axle Load Distribution Factors: **Variable**

General Traffic Inputs

Mean wheel location (inches from the lane marking): 18

Traffic wander standard deviation (in): 10

Design lane width (ft): 12

Number of Axles per Truck: **Variable**

Axle Configuration

Average Axle Width (edge-to-edge outside dimensions, ft): 8.5

Dual Tire Spacing (in): 12

Tire Pressure

Single (psi): 95

Dual (psi): 95

Axle Spacing

Tandem (in): 51.6

Tridem (in): 49.2

Quad (in): 49.2

Wheelbase

Average Axle Spacing (ft)

Short: 12

Medium: 15

Long: 18

Percent of trucks

Short: 33.0

Medium: 33.0

Long: 34.0

Figure E.1: Hourly Truck Distribution

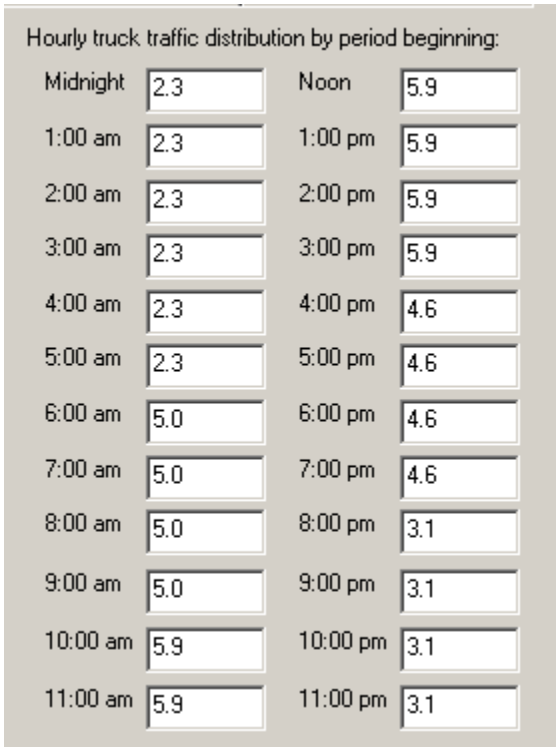

APPENDIX F

PAVEMENT PERFORMANCE YEARS

All pavement sections were analyzed using the AASHTO 2002 PDG. This section contains the life of the pavement sections in absolute terms (years).

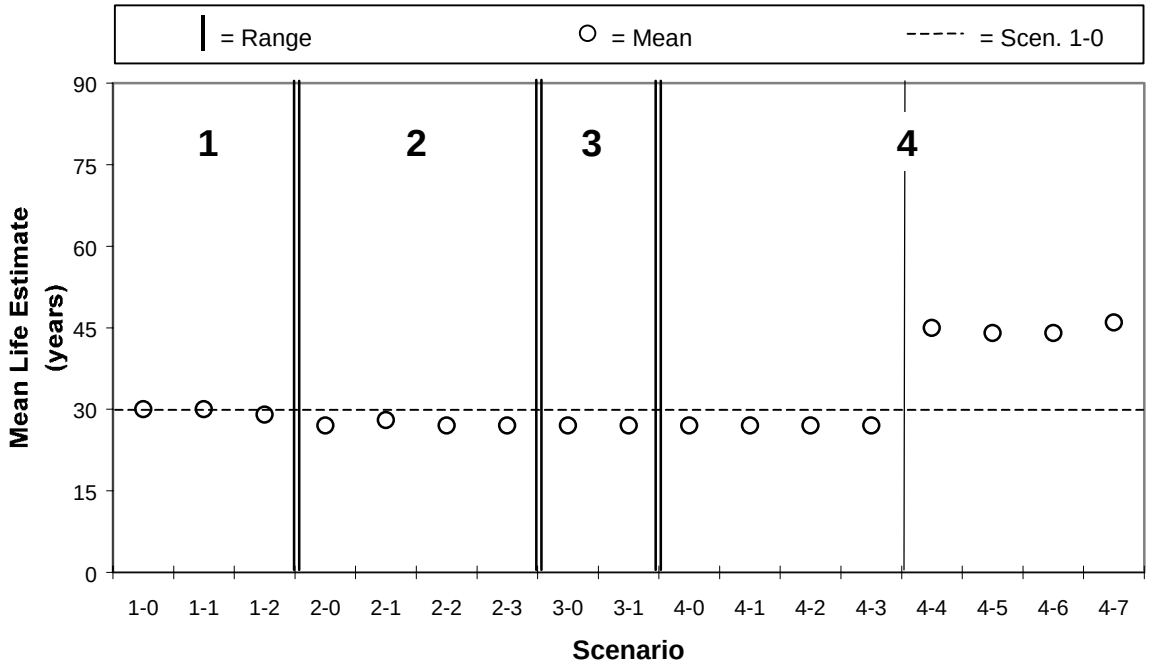

Figure F.1: Flexible Site 18_1028, 50th Percentile Range in Life Overestimation

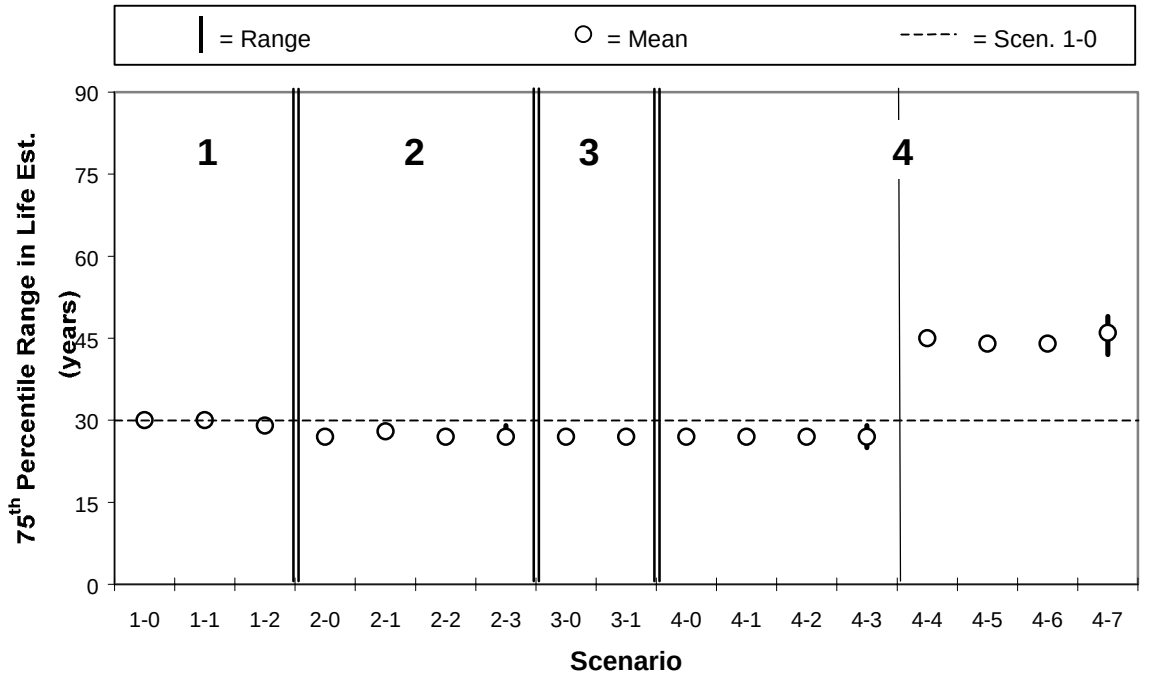

Figure F.2: Flexible Site 18_1028, 75th Percentile Range in Life Overestimation

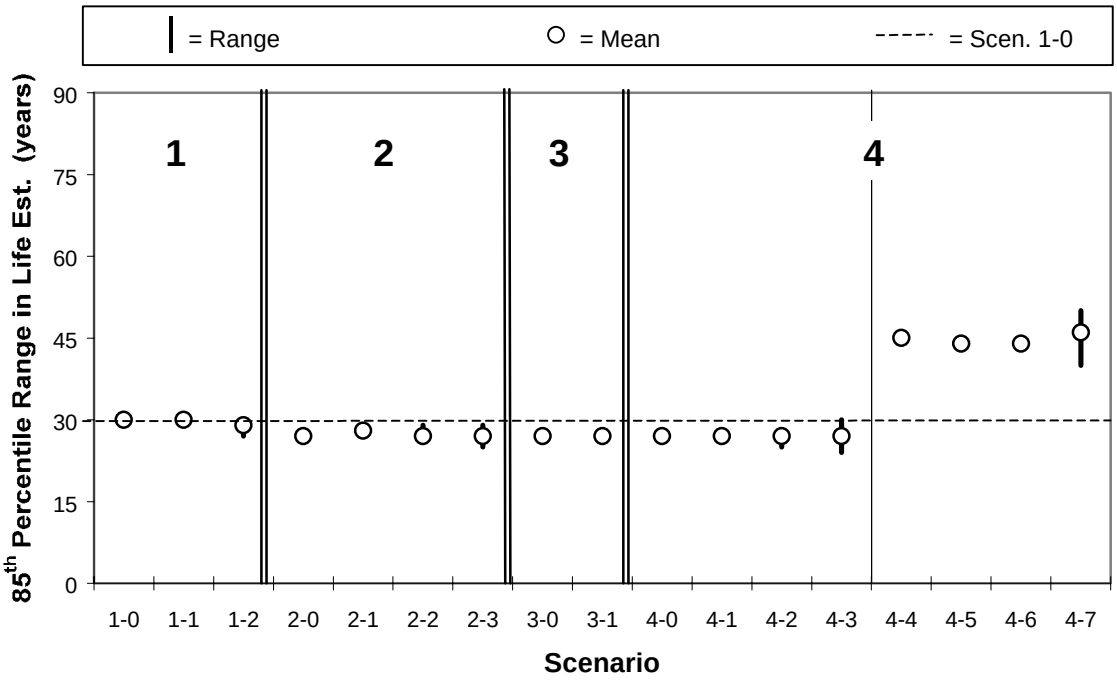

Figure F.3: Flexible Site 18_1028, 85th Percentile Range in Life Overestimation

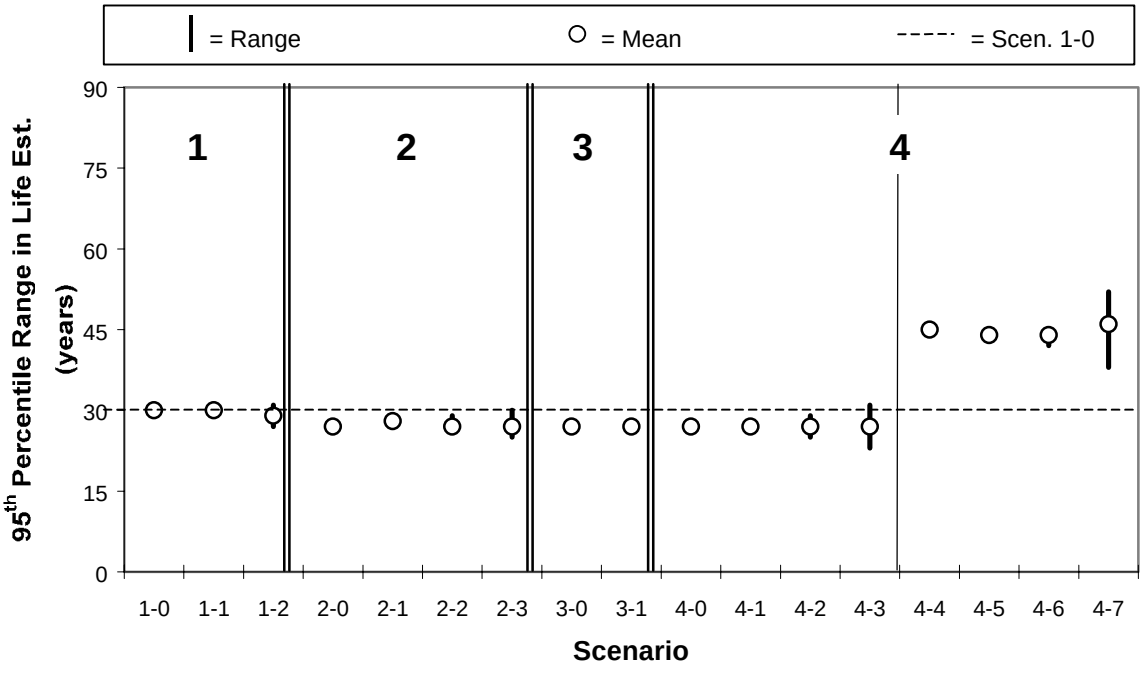

Figure F.4: Flexible Site 18_1028, 95th Percentile Range in Life Overestimation

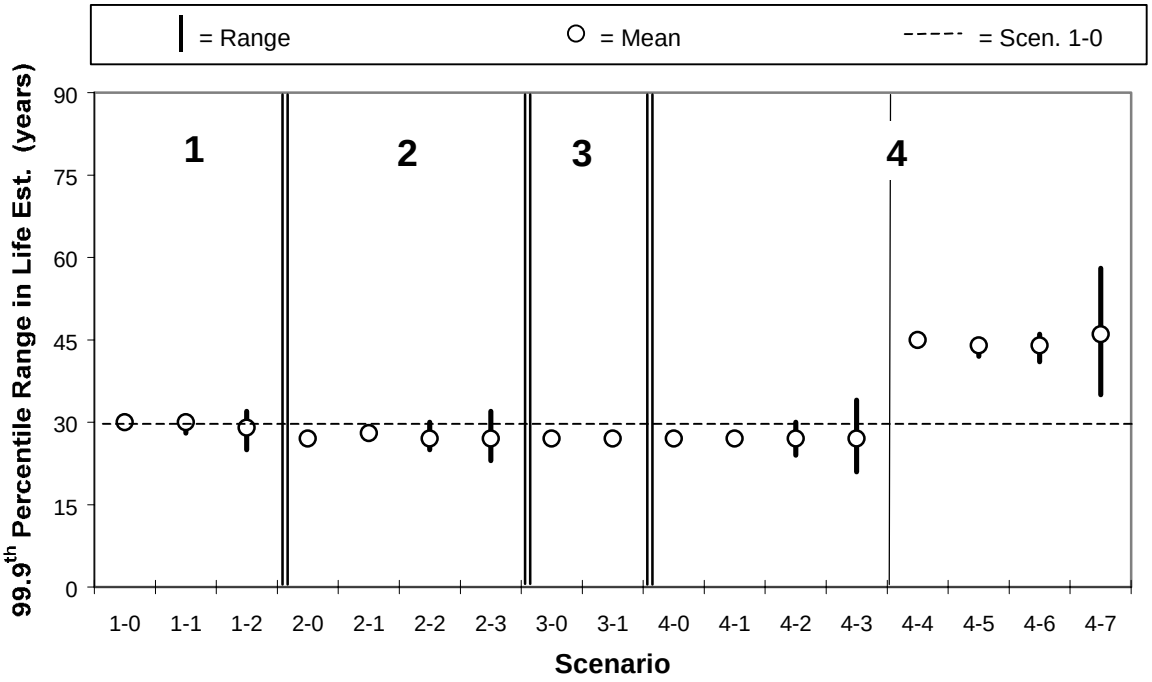

Figure F.5: Flexible Site 18_1028, 99.9th Percentile Range in Life Overestimation

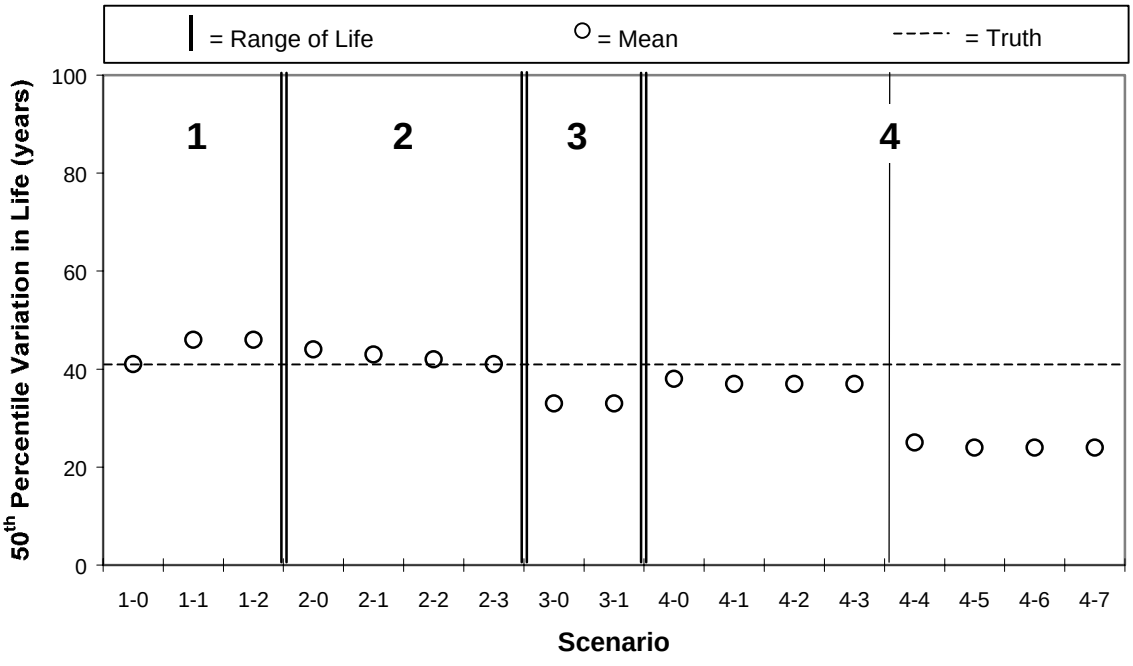

Figure F.6: Flexible Site 26_1010, 50th Percentile Range in Life Overestimation

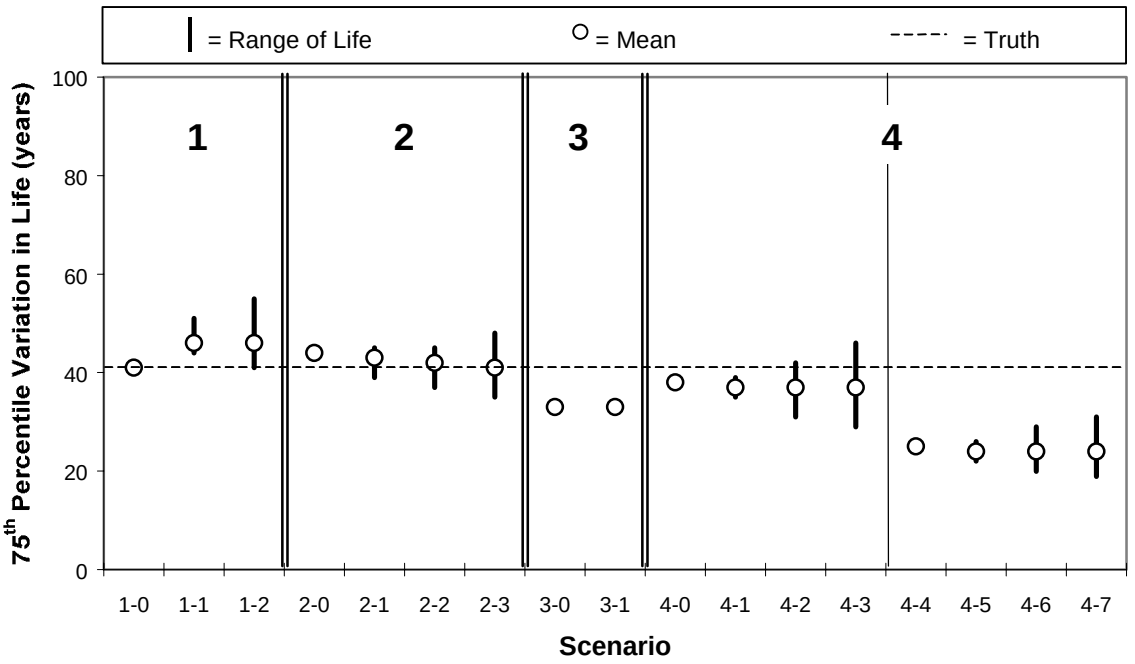

Figure F.7: Flexible Site 26_1010, 75th Percentile Range in Life Overestimation

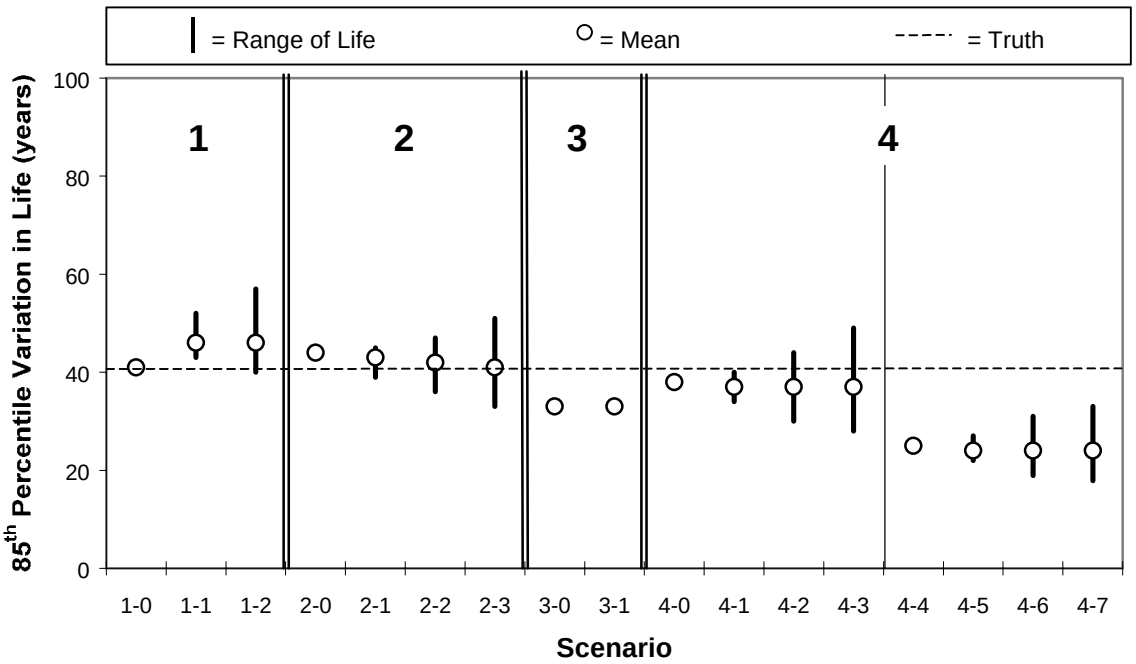

Figure F.8: Flexible Site 26_1010, 85th Percentile Range in Life Overestimation

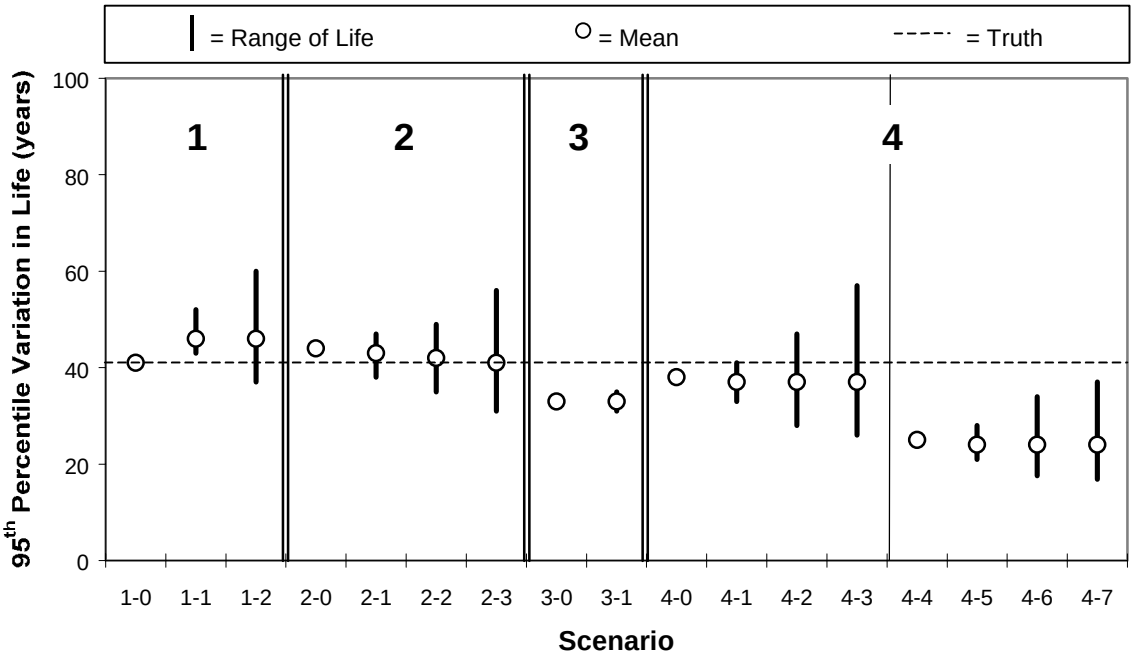

Figure F.9: Flexible Site 26_1010, 95th Percentile Range in Life Overestimation

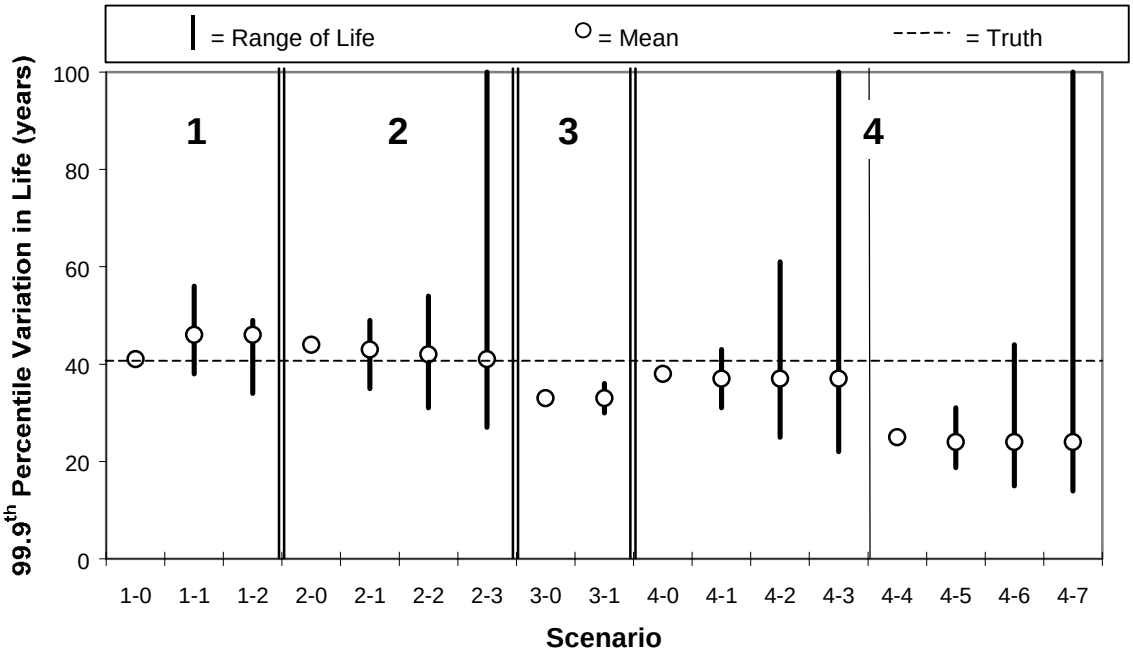

Figure F.10: Flexible Site 26_1010, 99.9th Percentile Range in Life Overestimation

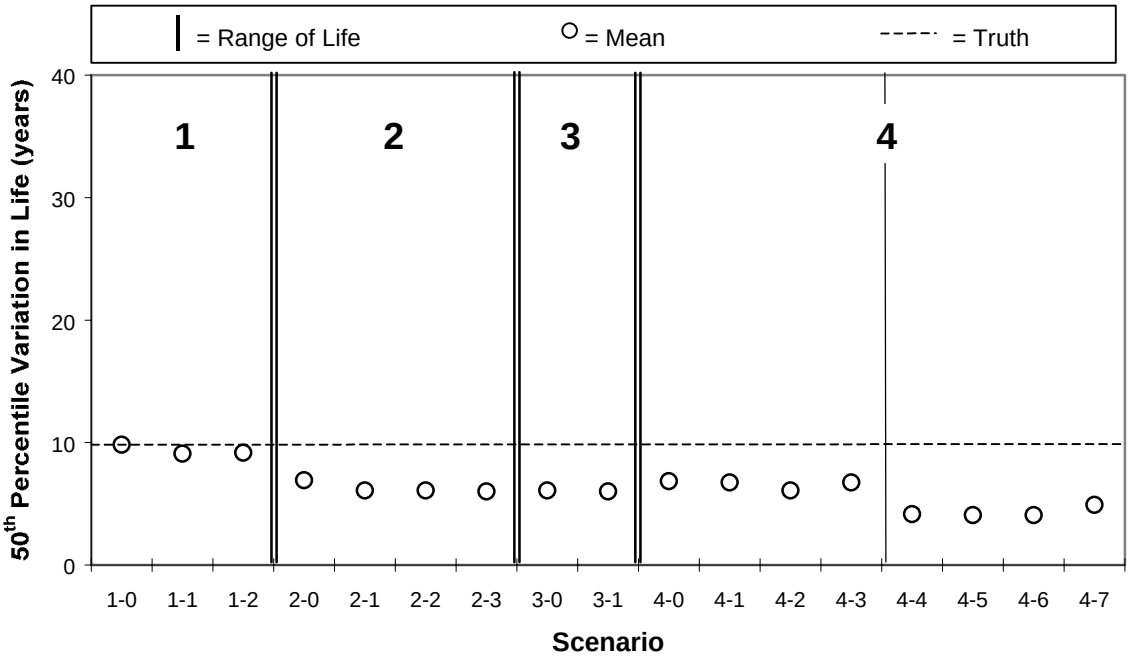

Figure F.11: Flexible Site 53_6048, 50th Percentile Range in Life Overestimation

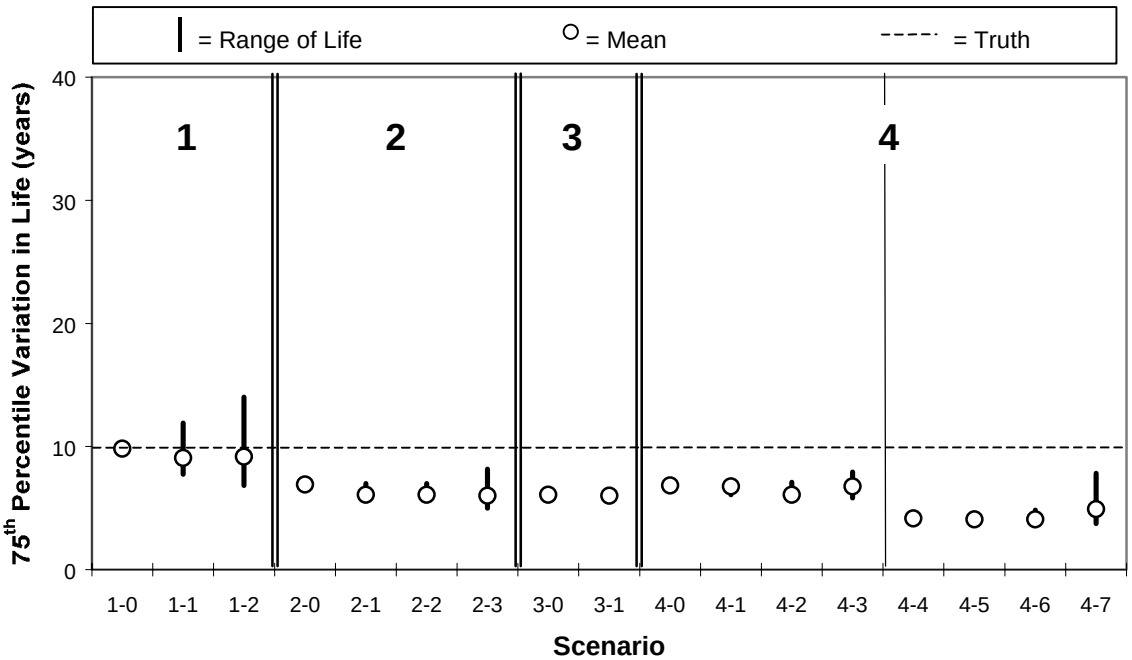

Figure F.12: Flexible Site 53_6048, 75th Percentile Range in Life Overestimation

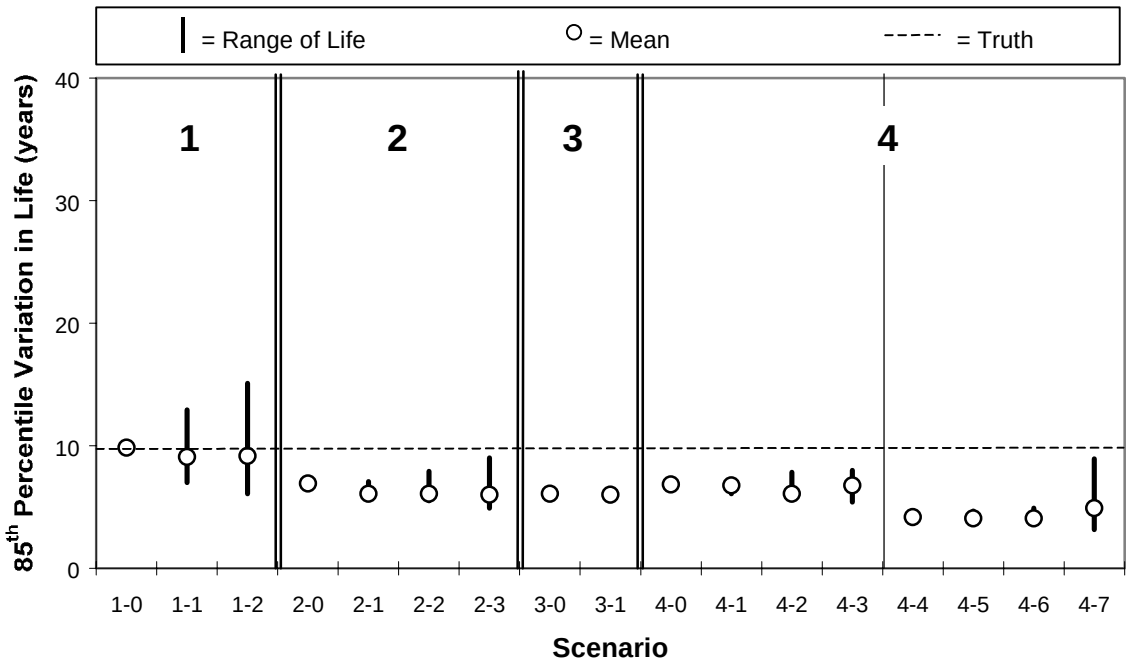

Figure F.13: Flexible Site 53_6048, 85th Percentile Range in Life Overestimation

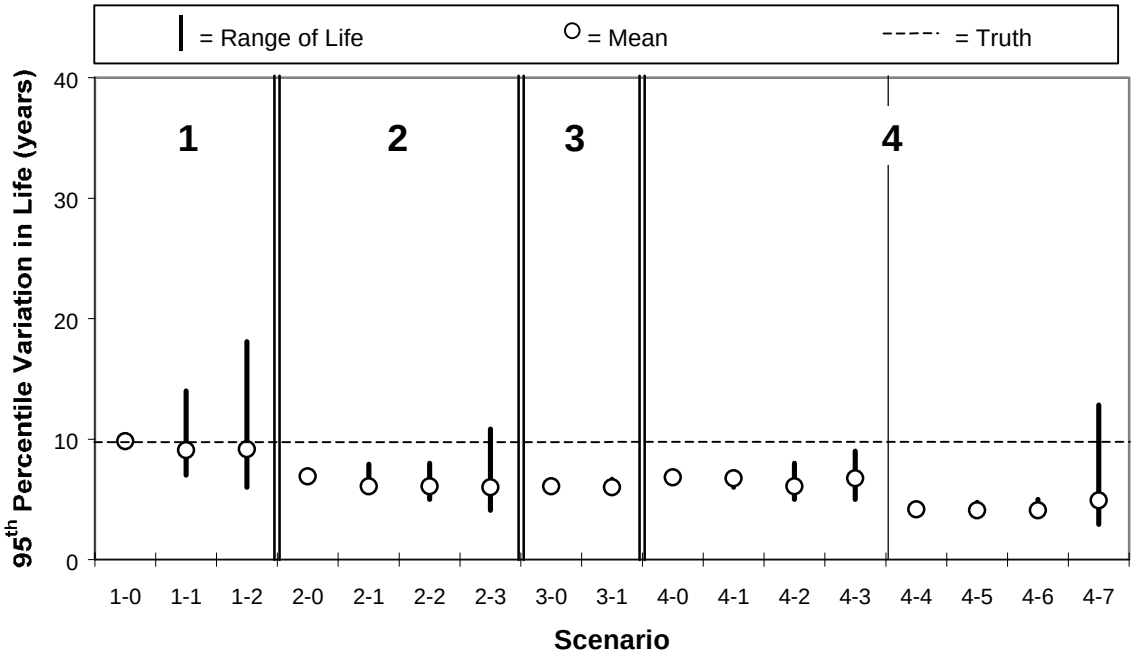

Figure F.14: Flexible Site 53_6048, 95th Percentile Range in Life Overestimation

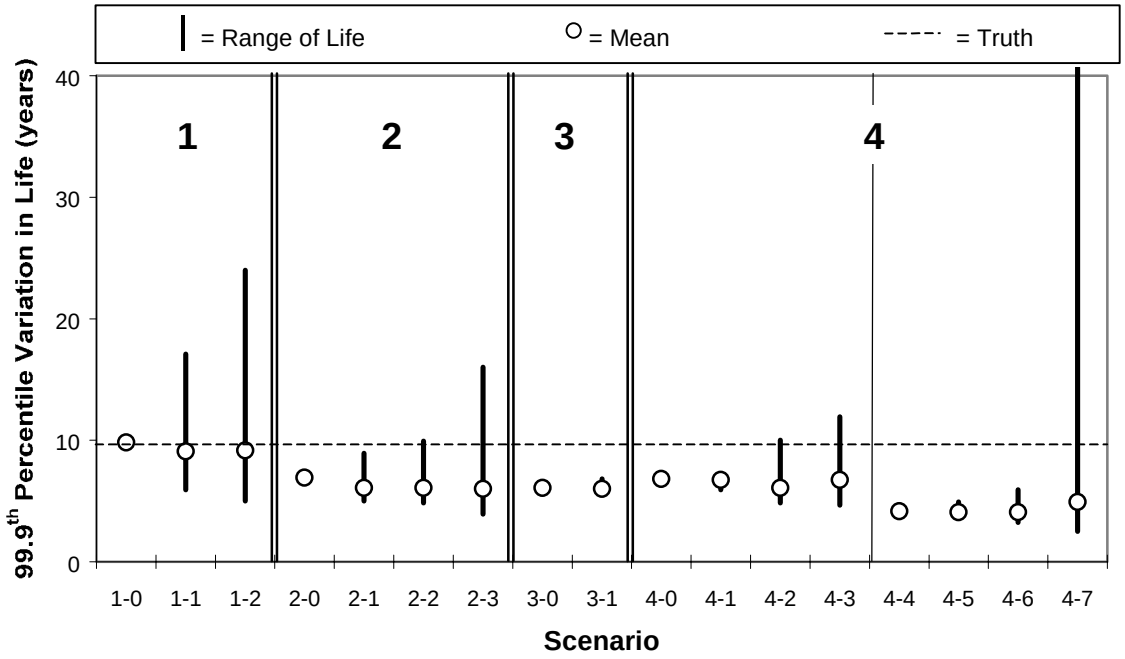

Figure F.15: Flexible Site 53_6048, 99.9th Percentile Range in Life Overestimation

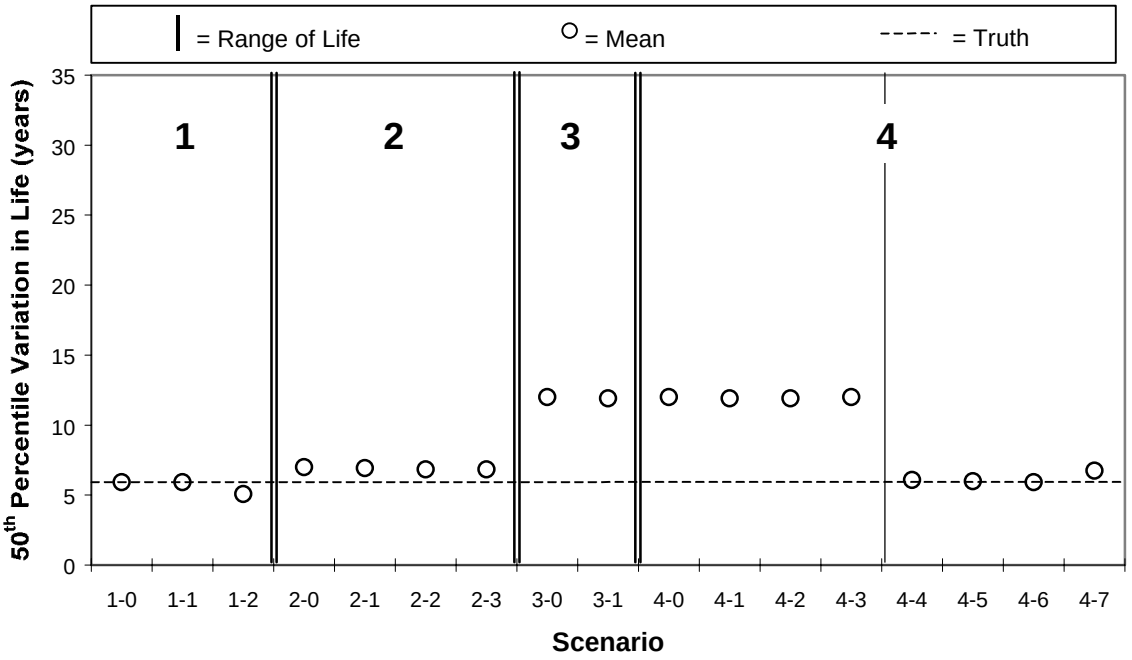

Figure F.16: Flexible Site 28_2807, 50th Percentile Range in Life Overestimation

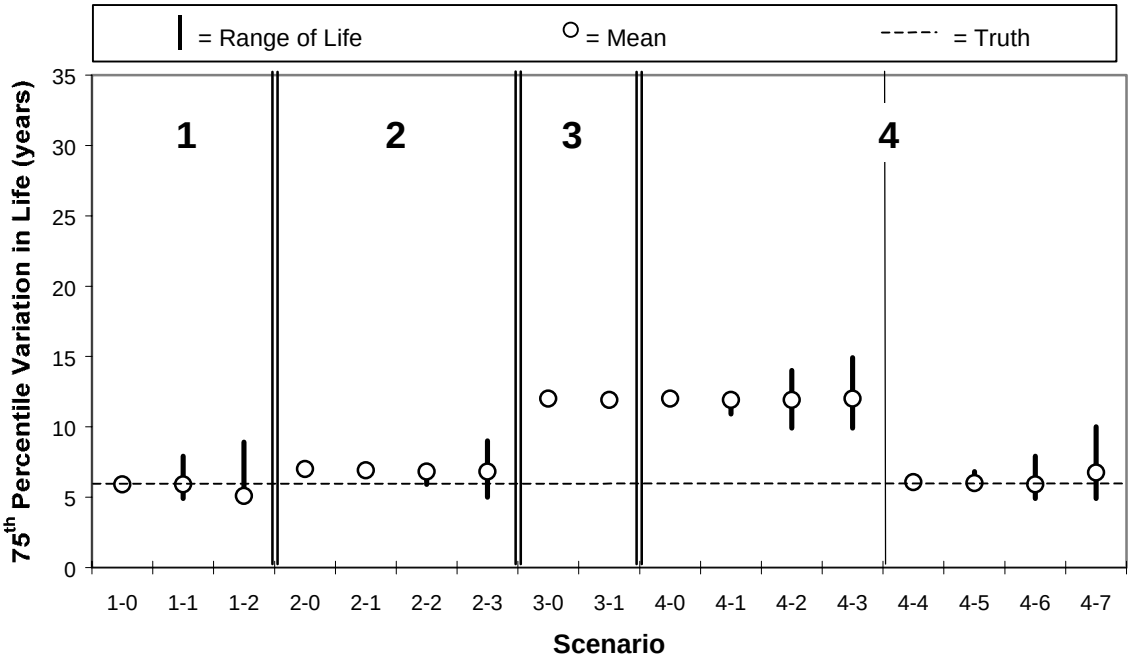

Figure F.17: Flexible Site 28_2807, 75th Percentile Range in Life Overestimation

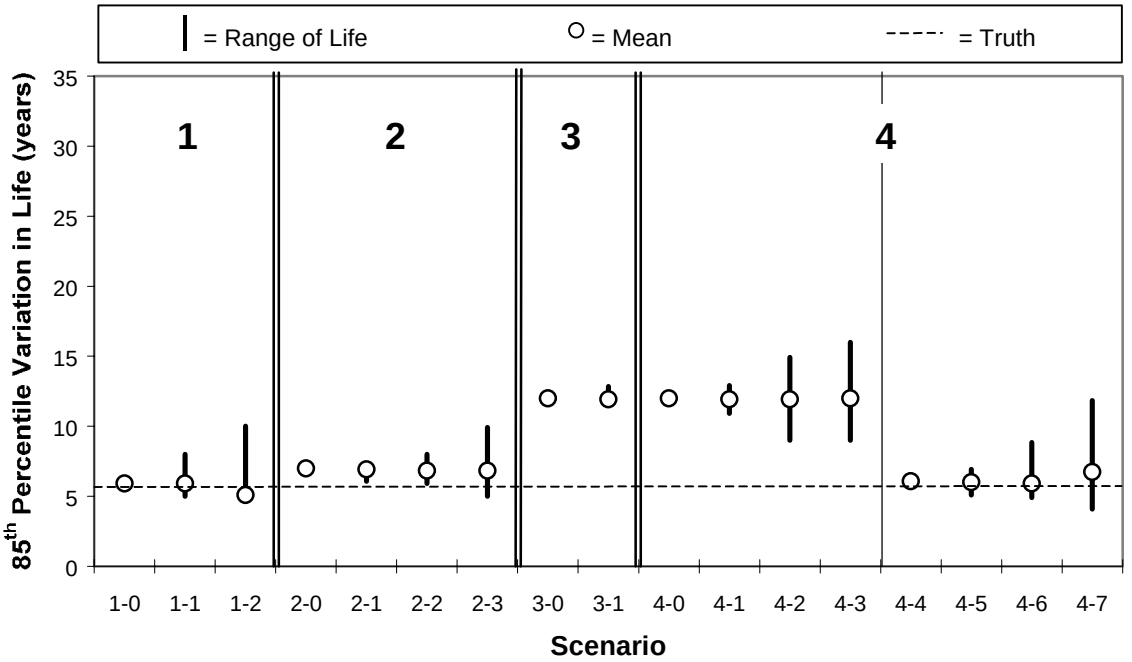

Figure F.18: Flexible Site 28_2807, 85th Percentile Range in Life Overestimation

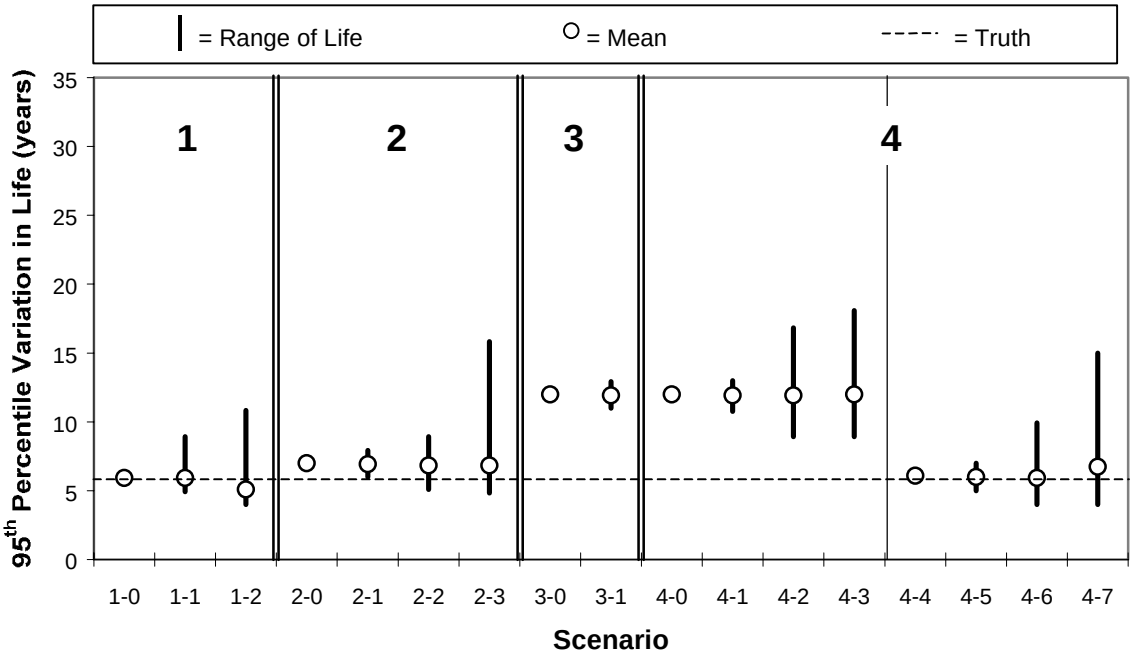

Figure F.19: Flexible Site 28_2807, 95th Percentile Range in Life Overestimation

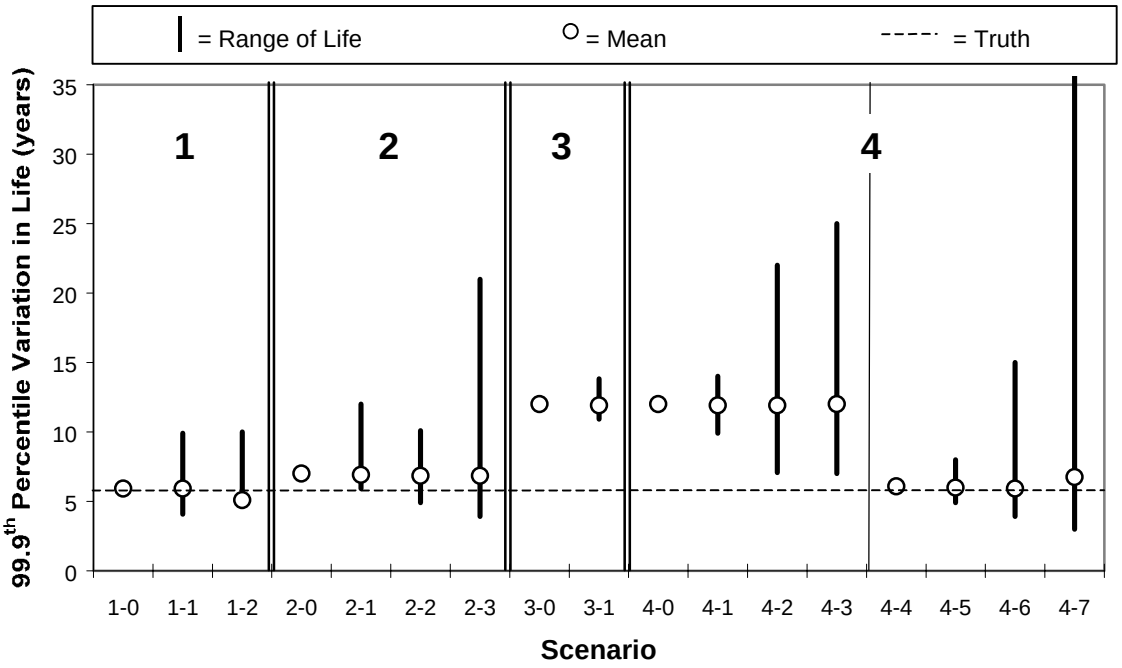

Figure F.20: Flexible Site 28_2807, 99.9th Percentile Range in Life Overestimation

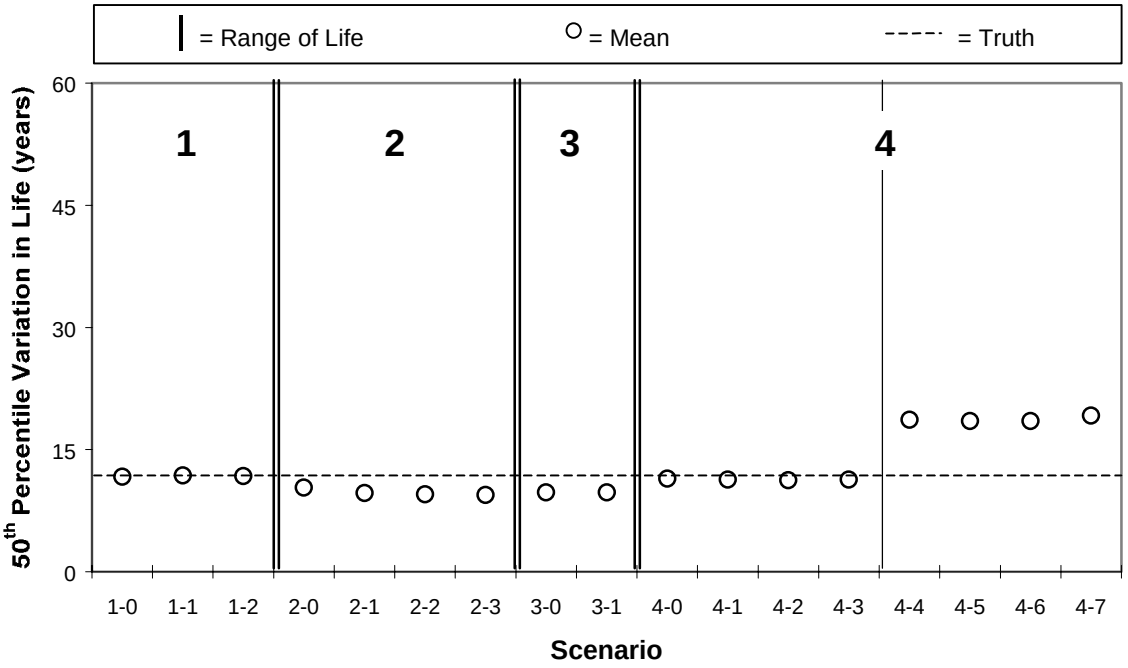

Figure F.21: Rigid Site 18_5518, 50th Percentile Range in Life Overestimation

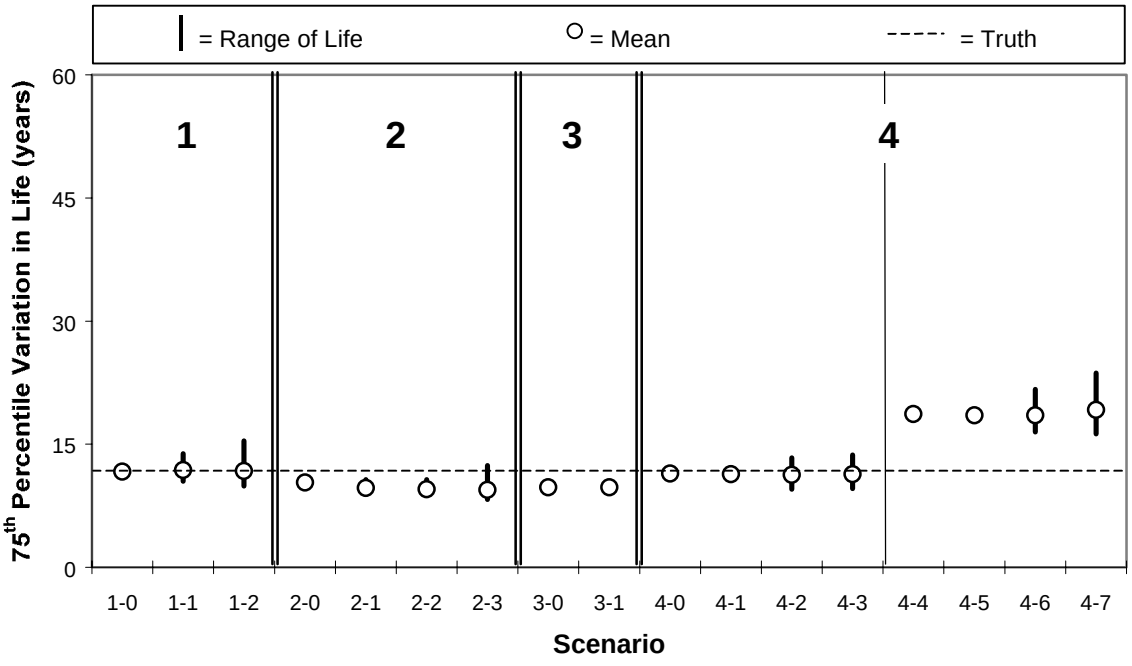

Figure F.22: Rigid Site 18_5518, 75th Percentile Range in Life Overestimation

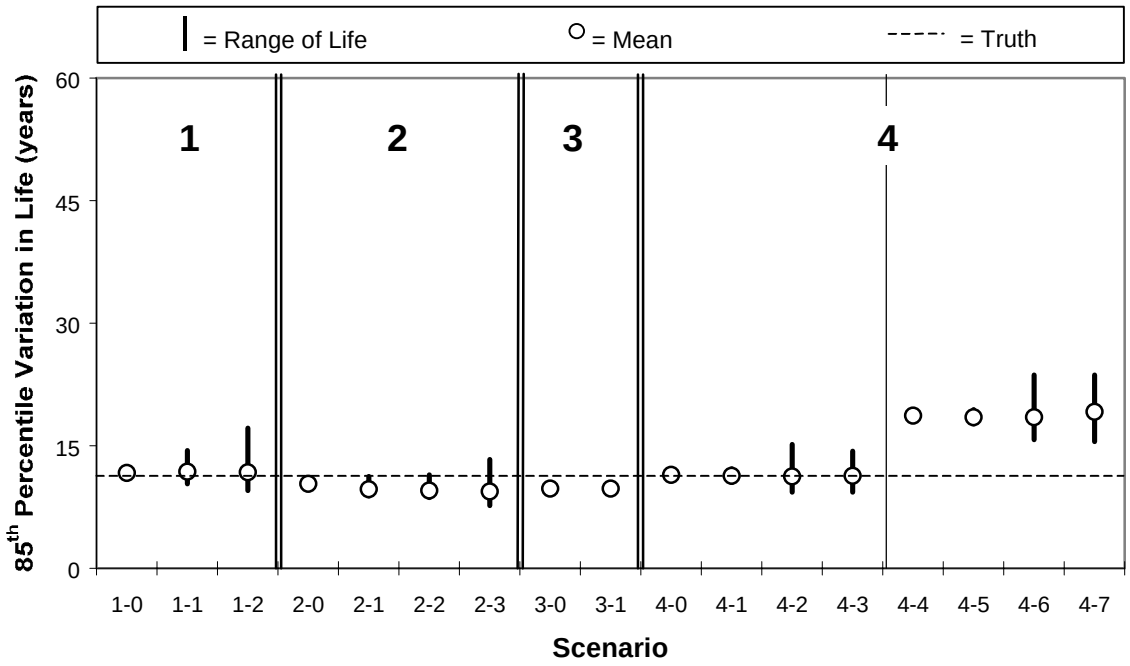

Figure F.23: Rigid Site 18_5518, 85th Percentile Range in Life Overestimation

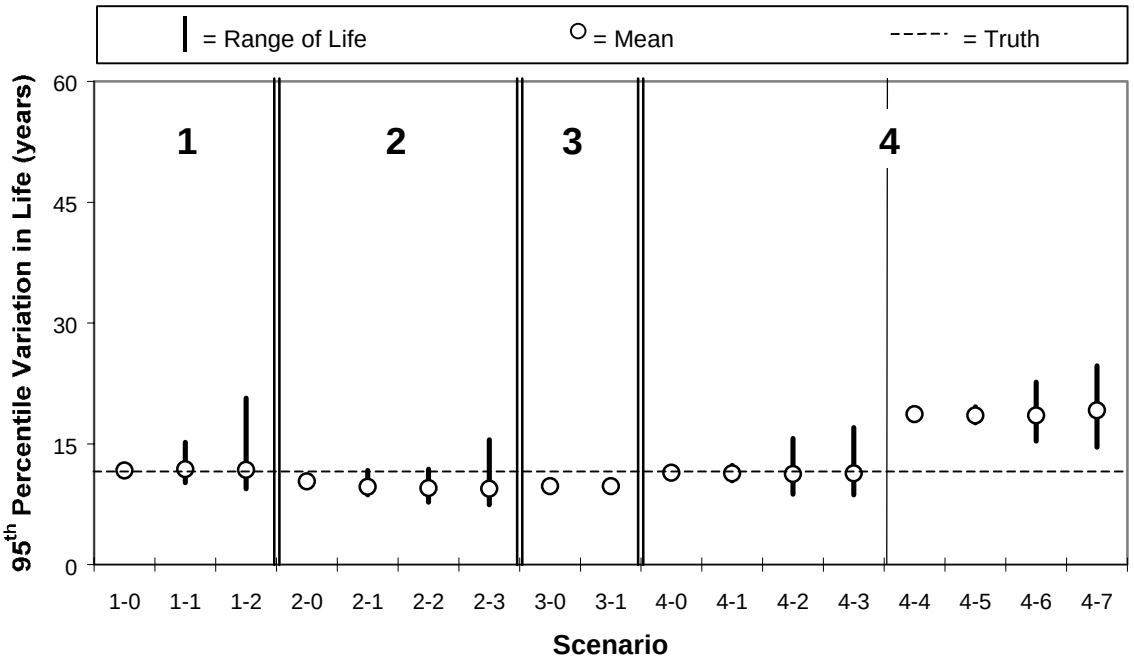

Figure F.24: Rigid Site 18_5518, 95th Percentile Range in Life Overestimation

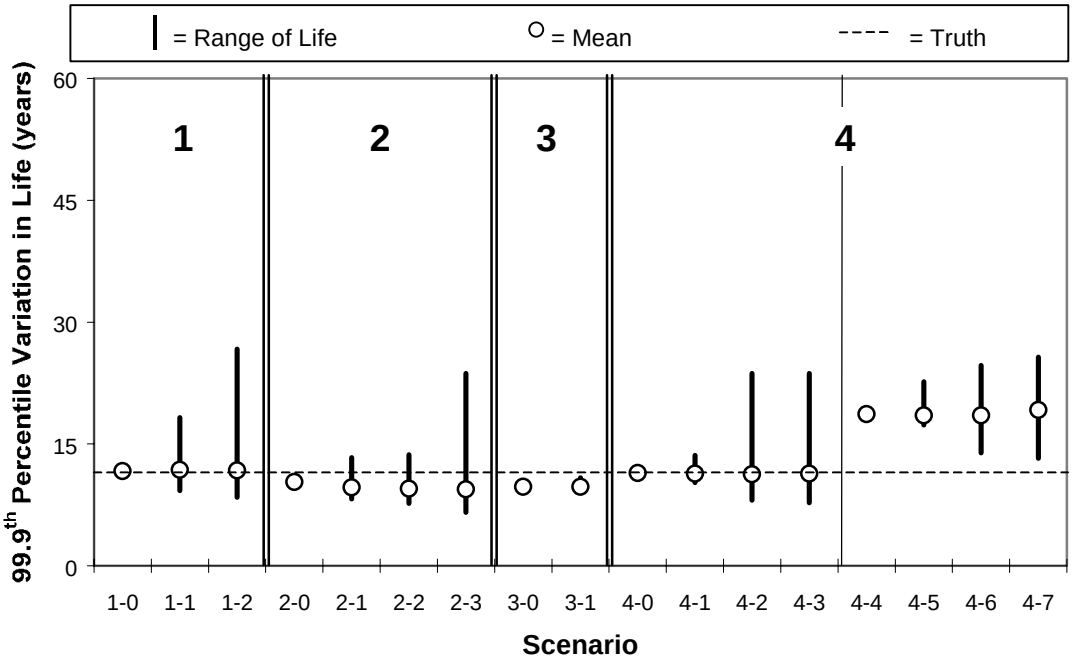

Figure F.25: Rigid Site 18_5518, 99.9th Percentile Range in Life Overestimation

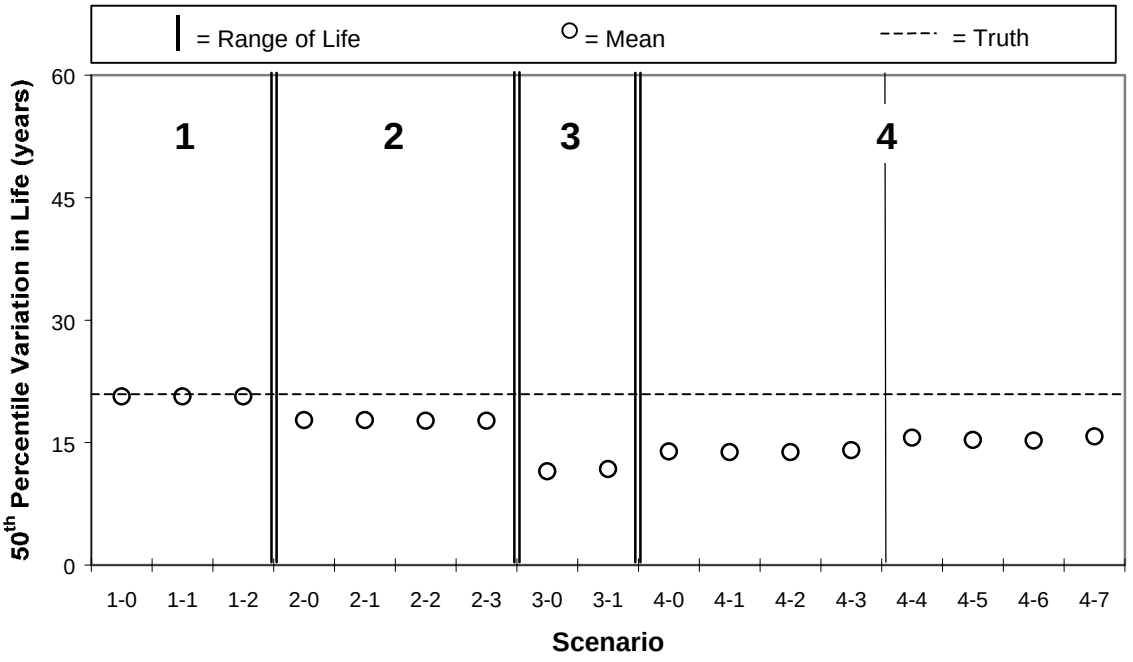

Figure F.26: Rigid Site 27_5076, 50th Percentile Range in Life Overestimation

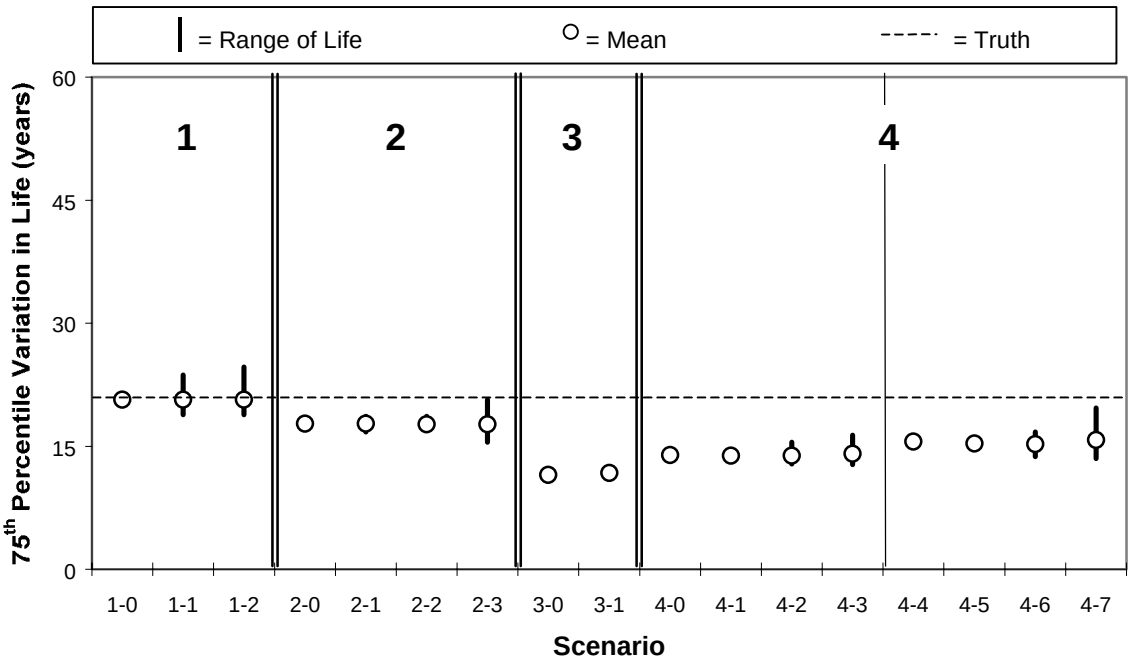

Figure F.27: Rigid Site 27_5076, 75th Percentile Range in Life Overestimation

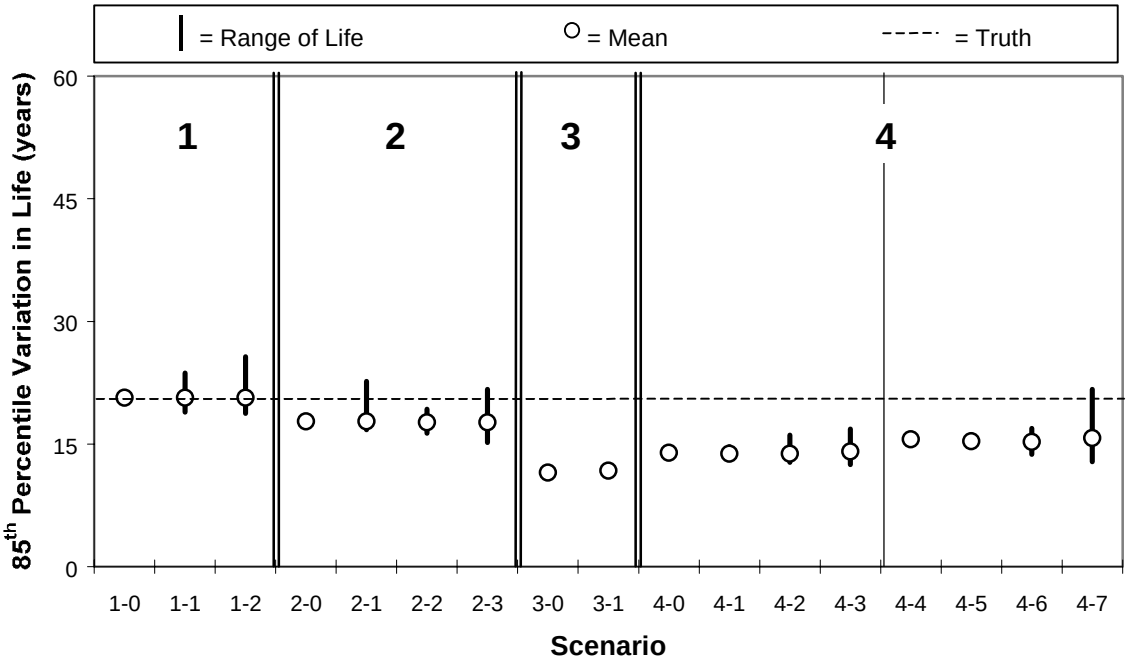

Figure F.28: Rigid Site 27_5076, 85th Percentile Range in Life Overestimation

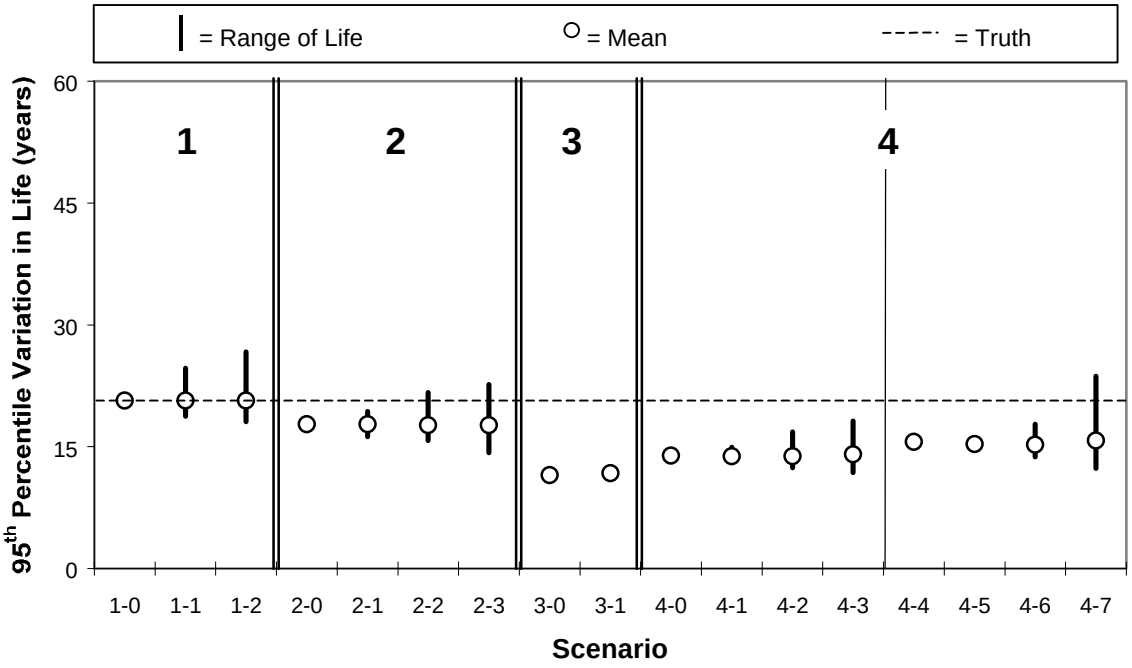

Figure F.29: Rigid Site 27_5076, 95th Percentile Range in Life Overestimation

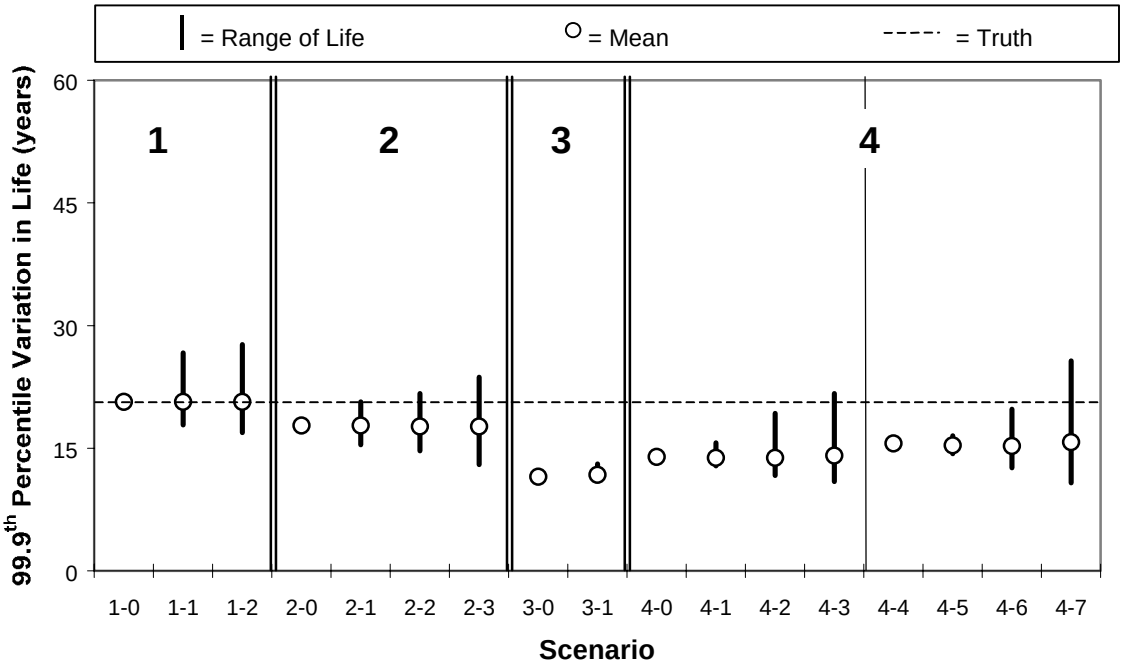

Figure F.30: Rigid Site 27_5076, 99.9th Percentile Range in Life Overestimation

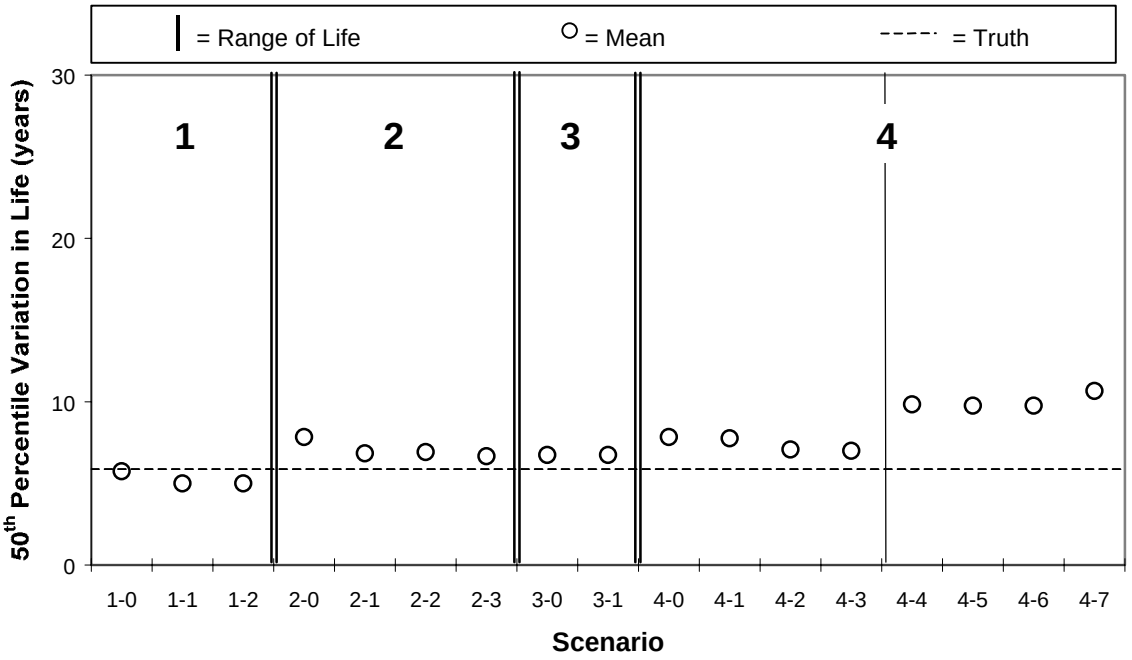

Figure F.31: Rigid Site 9_4008, 50th Percentile Range in Life Overestimation

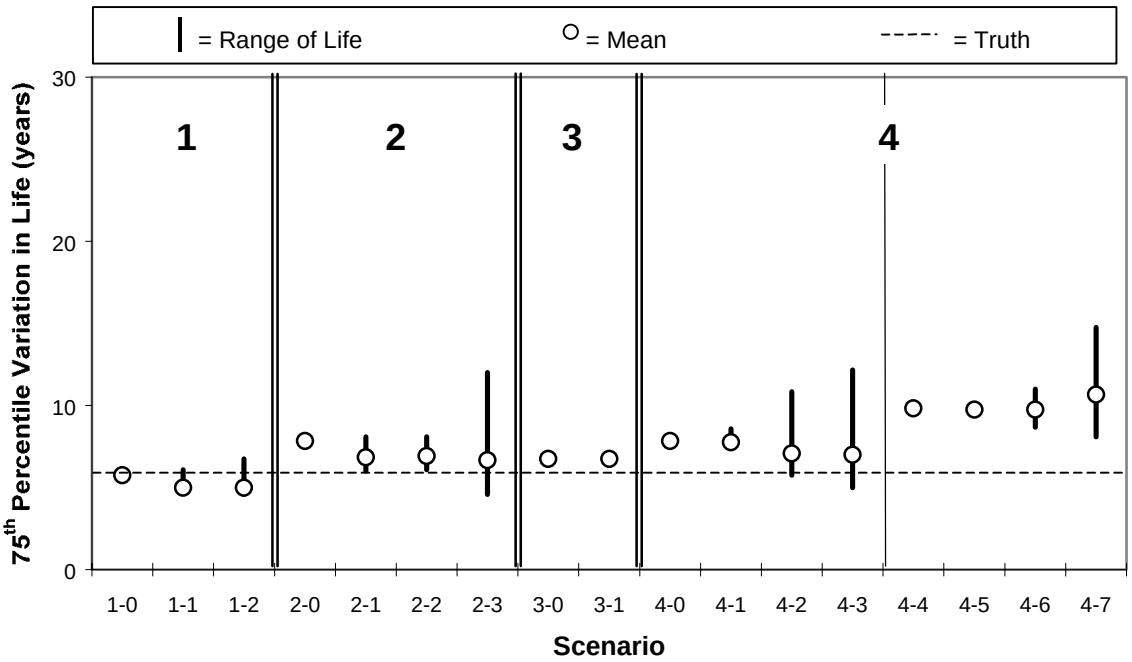

Figure F.32: Rigid Site 9_4008, 75th Percentile Range in Life Overestimation

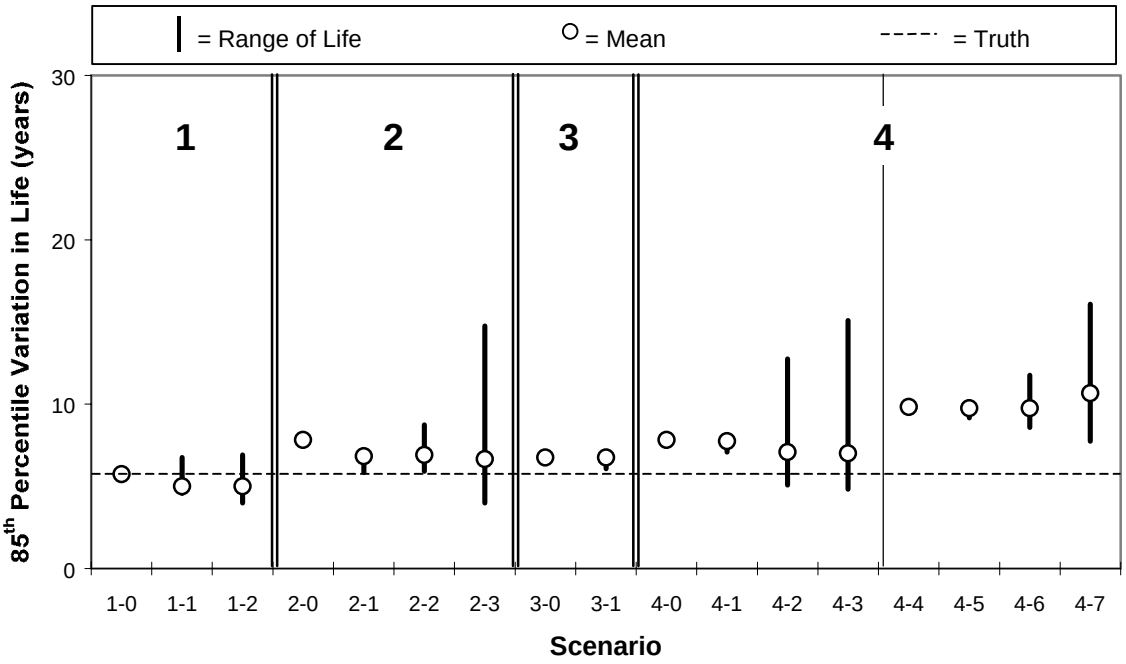

Figure F.33: Rigid Site 9_4008, 85th Percentile Range in Life Overestimation

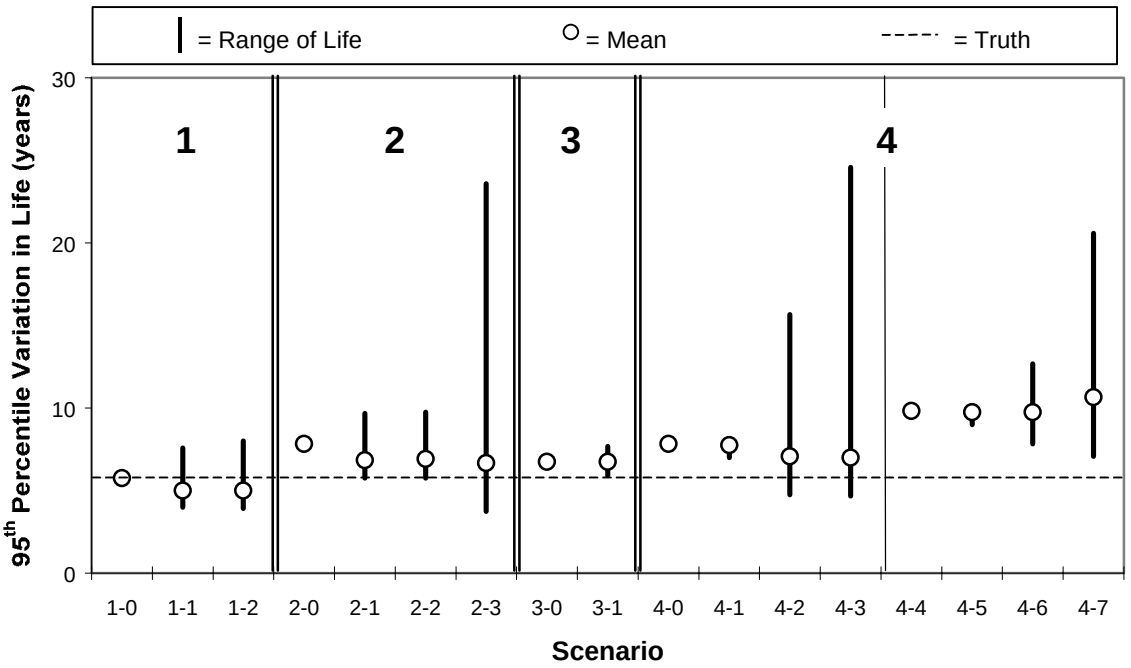

Figure F.34: Rigid Site 9_4008, 95th Percentile Range in Life Overestimation

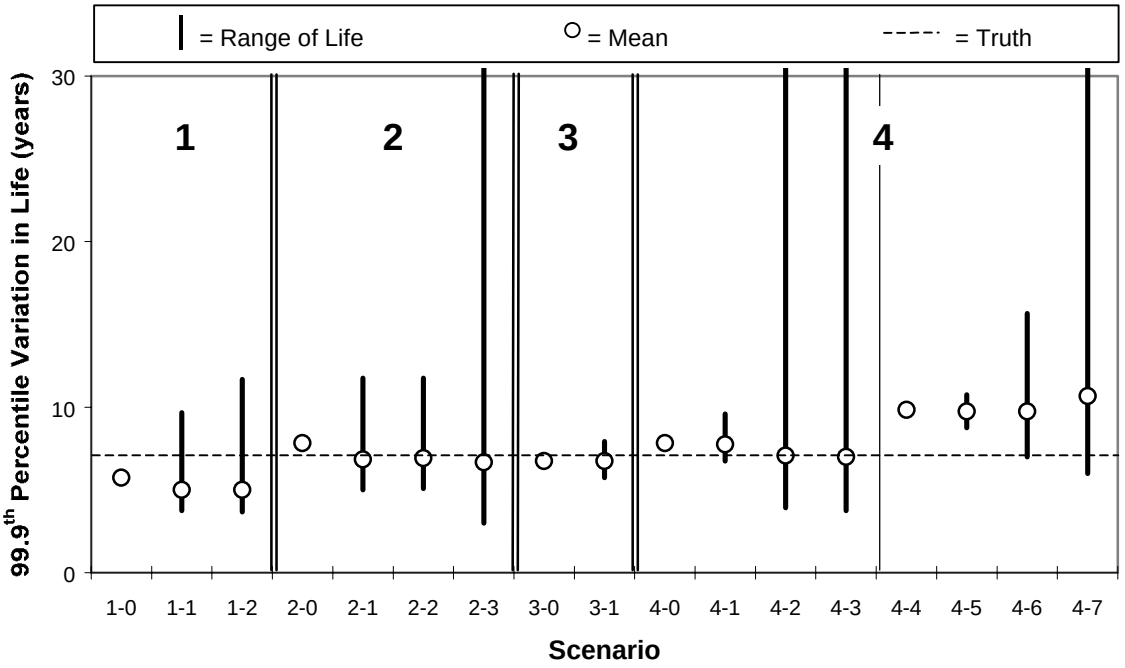

Figure F.35: Rigid Site 9_4008, 99.9th Percentile Range in Life Overestimation

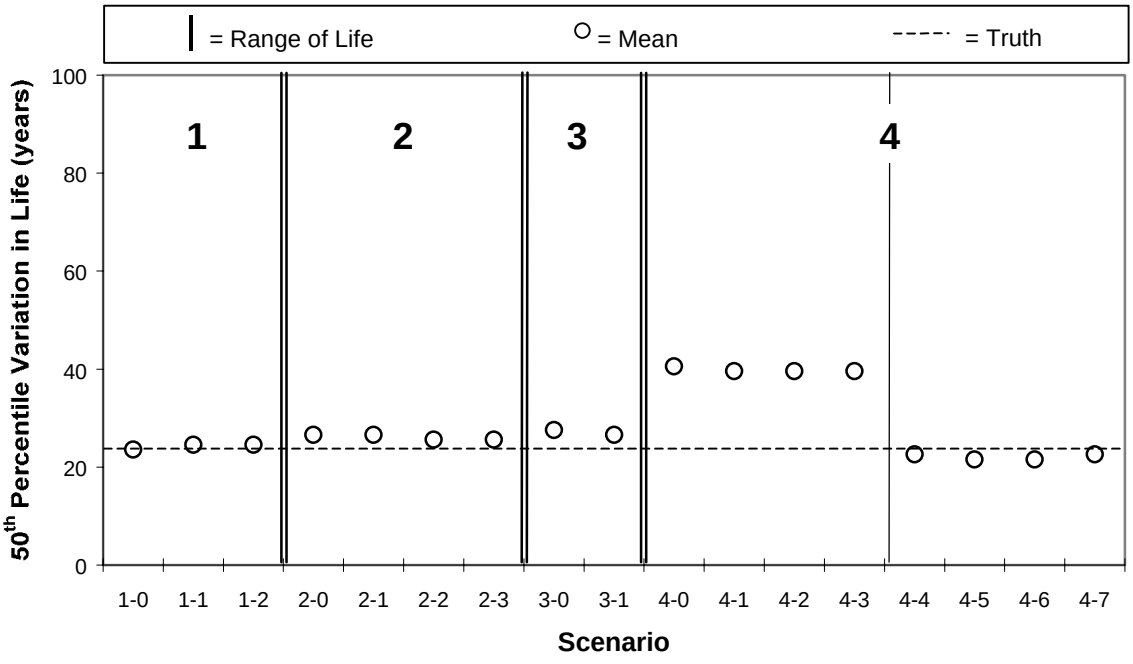

Figure F.36: Rigid Site 50_1682, 50th Percentile Range in Life Overestimation

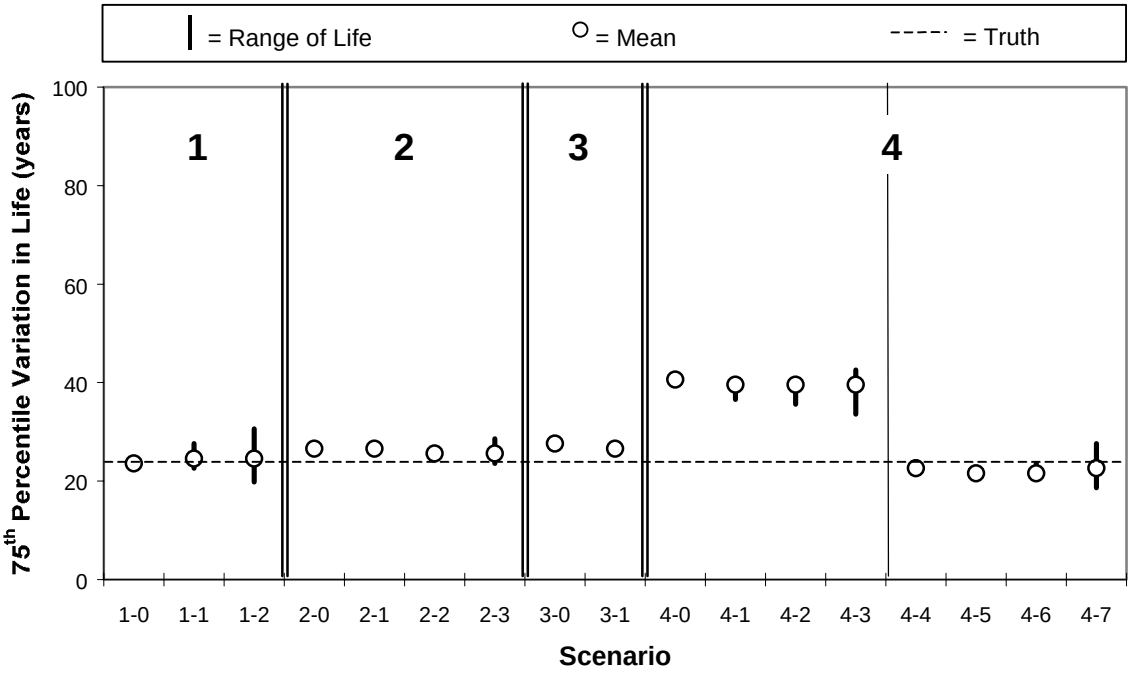

Figure F.37: Rigid Site 50_1682, 75th Percentile Range in Life Overestimation

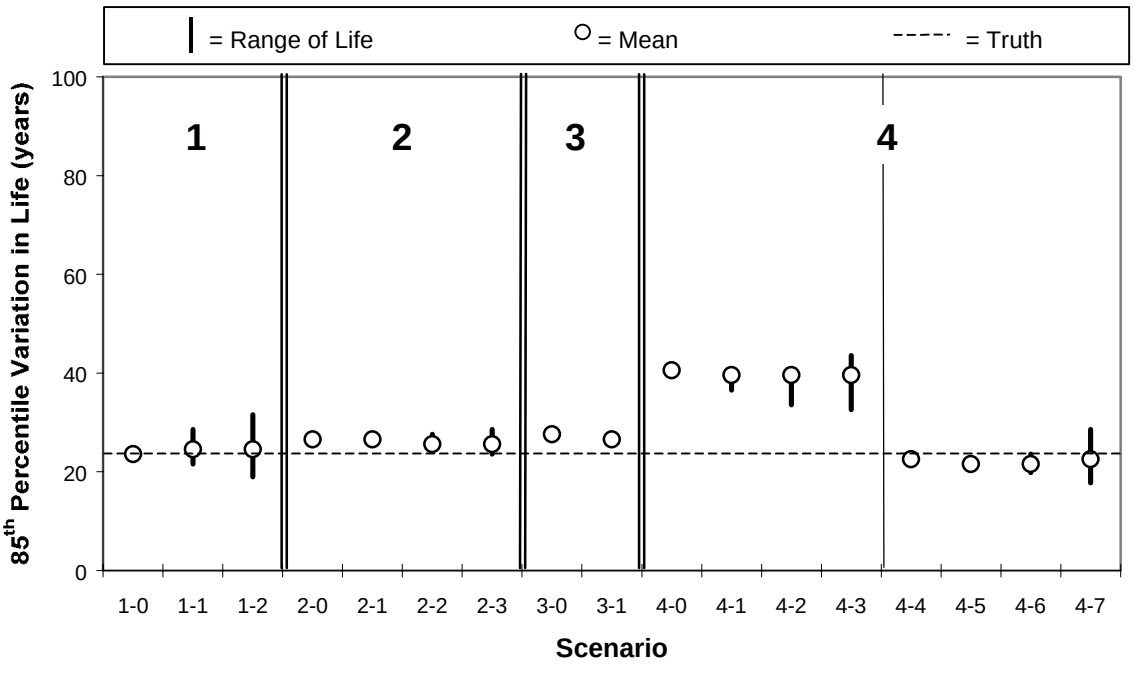

Figure F.38: Rigid Site 50_1682, 85th Percentile Range in Life Overestimation

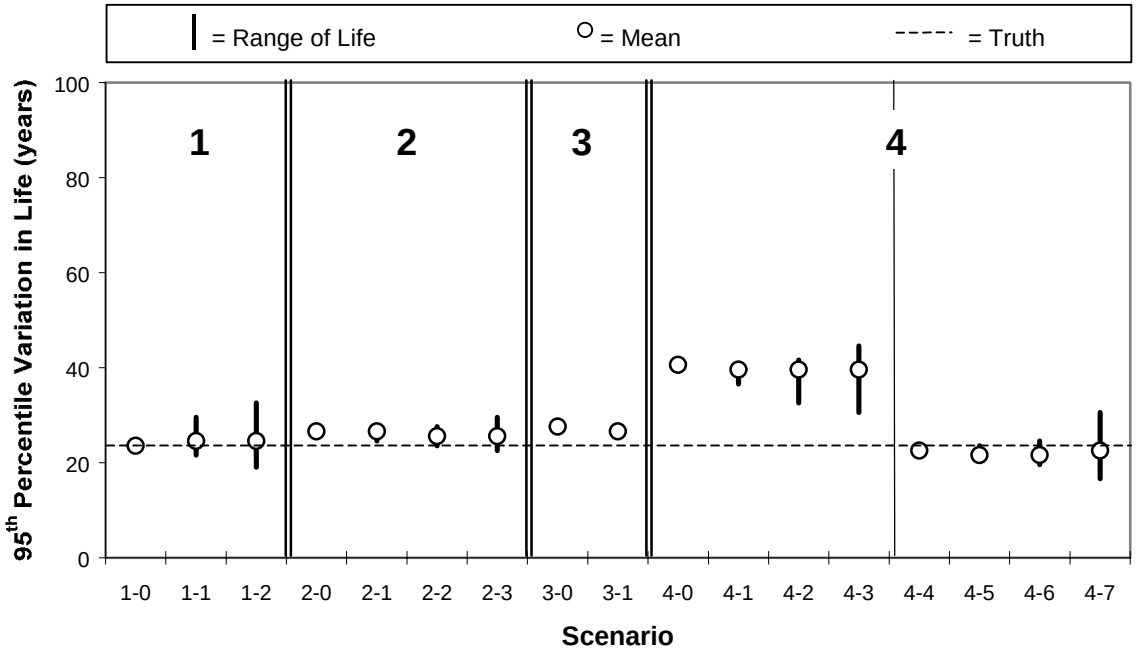

Figure F.39: Rigid Site 50_1682, 95th Percentile Range in Life Overestimation

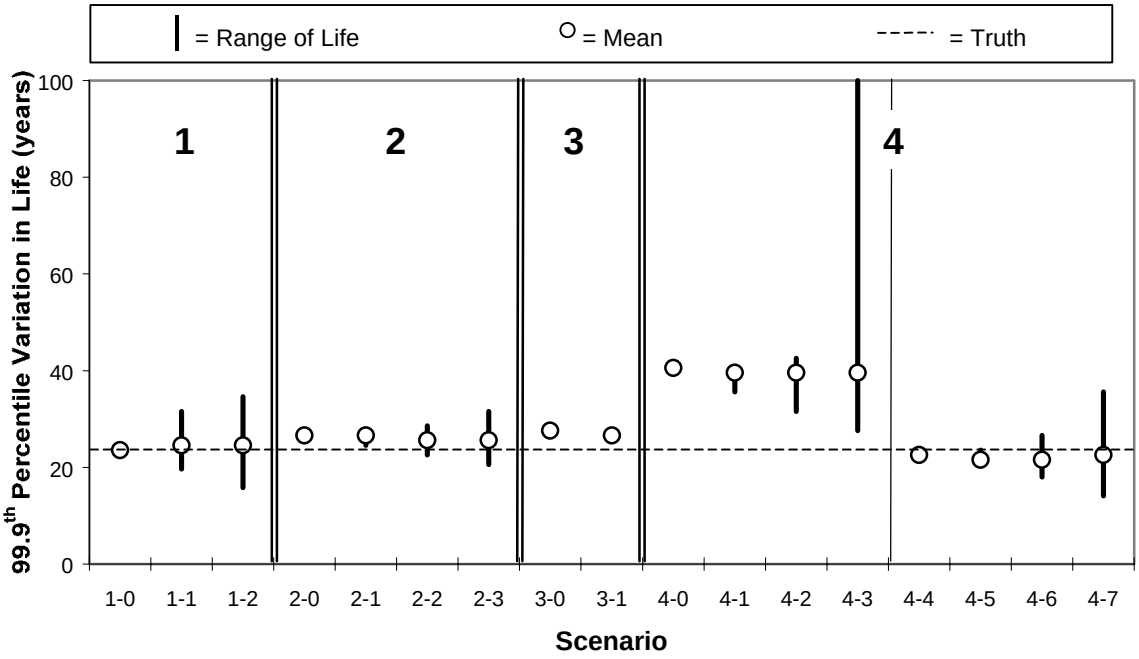

Figure F.40: Rigid Site 50_1682, 99.9th Percentile Range in Life Overestimation

APPENDIX G

Pavement Performance

All pavement sections were analyzed using the 2002 PDG. This section contains the life of pavement sections as a function of traffic sampling scenario.

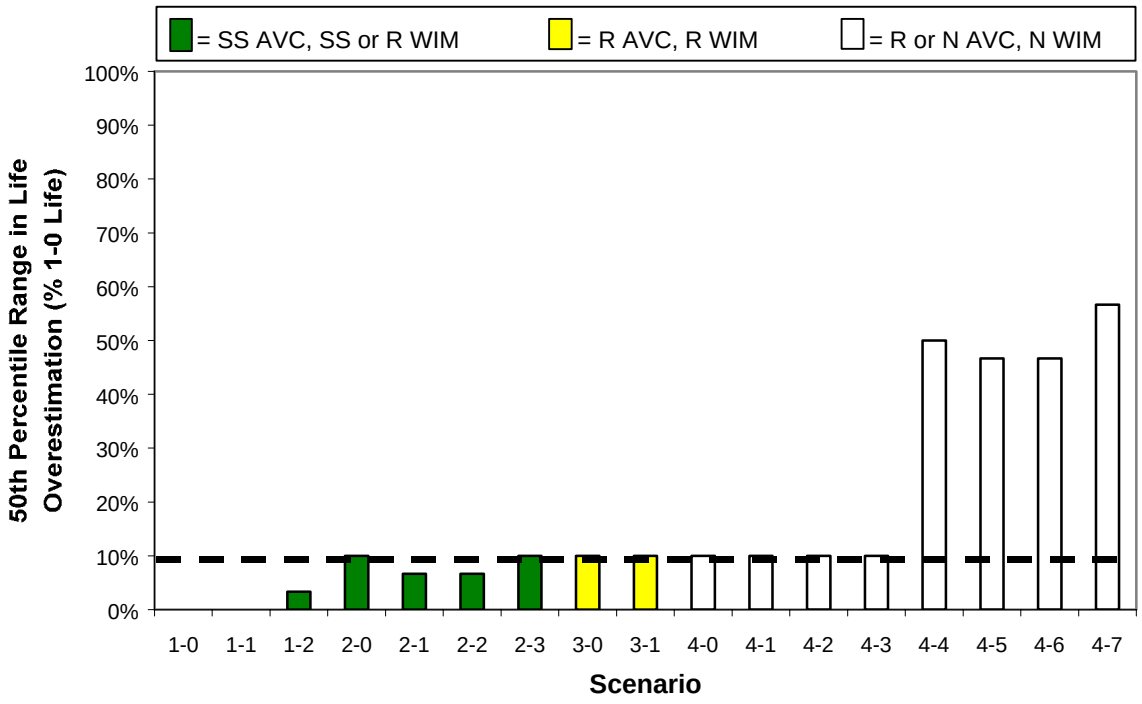

Figure G.1: Flexible Site 18_1028, 50th Percentile, % Life Overestimation

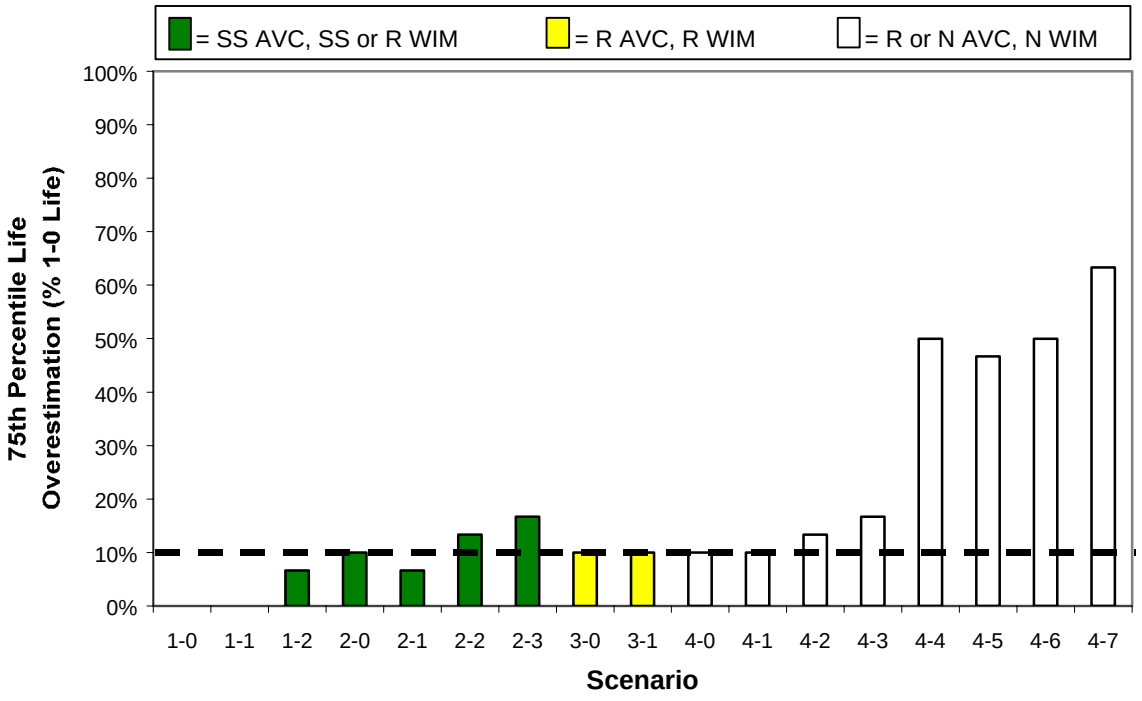

Figure G.2: Flexible Site 18_1028, 75th Percentile, % Life Overestimation

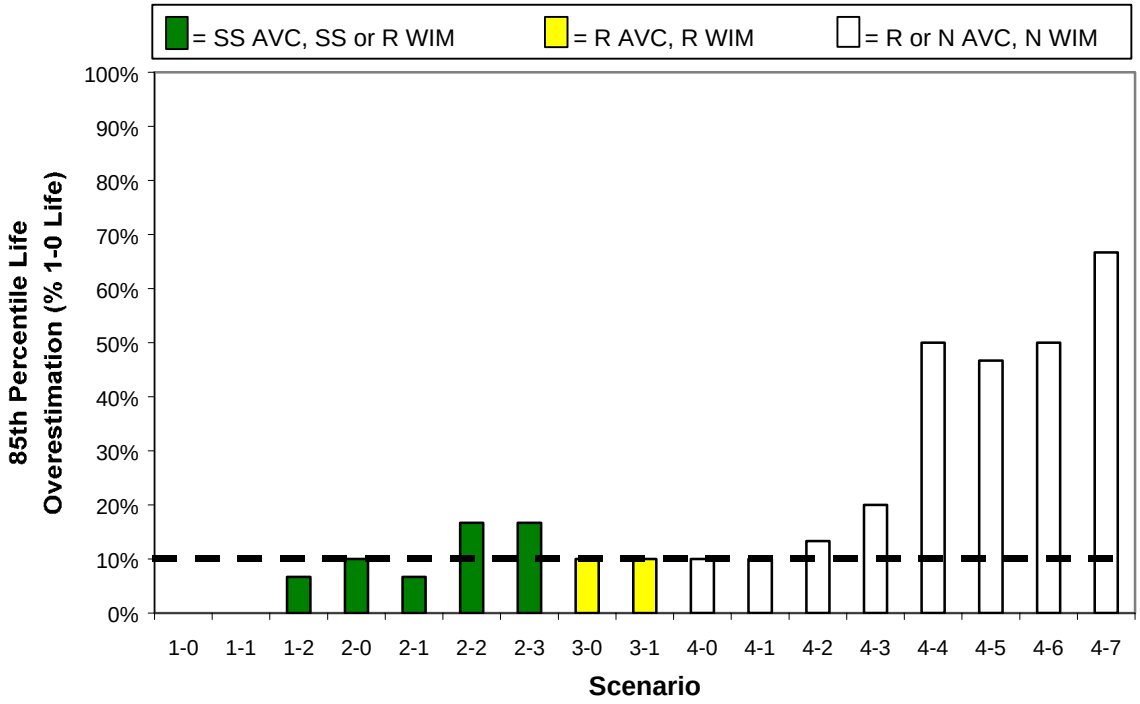

Figure G.3: Flexible Site 18_1028, 85th Percentile, % Life Overestimation

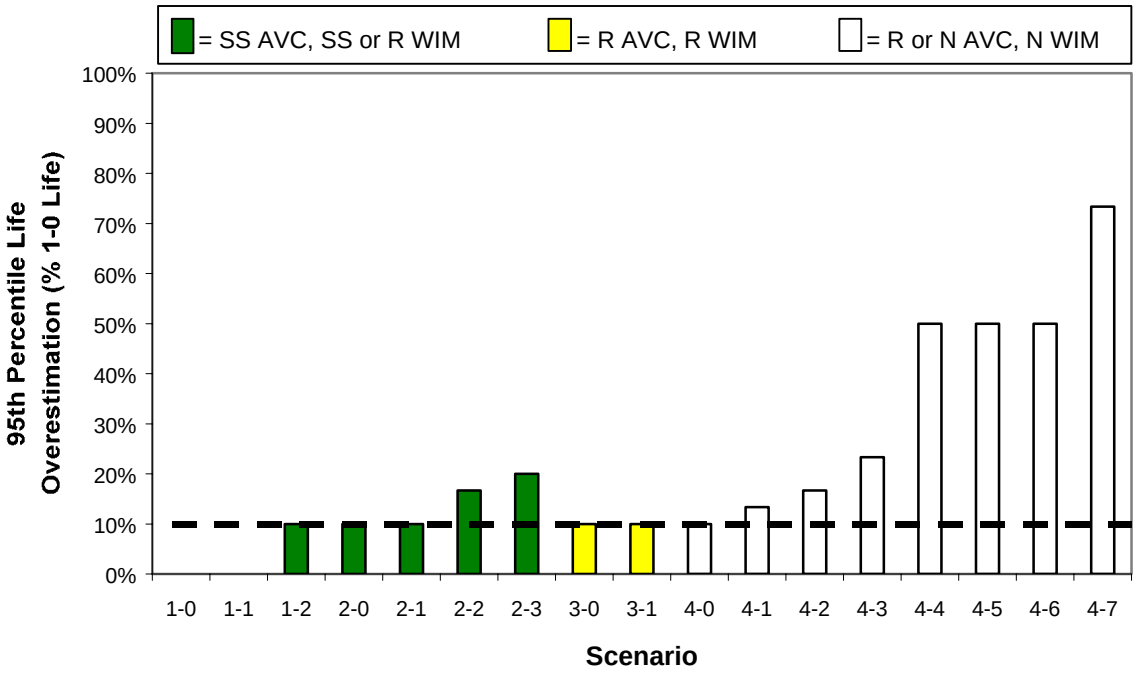

Figure G.4: Flexible Site 18_1028, 95th Percentile, % Life Overestimation

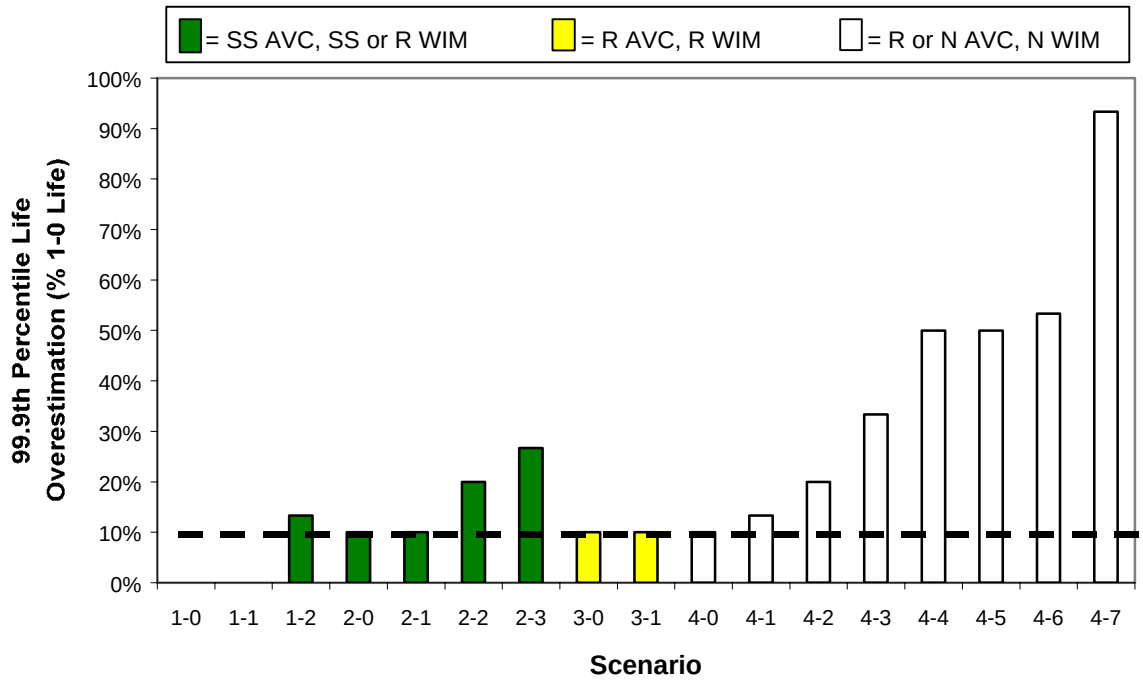

Figure G.5: Flexible Site 18_1028, 99.9th Percentile, % Life Overestimation

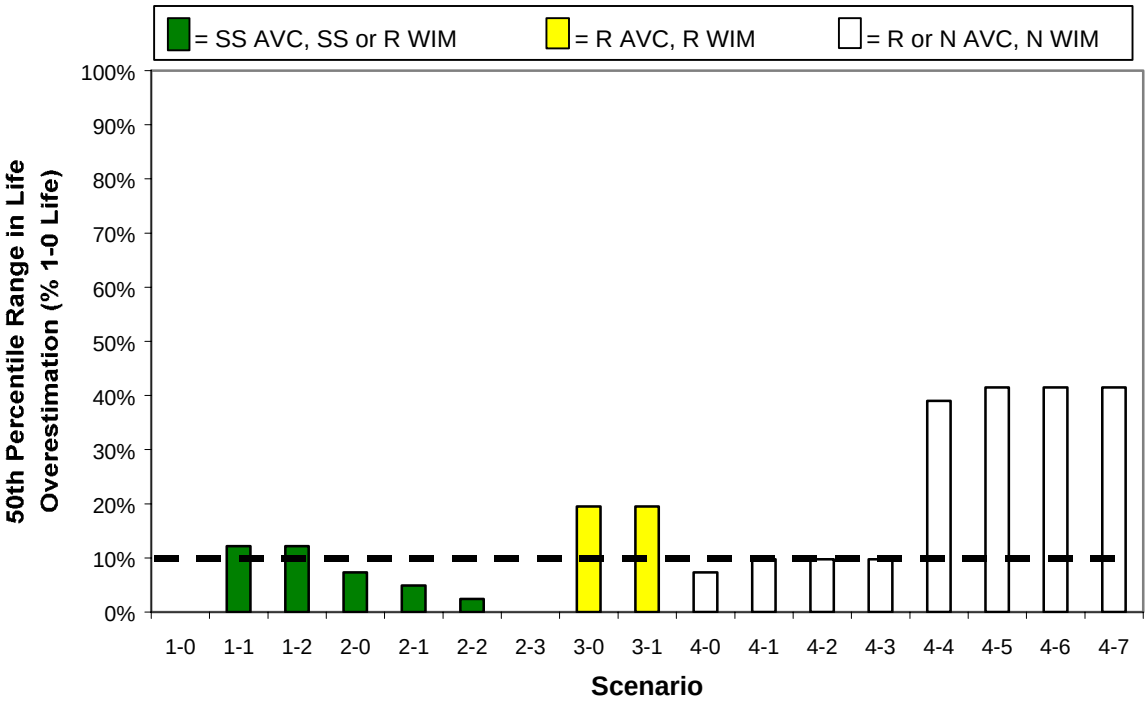

Figure G.6: Flexible Site 26_1010, 50th Percentile, % Life Overestimation

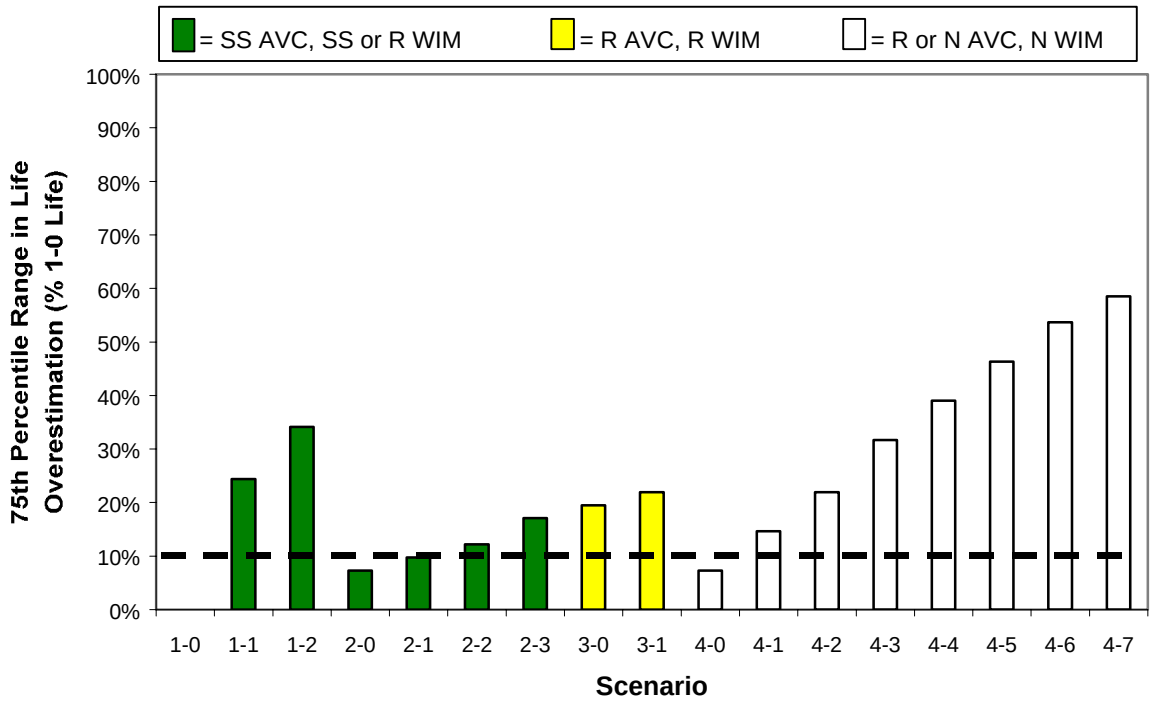

Figure G.7: Flexible Site 26_1010, 75th Percentile, % Life Overestimation

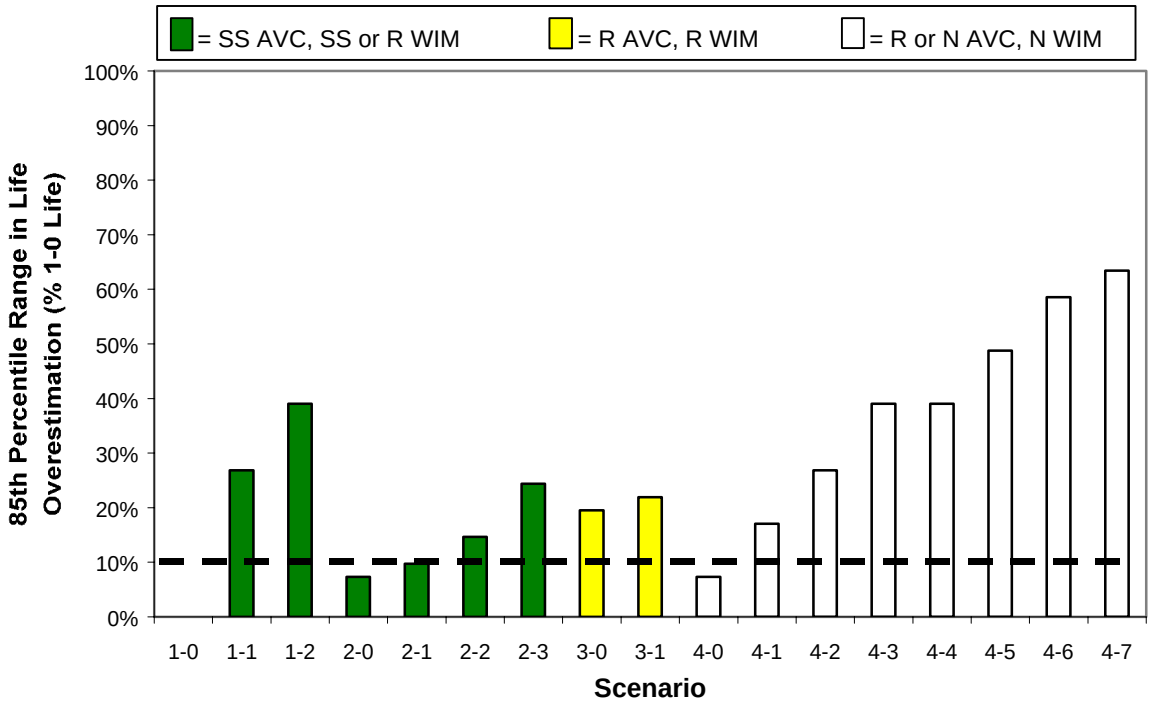

Figure G.8: Flexible Site 26_1010, 85th Percentile, % Life Overestimation

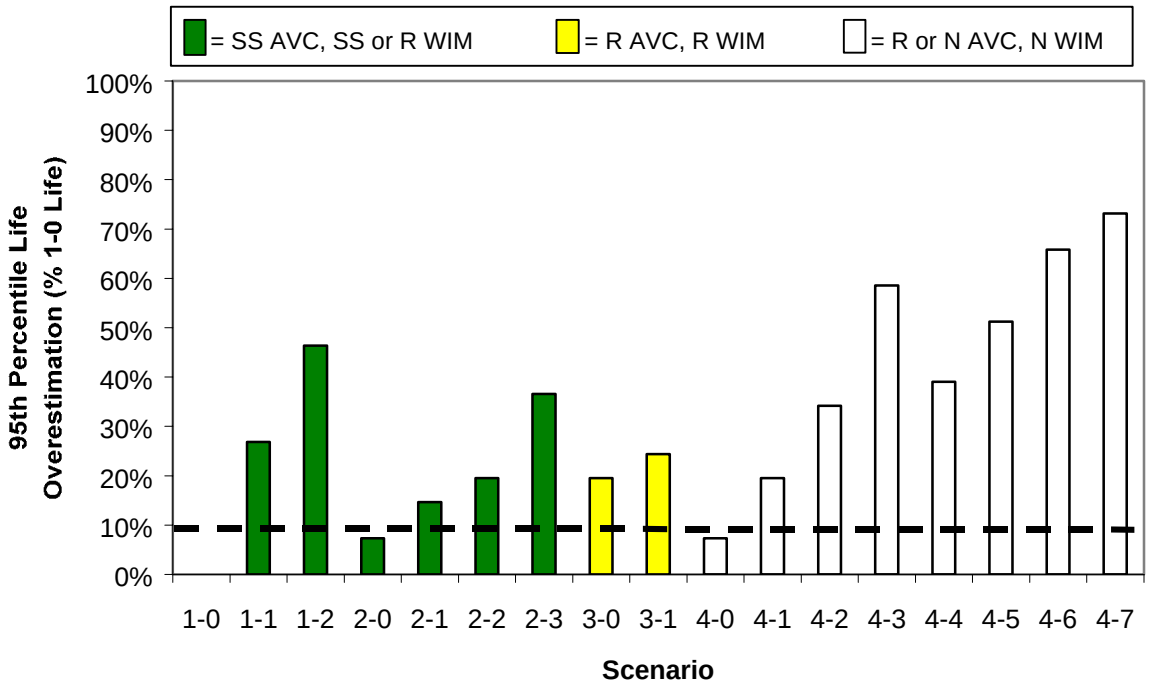

Figure G.9: Flexible Site 26_1010, 95th Percentile, % Life Overestimation

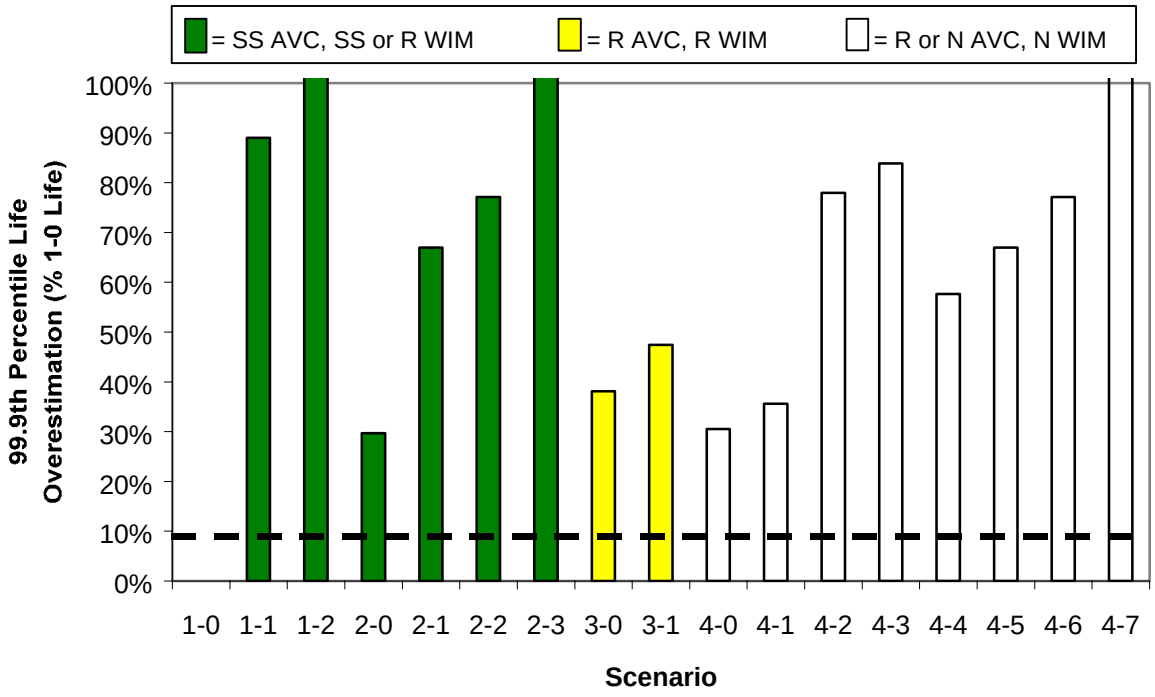

Figure G.10: Flexible Site 26_1010, 99.9th Percentile, % Life Overestimation

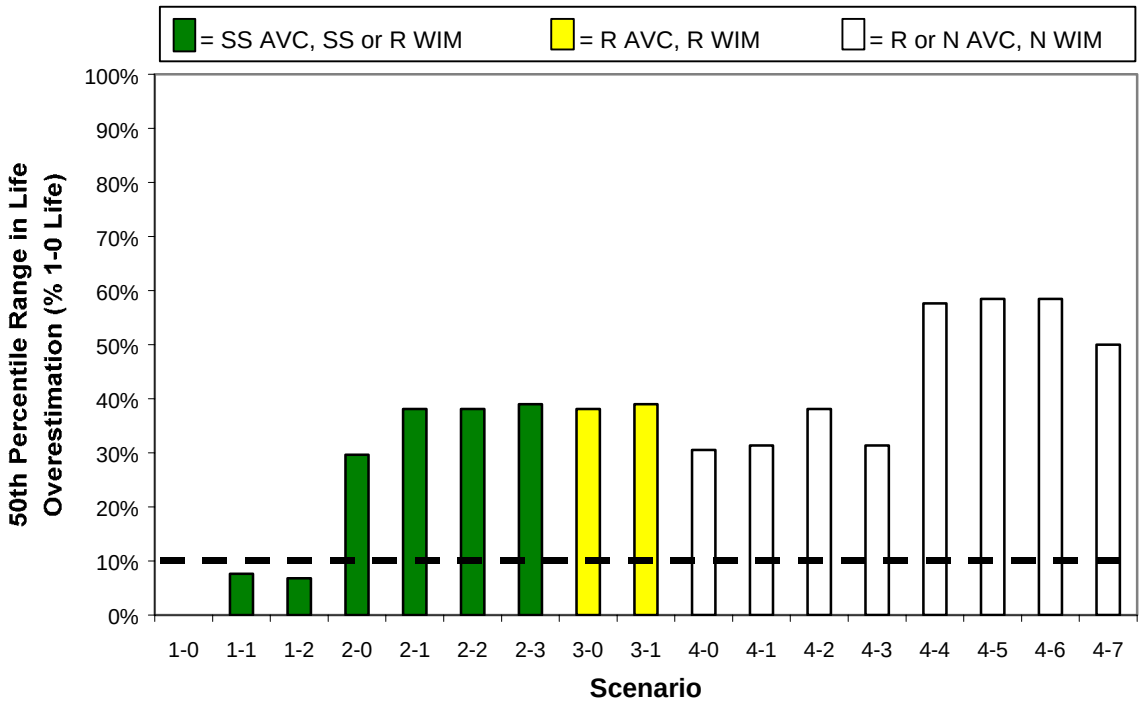

Figure G.11: Flexible Site 53_6048, 50th Percentile, % Life Overestimation

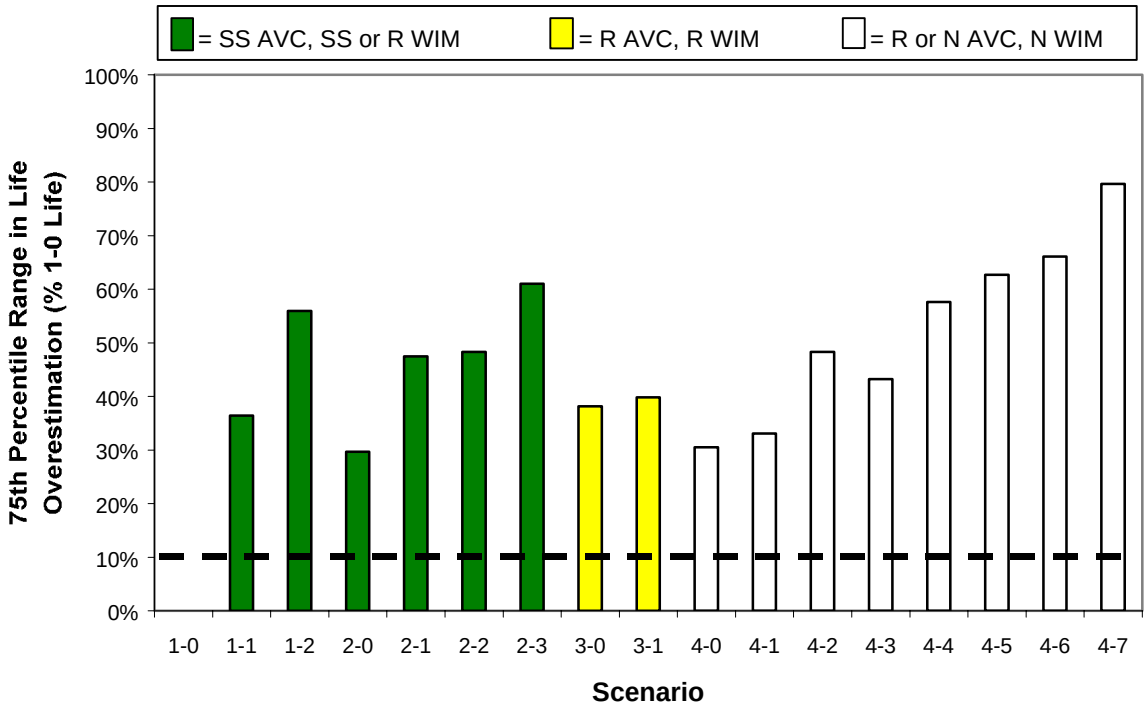

Figure G.12: Flexible Site 53_6048, 75th Percentile, % Life Overestimation

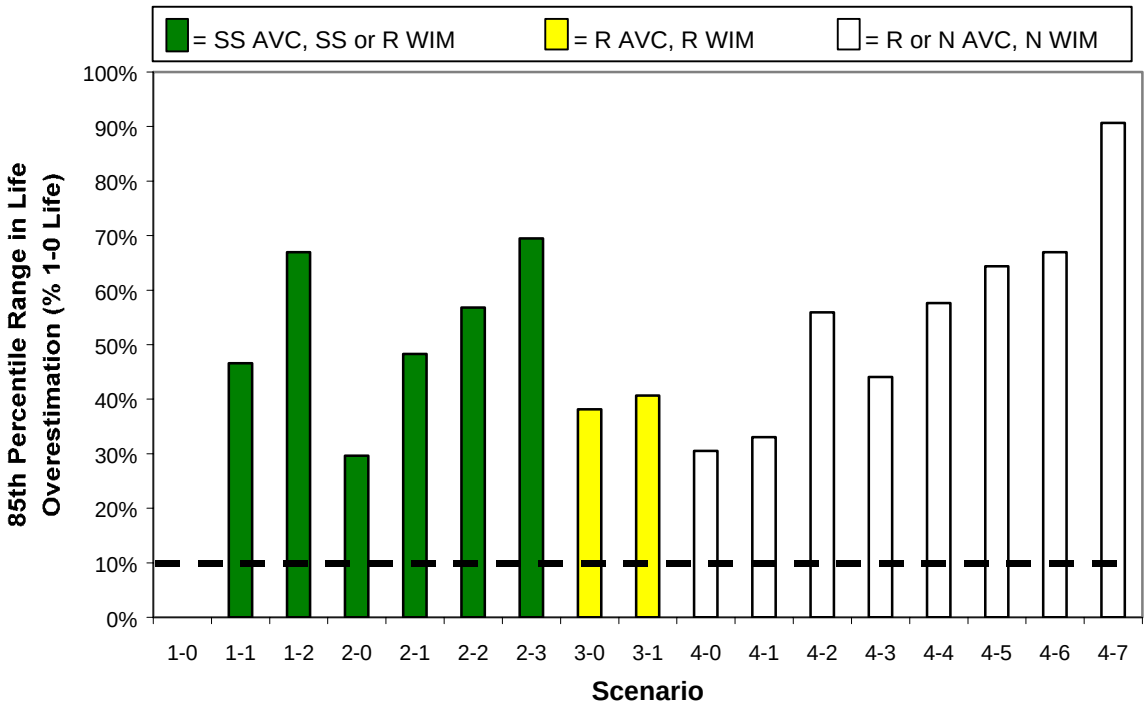

Figure G.13: Flexible Site 53_6048, 85th Percentile, % Life Overestimation

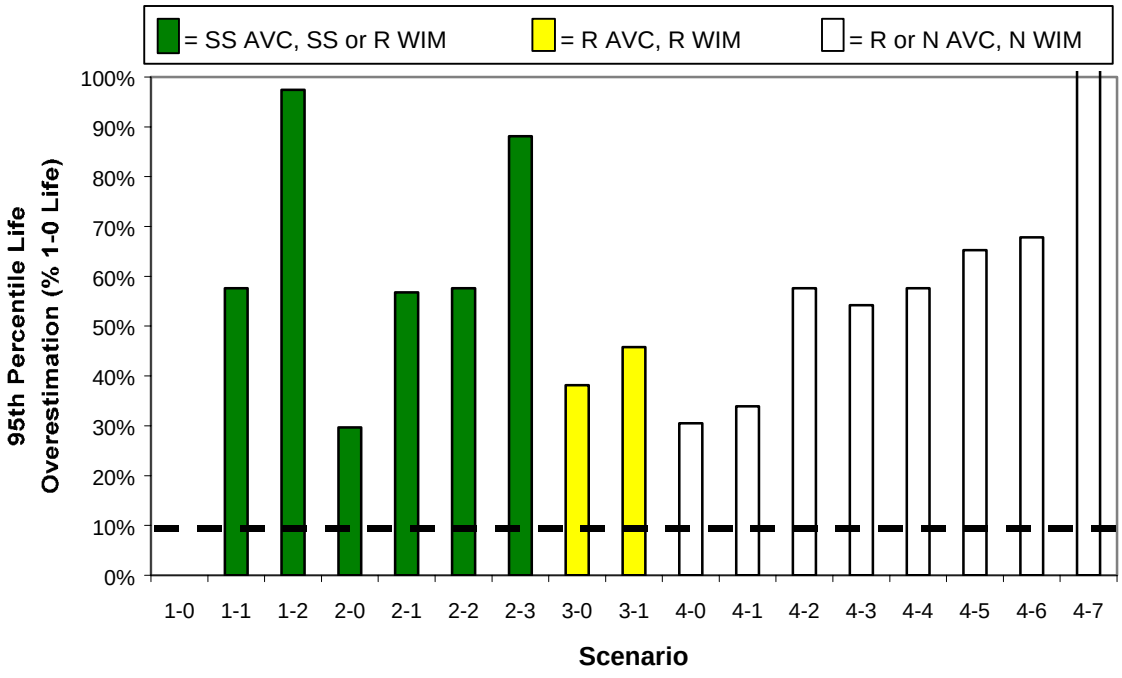

Figure G.14: Flexible Site 53_6048, 95th Percentile, % Life Overestimation

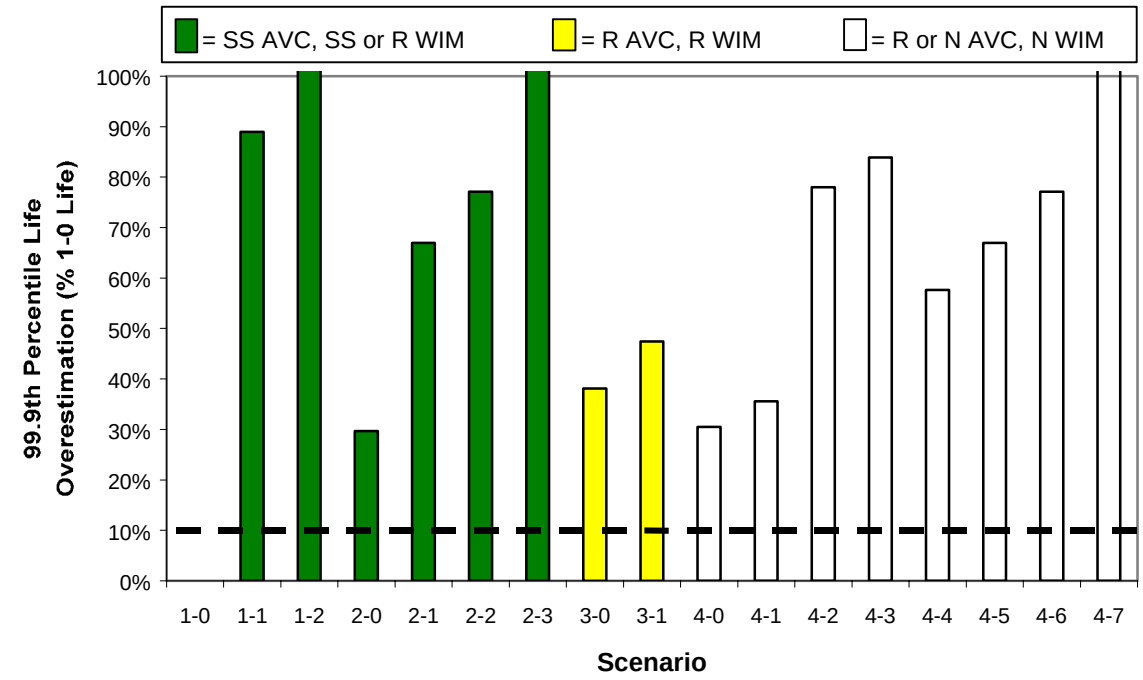

Figure G.15: Flexible Site 53_6048, 99.9th Percentile, % Life Overestimation

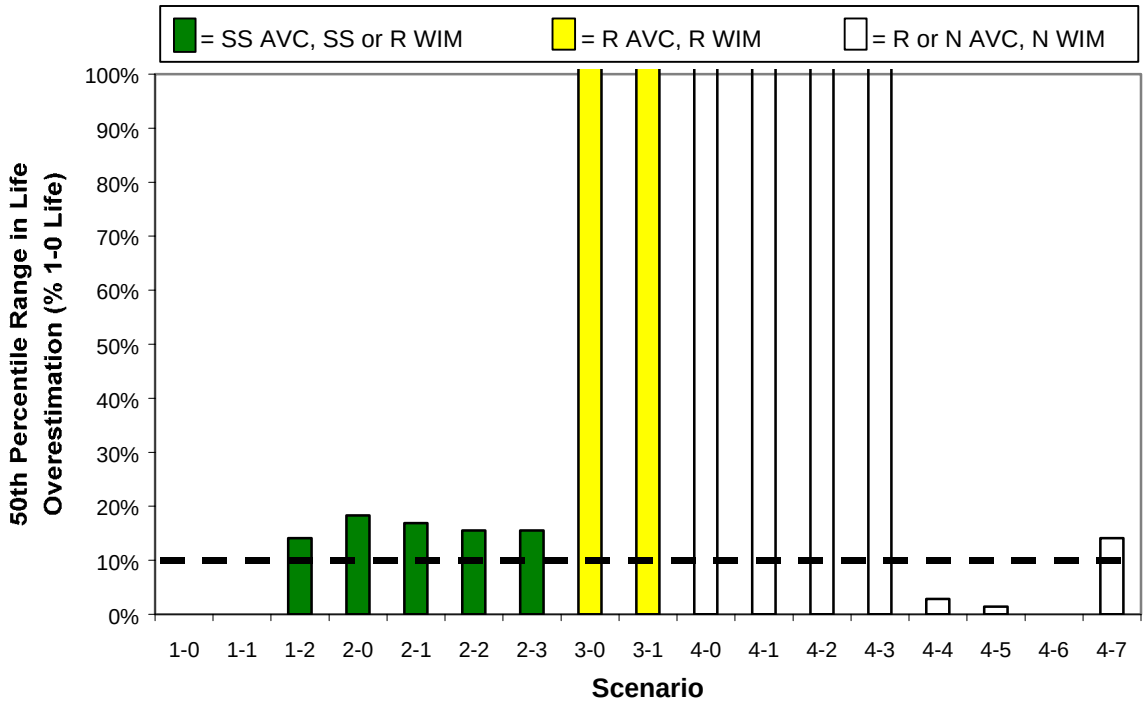

Figure G.16: Flexible Site 28_2807, 50th Percentile, % Life Overestimation

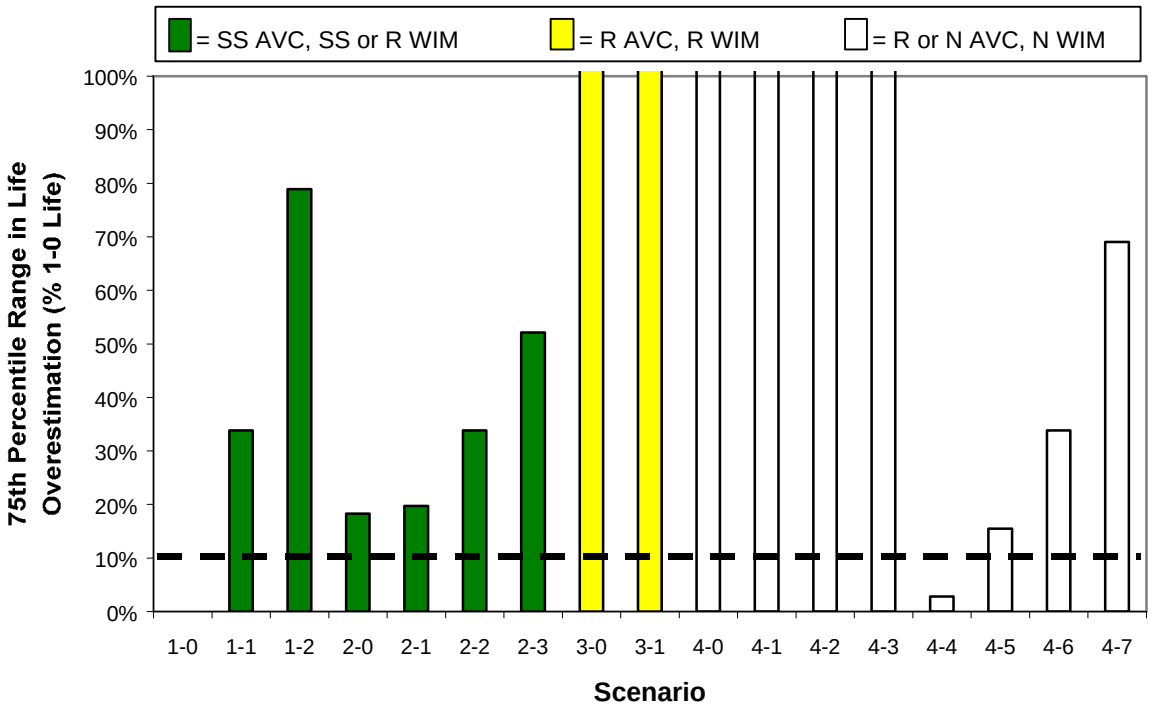

Figure G.17: Flexible Site 28_2807, 75th Percentile, % Life Overestimation

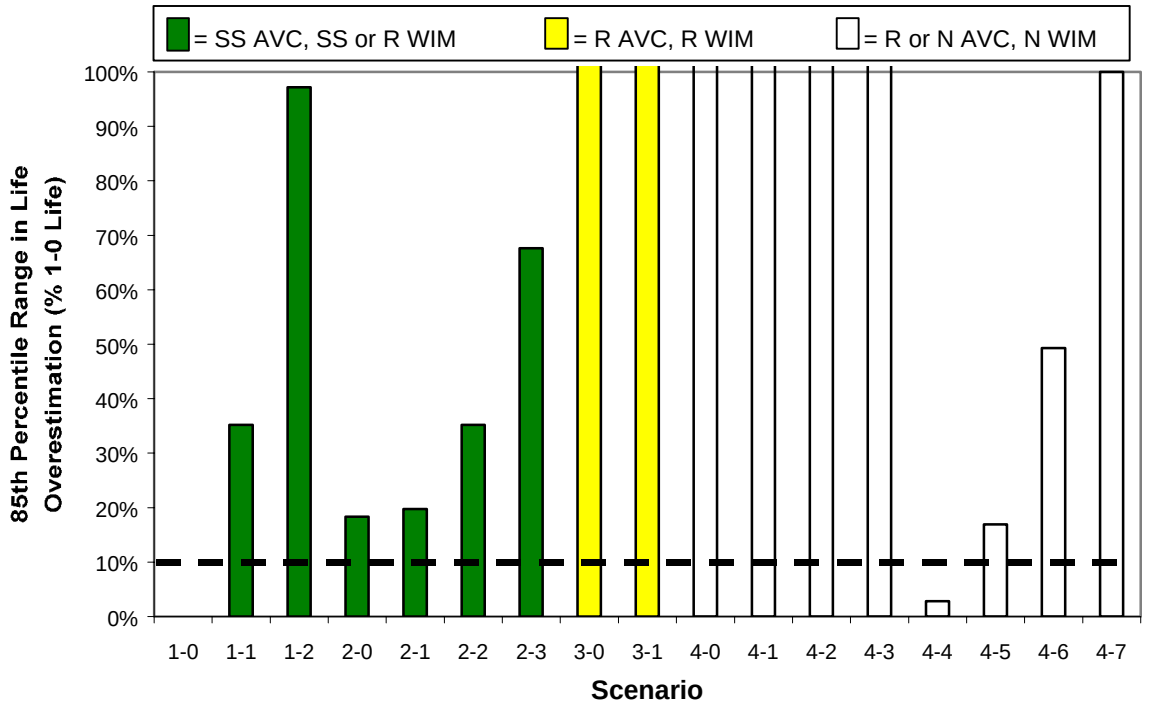

Figure G.18: Flexible Site 28_2807, 85th Percentile, % Life Overestimation

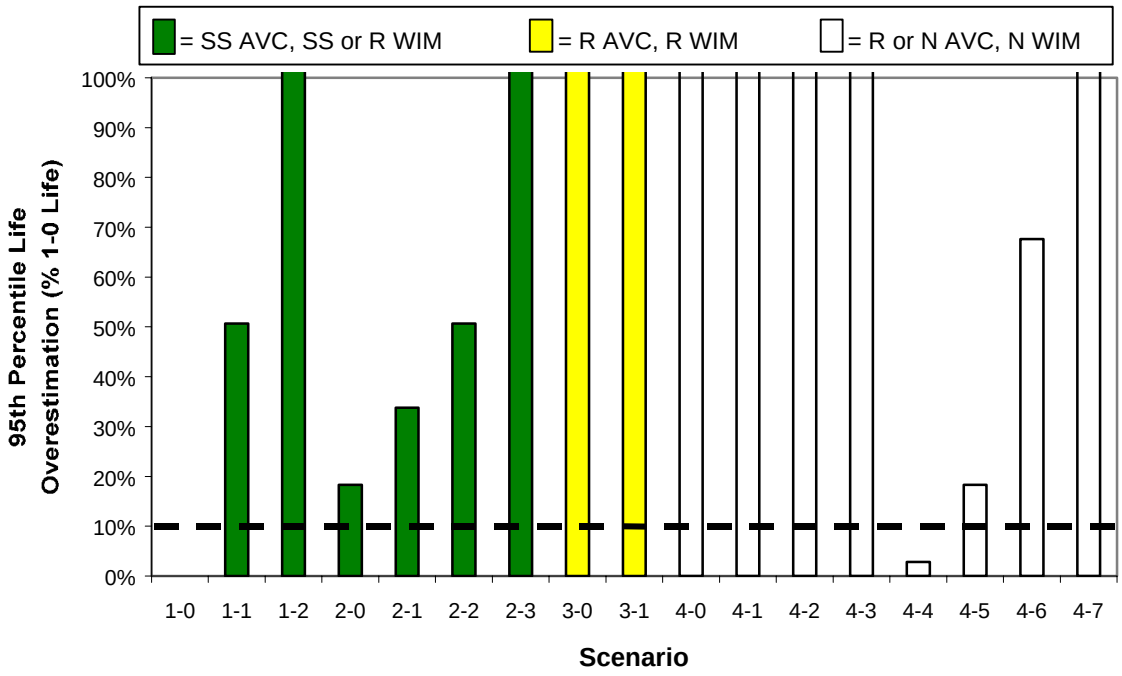

Figure G.19: Flexible Site 28_2807, 95th Percentile, % Life Overestimation

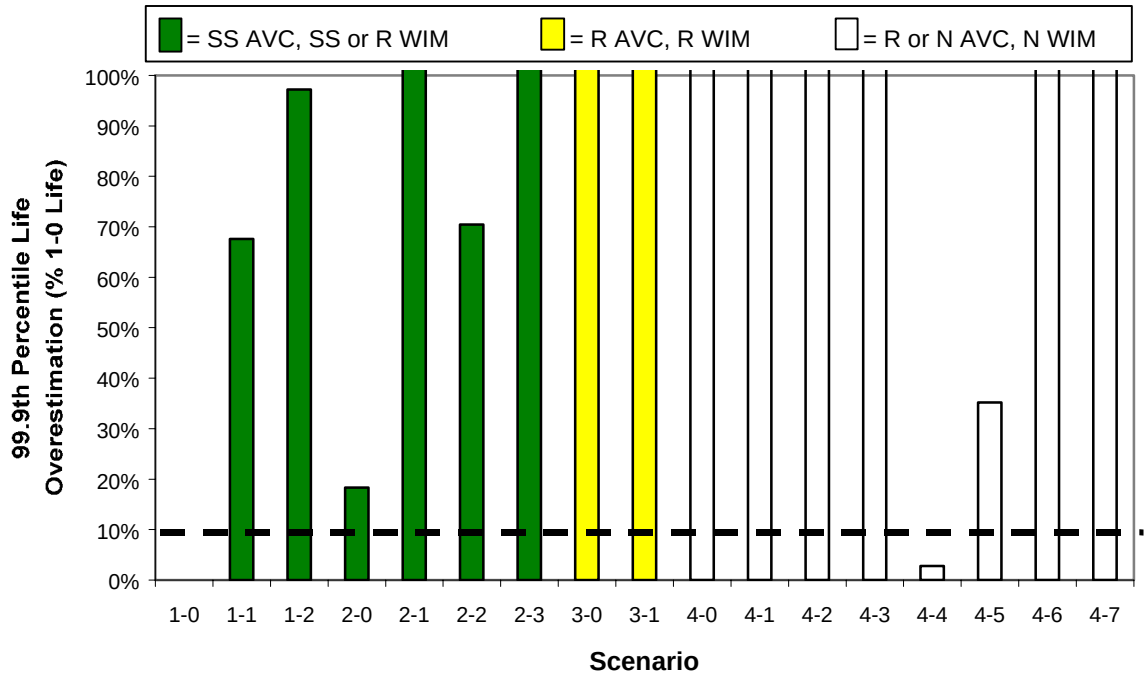

Figure G.20: Flexible Site 28_2807, 99.9th Percentile, % Life Overestimation

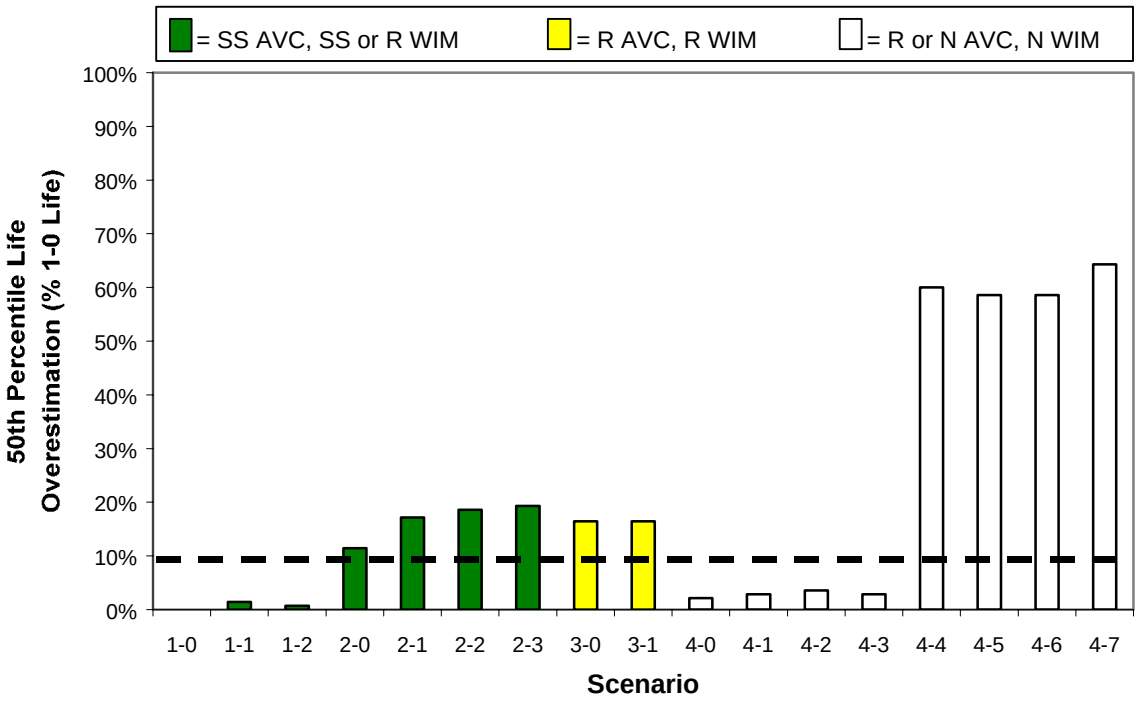

Figure G.21: Rigid Site 18_5518, 50th Percentile, % Life Overestimation

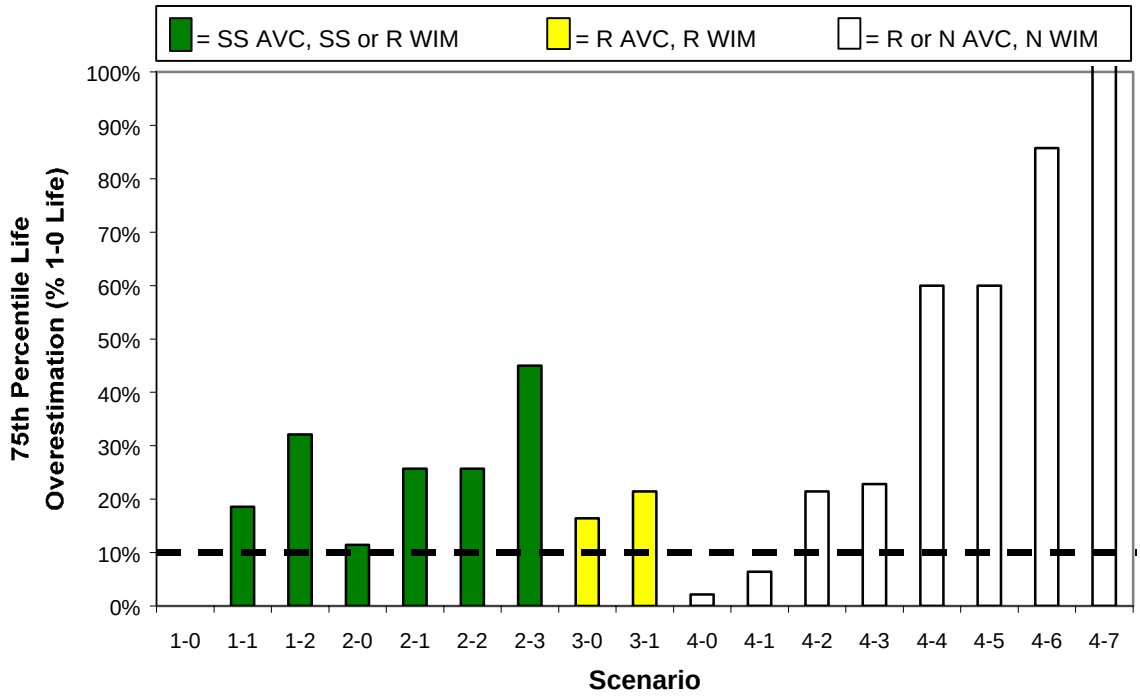

Figure G.22: Rigid Site 18_5518, 75th Percentile, % Life Overestimation

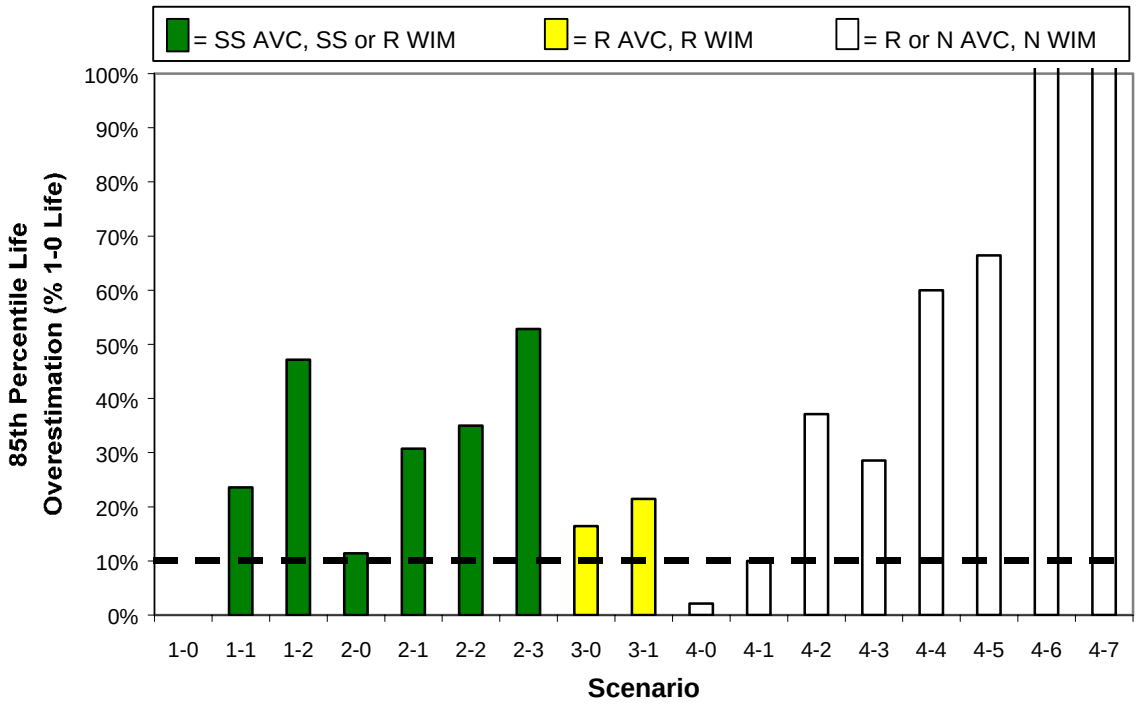

Figure G.23: Rigid Site 18_5518, 85th Percentile, % Life Overestimation

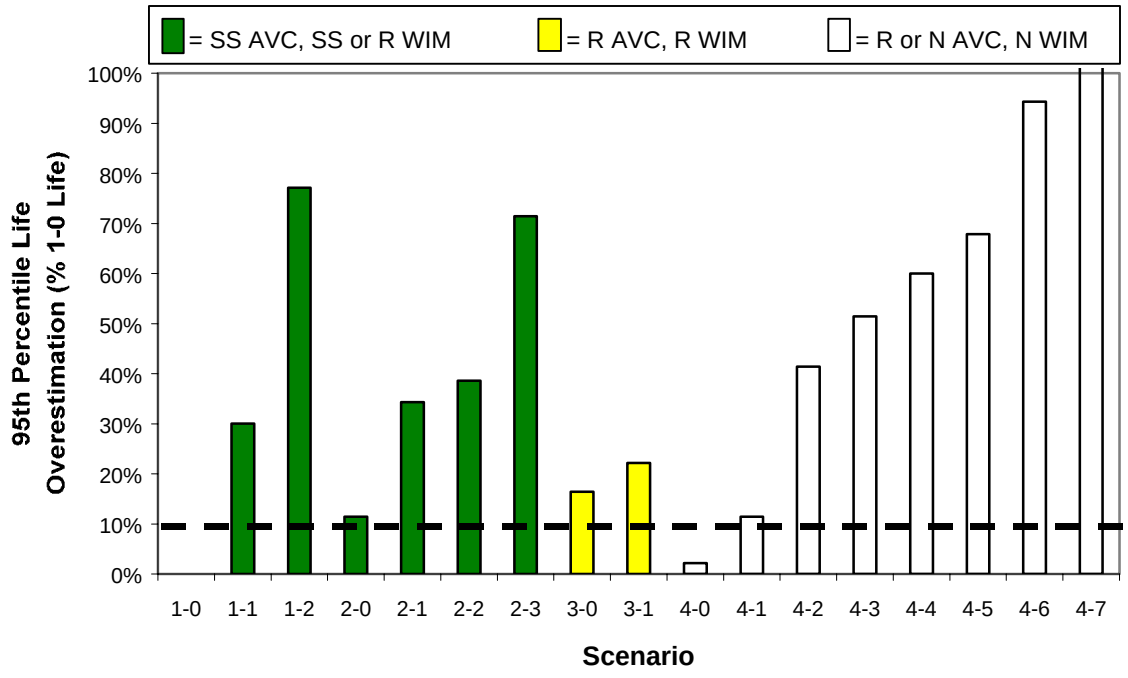

Figure G.24: Rigid Site 18_5518, 95th Percentile, % Life Overestimation

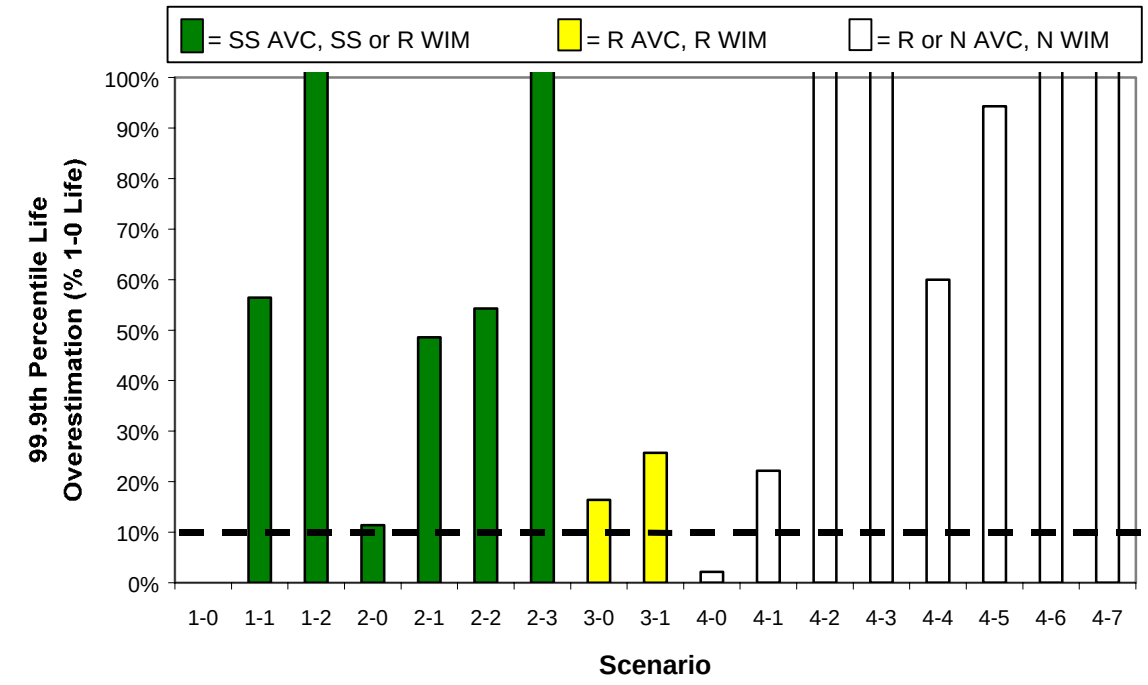

Figure G.25: Rigid Site 18_5518, 99.9th Percentile, % Life Overestimation

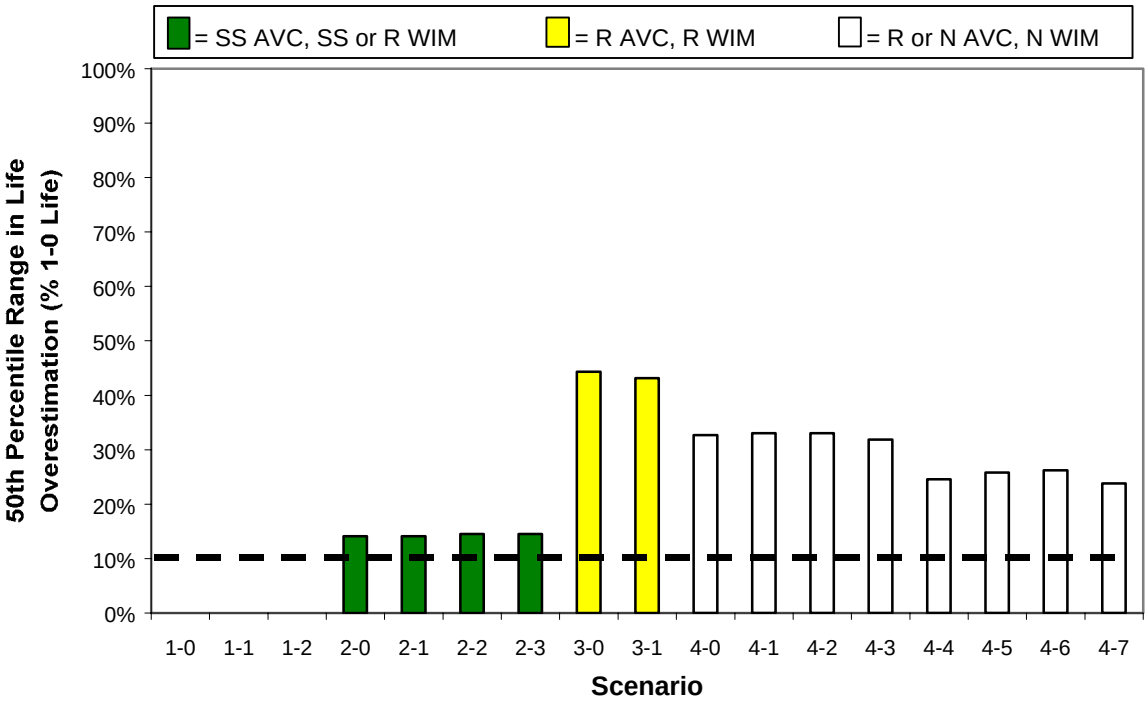

Figure G.26: Rigid Site 27_5076, 50th Percentile, % Life Overestimation

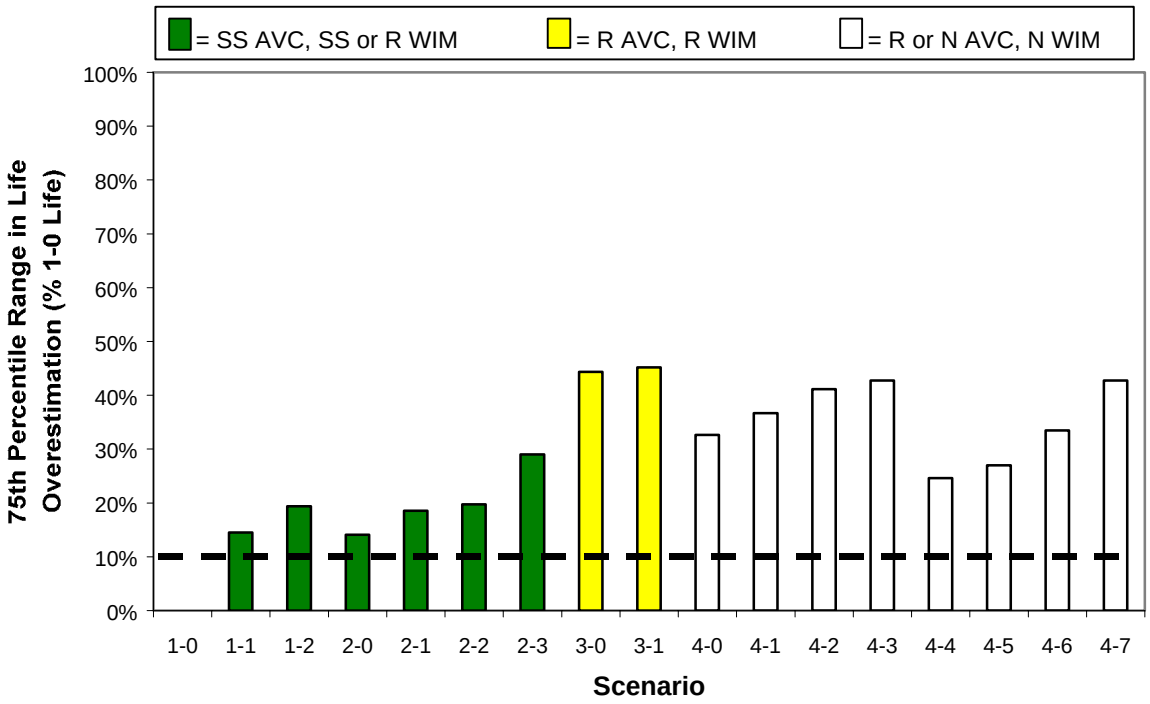

Figure G.27: Rigid Site 27_5076, 75th Percentile, % Life Overestimation

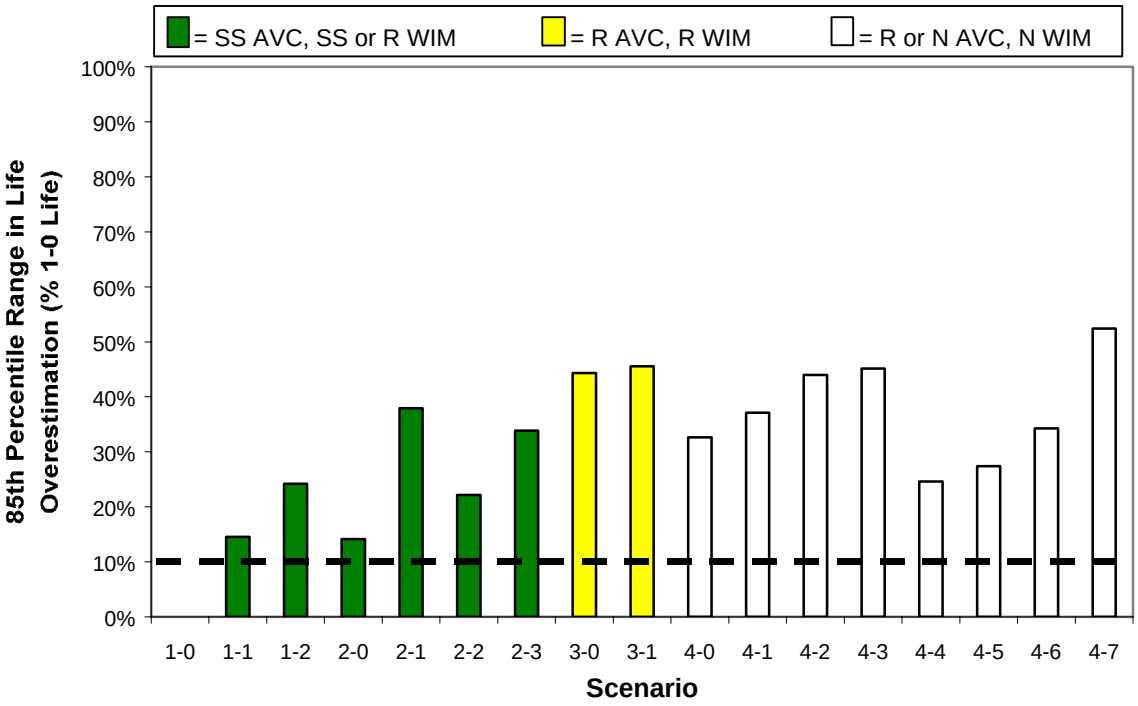

Figure G.28: Rigid Site 27_5076, 85th Percentile, % Life Overestimation

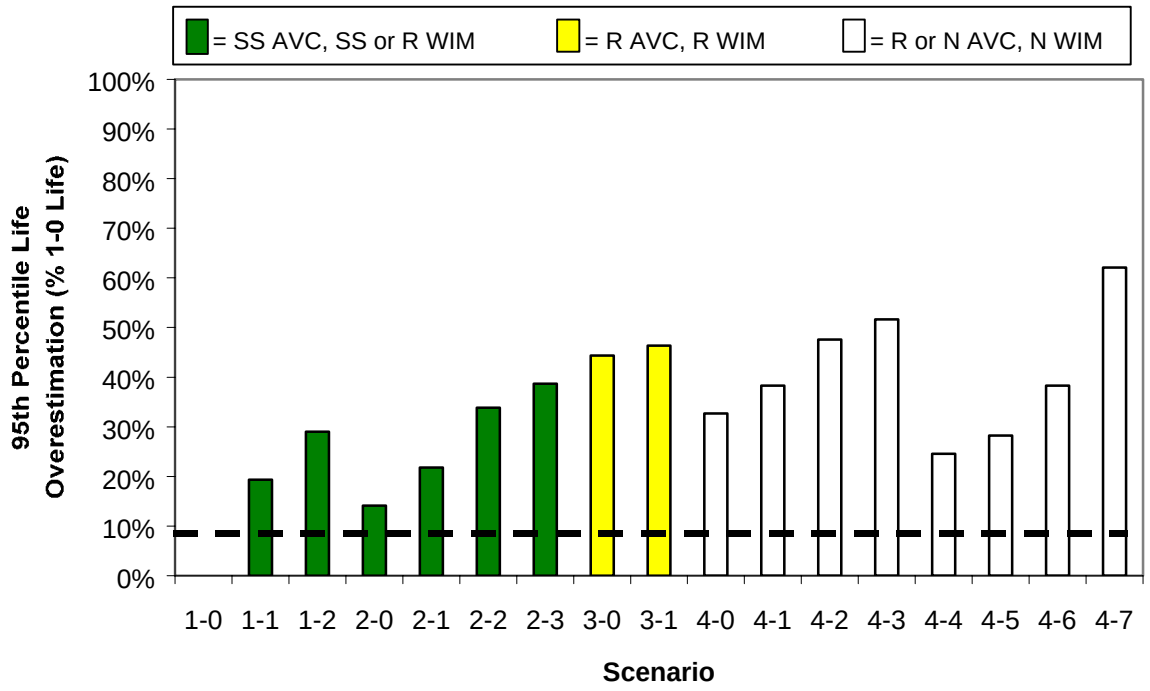

Figure G.29: Rigid Site 27_5076, 95th Percentile, % Life Overestimation

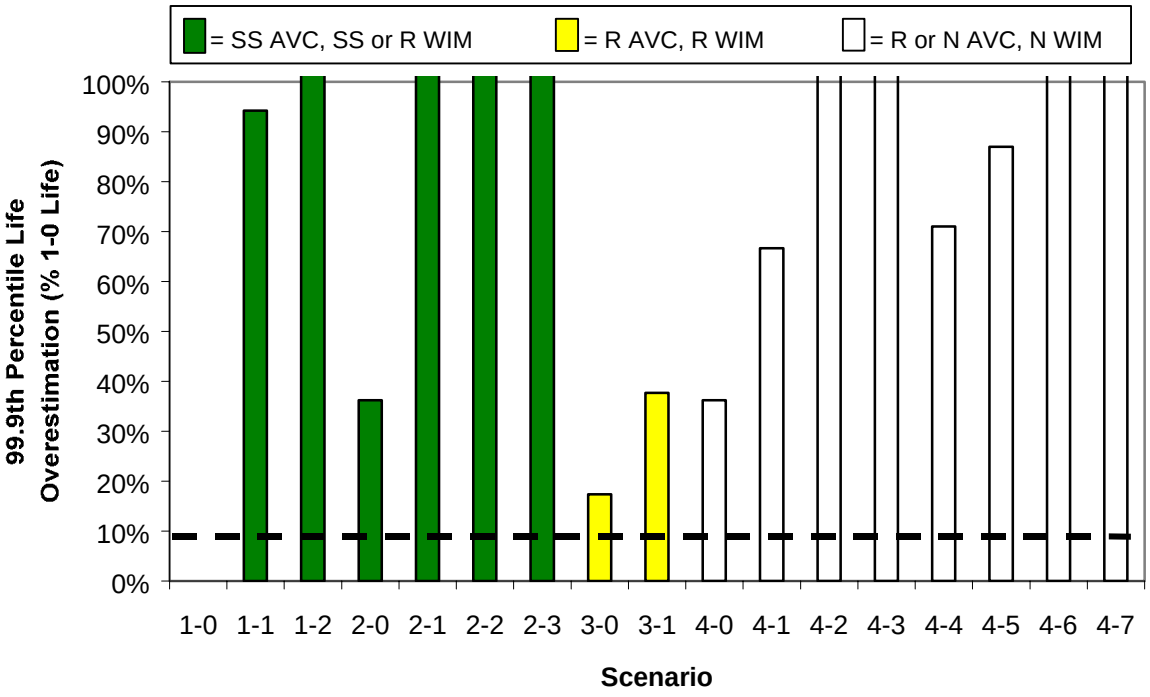

Figure G.30: Rigid Site 27_5076, 99.9th Percentile, % Life Overestimation

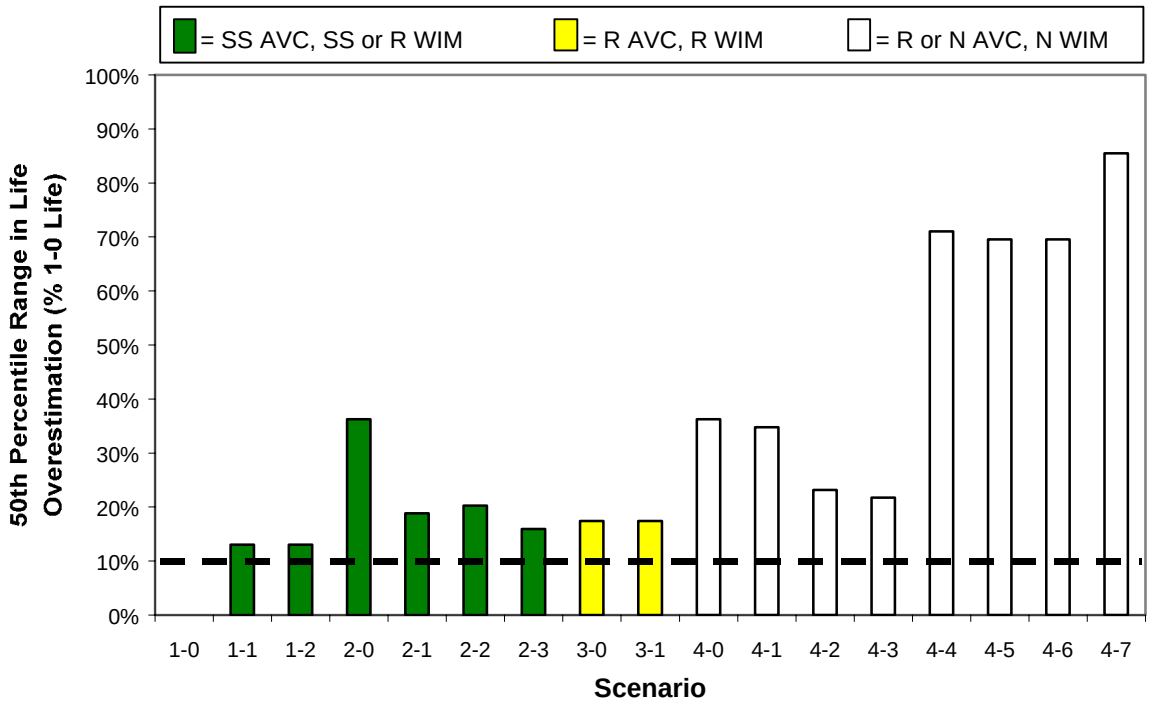

Figure G.31: Rigid Site 9_4008, 50th Percentile, % Life Overestimation

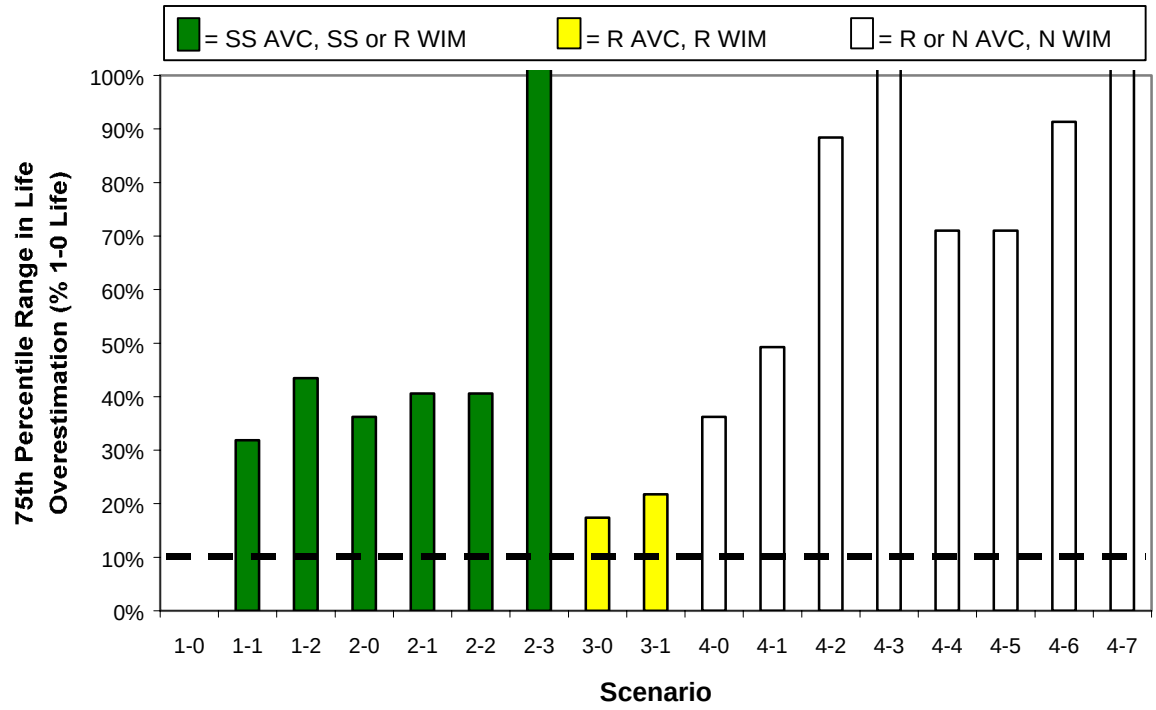

Figure G.32: Rigid Site 9_4008, 75th Percentile, % Life Overestimation

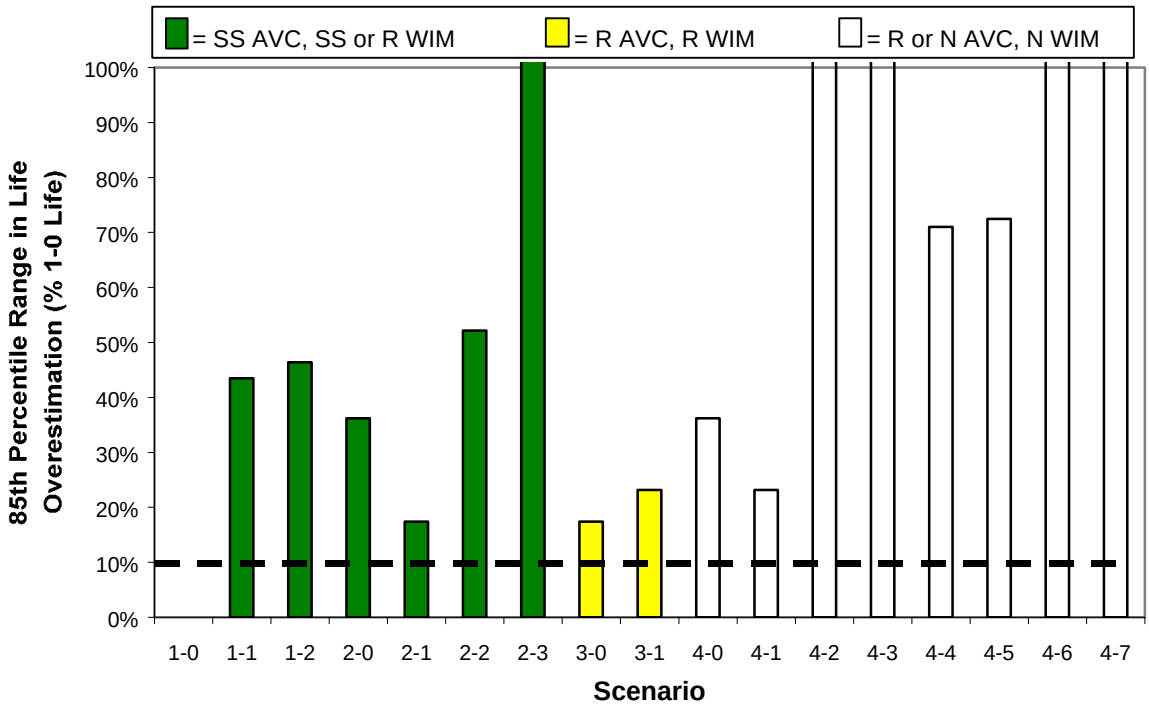

Figure G.33: Rigid Site 9_4008, 85th Percentile, % Life Overestimation

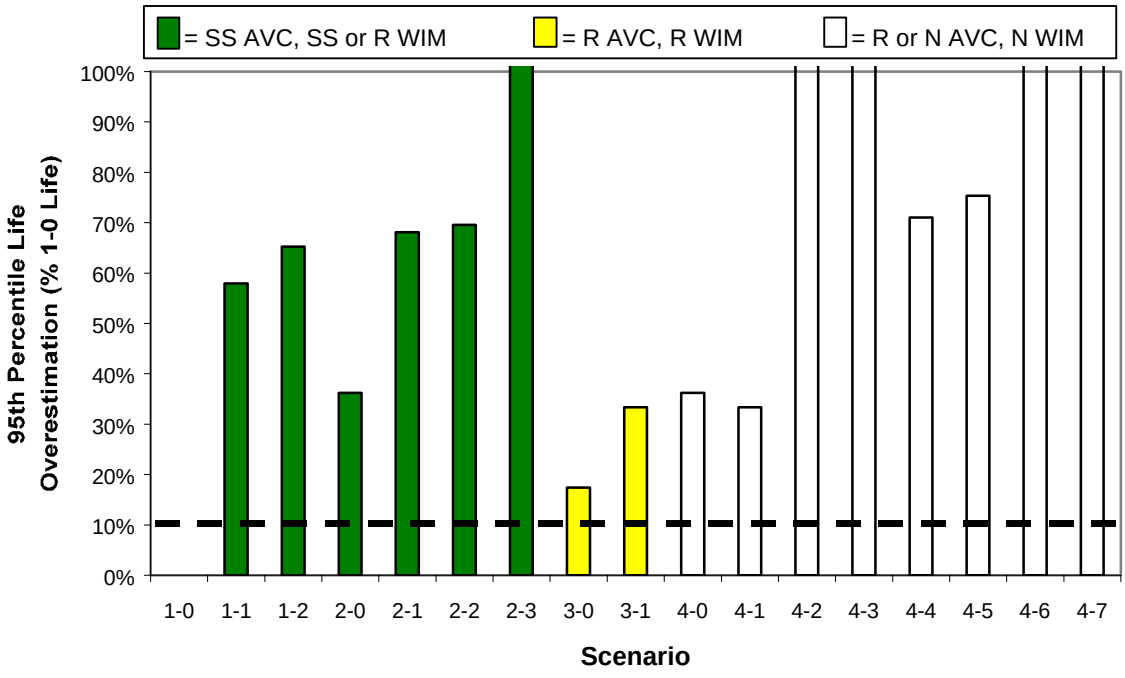

Figure G.34: Rigid Site 9_4008, 95th Percentile, % Life Overestimation

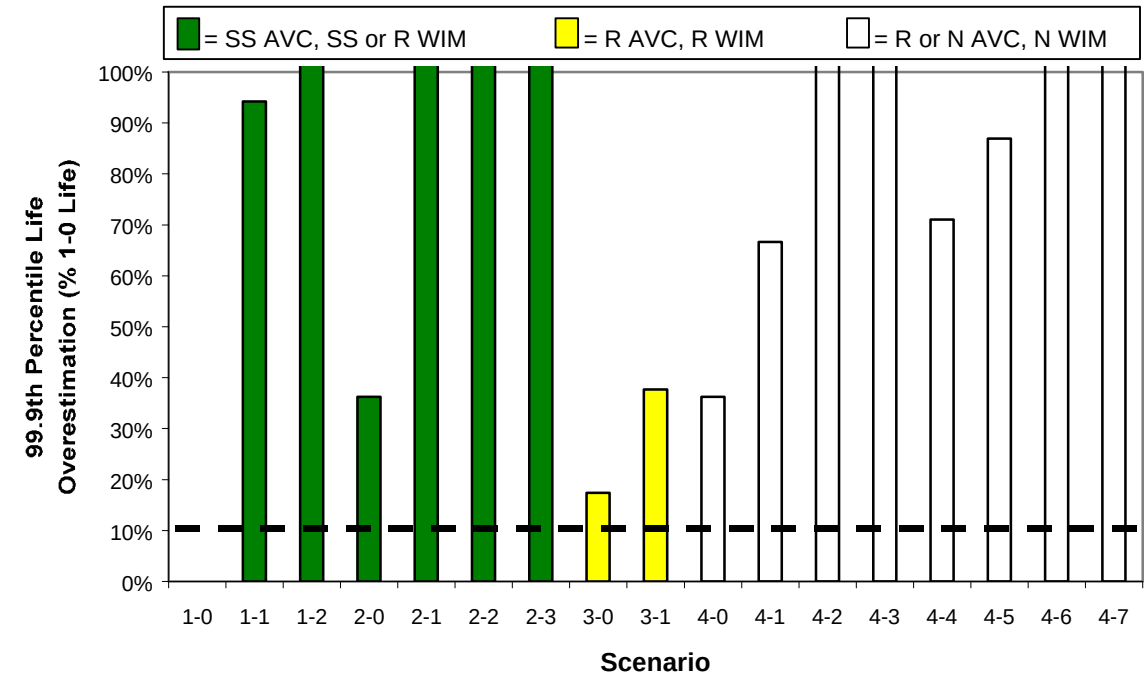

Figure G.35: Rigid Site 9_4008, 99.9th Percentile, % Life Overestimation

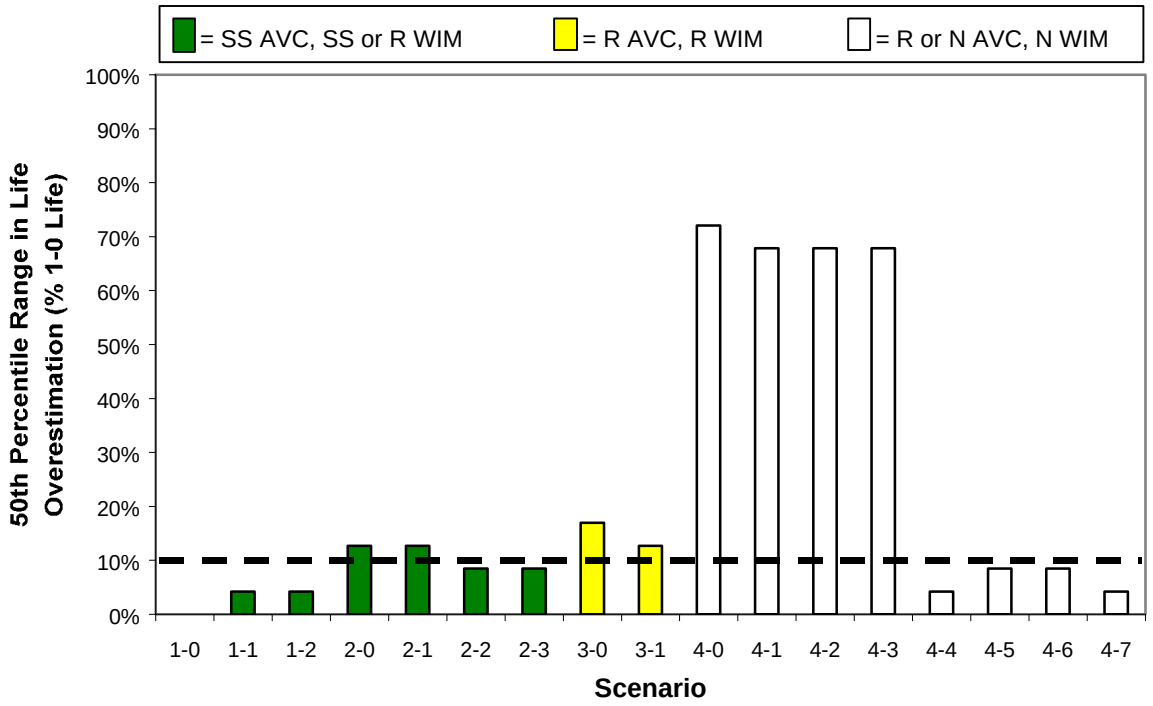

Figure G.36: Rigid Site 50_1682, 50th Percentile, % Life Overestimation

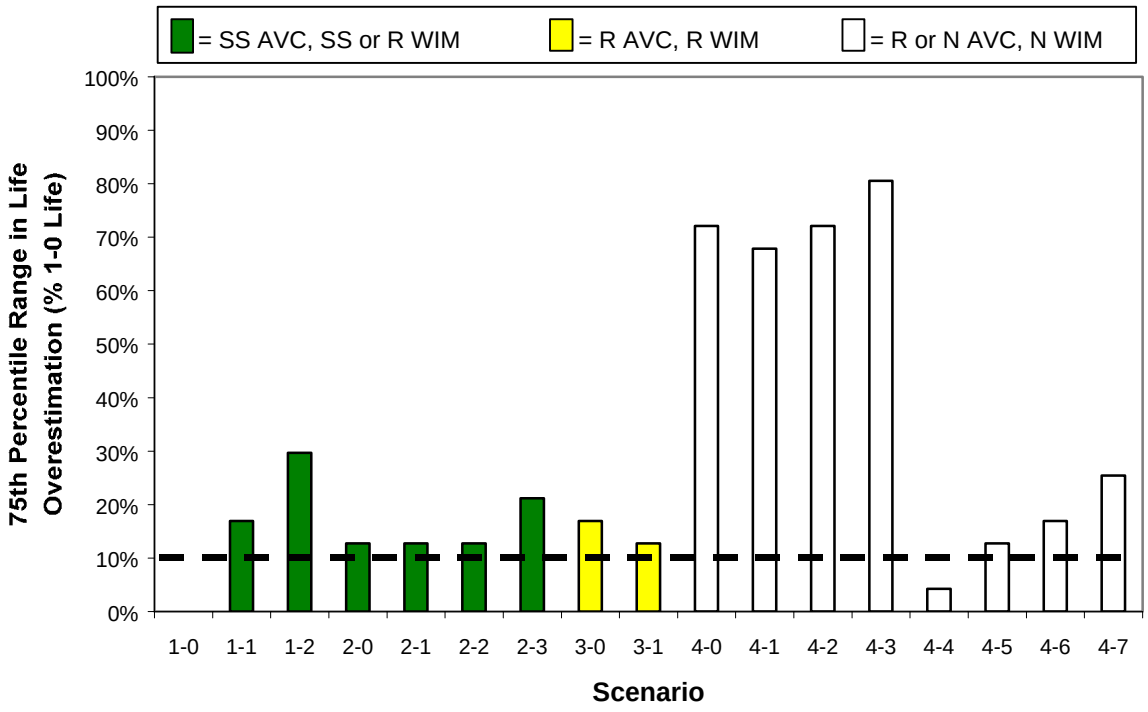

Figure G.37: Rigid Site 50_1682, 75th Percentile, % Life Overestimation

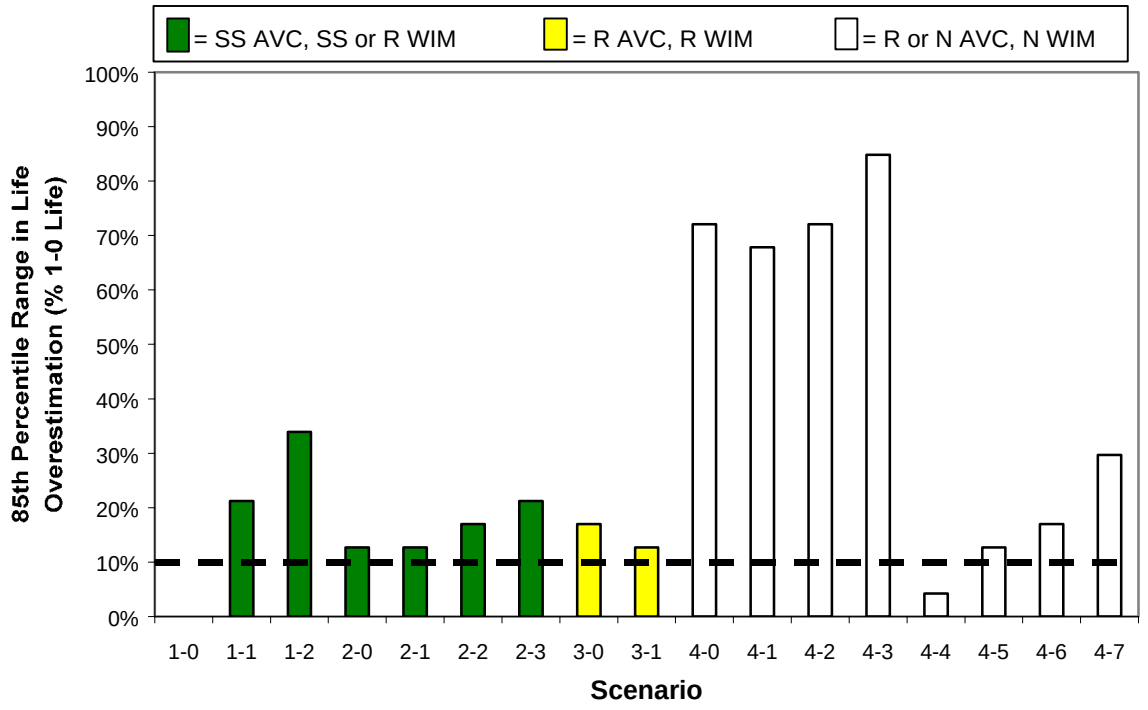

Figure G.38: Rigid Site 50_1682, 85th Percentile, % Life Overestimation

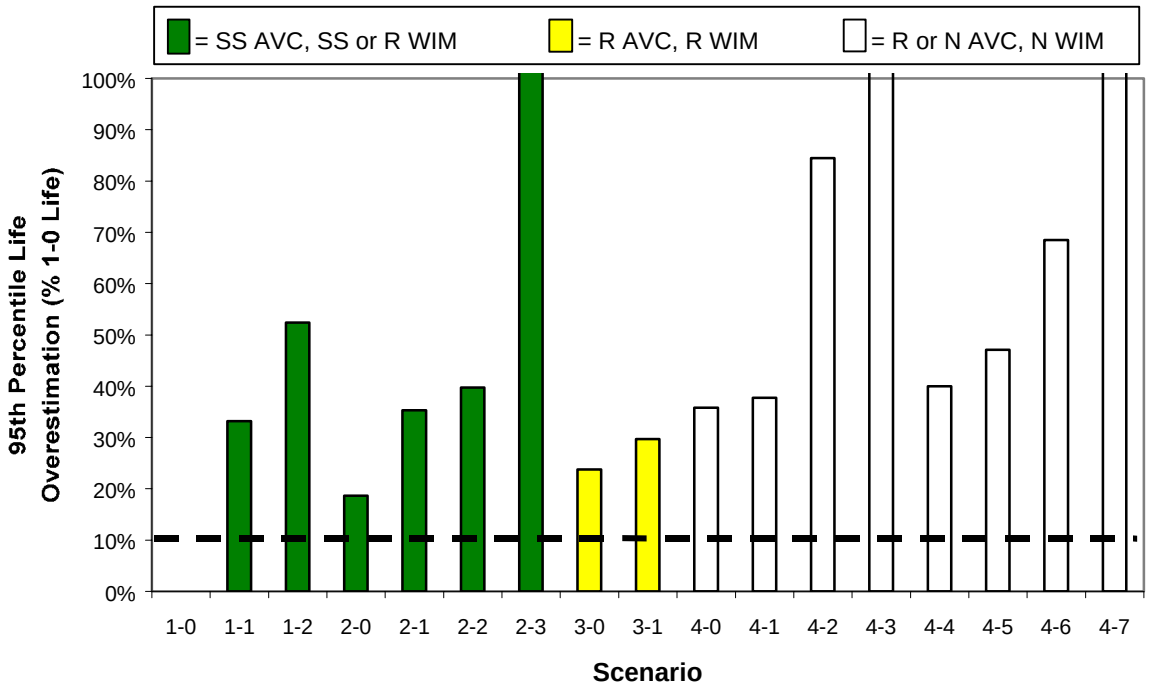

Figure G.39: Rigid Site 50_1682, 95th Percentile, % Life Overestimation

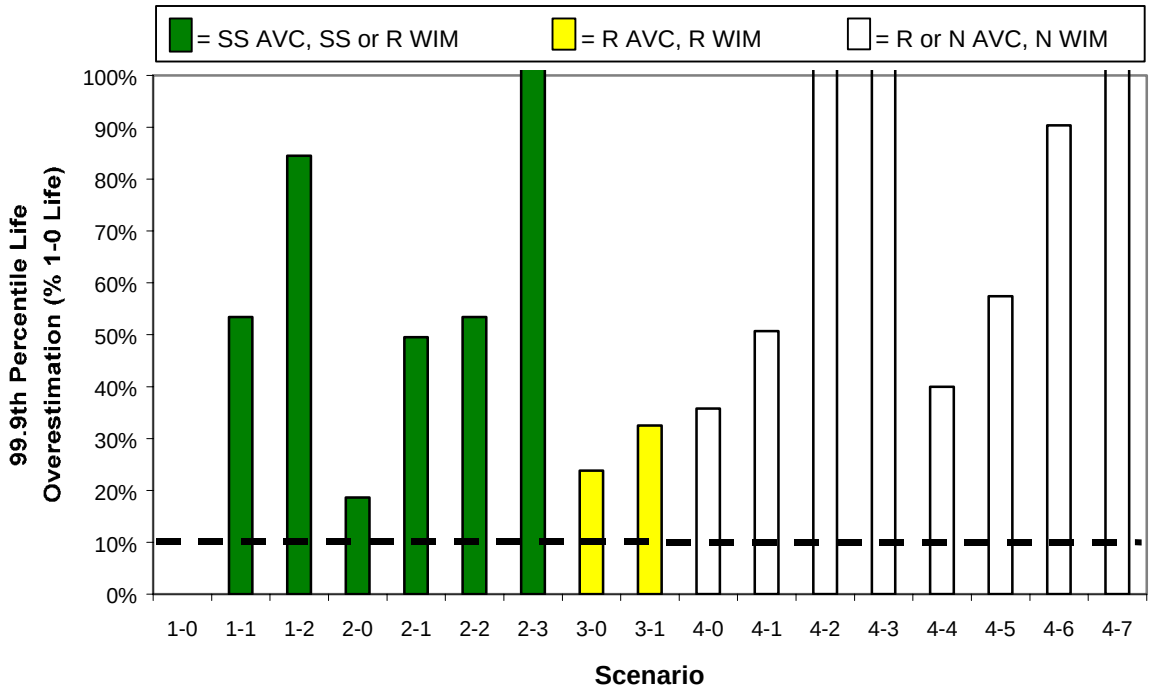

Figure G-40: Rigid Site 50_1682, 99.9th Percentile, % Life Overestimation